Synthesis, characterisation and biological studies of copper(I) and copper(II) pyridinyl Schiff base complexes

UNIVERSITY OF
KWAZULU-NATAL

INYUVESI
YAKWAZULU-NATALI

Supervisors: Prof VO Nyamori and Prof BO Owaga

By Mthokozisi Mkhize

Synthesis, characterisation and biological studies of copper(I) and copper(II) pyridinyl Schiff base complexes

by

Mthokozisi Mkhize

A thesis submitted in fulfilment of the academic requirements for a masters degree in Chemistry in the School of Chemistry and Physics, University of KwaZulu-Natal, Westville Campus, Durban

November 2019

As the candidate's supervisors, we have approved this thesis for submission.

Signed: _____ Name: _____ Date: _____

Signed: _____ Name: _____ Date: _____

Abstract

Coordination complexes have numerous applications ranging from industrial processes to pharmaceuticals. Schiff base ligands, along with copper(I) and copper(II) metal complexes have been investigated and reported in the literature for their potential as antibacterial agents. This thesis reports the synthesis, characterisation of Schiff base ligands and their corresponding copper(I) and copper(II) complexes for antibacterial application investigations.

A total of fourteen Schiff base ligand derivatives (**L1** – **L14**) were synthesised, purified and characterised. They were analysed by nuclear magnetic resonance (^{1}H-NMR & ^{13}C-NMR) spectroscopy, UV-Vis spectroscopy, infrared (IR) spectroscopy and also melting point determinations. **L1** – **L14** were synthesised *via* the solvent-free grinding technique, whilst **L3** and **L11** – **L14** were also synthesised by the microwave-assisted heating for comparative purposes. It was found that both the solvent-free grinding and microwave-assisted techniques were efficient, timeous, clean and high yielding, (83 – 98%) and (85 – 91%), respectively.

L1 – **L10** were used in the synthesis (two-stage) of fifteen copper complexes in reactions done under an inert atmosphere. Of the fifteen complexes, **1** – **7** were copper(I) pyridinyl Schiff base complexes, while **8** – **15** were copper(II) Schiff base complexes. Additionally, **8 – 15** were also prepared using a one-pot approach in which the respective ligand precursors and the copper(I) or copper(II) metal salts were mixed together. Both techniques resulted in high yields, (84 – 94%) and (77 – 89%) for two-stage and one-pot reactions, respectively. The two-stage reactions showed to be efficient with higher yields and is suitable for both copper(I) and copper(II) Schiff base synthesis by allowing controlled reaction conditions. The Schiff base complexes were analysed by nuclear magnetic resonance (^{1}H-NMR & ^{13}C-NMR), UV-Vis spectroscopy, infrared (IR) spectroscopy, elemental analysis (EA), electrospray ionisation mass spectroscopy (ESI-MS) and their melting points were determined. Finally, the single-crystal structures of derivatives of **10** and **12**, (**10**$_{\mathbf{py}}$ and **12**$_{\mathbf{py}}$) were solved using the single-crystal X-ray diffraction (SC-XRD). The structures of **10**$_{\mathbf{py}}$ and **12**$_{\mathbf{py}}$ adopt the distorted trigonal bipyramidal geometry around Cu(II) centre.

All complexes (**1** – **15**) were tested for their antimicrobial potency against four gram-negative, *i.e.*, *Escherichia coli* ATCC 25922 (*E. coli*), *Pseudomonas aeruginosa* ATCC 27853 (*P. aeruginosa*), *Klebsiella pneumoniae,* ATCC 31488 (*K. pneumonia*) *Salmonella typhimurium* ATCC 14028 (*S. typhimurium*); two gram-positive, *i.e.*, *Staphylococcus aureus* ATCC 25923 (*S. aureus*) and Methicillin-resistant *Staphylococcus aureus* ATCC 700699 (MRSA) bacteria. The copper(I) complexes (**1** – **7**) were inactive against all tested bacteria, while copper(II) complexes (**8** – **15**) showed bactericidal activities but did not demonstrate a wide spectrum of activities. Notably, **10**, **11** and **12** were appreciably active against five of six bacterial strains, except for the *Staphylococcus aureus* bacterium. Some of the Cu(II) Schiff base complexes displayed lower minimum inhibitory concentration (MIC) values in comparison with the standard reference, ciprofloxacin.

Preface

The experimental work was carried out in the School of Chemistry and Physics, University of KwaZulu-Natal, Westville campus from March 2017 to November 2019, under the supervision of Prof VO Nyamori and Prof BO Owaga.

The work reported in this thesis has been carried out by the author and has not been submitted into any other tertiary institution in any form, and the utilization of other individual's work has been acknowledged through appropriate referencing.

Sign…….… Date……

Declaration 1: Plagiarism

I, **Mthokozisi Mkhize** declare that;

1. The research reported in the thesis, except where otherwise indicated, is my original research.
2. This thesis has not been submitted for any degree or examination at any other University.
3. This thesis does not contain other person's data, pictures, graphs or other information unless specifically acknowledged as being sourced from the persons.
4. This thesis does not contain another person's writing unless specifically acknowledged as being sourced from other researchers. Where other written sources have been quoted, then:
    a. Their words have been re-written but, the general information attributed to them has been referenced.
    b. Where exact words have been used, then their writing has been placed in italics and inside quotation marks and referenced.
5. This thesis does not contain text, graphics or tables copied and pasted from the internet, unless specifically acknowledged and the source being detailed in the thesis and in the reference sections.

Signed……...Date…..……

Declaration 2: Scientific communications

Presentations

1 Faculty of Agriculture, Engineering and Science Postgraduate Research Day.
University of KwaZulu-Natal, Westville campus, 10 October 2018.
(Poster presentation)

Title: *Synthesis, structural and biological studies of copper(I) and copper(II) pyridinyl Schiff base complexes*

Authors: Mthokozisi Mkhize, Bernard Owaga and Vincent O. Nyamori

2 SACI/ChromSA Postgraduate Research Colloquium.
Durban University of Technology, Durban campus, 6 March 2019.
(Oral presentation)

Title: *Biological studies of copper(I) and copper(II) pyridinyl Schiff base complexes*

Authors: Mthokozisi Mkhize, Bernard Owaga and Vincent O. Nyamori

Signed……..……. Date……

Dedication

I dedicate this thesis to my family and friends with modesty and deep gratitude. For not only did I make it, but together we have made it.

There is no better way that I could possibly thank you, other than by getting this MSc degree, which somehow almost slipped our grasps. Thank you for support, you could have deserted me along the way. *Impela awukho umgodi wokulahla umuntu*. Please read this with a huge smile and pride, for we have made it, as a team.

Acknowledgements

Firstly, I would like to thank my former primary to high school teachers, emphasis going to Mabuthela High school amazing teachers, Mr Ngcobo, Mrs Qozo, Mrs Mvuna, Mr Nikwe and Mr Mwamuka who were more than teachers but also motivators especially during my difficult times whilst a learner. Not forgetting Mr Mshengu whom I solely owe my affection for science and yes especially the chemistry branch.

Secondly, I would also wish to thank the University of KwaZulu-Natal, College of Agriculture, Engineering and Science for giving me such a precious opportunity to further my studies. All lectures for their different contributions towards my studies, particularly my two lectures, Prof. VO Nyamori and Prof. BO Owaga, for giving me the honour to work under their supervision. I thank Dr C Mocktar for the biological application supervision. Not forgetting the invaluable inputs of Prof. BS Martincigh and Dr OS Olatunji.

Thirdly, I thank the NanoChemistry Research Group who walked me throughout the project, giving their all and always helped in every way possible. Nonjabulo Ngidi, Hassan Shoyiga, Simphiwe Ngwenya, Samantha Ndlovu, Regina Egbele and Kudzai Mugadza.

Fourthly, I thank my friends and colleagues for proofreading my work with a keen eye. Nicholas Rono, Siphiwe Mdutyana, Ayomide Labulo, Nokuthula Mtshali and Ayanda Hlophe, your efforts did not go in vain. I appreciate your time and selflessness.

Fifthly, I thank my parents (Mr Sibongiseni and Mrs Nompumelelo Mkhize), my siblings (Xolisile Mkhize, Thulani Mkhize, Hlobisile Mkhize, Zamani Mkhize and Siyamthanda Mkhize), my uncles (Sicelo Mkhize and Sishosonke Mkhize) for their continuous love and support and the rest of family and friends for their prayers.

Lastly, All the UKZN Westville staff for their help in many ways. Particularly, Sizwe Zamisa for SC-XRD structural analysis. Not forgetting Unathi Bongoza, Anita Naidoo, Renee Naidoo, Gregory Moodley, Vuyisa Mzozoyana, Raj Somaru, Nundkumar Miller, Fikile Gumede, Padayachee Malini and all who weren't mentioned herein.

Special thanks go to God almighty for life and everything: *uShembe uyindlela neqiniso*

“Our cells engage in protein production and many of those proteins are enzymes responsible for the chemistry of life” - *Randy Schekman*

“We think there is colour, we think there is sweet, we think there is bitter, but in reality, there are atoms and a void” - *Democritus*

Table of Contents

3. Chapter 3: Experimental

4. Chapter 4: Results and discussions

Appendices

List of tables

List of figures

Content **Page**

List of schemes

Content **Page**

Abbreviation

AmB	Amphotericin B
ATP	Adenosine triphosphate
BAMs	Biological active molecules
$CDCL_3$	Deuterated chloroform
cisplatin	*cis*-diamminedichloroplatinum(II) complex
DMSO	Deuterated dimethyl sulfoxide
DNA	Deoxyribonucleic acid
E coli	*Escherichia coli*
EA	Elemental analysis
EDG	Electron-donating group
ESI-MS	Electrospray ionisation mass spectroscopy
EWG	Electron-withdrawing group
HIV	Human immunodeficiency virus
HSAB	Hard and soft, acid and base
IR	Infrared spectroscopy
K. pneumoniae	*Klebsiella pneumoniae*
MeCN	Acetonitrile
MHA	Mueller-Hinton Agar
MIC	Minimum inhibitory concentration
MLCT	Metal to ligand charge transfer
MRSA	Methicillin-resistant *Staphylococcus aureus*
MW-assisted	Microwave-assisted
NB	Nutrient Broth
NMR	Nuclear magnetic resonance
PMI	Phosphomannose isomerase
ppm	Parts per million
PSB	Pyridinyl Schiff base
QSB	Quinoline Schiff base
RNS	Reactive nitrogen species
ROS	Reactive oxygen species

S. aureus	*Staphylococcus aureus*
S. typhimurium	*Salmonella typhimurium*
SB	Schiff base
SC-XRD	Single-crystal X-ray diffractometer
SOD	Superoxide dismutase
TLC	Thin layer chromatography
UV-Vis	Ultraviolet-visible
Vfend	Voriconazole

List of compounds

L1	(*E*)-2,6-dimethyl-*N*-(pyridin-4-ylmethylene)aniline ligand
L10	(*E*)-2,4,6-tri-*tert*-butyl-*N*-(pyridin-2-ylmethylene)aniline ligand
L11	(*E*)-*N*-(1-(pyridin-2-yl)ethylidene)aniline ligand
L12	(*E*)-*N*-(pyridin-3-ylmethylene)aniline ligand
L13	(*E*)-*N*-(pyridin-4-ylmethylene)aniline ligand
L14	(*E*)-3-nitro-*N*-(pyridin-3-ylmethylene)aniline ligand
L2	(*E*)-2,6-dimethyl-*N*-(pyridin-2-ylmethylene)aniline ligand
L3	(*E*)-*N*-(pyridin-2-ylmethylene)aniline ligand
L4	(*E*)-2,6-dichloro-*N*-(pyridin-2-ylmethylene)aniline ligand
L5	(*E*)-2,6-dichloro-*N*-(pyridin-4-ylmethylene)aniline ligand
L6	(*E*)-3-nitro-*N*-(pyridin-2-ylmethylene)aniline ligand
L7	(*E*)-3-nitro-*N*-(pyridin-4-ylmethylene)aniline ligand
L8	(*E*)-4-bromo-2,6-dichloro-*N*-(pyridin-2-ylmethylene)aniline ligand
L9	(*E*)-2,6-dimethyl-*N*-(quinolin-2-ylmethylene)aniline ligand
1	$[Cu(L1)_2]Cl^-$
2	$[Cu(L2)_2]Cl^-$
3	$[Cu(L3)_2]Cl^-$
4	$[Cu(L4)_2]Cl^-$
5	CuL5Cl
6	$[Cu(L6)_2]Cl^-$
7	$[CuCl(L7)_2]$
8	$[Cu(L10)_2]2Cl^-$
9	$[Cu(L1)_2]2Cl^-$
10	$[Cu(L2)_2]2Cl^-$
11	$[Cu(L9)_2]2Cl^-$
12	$[Cu(L3)_2]2Cl^-$
13	$[Cu(L8)_2]2Cl^-$
14	$[Cu(Cl)_2(L6)_2]$
15	$[Cu(Cl)_2L7]$

Chapter 1

1. Introduction

The chapter gives a brief overview of the challenges faced in managing the diseases that are caused by bacteria. The rationale behind the choice of ligands and their corresponding copper(I) and copper(II) Schiff base complexes for the antibacterial application is then discussed. This is then followed by the aims, objectives of the project, research questions and approach to be investigated in the project.

1.1 Disease management

Many drugs have been developed to manage different kinds of diseases, yet there is still a need to develop more drugs. Some diseases cannot be effectively treated by one drug because some pathogens may become resistance to the drug while some drugs are only effective when administered in high quantities.[1-4] There is a need to develop drugs which are affordable and environmentally benign after excretion from the system of the host.

Diseases can be infectious or non-infectious. The later includes diseases like cancer, diabetes, osteoporosis, chronic lung and heart diseases. Infectious diseases are caused and transmitted by bacteria, fungi or viruses. The infectious diseases that are caused by bacteria have emerged as the major threat to the social welfare of humans across the globe.[4-6] This has led to the investigation of the designed copper(I) and copper(II) coordination complexes as potential antibacterial agents.

The pharmaceutical potency of complexes is determined by the choice of coordinated ligands, the size and oxidation state of the metal centre.[7,8] Many transition metals have been used for this purpose, but compounds of bio-essential ions such as silver(I), copper(I) and copper(II) have been used as metallo-bactericides and their use in other medical applications can be dated back to the 19th century.[9,10] For instance, silver(I) compounds are incorporated in wound dressings due to their antimicrobial properties. Copper(I) and copper(II) metal salts or complexes, especially for those coordinated *via* nitrogen-, oxygen-, sulphur- or a combination of these donor atoms have generated a library of complexes for medicinal studies.[11-14] These complexes have been found to interact with deoxyribonucleic acid (DNA), thus, serving as antitumor agents.[7,10]

1.1.1 Bacteria and bacterial roles

Bacteria are single cell microorganisms and are deemed to be the first form of life to habitat on the earth. Also, bacteria are the most abundant living organisms and can be pathogenic or beneficial to its host environment. In some organisms, bacteria can have the symbiotic (mutual) benefits with the host. The mitochondria are believed to have originally been bacteria due to their close similarities. For this reason, mitochondria having the symbiotic relationship with mammals is the best example of a beneficial relationship between bacteria and its host cell.[15-18] Mitochondrion produces energy for animal cells. This is because the animal cells cannot convert oxygen and nutrients into useful energy known as adenosine triphosphate (ATP), the energy used for different chemical and biological reactions.[18-21] Also, ATP has showed to be involved in apoptosis by the careful and calculated release of pro-apoptotic redox proteins that induce cell death followed by phagocytic attack and removal unwanted cells.[17,22]

Bacteria generally play different roles in life. Bacteria can be good, *e.g.*, in the human bodies, there are those that help perform beneficial biochemical processes while others are used in medicine. Examples of beneficial bacteria include strains that digest food, which is made possible by catalytic reactions using enterocytes microbiomes.[17,23-26] Others are used in the production of food, *i.e.*, yoghurt, bread and alcohol beverages.[27-34] However, some bacteria are infectious and thus can cause diseases in plants, animals and humans.[35] In humans, the bacterial infections can lead to simple allergies or even result in diseases such as cancer, diabetes, cardiovascular, chronic inflammation and tooth decay. An example of a bacteria responsible for tooth decay is the *Porphyromonas gingivalis* (*P. gingivalis*), along with other bacteria, they can also cause life-threatening conditions.[36] Infections caused by bacteria such as *Pseudomonas aeruginosa, Methicillin-resistant staphylococcus aureus* (MRSA), *Escherichia coli (E coli), Staphylococcus aureus (S aureus), Enterobacter, Acinetobacter* and *Enterococcus* bacteria have been studied extensively due to their resistance to the antibiotics and lethality nature.[37-39]

1.1.2 The two classes of bacteria

There are two main classes of bacteria, known as the gram-positive and gram-negative. They are classified according to their tendency towards dye-staining since their outermost membranes react differently towards the staining dyes. The gram-positive bacteria consist of a thicker peptidoglycan outer membrane containing the lipoteichoic and teichoic acids (Figure

1.1(b)). The inner hydrophobic cell membrane and lipoproteins are both found in the gram-positive and gram-negative bacteria, whilst the gram-negative bacteria consist of two hydrophobic inner and outer cell membranes and a thin peptidoglycan layer in between the two membranes (Figure 1.1(a)). The gram-negative bacteria outermost layer consists of the lipopolysaccharides and proteins for transporting substances in and out of the microbe.[40]

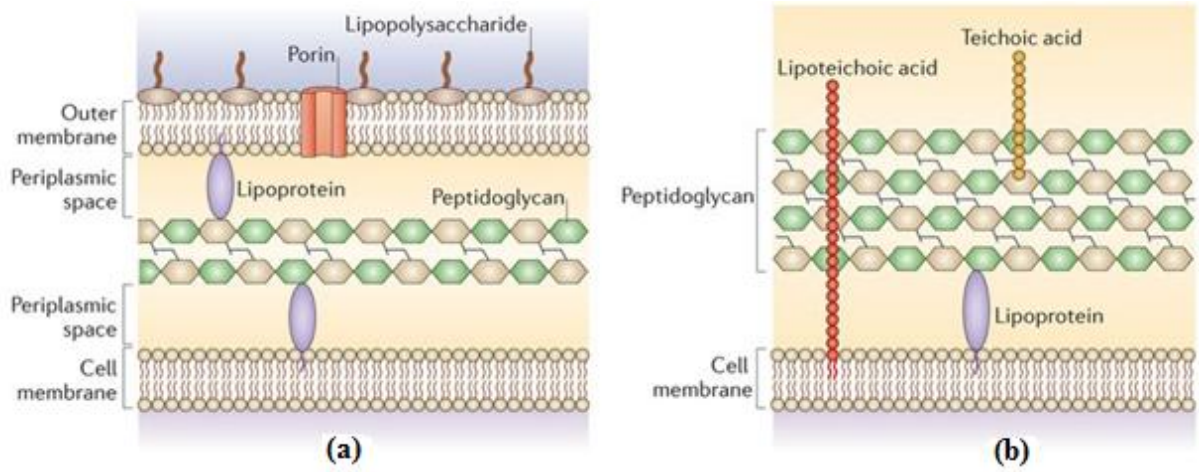

Figure 1.1: The cell wall structure of (a) gram-negative and (b) gram-positive bacteria[40]

Gram-positive bacteria are a sub-group of bacteria that include the MRSA and *S. aureus* bacteria. The *Staphylococcus aureus* bacteria are the human pathogenic microorganisms that are mainly found in the outermost skin cells in the body.[41] Bacterial infections caused by *Staphylococcus aureus* are easily transmitted through contact since these bacteria are found to habitat the outer skin environment. *Staphylococcus aureus* bacteria are responsible for several diseases, which include boils, impetigo, food poisoning, cellulitis and toxic shock syndrome.[42] MRSA bacteria are a group of *Staphylococcus aureus* bacteria that resists the methicillin antibiotics. Hence, they are referred to, as the Methicillin-resistant *staphylococcus aureus* (MRSA) bacteria.[2] The MRSA bacteria, like the *Staphylococcus aureus* bacteria, can be both commensal and pathogenic in human beings.[41] The MRSA infections have severe consequences compared to the *Staphylococcus aureus* bacteria counterparts. This is due to the pathogenic superiority of MRSA bacteria.[43,44] In its worst-case scenario, the MRSA bacteria can be directly linked to the sepsis and acute endocarditis infections.[45] These infections are quite a challenge to treat since the MRSA bacteria are situated on the inner organs of human beings. However, the gram-positive bacterial infections are less severe in comparison to those of gram-negative.

The gram-negative bacterial outer membrane is similar to those found in human beings. This camouflage enables gram-negative bacteria to survive thereby causing more damage. This is because the human host cells cannot identify gram-negative bacteria as a threat due to their close similarities. Examples of gram-negative bacteria include the *Escherichia coli* (*E coli*) and *Pseudomonas aeruginosa* (*P. aeruginosa*) bacteria, amongst others. The *Pseudomonas aeruginosa* and the *E coli* bacteria have rod-like shapes and they are responsible for numerous plant and animal diseases. In humans, the *Pseudomonas aeruginosa* bacteria cause infections of the urinary tract, gastrointestinal, dermatitis and respiratory systems. This is usually worse in humans with impaired immune systems. Most of the *E coli* bacterial strains are harmless and found in the human intestines, while some *E coli* strains have been reported to cause food and blood poisoning, pneumonia, urinary tract infections and diarrhoea, amongst other diseases.[42]

1.1.3 Setbacks of bacterial diseases

The discovery of potent antibiotics has saved lives of many people. However, bacterial resistance is a major drawback in the effective management of infectious diseases. Thus, there is always a need for research of alternative agents because some bacteria can quickly develop resistance to available drugs.[46,47] This is attributed to the short life span of bacteria. Hence, their genetic modifications allow for resistance within a short period of time.

The side effects of readily approved drugs are also a problem, *e.g.*, patients who are treated with dental bacterial infections may end up suffering from the bad taste, irritability and gum or teeth staining.[48] Thus, more research should be conducted on plague antibacterial agents that cannot cause irritation on patients, but are odourless, colourless and tasteless. Some prolonged treatment by inorganic antibiotics have shown serious life-threatening side effects which include cardiovascular, gastrointestinal, pneumonia, diabetes, kidneys and liver dysfunction while bone deterioration may be experienced upon discontinued use of therapy.[36,49] Due to the side effects that can possibly be lethal, the new antibacterial agents with minimal side effects are currently being researched for their roles and mechanisms as pharmacological agents.

The mechanisms of metal-based antibacterial drugs are not clearly understood, especially in the biological point of view. However, the bactericidal activity of silver nanoparticles is believed to be through induction of reactive oxygen species (ROS) in the cytoplasm of a microorganism. This can occur by both the release of Ag(I) ions or by binding of organic

ligands into the bacterial outer membrane and cause cell membrane permeability.[46] Hence, more studies should be conducted for a better understanding and design of antibacterial agents. The development of antibacterial agents with low inhibition concentration and selectivity is still a challenge for approved drugs. This is because drugs may be toxic to the host in high quantities.[50] The antibacterial candidates should also demonstrate a wide-spectrum of antibacterial activities, which is hard to achieve. The antimicrobial activity of some copper(I) and copper(II) complexes will be reported in this thesis.

1.1.4 Use of metal complexes as antibacterial agents

Metal complexes are formed when organic molecules (ligands) get coordinated to mostly transition metal centres. Complexes are widely used in different applications. Some metal complexes are active as antibacterial agents.[51-55] Different complexes spanning a wide range of transition metal centres have been investigated for antibacterial activities and of interests has been complexes of biological essential ions, *e.g.*, copper metal centre. This is because they are assumed to be less toxic, should they be administered in human beings. Apart from the metal centres, the coordinated ligands also play a role in the activity of complexes. The properties of ligands somehow carry over to the final complex, *i.e.*, the hydrophilic ligands can result in hydrophilic complexes. Hence the choice of ligands deserves a great deal of attention.

Schiff base ligands are organic compounds containing an imine functional group (C=N) formed *via* condensation of an amine (or related nucleophiles) and a carbonyl group.[56-66] Schiff bases (SBs) have been exploited for their attractive properties such as antibacterial, antifungal and facile coordination to most transition metals.[67-71] In metal coordination, Schiff bases form complexes that have numerous biological importance.[72,73] The use of complexes with known biochemical pathways ensures the limitation of side effects as pharmacological agents.[10,74] Due to the potential use of copper(I) and copper(II) complexes in other medical applications, we have designed, synthesised and explored their chemical, physical, structural properties and antimicrobial activities.

1.1.5 Green synthesis of ligands and complexes

Green chemistry, also known as the sustainable chemistry, is the design of chemical products and processes that reduce or eliminate the use or generation of hazardous substances.[75] Green chemistry is a highly effective approach to prevent pollution.[76,77] Hence, adhering to the principles of green chemistry has become an inevitable synthetic strategy in modern day chemistry. Green chemistry is premised on 12 principles, which shall not be discussed in details.[78] The aim is to reduce wastes produced from chemical industries and academia which has led to numerous health problems, toxicity, depletion of renewable resources and global warming phenomena. In this project, Schiff base ligands were synthesised by two potentially green methods, namely; the solvent-free grinding and microwave-assisted techniques. This was followed by the synthesis of complexes using two green techniques, namely; the two-stage and one-pot approaches under ambient conditions.

The mechanochemical technique involves chemical reaction by application of the mechanical force, *e.g.*, in the form of grinding.[79-82] There are three types of mechanical synthetic techniques.[67,82,83] The neat grinding is the most common, simplest and effective of the three techniques.[67] Neat grinding reactions can proceed at room conditions and does not require the use of a solvent (solvent-free grinding). This is advantageous since the volatile wastes are not emitted from the reaction. The solvent-free grinding affords close proximity of reacting molecules since they are not dispersed in a solvent medium, which favours the forward reaction.[8,81-86] Hence, the solvent-free grinding synthesis has been widely used because of the said advantages. The neat grinding also allows for exceptional stoichiometric control of the reaction mixture as there is no addition of a catalyst or solvent, which allows for a good control of products.[67,81] Besides the neat grinding technique, microwave-assisted (MW-assisted) is a also popular green synthetic technique.

The microwave-assisted technique provides an alternative procedure to synthesise compounds and involves the application of microwave radiation to heat up chemical reactions in polar reaction media. The microwave radiation is absorbed as heat. The employment of polar solvent, *i.e.*, minimal ethanol (EtOH) is useful in the conversion of microwave radiation into heat energy. The heat energy speed-up the reaction rate.[13-15] This technique is easy to operate and afford high yields, while the clean-up of product is minimal.[87-97] Thus, microwave-assisted (MW-assisted) has been widely employed as an efficient synthetic technique for heterogeneous Schiff base ligands and complexes.[93-95]

The compounds can also be synthesised using a conventional method by mixing reactants in a solvent. This method relies more on the nature of the solvents. The advantages of a conventional method are the operational easiness and can proceed at normal room conditions. However, heating the reaction usually speeds-up the reaction. Stirring the reaction increases homogeneity and improve contact of molecules. Also, stirring avoids development of hot-spots in a reaction.[98] Some reactions cannot proceed under solvent-free conditions, especially in the case of solid reactants.[99,100] However, green solvents like water and EtOH can be used in minimal quantities to suit the greener synthetic approach. The conventional method can be done in many steps (two-stage) or in a single step (one-pot) approach.

The two-stage conventional reaction involves the synthesis of organometallic complexes using pre-synthesised and characterised ligands, *i.e.*, the ligand precursors are synthesised and purified before the complexation to afford complexes. This allows for better control of the structure of the complex, which is easily achieved by using the specific ratio of ligands and metal salts. On the other hand, one-pot synthetic technique contains just a single step synthesis of metal complexes. Thus, the one-pot approach is devoid of the monotonous multistep purifications that are required in the two-stage approach. However, one-pot approach is less selective when the starting reactants contain multiple functional groups.[101] This lowers yields of the desired product since the approach can potentially form a number of side products. This can become tedious during the purification stage.

1.2 Problem statement

Bacterial related diseases have been a challenge before the civilisation of mankind and continue to be a major global challenge to date. Disease management by antimicrobial drugs has numerous setbacks, including non-selectivity or specificity and development of resistance by the bacteria. Hence, there is still a need for research of potential antibacterial drugs. The major challenge is to develop drug candidates that can have a wide spectrum of antibacterial activities, especially candidates that can show potency in both the gram-negative and gram-positive bacteria. Another challenge is the design of drug candidates which are effective at low dose concentration.

SBs have generated lots of interest because they exhibit a wide range of attractive properties such as antibacterial and antifungal potency.[102-104] In addition, Schiff base ligands have been vastly used in metal coordination that is applied in different biochemical substrates.[67,70,105]

These complexes of copper with pyridinyl Schiff base derivatives, especially copper(I) complexes have not been explored in detail. Thus, the copper(I) and copper(II) complexes were synthesised and investigated for the antibacterial potency.

1.3 Aims and objectives

The primary aims of the project were:

1. To synthesise, characterise and investigate biological activities of copper(I) and copper(II) pyridinyl Schiff base complexes.
2. To test the antibacterial potency of synthesised complexes.

The primary aims of the project were achieved by following the specific objectives of the study, which were to:

1. Synthesise and characterise pyridinyl Schiff base ligands using a green neat grinding technique under solvent-free conditions (solvent-free grinding) and compare the results with those obtained using the microwave-assisted method.
2. Compare conventional two-stage and one-pot approach techniques for the synthesis of complexes.
3. Characterise the ligands and complexes using spectroscopic and analytical techniques.
4. Utilise the Kirby-Bauer technique to evaluate susceptibilities of bacteria towards the compounds and compare to the parent complex (**12**) by working out the minimum inhibitory concentration (MIC) values.

1.4 Research questions

1 What is the most efficient synthetic route for pyridinyl/quinolinyl ligands between the solvent-free grinding and microwave-assisted techniques?
2 Which technique produces higher yields between the conventional two-stage and one-pot approach in the synthesis of complexes?
3 Does the oxidation state of copper metal centre affect the activity against bacteria?
4 Which R-group substituent enhances the antimicrobial activity between the electron-withdrawing group (EWG) and electron-donating group (EDG) appended complexes?
5 Does quinoline moiety improve the antibacterial activity over pyridine moiety in the ligand backbone structure?

1.5 Research approach

The ligands were synthesised by the solvent-free grinding technique. This technique was compared with the microwave-assisted technique to deduce a better route for the ligand synthesis. This was followed by the synthesis of metal complexes. The techniques that were employed in the synthesis of complexes were either or both the two-stage and one-pot reactions at temperate (~25 ºC) conditions. The two techniques employed were compared to determine a better technique for the synthesis of complexes. The synthesised complexes were purified and analysed using various spectroscopic and analytical techniques. The structure of complexes $\mathbf{10}_{\mathbf{py}}$ and $\mathbf{12}_{\mathbf{py}}$ were determined using the single-crystal X-ray diffraction (SC-XRD) instrument.

The synthesised and purified complexes were tested against six bacteria, two of which were gram-positive and four gram-negative bacteria. The technique used for antibacterial assay was the Kirby-Bauer method or simply disc diffusion technique utilizing dimethyl sulfoxide (DMSO) as a negative control, while ciprofloxacin standard drug was used as a positive reference. This was then followed by determination of the minimum inhibitory concentration (MIC) values by use of the dilution method to establish the lowest amount of a certain compound required for bactericidal activities.

1.6 Outline of thesis

Chapter One

Chapter One first discusses the general background, followed by the motivation for the choice of compounds that are examined for biological studies in this project. The aims and objectives to justify the logic behind the research project are stated and how the research questions will be answered by following the clearly stated research approach.

Chapter Two

Chapter Two is the literature review based on the project rationale to employ the pyridinyl Schiff base copper complexes for the antibacterial application. The literature summary and project rationale are stated at the end of the chapter.

Chapter Three

Chapter Three reports the experimental procedures from the synthesis and characterisation of ligands, to the synthesis and characterisation of copper complexes. Further, the methods for biological application are stated.

Chapter Four

Chapter Four reports results and discussions on the synthesis and characterisation of all synthesised compounds. This starts with the synthesis of donor ligands and coordination complexes. The conclusion is drawn based on the results obtained in correlation to the structures.

Chapter Five

Chapter Five provides the results and discussions behind all biological studies and techniques employed in the antibacterial activity of the tested compounds.

Chapter Six

This chapter report the results and drawn conclusions based on project questions. The chapter ends with the future work and recommendations, which are clearly stated for project continuation.

References

1. B. Aslam, W. Wang, M. I. Arshad, M. Khurshid, S. Muzammil, M. H. Rasool, M. A. Nisar, R. F. Alvi, M. A. Aslam, M. U. Qamar, M. K. F. Salamat and Z. Baloch, *Infection and Drug Resistance*, 2018, **11**, 1645.
2. R. Kanchanapally, B. P. V. Nellore, S. S. Sinha, F. Pedraza, S. J. Jones, A. Pramanik, S. R. Chavva, C. Tchounwou, Y. Shi and A. Vangara, *RSC Advances*, 2015, **5**, 18881.
3. W. Li, K. Dong, J. Ren and X. Qu, *Angewandte Chemie International Edition*, 2016, **55**, 8049.
4. P. Wikaningtyas and E. Y. Sukandar, *Asian Pacific Journal of Tropical Biomedicine*, 2016, **6**, 16.
5. G. Fang, W. Li, X. Shen, J. M. Perez-Aguilar, Y. Chong, X. Gao, Z. Chai, C. Chen, C. Ge and R. Zhou, *Nature Communications*, 2018, **9**, 129.
6. S. V. Kumar, S. Ø. Scottwell, E. Waugh, C. J. McAdam, L. R. Hanton, H. J. L. Brooks and J. D. Crowley, *Inorganic Chemistry*, 2016, **55**, 9767.
7. K. A. Ali, M. M. Abd-Elzaher and K. Mahmoud, *International Journal of Medicinal Chemistry*, 2013, **2013**, 7.
8. A. K. Ghosh, M. Mitra, A. Fathima, H. Yadav, A. Roy Choudhury, B. U. Nair and R. Ghosh, *Polyhedron*, 2016, **107**, 1.
9. W. J. Lian, X. T. Wang, C. Z. Xie, H. Tian, X. Q. Song, H. T. Pan, X. Qiao and J. Y. Xu, *Dalton Transactions*, 2016, **45**, 9073.
10. S. Kathiresan, S. Mugesh, J. Annaraj and M. Murugan, *New Journal of Chemistry*, 2017, **41**, 1267.
11. G. K. Patra and I. Goldberg, *New Journal of Chemistry*, 2003, **27**, 1124.
12. M. Hazra, T. Dolai, A. Pandey, S. K. Dey and A. Patra, *Bioinorganic Chemistry and Applications*, 2014, **2014**, 13.
13. B. Geeta, K. Shravankumar, P. M. Reddy, E. Ravikrishna, M. Sarangapani, K. K. Reddy and V. Ravinder, *Spectrochimica Acta Part A: Molecular and Biomolecular Spectroscopy*, 2010, **77**, 911.
14. F. Shabani, S. Ghammamy, K. Mehrani, M. B. Teimouri, M. Soleimani and S. Kaviani, *Bioinorganic Chemistry and Applications*, 2008, **2008**, 5.
15. N. S. Chandel, *Cell Metabolism*, 2015, **22**, 204.
16. D. R. Green and J. C. Reed, *Science*, 1998, **281**, 1309.
17. V. Punj and A. Chakrabarty, *Cellular Microbiology*, 2003, **5**, 225.

18. M. Webb, D. P. Sideris and M. Biddle, *Bioorganic & Medicinal Chemistry Letters*, 2019, **29**, 1270.
19. J. Barber, *Chemical Society Reviews*, 2009, **38**, 185.
20. J. Krutmann and P. Schroeder, *Journal of Investigative Dermatology Symposium Proceedings*, 2009, **14**, 44.
21. E. Cadenas, *Molecular Aspects of Medicine*, 2004, **25**, 17.
22. E. H. Y. A. Cheng, M. C. Wei, S. Weiler, R. A. Flavell, T. W. Mak, T. Lindsten and S. J. Korsmeyer, *Molecular Cell*, 2001, **8**, 705.
23. L. Flandroy, T. Poutahidis, G. Berg, G. Clarke, M. C. Dao, E. Decaestecker, E. Furman, T. Haahtela, S. Massart, H. Plovier, Y. Sanz and G. Rook, *Science of The Total Environment*, 2018, **627**, 1018.
24. S. F. Gilbert, J. Sapp and A. I. Tauber, *The Quarterly Review of Biology*, 2012, **87**, 325.
25. H. J. Flint, K. P. Scott, P. Louis and S. H. Duncan, *Nature Reviews Gastroenterology & Hepatology*, 2012, **9**, 577.
26. S. M. Jandhyala, R. Talukdar, C. Subramanyam, H. Vuyyuru, M. Sasikala and D. N. Reddy, *World Journal of Gastroenterology*, 2015, **21**, 8787.
27. M. Arici Muhammet, G. Ozulku, R. M. Yildirim, O. Sagdic and M. Z. Durak, *Food Science and Biotechnology*, 2018, **27**, 499.
28. A. Corsetti, M. Gobbetti, F. Balestrieri, F. Paoletti, L. Russi and J. Rossi, *Journal of Food Science*, 1998, **63**, 347.
29. K. Sigler, D. Matoulková, M. Dienstbier and P. Gabriel, *Applied Microbiology and Biotechnology*, 2009, **82**, 1027.
30. E. J. Pires, J. A. Teixeira, T. Brányik and A. A. Vicente, *Applied Microbiology and Biotechnology*, 2014, **98**, 1937.
31. D. Smogrovicová, Z. Dömény, P. Gemeiner, A. Malovíková and E. Sturdík, *Biotechnology Techniques*, 1997, **11**, 261.
32. F. Kobayashi and S. Odake, *Food and Bioprocess Technology*, 2015, **8**, 1690.
33. F. F. Jacob, M. Hutzler and F. J. Methner, *European Food Research and Technology*, 2019, **245**, 95.
34. J. J. Wang, W. N. Xu, X. E. Li, J. Li and Q. Li, *World Journal of Microbiology and Biotechnology*, 2014, **30**, 1901.
35. C. Sharma, N. Rokana, M. Chandra, B. P. Singh, R. D. Gulhane, J. P. S. Gill, P. Ray, A. K. Puniya and H. Panwar, *Frontiers in Veterinary Science*, 2018, **4**, 237.

36. Y. Wang, Y. Zhang, Y. Q. Shi, X. H. Pan, Y. H. Lu and P. Cao, *Microbial Pathogenesis*, 2018, **116**, 26.
37. M. S. Aljahdali, A. A. El-Sherif, R. H. Hilal and A. T. Abdel-Karim, *European Journal of Chemistry*, 2013, **4**, 370.
38. J. C. Y. Lin, R. T. W. Huang, C. S. Lee, A. Bhattacharyya, W. S. Hwang and I. J. B. Lin, *Chemical Reviews*, 2009, **109**, 3561.
39. M. A. Malik, O. A. Dar, P. Gull, M. Y. Wani and A. A. Hashmi, *Medicinal Chemistry Communications*, 2018, **9**, 409.
40. L. Brown, J. M. Wolf, R. Prados-Rosales and A. Casadevall, *Nature Reviews Microbiology*, 2015, **13**, 620.
41. S. Y. C. Tong, J. S. Davis, E. Eichenberger, T. L. Holland and V. G. Fowler, *Clinical Microbiology Reviews*, 2015, **28**, 603.
42. Y. Zhang, X. Liu, Y. Wang, P. Jiang and S. Quek, *Food Control*, 2016, **59**, 282.
43. S. Müller, A. J. Wolf, I. D. Iliev, B. L. Berg, D. M. Underhill and G. Y. Liu, *Cell Host & Microbe*, 2015, **18**, 604.
44. R. S. Kalhapure, S. J. Sonawane, D. R. Sikwal, M. Jadhav, S. Rambharose, C. Mocktar and T. Govender, *Colloids and Surfaces B: Biointerfaces*, 2015, **136**, 651.
45. Z. Zhao, R. Yan, X. Yi, J. Li, J. Rao, Z. Guo, Y. Yang, W. Li, Y. Li and C. Chen, *American Chemical Society: Nano*, 2017, **11**, 4428.
46. L. Rizzello and P. P. Pompa, *Chemical Society Reviews*, 2014, **43**, 1501.
47. J. L. Fox, *Nature Biotechnology*, 2006, **24**, 1521.
48. A. Pepperney and M. L. Chikindas, *Probiotics and Antimicrobial Proteins*, 2011, **3**, 68.
49. L. M. Golub, M. S. Elburki, C. Walker, M. Ryan, T. Sorsa, H. Tenenbaum, M. Goldberg, M. Wolff and Y. Gu, *International Dental Journal*, 2016, **66**, 127.
50. S. M. Nabavi, A. Marchese, M. Izadi, V. Curti, M. Daglia and S. F. Nabavi, *Food Chemistry*, 2015, **173**, 339.
51. M. M. Abd-Elzaher, A. A. Labib, H. A. Mousa, S. A. Moustafa, M. M. Ali and A. A. El-Rashedy, *Beni-Suef University Journal of Basic and Applied Sciences*, 2016, **5**, 85.
52. M. Nath and P. K. Saini, *Dalton Transactions*, 2011, **40**, 7077.
53. I. Turel, *Molecules (Basel, Switzerland)*, 2015, **20**, 7951.
54. A. Kourtellaris, E. E. Moushi, I. Spanopoulos, C. Tampaxis, G. Charalambopoulou, T. A. Steriotis, G. S. Papaefstathiou, P. N. Trikalitis and A. J. Tasiopoulos, *Inorganic Chemistry Frontiers*, 2016, **3**, 1527.

55. S. Yavuz and H. Yildirim, *Journal of Chemistry*, 2013, **2013**, 7.
56. M. Zbacnik and B. Kaitner, *Crystal Engineering Communications*, 2014, **16**, 4162.
57. Z. D. Petrović, J. Đorović, D. Simijonović, V. P. Petrović and Z. Marković, *RSC Advances*, 2015, **5**, 24094.
58. N. G. Khaligh, H. S. Abbo and S. J. J. Titinchi, *Research on Chemical Intermediates*, 2017, **43**, 901.
59. M. Khorshidifard, H. A. Rudbari, B. Askari, M. Sahihi, M. R. Farsani, F. Jalilian and G. Bruno, *Polyhedron*, 2015, **95**, 1.
60. T. Baran, I. Sargin, M. Kaya and A. Menteş, *Carbohydrate Polymers*, 2016, **152**, 181.
61. Y. Zhang, J. Fan, B. Yang and L. Ma, *Chemical Engineering Journal*, 2017, **326**, 612.
62. M. Zbačnik, K. Pičuljan, J. Parlov-Vuković, P. Novak and A. Roodt, *Crystals*, 2017, **7**, 25.
63. M. Sutradhar, L. M. D. R. S. Martins, M. F. C. Guedes da Silva and A. J. L. Pombeiro, *Applied Catalysis A: General*, 2015, **493**, 50.
64. W. Al Zoubi, A. A. S. Al-Hamdani, S. D. Ahmed and Y. G. Ko, *Applied Organometallic Chemistry*, 2018, **32**, 3895.
65. M. Galini, M. Salehi, M. Kubicki, A. Amiri and A. Khaleghian, *Inorganica Chimica Acta*, 2017, **461**, 167.
66. E. Q. Gao, Y. F. Yue, S. Q. Bai, Z. He and C. H. Yan, *Crystal Growth & Design*, 2005, **5**, 1119.
67. K. Venugopala and B. Jayashree, *Indian Journal of Pharmaceutical Sciences*, 2008, **70**, 88.
68. D. Chaturvedi and M. Kamboj, *Chemical Sciences Journal*, 2016, **7**, 1.
69. O. G. Idemudia, A. P. Sadimenko, A. J. Afolayan and E. C. Hosten, *Bioinorganic Chemistry and Applications*, 2015, **2015**, 14.
70. C. M. Da Silva, D. L. da Silva, L. V. Modolo, R. B. Alves, M. A. de Resende, C. V. Martins and Â. de Fátima, *Journal of Advanced Research*, 2011, **2**, 1.
71. U. Kalinowska-Lis, A. Felczak, L. Chęcińska, I. Szabłowska-Gadomska, E. Patyna, M. Małecki, K. Lisowska and J. Ochocki, *Molecules*, 2016, **21**, 87.
72. F. Xie and F. Peng, *Journal of Fluorescence*, 2018, **28**, 89.
73. J. Shin, A. Eskandari and K. Suntharalingam, *Molecules*, 2019, **24**, 1677.
74. K. L. Haas and K. J. Franz, *Chemical reviews*, 2009, **109**, 4921.

75. N. S. Radulović, A. B. Miltojević and R. D. Vukićević, *Comptes Rendus Chimie*, 2013, **16**, 257.
76. Neelima, K. Poonia, S. Siddiqui, M. Arshad and D. Kumar, *Spectrochimica Acta Part A: Molecular and Biomolecular Spectroscopy*, 2016, **155**, 146.
77. O. L. Cifuentes-Vaca, J. Andrades-Lagos, J. Campanini-Salinas, A. Laguna, D. Vásquez-Velásquez and M. Concepción Gimeno, *Inorganica Chimica Acta*, 2019, **489**, 275.
78. J. R. Anacona and I. Osorio, *Transition Metal Chemistry*, 2008, **33**, 517.
79. L. H. Abdel-Rahman, N. M. Ismail, M. Ismael, A. M. Abu-Dief and A. E. Abdel-Hameed, *Journal of Molecular Structure*, 2017, **1134**, 851.
80. M. Ghosh, M. Layek, M. Fleck, R. Saha and D. Bandyopadhyay, *Polyhedron*, 2015, **85**, 312.
81. N. Raman, A. Kulandaisamy, C. Thangaraja, P. Manisankar, S. Viswanathan and C. Vedhi, *Transition Metal Chemistry*, 2004, **29**, 129.
82. A. S. Abd El-All, S. A. Osman, H. M. F. Roaiah, M. M. Abdalla, A. A. Abd El Aty and W. H. AbdEl-Hady, *Medicinal Chemistry Research*, 2015, **24**, 4093.
83. G. Y. Nagesh and B. H. M. Mruthyunjayaswamy, *Journal of Molecular Structure*, 2015, **1085**, 198.
84. L. H. Abdel-Rahman, N. M. Ismail, M. Ismael, A. M. Abu-Dief and E. A. Ahmed, *Journal of Molecular Structure*, 2017, **1134**, 851.
85. M. T. Kaczmarek, M. Zabiszak, M. Nowak and R. Jastrzab, *Coordination Chemistry Reviews*, 2018, **370**, 42.
86. I. P. Ejidike and P. A. Ajibade, *Molecules*, 2015, **20**, 9788.
87. T. Baran, A. Menteş and H. Arslan, *International Journal of Biological Macromolecules*, 2015, **72**, 94.
88. S. Bernardini, A. Tiezzi, V. Laghezza Masci and E. Ovidi, *Natural Product Research*, 2018, **32**, 1926.
89. Y. Yang, Y. Lin, L. Li, R. J. Linhardt and Y. Yan, *Metabolic Engineering*, 2015, **29**, 217.
90. E. Patridge, P. Gareiss, M. S. Kinch and D. Hoyer, *Drug Discovery Today*, 2016, **21**, 204.
91. C. O. Kappe and D. Dallinger, *Nature Reviews Drug Discovery*, 2006, **5**, 51.
92. E. D. Brown and G. D. Wright, *Nature*, 2016, **529**, 336.

93. D. Sriram, P. Yogeeswari, N. S. Myneedu and V. Saraswat, *Bioorganic & Medicinal Chemistry Letters*, 2006, **16**, 2127.
94. R. V. Singh, P. Chaudhary, S. Chauhan and M. Swami, *Spectrochimica Acta Part A: Molecular and Biomolecular Spectroscopy*, 2009, **72**, 260.
95. M. C. García-López, B. M. Muñoz-Flores, R. Chan-Navarro, V. M. Jiménez-Pérez, I. Moggio, E. Arias, A. Rodríguez-Ortega and M. E. Ochoa, *Journal of Organometallic Chemistry*, 2016, **806**, 68.
96. A. K. Bose, M. Jayaraman, A. Okawa, S. S. Bari, E. W. Robb and M. S. Manhas, *Tetrahedron Letters*, 1996, **37**, 6989.
97. N. Kavitha and P. V. Anantha Lakshmi, *Journal of Saudi Chemical Society*, 2017, **21**, S457.
98. J. J. Shah and K. Mohanraj, *Indian Journal of Pharmaceutical Sciences*, 2014, **76**, 46.
99. K. Singh, Y. Kumar, P. Puri, M. Kumar and C. Sharma, *European Journal of Medicinal Chemistry*, 2012, **52**, 313.
100. O. A. El-Gammal, M. M. Bekheit and M. Tahoon, *Spectrochimica Acta Part A: Molecular and Biomolecular Spectroscopy*, 2015, **135**, 597.
101. V. Rakers, P. Cadinu, J. B. Edel and R. Vilar, *Chemical Science*, 2018, **9**, 3459.
102. X. Liu and J.-R. Hamon, *Coordination Chemistry Reviews*, 2019, **389**, 94.
103. S. S. A. Fathima, M. M. S. Meeran and E. R. Nagarajan, *Journal of Molecular Liquids*, 2019, **279**, 177.
104. V. R. Mishra, C. W. Ghanavatkar, S. N. Mali, H. K. Chaudhari and N. Sekar, *Journal of Biomolecular Structure and Dynamics*, 2019, 1.
105. R. Casasnovas, M. Adrover, J. Ortega-Castro, J. Frau, J. Donoso and F. Muñoz, *The Journal of Physical Chemistry B*, 2012, **116**, 10665.

Chapter 2

2 Literature review

This chapter is a review of the work previously done to tackle the biological problems in disease management and documented in the literature. It covers the core antimicrobial activity, shortfalls and the role of Schiff base ligands along with their corresponding complexes. Subsequently, the project rationale is stated.

2.1 Introduction

Microorganisms are of great importance in a balanced ecosystem, they are just as important as herbivores that feed on plants and the plants that harvest energy from the sun.[1,2] Microorganisms encompasses bacteria, fungi and yeasts that can be used in the production of food and beverages.[3-10] Some microorganisms are involved in a number of human biochemical pathways and can be used for medicinal purposes.[11-15] However, other microorganisms cause infectious diseases to the host cells.[16] For this reason, we look at the pharmaceutical management of diseases that are caused by microbes.

2.2 Biological application of approved drugs

An era of antibiotic discovery was a major turnaround in pharma-therapeutics. This ensured that diseases could be treated with success. Drug discovery is a lengthy and costly process that culminates in evaluative biological trials before the drug candidate can be approved for use. It starts from basic synthetic and evaluative (*in vitro* to *in vivo*) research in the academia and pharmaceutic industry. The process requires a huge amount of support funding and is usually lengthy and slow. However, evolution of pathogenic bacteria and the diseases they cause is usually complex and fast-paced. This creates a challenge in the effective management of such diseases and create a demand for new drugs that are more effective and at the same time have minimum side effects. Table 2.1 shows the antibacterial FDA approved drugs in a period of five years, *i.e.*, between the year 2011 and 2016.

Table 2.1: Drugs approved by the FDA from 2011 to 2016[17]

Drug	Indication	Company (year)
Avycaz (ceftazidime–avibactam)	For complicated intra-abdominal and urinary tract infections caused by *E. coli*, *K. pneumoniae*, *C. koseri*, *E. aerogenes*, *E. cloacae* and *P. aeruginosa*	Actavis (February 2015)
Dalvance (dalbavancin)	For acute bacterial skin and skin structure infections caused by *S. aureus* (methicillin resistant/susceptible strains), *S. pyogenes*, *S. agalactiae* and *S. anginosus*	Durata Therapeutics (May 2014)
Metronidazole 1.3% Vaginal Gel	For the treatment of bacterial vaginosis caused by anaerobic bacteria and protozoa	Actavis, Inc. (April 2014)
Orbactiv (oritavancin)	For acute bacterial skin and skin structure infections caused by *S. aureus* (including methicillin-susceptible/resistant isolates), *S. pyogenes, S. agalactiae, S. dysgalactiae, S. anginosus group* (including *S. anginosus, S. intermedius and S. constellatus*) *and E. faecalis*(vancomycin-susceptible isolates only).	The Medicines Company (August 2014)
Sivextro (tedizolid phosphate)	For acute bacterial skin and skin structure infections caused by *S. aureus* (including MRSA and methicillin-susceptible [MSSA] isolates), *S. pyogenes, S. agalactiae, S. anginosus* Group (including *S. anginosus, S. intermedius and S. constellatus*) and *E. faecalis.*	Cubist Pharmaceuticals (June 2014)
Sirturo (bedaquiline)	For multi-drug resistant tubercolosis	Janssen Therapeutics (December 2012)
Abthrax (raxibacumab)	For anthrax	GlaxoSmithKline (December 2012)
Dificid (fidaxomicin)	For *C. difficile*-associated diarrhoea	Optimer Pharmaceuticals (May 2011)

2.2.1 Selected antifungal agents that are currently in use

There is an increasing need for the development of better and new strategies in disease management.[18,19] An example illustrating this is amphotericin B (AmB), an approved antifungal drug. It is used to treat severe systemic fungal infections.[20-22] The AmB drug suffers numerous setbacks, such as toxicity. These include the renal dysfunction which can only be reversed upon discontinued use of the drug.[23-25] Even worse, AmB is carcinogenic.[20,22] Later on, azole-derived antimycotic agents such as fluconazole and itraconazole were developed. These proved to have reduced side effects.[26] The fluconazole and itraconazole (Figure 2.1(a) and (b), respectively) both contain the triazole functional groups. The triazole drugs are noncancerous since they have not shown to participate in DNA damage.

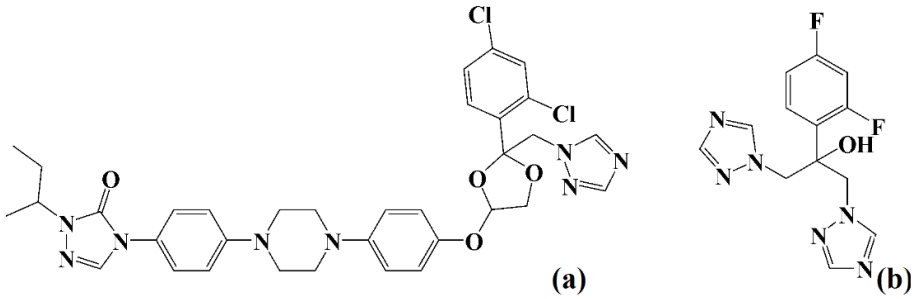

Figure 2.1: Structure of (a) itraconazole and (b) fluconazole compounds

Jonson *et al*.[21] compared the fungal susceptibility of voriconazole (Vfend) (Figure 2.2), AmB, itraconazole and fluconazole against several fungal yeasts extracted from different patients. The *in vitro* studies did not demonstrate any observed correlation nor distinct differences in activities between Vfend and AmB fungal treatments. Vfend and the itraconazole showed parallel antifungal activities against most yeasts, whilst Vfend surpasses the activities of fluconazole in both the biological potency and spectrum of activities.[21] Thus, Vfend is employed in serious fungal infections management, especially in patients with the impaired immune system. The triazole derivatives biological potency is not limited to the antifungal potency, but they have also shown the microbial (bacterial) inhibition.[27,28]

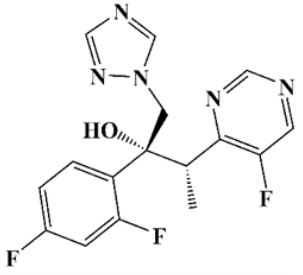

Figure 2.2: Structure of voriconazole (Vfend) compound

2.2.2 Selected antibacterial agents that are currently in use

Heterocyclic compounds have been used for different applications in material and biological sciences.[29,30] Heterocyclic compounds are also used in biochemical pathways as antimicrobial agents. Triazole and pyridine have versatile activities, owing their potency to the presence of their multifunctional groups.[30,31] Hence, the triazole derivatives have many biological applications because of their biochemical importance in protein binding stability. Holland-Nell *et al*.[32] demonstrated and explained that disulphide linked peptides stability can be enhanced by protein-triazole linkage.[32] This feature enabled their use as pesticides approved drugs. The improvement of the peptide structure is important in the design of novel antibacterial potential compounds.

The triazole compounds have been studied for the antibacterial properties and they are suitable candidates as antibacterial drugs. Angajala *et al*.[33] worked on triazole derivatives and compared the effects of triazole substituents based on their antibacterial activities. Generally, the triazole compounds with appended electron-withdrawing groups (EWGs), like NO_2 or Cl, showed superior antibacterial activities. This is not the case with the electron-donating group (EDG) substituted triazoles.[34] *Meta* EWG substituted triazoles have reasonable activities, while *para*-substituted benzyl or phenyl ring (Figure 2.3) showed a significant increase in the bactericidal activity. Furthermore, it was observed that the triazole derivatives demonstrated better activities towards the gram-positive bacteria. Particularly, towards the Methicillin-resistant *Staphylococcus aureus* (MRSA) bacteria.[33] However, the triazole compounds (Figure 2.3(a) and (b)) lacked a wide-spectrum of antibacterial activities.[33] This impedes their usage as suitable as antibacterial drugs.

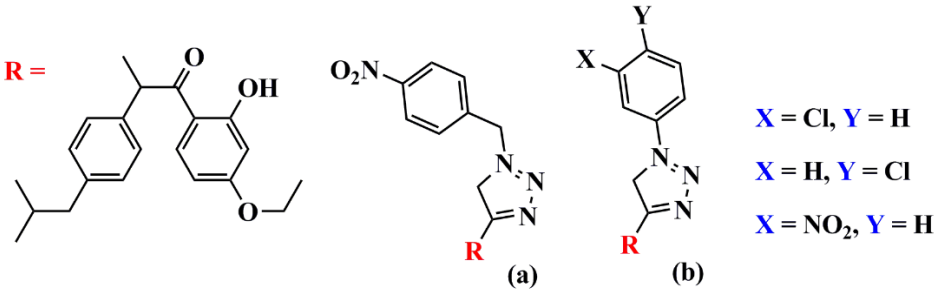

Figure 2.3: (R) primary backbone, (a) and (b) triazole antibacterial active compounds

It has been reported in the literature that the potency of organic compounds can be improved by the complexation, forming coordination complexes.[29] Thus, Murcia *et al*.[26] synthesised the triazole cobalt [Co(II)] and chromium [Cr(III)] complexes (Figure 2.4). The ligands along with their Co(II) and Cr(III) bidentate and tridentate coordinated complexes were investigated for their antibacterial activities against *Escherichia coli* (E coli), *Staphylococcus aureus* (*S. aureus*) and *Salmonella typhimurium* (*S. typhimurium*). Expectedly, the metal complexes were more biologically active compared to their free organic triazole ligands, while complexes (Figure 2.4(a-c)) showed greater activities. The *in vitro* assays of chromium complexes (Figure 2.4(d-f)) did not show activities against bacteria. It can be seen that the compounds with permanent dipole moment showed higher biological activities.[26]

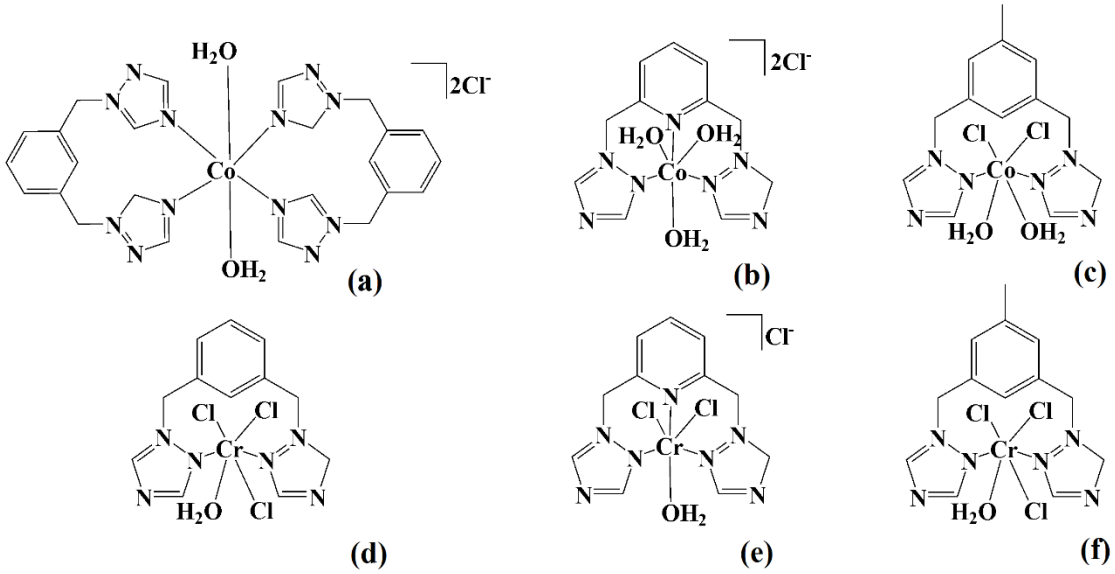

Figure 2.4: Chromium (a, b and c) and cobalt (d, e and f) triazole complexes

Singh *et al*.[35] investigated the Schiff bases (SBs) containing the triazole moiety complexes of cobalt, zinc, nickel and copper. The metal complexes exhibited a broad range of antibacterial activities against *S. aureus*, Bacillus subtilis (*B. subtilis*), *E. coli* and Pseudomonas aeruginosa (*P. aeruginosa*) test bacteria. This was explained by the reduction of metal centre polarity in the resulting complexes. The complexes generally showed a wide biological activity. Zn(II) complexes demonstrated greater activities and wide inhibition zones against tested bacteria compared with other metal centres.[35] Complex (Figure 2.5a) containing a single bidentate ligand showed better activities compared to complex (Figure 2.5b). In was concluded that the introduction of methyl substitution does not show any significant biological effects.

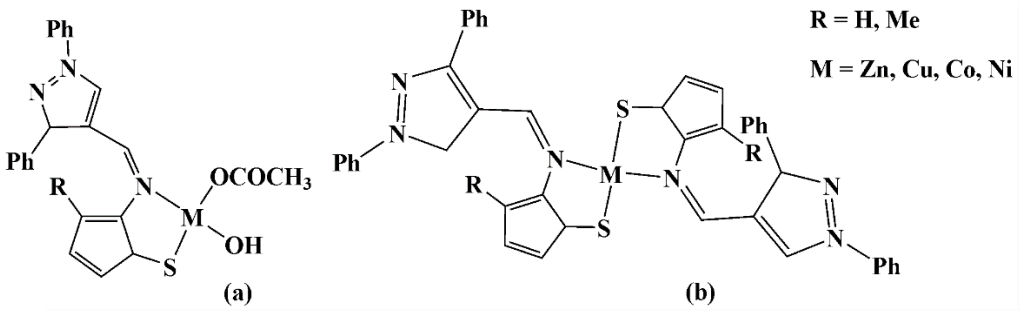

Figure 2.5: Schiff bases with triazole moiety complexes with cobalt, nickel, copper and zinc metal centres

2.2.3 Pyridinyl Schiff base complexes as antibacterial candidates

Alias *et al.*[36] studied the antibacterial potential of trithiocarbonate derivatives with the introduction of the biologically active azomethine functional group. Trithiocarbonate complexes containing *N*-, *O*- and, or *S*-donor atoms have showed different biological roles, *e.g.*, antibacterial roles.[36,37] The antibacterial activities reported by Alias *et al.*[36] were lower than that of the standard drug and this drove further design and synthesis of penicillin-based pyridinyl Schiff base by Chaudhary *et al.*[38] The pyridine moiety in the ligand backbone was introduced, bearing in mind that the heterocyclic aromatic moiety also affords advantages in the biological application qualities.[39] Complexes (Figure 2.6(a) and (b)) antibacterial activities were tested and showed improved activities in all Co(II), Ni(II) and Zn(II) complexes. The results postulated that the azomethine and pyridine moiety enhances the biological activity.[38]

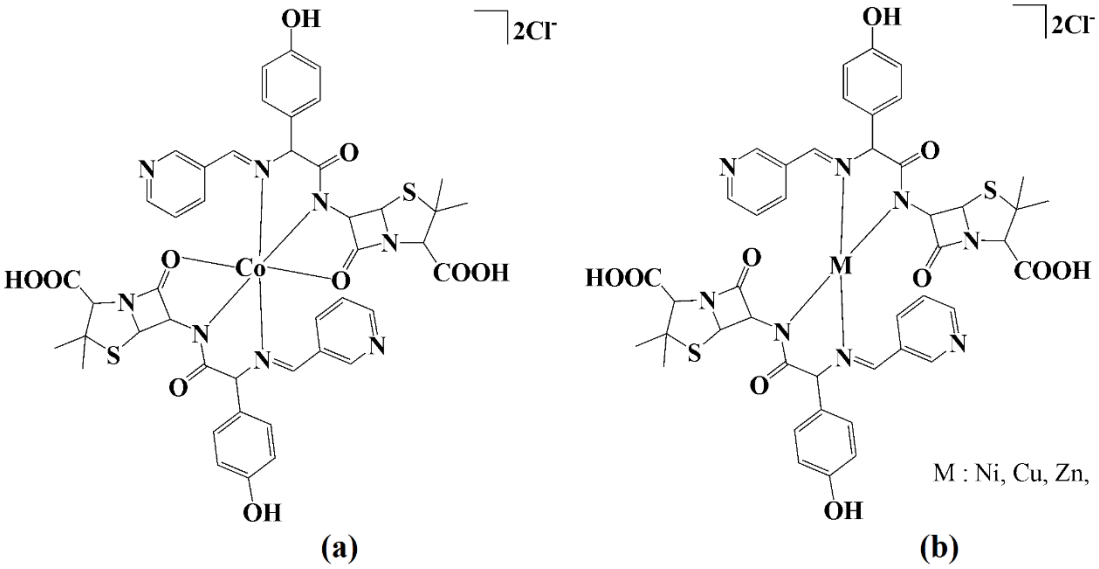

Figure 2.6: (a) Tri-coordinated Co(II); and (b) bi-coordinating Ni(II), Cu(II) and Zn(II) complexes

2.3 Schiff base ligands

Schiff base ligands have been studied for their antibacterial properties as well. SBs are sub-class of imine ligands with very stable coordinative behaviour.[40-42] SBs are versatile compounds that are synthesised from the condensation of aldehydes or ketones and amines.[43-45] Many imine-containing compounds of diverse structures can easily be synthesised by attaching different substituents to either of the precursors.[27,46-53] They have many important properties which includes antimicrobial.[27,48,50,54-57] An imine (C=N) functional group plays a role in many biochemical pathways by the provision of a biological active site within a molecule.[36,58,59] More importantly, SBs (imines) have high potency in disease management and are less toxic as they are readily incorporated within the system of an organism.[52] As SBs shown in Figure 2.7(a), (b) and (c), these ligands have multi-denticity, namely; mono/bi, tri and tetradentate ligands in the corresponding order.[60-64]

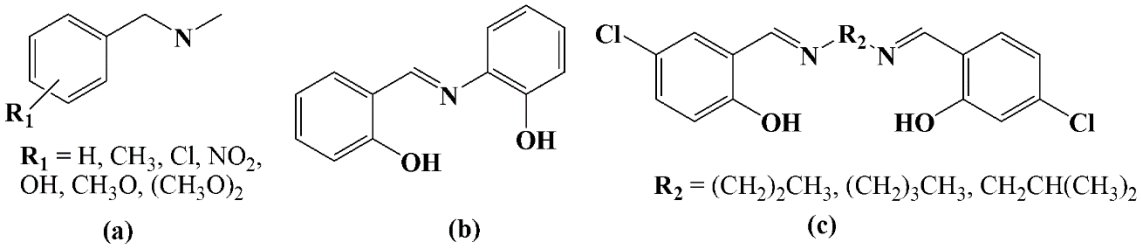

Figure 2.7: (a) Mono or bidentate, (b) tridentate and (c) tetradentate Schiff base ligands

Schiff base containing a pyridinyl moiety (Figure 2.8 (a) and (c)) are termed the pyridinyl Schiff bases (PSBs).[65] PSBs exhibit a broad range of biological activities, including antifungal, antibacterial, antimalarial, anti-inflammatory, antiviral, anticancer, antitubercolosis and antipyretic activities.[50,66] The examples of PSBs showing theses biological properties are shown in Figure 2.8.

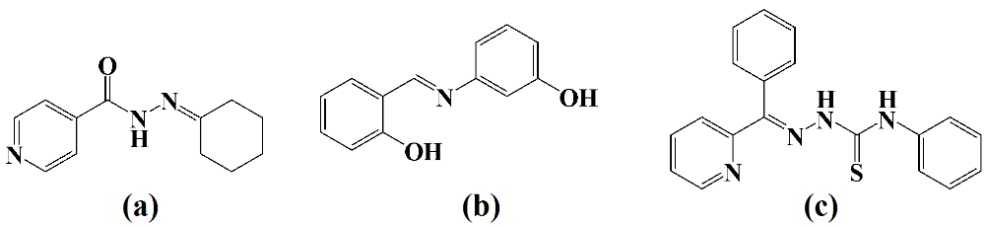

Figure 2.8: Schiff bases with (a) antitubercolosis, (b) antibacterial and (c) anticancer activity

The application of complexes considerably relies in the steric and electronic properties of the parent organic ligands.[67] Hence, varying the ligand backbone substituents provides the desired properties, suiting the needs for a specific application. PSBs and their corresponding complexes merit a great their attention.[68-70]

2.3.1 Pyridinyl Schiff base complexes

Complexes of PSBs are versatile, stable and have ease preparative accessibility. The SBs coordinate in most instance *via* the N_{imino} and N_{py} atoms.[71-73] The complexes also derive the bioactivity of the pyridinyl Schiff base.[74-76] Hence, the resulting complexes can have several coordination modes (Figure 2.9), *i.e.*, (a) metallocycle (mono-metallic) and (b) linear polymer (multi-metallic) and (c) discrete or bridged (multi-metallic) coordinated complexes.

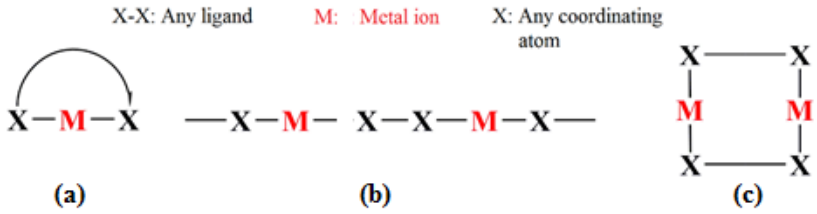

Figure 2.9: (a) Metallocycle, (b) linear and (c) discrete multinuclear coordination modes

The coordination mode of the metal centre is driven by different conditions. These conditions include the type of metal centre, counter ions, ligand structure and denticity, and also the π-π interaction of molecules within a sample. Furthermore, the nature of the solvent that is used in crystallisation or reaction, crystallisation technique and ratio of reagents during the synthesis reactions all determine the structural mode of a complex.[77,78] All the aforementioned conditions are responsible for both the physical and chemical properties of a resulting complex. Hence, manipulating any of the conditions can have a significant effect in the final complex. For instance, changing the nature of solvent from non-coordinating like THF to coordinating pyridine can affect the type of coordinated ligands, as pyridine can act as a ligand itself through oxidative addition or substitution. Discrete multinuclear bridged complexes are often more stable in solution compared to the metallocycle and linear complexes.[79] Hence, discrete multinuclear-bridged complexes can be applied in reactions that are in solution. Furthermore, these complexes form numerous structural derivatives. Thus, a library can be generated in the study of their coordination behaviour and biological aspects.

As previously mentioned, PSB ligands alone are biologically active. The introduction of a metal centre has been reported to form complexes with enhanced biological activities over their corresponding precursor ligands.[80,81] These biological activities include, but not limited to the antimicrobial application.[31,82-85] The Overtone's concept and the Tweedy's chelation theory have been proposed to account for the enhanced antimicrobial activities of complexes over their corresponding ligands.[26,35,86] Pyridinyl Schiff base ligand can form complexes with numerous metal ions and silver is one of those metal centres.[87]

2.3.2 Silver containing complexes

Silver(I) is the most stable oxidation state of silver ion. Silver(I) can support a coordination number of 2 – 6 to afford a number of geometries.[78] The Ag(I) centre can form trigonal, trigonal pyramidal, tetrahedral, square-planar and octahedral coordination geometries. The geometry around silver(I) metal centre plays a role in the activity of the resulting complex. Multinuclear complexes coordinated to the multidentate ligands generally form stable complexes with an increased number of active sites.[88] Silver complexes containing *N*-donor ligands readily form in aqueous solutions with high formation constants. Hence, they result in stable complexes with pyridinyl Schiff base ligands. The pyridine derivatives have been investigated for their medicinal purposes since they showed high potential of interesting properties, *i.e.*, as antimicrobial[89,90] and anticancer agents.[41,90-92]

2.3.3 Chemistry and application of silver containing complexes

The use of silver(I) for biological applications can be traced back to the 19th century, before an era of the antibiotics. They have once again regained attention as a viable treatment option for infections encountered in burns, open wounds and chronic ulcers.[93,94] Microbes have resistance tendency towards silver(I) as a heavy metal. However, the microorganisms that are resistant to silver(I), do not show any serious clinical problem.[95] Silver(I) Schiff base complexes are used in diverse applications including wound dressing to treat infections caused by microbes.[96] Silver(I) complexes have potential as new antimicrobial agents for clinical application,[97] since silver(I) does not show a significant toxicity in a living organism in minimal concentrations.[98]

The antimicrobial activity of a complex is greatly affected by the choice of the metal centre and the coordinated ligands.[96,99] Like other complexes, silver(I) Schiff base complexes have been reported with superior antibacterial activities over their organic ligands.[40,51] The complexes with exposed metal centre (Figure 2.10(a)) have greater activities in relation to those with saturated coordinated ligands (Figure 2.10(b1) and (b2)), regardless of the counter ion. Silver(I) complexes bactericidal activity is greatly influenced by two properties, the reactive oxygen species (ROS) induction capabilities and their cysteine thiol groups binding affinity. The results showed that complexes containing bio-essential elements like Cu(I) (Figure 2.10(c)) do not always show enhanced potency over metals like Ag(I) complexes (Figure 2.10(b2)). This could be explained by the tendency of cells to have elevated tolerance towards copper ions poisoning. This enables the microorganisms to effectively avoid protein poisoning and binding to copper complexes by a number of different mechanisms that are already established by the body cells.[100] Copper complexes will be discussed further in the following sections.

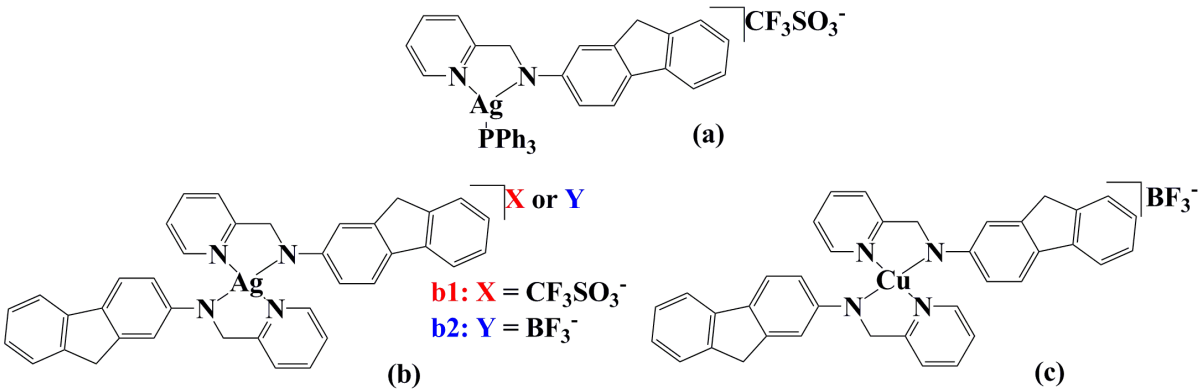

Figure 2.10: Complexes of (a) Ag(I) PPh_3, (b) Ag(I) and (c) Cu(I) structures

2.3.4 Copper containing complexes

Copper(I) or copper(II) form stable complexes with various Schiff base ligands *via* *N*-, *S*-, *O*-donor atoms. Copper Schiff base complexes play a role in a number of biochemical pathways in both human beings and microorganisms. The importance of Cu(I) and Cu(II) Schiff base complexes as antibacterial drug candidates will be discussed in the following sections.

2.3.5 Chemistry and application of copper containing complexes

Copper ions are bio-essential and their complexes that are involved in many cell survival biochemical reactions, including in the regular functioning of body cells.[100-103] Well-defined redox-active copper(I) complexes are potent efficient antioxidants, antimicrobials, antiparasitic and antitumor agents.[104] Their biological evaluation have shown fascinating properties as potential use in biological medication.

A number of Cu(I) and Cu(II) complexes have been evaluated for medicinal use in recent years. Examples with *S*-, *N*- and *O*- donor atoms are depicted in Figure 2.11. The efficient uptake of copper(I) Schiff base complexes in living cells has enabled the use of copper complexes in drug delivery as anticancer drug carriers. Copper(I) thiadiazole complexes have been investigated for pharmacological applications due to their good coordination behaviour and biological activities. They are used to inhibit the human immunodeficiency virus (HIV) and metastatic cancer cells.[105] The hydrazine copper(I) Schiff base complexes containing the *N*- or *O*-atom coordination have been found in certain biochemical reactions to improve the selectivity towards specific antitumour cells, since they behave like anticancer drug carriers within a systems.[106-108]

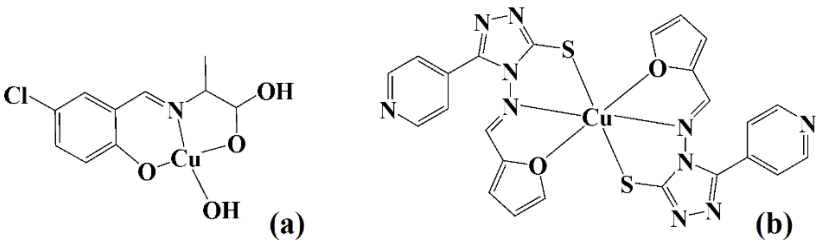

Figure 2.11: Structures of complexes (a) Cu(I) and (b) Cu(II) with medicinal potency

2.3.6 Copper(I) complexes

Copper(I) metals can participate in quite a number of biological functions as biological co-catalysts. The copper(I) pyridine Schiff base complexes interact with DNA to inhibit the spread of cancer.[109-111] Their pyridinyl Schiff base complexes are antibacterial active compounds and inhibits of the phosphomannose isomerase (PMI) enzyme. Thus, in the process disrupting the bacterial cell wall synthesis.[112] Copper(I) redox reactions are important for molecular oxygen-rich cells, as copper in return switches between +1 and +2 oxidation states.[113-116] Copper(I) pyridinyl Schiff base complexes are not stable and thus not so many reports have been

generated on their biological evaluations. The opposite can be said with copper(II) complexes as they form pretty stable complexes along with *N*-donor ligands.

2.3.7 Copper(II) complexes

Copper(II) complexes are relatively stable and have been extensively studied.[117] For example, Pitchunami *et al.*[118] reported a theoretical order of relative stability of M(II) chalcone-based Schiff base complexes to be Cu > Ni > Co > Zn. Thus, copper(II) complexes are good candidates for biological employment since they are less likely to degrade in harsh biological environment to form more toxic metabolites.[118] Copper(II) form stable complexes with PSBs that contain *N*-donor atoms as per Pearson's coordination theory (Table 2.2).[88] Numerous copper(II) pyridinyl Schiff base complexes have been synthesised and explored but the list is far from exhausting their structural activity studies. Copper(II) pyridinyl Schiff base complexes have shown various biological potency and their antimicrobial applications have also received quite a share of studies.[119]

Table 2.2: Pearson's Principle classification of some metal ions and donor atoms[88]

Hard Lewis acids	Borderline acids	Soft Lewis acids
H^+, Li^+, Na^+, K^+, Be^{2+}, Mg^{2+}, Ca^{2+}, Sr^{2+}, Sc^{3+}, Ti^{4+}, Zr^{4+}, Cr^{3+}, Al^{3+}, Ga^{3+}, La^{3+}, Gd^{3+}, Co^{3+}, Fe^{3+}	Fe^{2+}, Co^{2+}, Ni^{2+}, Cu^{2+}, Zn^{2+}, Pb^{2+}, Bi^{3+}, Rh^{3+}, Ir^{3+}	Cu^+, Au^+, Ag^+, Tl^+, Hg^+, Pd^{2+}, Cd^{2+}, Pt^{2+}, Hg^{2+}
Hard Lewis bases	**Borderline bases**	**Soft Lewis bases**
OH^-, H_2O, ROH, Cl^-, RO^-, R_2O, CH_3CO_2 -, NH_3, RNH_2, NH_2NH_2, CO_3^{2-}, NO_3^-, O^{2-}, SO_4^{2-}, PO_4^{3-}, ClO_4^-, F^-	NO_2^-, Br^-, N_3^-, N_2, $C_6H_5NH_2$, pyridine, imidazole	RSH, RS^-, R_2S, S_2^-, CN^-, RNC, CO, I^-, R_3As, R_3P, C_6H_5, C_2H_4, H_2S, HS^-, H^-

Mishra *et al.*[31] designed and tested antibacterial activity of a series of Cr(III), Co(II), Ni(II) and Cu(II) Schiff base complexes. The results of varying the metal centre showed that copper(II) and cobalt(II) complexes have appreciable antimicrobial activities.[31] However, the activity of these complexes require high concentration doses. Making these complexes bad candidates for antibacterial application. Ghosh *et al.*[80] tested the antibacterial activities of mono and binuclear copper(II) complexes with a potential $N_{imino}N_{py}SH$ tridentate pyridinyl Schiff base ligand (Figure 2.12(a)). As predicted by the Pearson theory, $N_{imino}N_{py}SH$ coordinates copper(II) as a bidentate through the *N*-atoms. In both cases, the imino group attacks the thiol group to form a benzothiazole ring in the process.

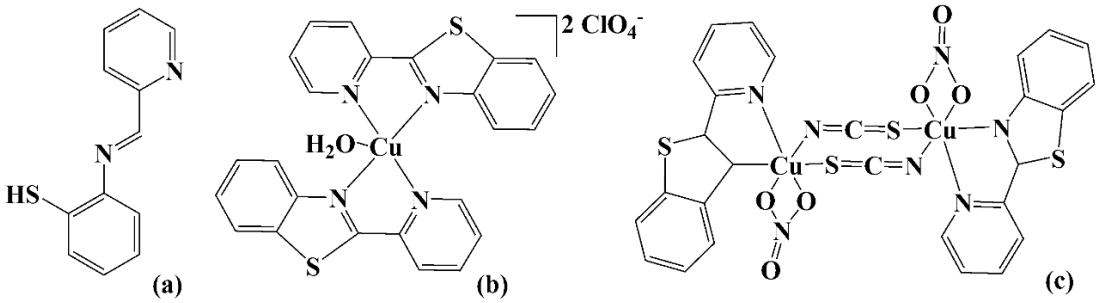

Figure 2.12: (a) Potential tridentate ligand (**L**), (b) Cu(II) $(\mathbf{L})_2$ and (c) (Cu(II) NCS NO_3 $\mathbf{L})_2$

The mononuclear formed a distorted square pyramidal geometry with spectator balancing perchlorate anions (Figure 2.12(b)), while the binuclear resulted in a thiocyanato-bridged species in which each copper(II) ion forms the distorted octahedral geometry with bidentate nitrate (NO_3^-) coordinated ligands (Figure 2.12(c)). The resulting complexes (Figure 2.12(b) and 2.12(c)) showed a wide-spectrum of antibacterial activities when tested against gram-negative and gram-positive bacteria. The mononuclear showed relatively higher antibacterial potency compared to the multinuclear complexes. This could be explained by the close engulfing of the metal centre by the binuclear complex, which lowered the activity of the complex. However, these complexes revealed higher MIC values.[80] It would be interesting to find out if there is any antibacterial potency enhancement, should one design the copper(II) complex with even more exposed metal centre, having a 1:1 metal to ligand ratio and non-coordinative anions. As these complexes have not been exhaustively investigated.

2.4 Literature summary

Researchers consider many coherent properties when designing structural compounds for an antibacterial application. In summary, for antibacterial evaluations, size, stability, solubility and substituted groups affects biochemistry of the ligand. However, there is no defined formula for a combination of factors that yields a ligand with high antibacterial activities. Nonetheless, the EDGs appended ligands are more active towards gram-negative bacteria while EWGs substituted ligands are more potent towards gram-positive bacteria. The solubility and stability of ligands favour antibacterial activities and usually show higher activities. The precursors carry over their attributes to a final complex. Small molecules can easily diffuse into the microbial outer membrane quite easily and are bacterial potent. The ligand biokinetics and choice of metal centre affects the antibacterial potency of a complex. At this point, even literature fails to pinpoint the best metal centre for best antibacterial results. Researchers opt for bio-essential metal ions, *i.e.* copper, with ligands that contain pyridinyl moieties.

2.5 Project rationale

PSBs have good stability, chelating properties and biological applications.[96,120] A great deal has been focused in PSBs complexes containing either or both the nitrogen and oxygen donor atom in their backbone structures.[85,120] Copper ions form very strong bonds with *N*-donor ligands as they form strong back bonding.[35,121-123] Among transition metal complexes, the activity of bio-essential and biocidal copper(I) and copper(II) complexes are usually ranked amongst the highest in various applications.[111,124,125] Surprisingly, with all the excitements and biological properties of copper, there is not even a single copper-based antibacterial approved drug that has been documented.[100] Many copper(II) pyridinyl Schiff base complexes have been documented. This is because they are stable and can be synthesised with ease. Copper(I) pyridinyl Schiff base complexes lack the stability along with PSBs. Thus, there is a gap in the study of biological studies of copper, especially copper(I) pyridinyl Schiff derivatives. The antibacterial drug shortfall and aforesaid reasons have led to a justified motive for the synthesis of copper(I) and copper(II) Schiff base complexes. The ligand substitutions on the phenyl ring was varied to establish their effects on antibacterial activity of complexes.

References

1. J. Barber, *Chemical Society Reviews*, 2009, **38**, 185.
2. H. Lambers, F. S. Chapin and T. L. Pons, in *Plant Physiological Ecology*, Springer New York, New York, NY, 2008, pp. 11.
3. M. Arici Muhammet, G. Ozulku, R. M. Yildirim, O. Sagdic and M. Z. Durak, *Food Science and Biotechnology*, 2018, **27**, 499.
4. A. Corsetti, M. Gobbetti, F. Balestrieri, F. Paoletti, L. Russi and J. Rossi, *Journal of Food Science*, 1998, **63**, 347.
5. K. Sigler, D. Matoulková, M. Dienstbier and P. Gabriel, *Applied Microbiology and Biotechnology*, 2009, **82**, 1027.
6. E. J. Pires, J. A. Teixeira, T. Brányik and A. A. Vicente, *Applied Microbiology and Biotechnology*, 2014, **98**, 1937.
7. J. J. Wang, W. N. Xu, X. E. Li, J. Li and Q. Li, *World Journal of Microbiology and Biotechnology*, 2014, **30**, 1901.
8. D. Smogrovicová, Z. Dömény, P. Gemeiner, A. Malovíková and E. Sturdík, *Biotechnology Techniques*, 1997, **11**, 261.
9. F. Kobayashi and S. Odake, *Food and Bioprocess Technology*, 2015, **8**, 1690.
10. F. F. Jacob, M. Hutzler and F. J. Methner, *European Food Research and Technology*, 2019, **245**, 95.
11. L. Flandroy, T. Poutahidis, G. Berg, G. Clarke, M. C. Dao, E. Decaestecker, E. Furman, T. Haahtela, S. Massart, H. Plovier, Y. Sanz and G. Rook, *Science of The Total Environment*, 2018, **627**, 1018.
12. V. Punj and A. Chakrabarty, *Cellular Microbiology*, 2003, **5**, 225.
13. S. F. Gilbert, J. Sapp and A. I. Tauber, *The Quarterly Review of Biology*, 2012, **87**, 325.
14. H. J. Flint, K. P. Scott, P. Louis and S. H. Duncan, *Nature Reviews Gastroenterology & Hepatology*, 2012, **9**, 577.
15. S. M. Jandhyala, R. Talukdar, C. Subramanyam, H. Vuyyuru, M. Sasikala and D. N. Reddy, *World Journal of Gastroenterology*, 2015, **21**, 8787.
16. C. Sharma, N. Rokana, M. Chandra, B. P. Singh, R. D. Gulhane, J. P. S. Gill, P. Ray, A. K. Puniya and H. Panwar, *Frontiers in Veterinary Science*, 2018, **4**, 237.
17. A. S. Chaudhary, *Acta Pharmaceutica Sinica B*, 2016, **6**, 552.
18. Neelima, K. Poonia, S. Siddiqui, M. Arshad and D. Kumar, *Spectrochimica Acta Part A: Molecular and Biomolecular Spectroscopy*, 2016, **155**, 146.

19. S. Yavuz and H. Yildirim, *Journal of Chemistry*, 2013, **2013**, 7.
20. R. S. Saturnino, N. M. Machado, J. C. Lopes and J. C. Nepomuceno, *Drug and Chemical Toxicology*, 2018, **41**, 9.
21. E. Johnson, A. Espinel-Ingroff, A. Szekely, H. Hockey and P. Troke, *International Journal of Antimicrobial Agents*, 2008, **32**, 511.
22. T. Lin, C. R. Chin, A. R. Everitt, S. Clare, J. M. Perreira, G. Savidis, A. M. Aker, S. P. John, D. Sarlah and E. M. Carreira, *Cell Reports*, 2013, **5**, 895.
23. A. C. O. Souza, A. L. Nascimento, N. M. de Vasconcelos, M. S. Jerônimo, I. M. Siqueira, L. R-Santos, D. O. S. Cintra, L. L. Fuscaldi, O. R. Pires Júnior, R. Titze-de-Almeida, M. F. Borin, S. N. Báo, O. P. Martins, V. N. Cardoso, S. O. Fernandes, M. R. Mortari, A. C. Tedesco, A. C. Amaral, M. S. S. Felipe and A. L. Bocca, *European Journal of Medicinal Chemistry*, 2015, **95**, 267.
24. A. Ahmad, Y. Wei, F. Syed, S. Khan, G. M. Khan, K. Tahir, A. U. Khan, M. Raza, F. U. Khan and Q. Yuan, *Journal of Photochemistry and Photobiology B: Biology*, 2016, **161**, 17.
25. P. M. Peçanha, S. de Souza, A. Falqueto, T. R. Grão-Veloso, L. V. Lírio, C. U. G. Ferreira, A. R. Santos, H. G. Costa, L. R. M. de Souza and F. F. Tuon, *International Journal of Antimicrobial Agents*, 2016, **48**, 428.
26. R. Murcia, S. Leal, M. Roa, E. Nagles, A. Muñoz-Castro and J. Hurtado, *Molecules*, 2018, **23**, 2013.
27. M. M. Abd-Elzaher, A. A. Labib, H. A. Mousa, S. A. Moustafa, M. M. Ali and A. A. El-Rashedy, *Beni-Suef University Journal of Basic and Applied Sciences*, 2016, **5**, 85.
28. M. Shaikh, D. Wagare, M. Farooqui and A. Durrani, *Polycyclic Aromatic Compounds*, 2019, **39**, 1.
29. S. H. Sumrra, A. Suleman, Z. H. Chohan, M. N. Zafar, M. A. Raza and T. Iqbal, *Russian Journal of General Chemistry*, 2017, **87**, 1281.
30. N. Kaur, *Synthetic Communications*, 2015, **45**, 539.
31. A. P. Mishra and R. K. Jain, *Journal of Saudi Chemical Society*, 2014, **18**, 814.
32. K. Holland-Nell and M. Meldal, *Angewandte Chemie International Edition*, 2011, **50**, 5204.
33. K. K. Angajala, S. Vianala, R. Macha, M. Raghavender, M. K. Thupurani and P. J. Pathi, *SpringerPlus*, 2016, **5**, 423.

34. V. Bhardwaj, D. Gumber, V. Abbot, S. Dhiman and P. Sharma, *RSC Advances*, 2015, **5**, 15233.
35. K. Singh, Y. Kumar, P. Puri, M. Kumar and C. Sharma, *European Journal of Medicinal Chemistry*, 2012, **52**, 313.
36. M. Alias, H. Kassum and C. Shakir, *Journal of the Association of Arab Universities for Basic and Applied Sciences*, 2014, **15**, 28.
37. M. Rizzotto, in *A Search for Antibacterial Agents*, IntechOpen, 2012.
38. N. K. Chaudhary and P. Mishra, *Bioinorganic Chemistry and Applications*, 2017, **2017**, 6927675.
39. B. Koley Seth, A. Ray, A. Saha, P. Saha and S. Basu, *Journal of Photochemistry and Photobiology B: Biology*, 2014, **132**, 72.
40. M. A. Malik, O. A. Dar, P. Gull, M. Y. Wani and A. A. Hashmi, *Medicinal Chemistry Communications*, 2018, **9**, 409.
41. L. H. Abdel-Rahman, N. M. Ismail, M. Ismael, A. M. Abu-Dief and A. E. Abdel-Hameed, *Journal of Molecular Structure*, 2017, **1134**, 851.
42. N. G. Khaligh, H. S. Abbo and S. J. J. Titinchi, *Research on Chemical Intermediates*, 2017, **43**, 901.
43. V. Rosar, D. Dedeic, T. Nobile, F. Fini, G. Balducci, E. Alessio, C. Carfagna and B. Milani, *Dalton Transactions*, 2016, **45**, 14609.
44. G. Pampaloni, M. Guelfi, A. Sommazzi, G. Leone, F. Masi, S. Zacchini and G. Ricci, *Inorganica Chimica Acta*, 2019, **487**, 331.
45. N. S. Radulović, A. B. Miltojević and R. D. Vukićević, *Comptes Rendus Chimie*, 2013, **16**, 257.
46. A. G. Atanasov, B. Waltenberger, E. M. Pferschy-Wenzig, T. Linder, C. Wawrosch, P. Uhrin, V. Temml, L. Wang, S. Schwaiger, E. H. Heiss, J. M. Rollinger, D. Schuster, J. M. Breuss, V. Bochkov, M. D. Mihovilovic, B. Kopp, R. Bauer, V. M. Dirsch and H. Stuppner, *Biotechnology Advances*, 2015, **33**, 1582.
47. C. Wang, N. Xing, W. Feng, S. Guo, M. Liu, Y. Xu and Z. You, *Inorganica Chimica Acta*, 2019, **486**, 625.
48. M. Sivasankaran Nair, D. Arish and J. Johnson, *Journal of Saudi Chemical Society*, 2016, **20**, S591.
49. M. Cindrić, G. Pavlović, R. Katava and D. Agustin, *New Journal of Chemistry*, 2017, **41**, 594.

50. M. T. Kaczmarek, M. Zabiszak, M. Nowak and R. Jastrzab, *Coordination Chemistry Reviews*, 2018, **370**, 42.
51. R. V. Singh, P. Chaudhary, S. Chauhan and M. Swami, *Spectrochimica Acta Part A: Molecular and Biomolecular Spectroscopy*, 2009, **72**, 260.
52. G. Y. Nagesh and B. H. M. Mruthyunjayaswamy, *Journal of Molecular Structure*, 2015, **1085**, 198.
53. M. Salehi, F. Rahimifar, M. Kubicki and A. Asadi, *Inorganica Chimica Acta*, 2016, **443**, 28.
54. A. M. Abu-Dief and I. M. A. Mohamed, *Beni-Suef University Journal of Basic and Applied Sciences*, 2015, **4**, 119.
55. G. Nagesh and B. Mruthyunjayaswamy, *Journal of Molecular Structure*, 2015, **1085**, 198.
56. B. Ž. Jovanović, M. Mišić-Vuković, A. D. Marinković and V. Vajs, *Journal of Molecular Structure*, 1999, **482**, 375.
57. C. M. Da Silva, D. L. da Silva, L. V. Modolo, R. B. Alves, M. A. de Resende, C. V. Martins and Â. de Fátima, *Journal of Advanced Research*, 2011, **2**, 1.
58. K. Poonia, S. Siddiqui, M. Arshad and D. Kumar, *Spectrochimica Acta Part A: Molecular and Biomolecular Spectroscopy*, 2016, **155**, 146.
59. G. Yadav and J. V. Mani, *International Journal of Science and Research*, 2015, **4**, 121.
60. A. A. Abdulkarem, *Journal of Biophysical Chemistry*, 2017, **8**, 13.
61. E. Gungor, S. Celen, D. Azaz and H. Kara, *Spectrochimica Acta Part A: Molecular and Biomolecular Spectroscopy*, 2012, **94**, 216.
62. C. Camp, J. Andrez, J. Pécaut and M. Mazzanti, *Inorganic chemistry*, 2013, **52**, 7078.
63. A. Brink, H. G. Visser and A. Roodt, *Inorganic Chemistry*, 2014, **53**, 12480.
64. M. Amini, *Journal of Coordination Chemistry*, 2010, **63**, 3849.
65. A. Gencer Imer, R. H. B. Syan, M. Gülcan, Y. S. Ocak and A. Tombak, *Journal of Materials Science: Materials in Electronics*, 2018, **29**, 898.
66. S. G. Nayak and B. Poojary, *Heliyon*, 2019, **5**, e02318.
67. W. Al Zoubi, A. A. S. Al-Hamdani and M. Kaseem, *Applied Organometallic Chemistry*, 2016, **30**, 810.
68. J. L. Sebat, A. J. Paszczynski, M. S. Cortese and R. L. Crawford, *Applied and Environmental Microbiology*, 2001, **67**, 3934.

69. V. Bhardwaj, M. N. Noolvi, S. Jalhan and H. M. Patel, *Journal of Saudi Chemical Society*, 2016, **20**, 406.
70. N. B. Patel, S. N. Agravat and F. M. Shaikh, *Medicinal Chemistry Research*, 2011, **20**, 1033.
71. M. Rezaeivala and H. Keypour, *Coordination Chemistry Reviews*, 2014, **280**, 203.
72. A. A. Khandar, F. A. Afkhami, S. A. Hosseini-Yazdi, J. M. White, S. Kassel, W. G. Dougherty, J. Lipkowski, D. Van Derveer, G. Giester and F. Costantino, *Inorganica Chimica Acta*, 2015, **427**, 87.
73. T. Baran, I. Sargin, M. Kaya and A. Menteş, *Carbohydrate Polymers*, 2016, **152**, 181.
74. C. Valente, S. Calimsiz, K. H. Hoi, D. Mallik, M. Sayah and M. G. Organ, *Angewandte Chemie International Edition*, 2012, **51**, 3314.
75. Z. Uyar, D. Erdener, İ. Koyuncu and Ü. Arslan, *Journal of the Turkish Chemical Society, Section A: Chemistry*, 2017, **4**, 963.
76. P. R. Reddy and A. Shilpa, *Chemistry & biodiversity*, 2012, **9**, 2262.
77. H. He, L. Hashemi, M. L. Hu and A. Morsali, *Coordination Chemistry Reviews*, 2018, **376**, 319.
78. E. M. Njogu, B. Omondi and V. O. Nyamori, *Journal of Coordination Chemistry*, 2015, **68**, 3389.
79. D. Palomas, C. Kalamaras, P. Haycock, A. J. White, K. Hellgardt, A. Horton and M. R. Crimmin, *Catalysis Science & Technology*, 2015, **5**, 4108.
80. M. Ghosh, M. Layek, M. Fleck, R. Saha and D. Bandyopadhyay, *Polyhedron*, 2015, **85**, 312.
81. C. Chen, J. Zhang, Y. Zhang, Z. Yang, H. Wu, G. Pan and Y. Bai, *Journal of Coordination Chemistry*, 2015, **68**, 1054.
82. S. Zabin, M. Jammali and A. Alzahrani, *Journal of Organic and Inorganic Chemistry*, 2018, **4**, 6.
83. A. A. Abou-Hussein and W. Linert, *Spectrochimica Acta Part A: Molecular and Biomolecular Spectroscopy*, 2014, **117**, 763.
84. O. G. Idemudia, A. P. Sadimenko, A. J. Afolayan and E. C. Hosten, *Bioinorganic Chemistry and Applications*, 2015, **2015**, 14.
85. K. Buldurun, N. Turan, A. Savcı and N. Çolak, *Journal of Saudi Chemical Society*, 2019, **23**, 205.

86. O. A. El-Gammal, M. M. Bekheit and M. Tahoon, *Spectrochimica Acta Part A: Molecular and Biomolecular Spectroscopy*, 2015, **135**, 597.
87. I. P. Ejidike and P. A. Ajibade, *Bioinorganic Chemistry and Applications*, 2015, **2015**, 890734.
88. K. L. Haas and K. J. Franz, *Chemical Reviews*, 2009, **109**, 4921.
89. A. Lapasam, L. Dkhar, N. Joshi, K. M. Poluri and M. R. Kollipara, *Inorganica Chimica Acta*, 2019, **484**, 255.
90. M. Aidi, H. Keypour, A. Shooshtari, M. Mahmoudabadi, M. Bayat, Z. Ahmadvand, R. Karamian, M. Asadbegy, S. Tavatli and R. W. Gable, *Polyhedron*, 2019, **167**, 93.
91. A. S. Abd El-All, S. A. Osman, H. M. F. Roaiah, M. M. Abdalla, A. A. Abd El Aty and W. H. AbdEl-Hady, *Medicinal Chemistry Research*, 2015, **24**, 4093.
92. A. G. Blackman, *Polyhedron*, 2005, **24**, 1.
93. K. A. Ali, M. M. Abd-Elzaher and K. Mahmoud, *International Journal of Medicinal Chemistry*, 2013, **2013**, 7.
94. M. A. M. Abu-Youssef, R. Dey, Y. Gohar, A. A. Massoud, L. Öhrström and V. Langer, *Inorganic Chemistry*, 2007, **46**, 5893.
95. Y. Wang, X. Ding, Y. Chen, M. Guo, Y. Zhang, X. Guo and H. Gu, *Biomaterials*, 2016, **101**, 207.
96. A. Orabi, K. A. El-Nour, M. Youssef and H. Salem, *Arabian Journal of Chemistry*, 2018, In Press.
97. J. B. Wright, K. Lam and R. E. Burrell, *American Journal of Infection Control*, 1998, **26**, 572.
98. M. McCann, R. Curran, M. Ben-Shoshan, V. McKee, A. A. Tahir, M. Devereux, K. Kavanagh, B. S. Creaven and A. Kellett, *Dalton Transactions*, 2012, **41**, 6516.
99. M. N. Patel, H. N. Joshi and C. R. Patel, *Spectrochimica Acta Part A: Molecular and Biomolecular Spectroscopy*, 2013, **104**, 48.
100. O. L. Cifuentes-Vaca, J. Andrades-Lagos, J. Campanini-Salinas, A. Laguna, D. Vásquez-Velásquez and M. Concepción Gimeno, *Inorganica Chimica Acta*, 2019, **489**, 275.
101. R. A. Festa and D. J. Thiele, *Current Biology*, 2011, **21**, R877.
102. R. Hazra and G. K. Siberry, *Journal of the Pediatric Infectious Diseases Society*, 2014, **3**, S1.

103. S. Medici, M. Peana, V. M. Nurchi, J. I. Lachowicz, G. Crisponi and M. A. Zoroddu, *Coordination Chemistry Reviews*, 2015, **284**, 329.
104. S. Kathiresan, S. Mugesh, J. Annaraj and M. Murugan, *New Journal of Chemistry*, 2017, **41**, 1267.
105. M. Alias, H. Kassum and C. Shakir, *Journal of the Association of Arab Universities for Basic and Applied Sciences*, 2014, **15**, 28.
106. S. Y. Ebrahimipour, I. Sheikhshoaie, J. Castro, W. Haase, M. Mohamadi, S. Foro, M. Sheikhshoaie and S. Esmaeili-Mahani, *Inorganica Chimica Acta*, 2015, **430**, 245.
107. A. Li, Y. H. Liu, L. Z. Yuan, Z. Y. Ma, C. L. Zhao, C. Z. Xie, W. G. Bao and J. Y. Xu, *Journal of Inorganic Biochemistry*, 2015, **146**, 52.
108. P. Tyagi, S. Chandra, B. S. Saraswat and D. Yadav, *Spectrochimica Acta Part A: Molecular and Biomolecular Spectroscopy*, 2015, **145**, 155.
109. M. Barwiolek, E. Szlyk, A. Berg, A. Wojtczak, T. Muziol and J. Jezierska, *Dalton Transactions*, 2014, **43**, 9924.
110. N. Daneshvar, A. A. Entezami, A. A. Khandar and L. A. Saghatforoush, *Polyhedron*, 2003, **22**, 1437.
111. T. J. Khoo, M. K. b. Break, K. A. Crouse, M. I. M. Tahir, A. M. Ali, A. R. Cowley, D. J. Watkin and M. T. H. Tarafder, *Inorganica Chimica Acta*, 2014, **413**, 68.
112. A. S. Abu-Khadra, R. S. Farag and A. E. M. Abdel-Hady, *American Journal of Analytical Chemistry*, 2016, **7**, 1.
113. S. Tardito and L. Marchio, *Current Medicinal Chemistry*, 2009, **16**, 1325.
114. C. Marzano, M. Pellei, F. Tisato and C. Santini, *Anti-Cancer Agents in Medicinal Chemistry (Formerly Current Medicinal Chemistry-Anti-Cancer Agents)*, 2009, **9**, 185.
115. Y. Zhang, J. Fan, B. Yang and L. Ma, *Chemical Engineering Journal*, 2017, **326**, 612.
116. J. L. Rowland and M. Niederweis, *Tuberculosis*, 2012, **92**, 202.
117. P. Chakraborty, S. Purkait, S. Mondal, A. Bauzá, A. Frontera, C. Massera and D. Das, *Crystal Engineering Communications*, 2015, **17**, 4680.
118. C. Pitchumani Violet Mary, R. Shankar and S. Vijayakumar, *Molecular Simulation*, 2019, **45**, 1.
119. N. Raman, A. Kulandaisamy, C. Thangaraja, P. Manisankar, S. Viswanathan and C. Vedhi, *Transition Metal Chemistry*, 2004, **29**, 129.
120. J. L. Segura, M. J. Mancheno and F. Zamora, *Chemical Society Reviews*, 2016, **45**, 5635.

121. M. Akbar Ali and M. T. H. Tarafdar, *Journal of Inorganic and Nuclear Chemistry*, 1977, **39**, 1785.
122. A. Kourtellaris, E. E. Moushi, I. Spanopoulos, C. Tampaxis, G. Charalambopoulou, T. A. Steriotis, G. S. Papaefstathiou, P. N. Trikalitis and A. J. Tasiopoulos, *Inorganic Chemistry Frontiers*, 2016, **3**, 1527.
123. Y. Ji, B. Xu, W. Gong, X. Zhang, X. Jin, W. Ning, Y. Meng, W. Yang and Y. Chen, *Journal of the Taiwan Institute of Chemical Engineers*, 2016, **66**, 301.
124. J. R. Anacona and I. Osorio, *Transition Metal Chemistry*, 2008, **33**, 517.
125. A. Pizzi, *Annals of Forest Science*, 2016, **73**, 185.

Chapter 3

3 Experimental

This chapter reports the experimental procedures for the ligand and complex synthesis, characterisation and biological studies. The ligands were synthesised by employing the solvent-free grinding and microwave-assisted techniques. Synthesis of the Cu(I) and Cu(II) complexes was carried out through two conventional methods. The first was a two-stage involving the synthesis of ligands followed by their complexation to Cu(I) and Cu(II) while the second was a one-pot synthesis where precursors of the Schiff base ligands and the Cu(II) salt were directly reacted. The instrumentation and reagents employed in the project are also stated.

3.1 Materials

All commercial reagents were used without prior purification, except for the ethanol solvent and aniline reagent. Ethanol was dried using a slight modified magnesium turnings distillation[1], while aniline was purified by distillation. The other reagents and solvents used for this project were purchased from Sigma Aldrich (USA) and Merck (Germany) through their local suppliers. These chemicals were; deuterated chloroform (≥99.8%), deuterated dimethyl sulfoxide (≥99.8%), ethanol (≥99.8%), tetrahydrofuran (≥99.9%), diethyl ether (crude), dichloromethane (crude), hexane (crude), aniline (98%), 3-nitroaniline (≥99%), 2.6-dichloroaniline (≥98%), 2.6-dimethylaniline (99%), 4-bromo-2.6-dichloroaniline (97%), 2,4,6-tri-*tert*-butylaniline (99%), 2-acetylpyridine (≥99%), pyridine-3-carboxaldehyde (98%), pyridine-2-carboxyaldehyde (99%), pyridine-4-carboxyaldehyde (97%), pyridine (≥99%), quinoline-2-carboxaldehyde (97%), acetonitrile (≥99.93%), copper(I) chloride (≥90%), copper(II) chloride (99.99%) and argon gas, 5.0 technical grade (Airflex Industrial Gases, South Africa).

3.2 Instrumentation

All the ^{1}H-NMR and ^{13}C-NMR spectra were recorded on BRUKER 400 MHz and BRUKER 600 MHz spectrometers in DMSO–d_6 or $CDCl_3$. The ^{1}H-NMR chemical shifts are reported in parts per million (ppm) relative to the DMSO-d_6, δ = 2.5 ppm or $CDCl_3$, δ = 7.2 ppm respective residual peaks. Multiplicities are given as singlet (*s*), doublet (*d*) or triplet (*t*), while the coupling constants, *J*, are given in hertz (Hz). Infrared data is reported as percentage

transmittances at given wavenumbers between 4000 and 350 cm^{-1} and was recorded using a PerkinElmer 100 FT-IR spectrometer. High- and low-resolution electrospray ionization (ESI) mass spectrometry spectra were recorded using a Waters Micromass LCT Premier TOF-MS instrument with only molecular ions (M^+) and major fragmentation peaks being reported with intensities quoted as percentage of the respective base peak isotope. UV–Vis spectra were recorded on a Shimadzu UV-Vis spectrophotometer (UV-3600), in acetonitrile with 190 nm UV cut-off. All melting points (m.p) and melting point decompositions ($m.p_{dec}$)were determined using a Stuart Scientific melting point apparatus (SMP10) in open capillaries, or unless stated otherwise, where a TA Instruments Q series^{TM} thermal analysis instrument (DSC/TGA (SDT-Q600)) was applied. A Thermoscientific Flash 2000 elemental analyser (CNH) was used for elemental analysis. The single-crystal structures were obtained using the Bruker SMART APEXII diffractometer.

3.3 Solvent-free grinding synthesis of ligands

The Schiff base ligands were synthesised by manually grinding aniline and a corresponding pyridinyl aldehyde precursor, using mortar and pestle with a 1:1.1 (aldehyde to amine) stoichiometric ratio.[2] Solvent-free grinding for three minutes afforded yellow (in most cases) or white fine powders (**L6**, **L7**, **L8**, **L9**, **L10**, **L13** and **L14**). Ligand (**L4**) formed a paste, which was dried under vacuum to obtain powder.[3] Ligands, **L1**, **L2**, **L5**, **L11** and **L12** were obtained as oils, while **L3** was initially obtained as oil which was solidified by the aid of liquid nitrogen under reduced pressure Schlenk line apparatus. Thin layer chromatography (TLC) was used to confirm the reaction completion and purity along with the melting point determinations. Thereafter, followed by ligand purification by washing off excess aniline impurities.

3.3.1 (*E*)-2,6-dimethyl-*N*-(pyridin-4-ylmethylene)aniline, ligand (L1)

L1 was prepared using 2,6-dimethylaniline (0.56 mL, 4.723 mmol) and pyridine-4-carboxyaldehyde (0.44 mL, 4.671 mmol). The reaction afforded a yellow oil after three minutes. Yield 0.90 mL, 94%. FT-IR (cm^{-1}): 2907 (C–H), 1640 (C=N), 1470 (C=C). ^{1}H-NMR (400 MHz, $CDCL_3$-*d1*, δ ppm): 8.71 (2H, d, *J* =4.20 Hz Ha-C_5H_4N), 8.14 (1H, s, HC=N), 7.69 (2H, d, *J* = 5.80 Hz, Hc-C_5H_4N), 7.01 (2H, d, *J* = 7.52 Hd-C_6H_3), 6.92 (1H, t, *J* = 6.92 Hz, He-C_6H_3), 2.07 (6H, t, CH_3). ^{13}C-NMR (400 MHz, DMSO-*d6*, δ ppm): 161.12 (N=C), 150.26

(Cb-C_5H_4N), 150.14 (Cc-C_6H_3), 145.34 (Cd-C_5H_4N), 130.90 (Ce-C_6H_3), 129.31 (Cf-C_6H_3) 128.72 (Cg-C_6H_3), 121.22 (Ch-C_5H_4N), 19.27 (Ci-CH_3). UV-vis (CH_3CN): λ_{max} 200, 231 nm.

3.3.2 (*E*)-2,6-dimethyl-*N*-(pyridin-2-ylmethylene)aniline, ligand (L2)

L2 was prepared using 2,6-dimethylaniline (0.47 mL, 3.963 mmol) and pyridine-2-carboxyaldehyde (0.35 mL, 3.679 mmol). The reaction afforded a yellow oil after three minutes. Yield 0.72 mL, 95%, FT-IR (cm^{-1}): 3053 (C–H), 1638 (C=N), 1469 (C=C). ^{1}H-NMR (400 MHz, $CDCl_3$-*d1*, δ ppm): 8.66 (1H, d, *J* = 5.12 Hz Ha-C_5H_4N), 8.31 (1H, s, HC=N), 8.23 (1H, d, *J* = 7.84 Hz, Hc-C_5H_4N), 7.78 (1H, t, *J* = 6.20 Hd-C_5H_4N), 7.34 (1H, t, *J* = 3.84 Hz, He-C_5H_4N), 7.03 (2H, d, *J* = 7.52 Hz, Hf-C_6H_5), 6.92 (1H, t, *J* = 7.76 Hz, Hg-C_6H_5), 2.12 (1H, t, Hz, Hh-CH_3). ^{13}C-NMR (400 MHz, DMSO-d6, δ ppm): 152.21 (N=C), 149.05 (Cb-Cc-C_5H_4N), 149.01 (Cd-C_6H_3), 136.85 (Ce-C_5H_4N), 136.89 (Cf-C_5H_4N), 130.32 (Cg-C_6H_3) 128.75 (Ch-C_5H_3), 127.61 (Ci-C_6H_3), 127.60 (Cj-C_5H_4N), 19.12 (Ck-CH_3). UV-vis (CH_3CN): λ_{max} 238, 271 nm.

3.3.3 (*E*)-*N*-(pyridine-2-ylmethylene)aniline, ligand (L3)

L3 was prepared using aniline (0.44 mL, 4.819 mmol) and pyridine-2-carboxyaldehyde (0.45 mL, 4.731 mmol) as starting material. The reaction provided a brown oil after three minutes. The product was dried under reduced pressure for two hours to form a brown crystalline solid. Yield 0.8017 g, 93%, m.p 35 – 36 ºC. FT-IR (cm^{-1}): 3053 (C–H), 1627 (C=N), 1591 (C=C). ^{1}H-NMR (400 MHz, DMSO-*d6*, δ ppm): 8.71 (1H, d, *J* = 4.76 Hz Ha-C_5H_4N), 8.59 (1H, s, HC=N), 8.15 (1H, d, *J* = 7.88 Hz, Hc-C_5H_4N), 7.93 (1H, t, *J* = 6.64 Hd-C_5H_4N), 7.51 (1H, t, *J* = 5.08 Hz, He-C_5H_4N), 7.43 (2H, d, *J* = 7.64 Hz, Hf-C_6H_5), 7.32 (2H, d, *J* = 7.60 Hz, Hg-C_6H_5), 7.28 (1H, t, 7.32 Hz, Hh-C_6H_5). ^{13}C-NMR (400 MHz, DMSO-d6, δ ppm): 160.70 (N=C), 154.09 (Cb-C_5H_4N), 150.55 (Cc-C_5H_4N), 149.61 (Cd-C_5H_4N), 137.05 (Ce-C_5H_4N), 129.29 (Cf-C_6H_4) 126.72 (Cg-C_5H_4N), 125.60 (Ch-C_6H_4), 121.29 (Ci-C_5H_4N), 121.10 (Cj-C_5H_4). UV-vis (CH_3CN): λ_{max} 230, 283 nm.

3.3.4 (*E*)-2,6-dichloro-*N*-(pyridin-2-ylmethylene)aniline, ligand (L4)

L4 was prepared using 2,6-dichloroaniline (0.4901 g, 3.025 mmol) and pyridine-2-carboxyaldehyde (0.28 mL, 2.944 mmol). The reaction yielded a yellow oil after three minutes. The product was dried under reduced pressure for two hours to form a yellow solid. Yield 0.6949 g, 94%, m.p 119 – 121 ºC. FT-IR (cm^{-1}): 3056 (C–H), 1643 (C=N), 1469 (C=C). ^{1}H-

NMR (400 MHz, $CDCl_3$-*d1*, δ ppm): 8.78 (1H, s, HC=N) , 7.45 (1H, d, *J* = 3.48 Hz Hb-C_5H_4N), 6.63 (1H, d, *J* = 8.80 Hz, Hc-C_5H_4N), 6.54 (1H, t, *J* = 7.32 Hd-C_5H_4N), 6.19 (1H, t, *J* = 4.88 Hz, He-C_5H_4N), 5.83 (2H, t, *J* = 8.04 Hz, Hf-C_6H_3), 5.27 (1H, t, *J* = 16.0 Hz, Hg-C_6H_3). ^{13}C-NMR (400 MHz, DMSO-d6, δ ppm): 152.17 (N=C), 150.31 (Cb-C_5H_4N), 150.08 (Cc-C_5H_4N), 146.60 (Cd-C_5H_3), 137.01 (Ce-C_5H_4N), 136.04 (Cf-C_5H_4N) 129.67 (Cg-C_6H_3), 125.68 (Ch-C_6H_3), 126.20 (Ci-C_5H_4N), 122.44 (Cj-C_6H_3).

3.3.5 (*E*)-2,6-dichloro-*N*-(pyridin-4-ylmethylene)aniline, ligand (L5)

L5 was prepared using 2,6-dichloroaniline (0.8239 g, 5.085 mmol) and pyridine-4-carboxyaldehyde (0.47 mL, 4.989 mmol). Brown oil formed after three minutes. Yield 1.18 mL, 96%. FT-IR (cm^{-1}): 3042 (C–H), 1670 (C=N), 1469 (C=C). ^{1}H-NMR (400 MHz, $CDCL_3$-*d1*, δ ppm): 8.77 (2H, d, *J* = 5.68 Hz, Ha-C_5H_4N), 8.41 (1H, s, *J* = HC=N), 7.87 (2H, d, *J* = 5.56 Hz, Hc-C_5H_4N), 7.08 (2H, d, *J* = 8.04 Hz Hd-C_6H_3), 6.45 (1H, t, *J* = 8.04 Hz, Hf-C_6H_3). ^{13}C-NMR (400 MHz, DMSO-d6, δ ppm): 160.07 (N=C), 150.31 (Cb-C_5H_4N), 145.45 (Cc-C_5H_4N), 145.59 (Cd-C_6H_3), 130.80 (Ce-C_6H_3), 129.37 (Cf-C_6H_4) 122.71 (Cg-C_6H_3).

3.3.6 (*E*)-3-nitro-*N*-(pyridin-2-ylmethylene)aniline, ligand (L6)

L6 was prepared using 3-nitroaniline (0.6401 g, 4.634 mmol) and pyridine-2-carboxyaldehyde (0.28 mL, 4.520 mmol). The reaction yielded a brown paste after three minutes of grinding. Reaction mixture was left in air to form a completely dry solid, which was thereafter washed with diethyl ether, dried and then analysed. Yield 1.006 g, 98%, m.p 90 – 92 ºC. FT-IR (cm^{-1}): 3092 (C–H), 1620 (C=N), 1519 (N=O), 1568 (C=C), 1347 (N=O). ^{1}H-NMR (400 MHz, $CDCl_3$-*d6*, δ ppm): 8.67 (1H, d, *J* = 4.40 Hz Ha-C_5H_4N), 8.56 (1H, s, (HC=N), 8.13 (1H, d, *J* = 7.84 Hz, Hc-C_5H_4), 8.07 (1H, t, *J* = 2.48 Hf-C_5H_4N), 8.04 (1H, s, He-C_5H_4), 7.80 (1H, t, *J* = 7.91 Hz, Hi-C_6H_4N), 7.52 (1H, d, *J* = 5.05 Hz, Hd-C_6H_5), 7.49 (1H, d, *J* = 5.05 Hz, Hg-C_6H_4N), 7.36 (1H, t, *J* = 5.52 Hz, Hh-C_5H_4). ^{13}C-NMR (400 MHz, DMSO-d6, δ ppm): 151.84 (N=C), 150.13 (Ca-C_5H_4), 149.45 (Cc-C_5H_4), 149.33 (Cd-C_5H_4N), 148.17 (Ce-C_5H_4N), 137.04 (Cf-C_5H_4N) 136.38 (Cg-C_5H_4N), 132.87 (Ch-C_6H_4), 128.45 (Ci-C_6H_4), 126.38 (Cj-C_5H_4N), 122.67 (Ck-C_5H_4), 118.62 (Cl-C_5H_4). UV-vis (CH_3CN): λ_{max} 215, 253 nm.

3.3.7 (*E*)-3-nitro-*N*-(pyridine-4-ylmethylene)aniline, ligand (L7)

L7 was prepared using 3-nitroaniline (0.6526 g, 4.724 mmol) and pyridine-4-carboxyaldehyde (0.44 mL, 4.671 mmol). The reaction yielded an off-white powder after three minutes. Product

was washed with absolute dry ethanol then dried and analysed. Yield 0.9125 g, 96%, m.p 137-139 ºC (lit. 136 – 138 ºC)[4]. FT-IR (cm^{-1}): 3053 (C–H), 1632 (C=N), 1591 (C = C), 1517 (N = O), 1351 (N = O). ^{1}H-NMR (400 MHz, $CDCl_3$-*d1*, δ ppm): 8.74 (2H, d, *J* = 4.02 Hz, Ha-C_5H_4N), 8.45 (1H, s, HC=N), 8.07 (1H, dt, *J* = 3.84 Hz, Hc-C_6H_4), 7.99 (1H, t, *J* = 1.72 Hz, Hd-C_6H_4), 7.73 (2H, d, *J* = 5.32 Hz, He-C_5H_4N), 7.53 (1H, s, Hf-C_6H_4), 7.05 (1H, d, *J* = 2.60 Hz, Hg-C_6H_4). ^{13}C-NMR (400 MHz, DMSO-d6, δ ppm): 160.34 (N=C), 150.12 (Cb-C_5H_4), 1494.5 (Cc-C_5H_4N), 149.79 (Cd-C_5H_4N), 144.63 (Ce-C_5H_4N), 132.78 (Cf-C_6H_4), 128.55 (Cg-C_6H_4) 122.70 (Ch-C_5H_4), 120.56 (Ci-C_5H_4N), 118.71 (Cj-C_5H_4). UV-vis (CH_3CN): λ_{max} 213, 252 nm.

3.3.8 (*E*)-4-bromo-2,6-dichloro-*N*-(pyridin-2-ylmethylene)aniline, ligand (L8)

L8 was prepared using 4-bromo-2,6-dichloroaniline (1.1267 g, 5.259 mmol) and pyridine-2-carboxyaldehyde (0.50 mL, 5.247 mmol). This formed a dry brown paste within three minutes. The resulting paste was left in open air to dry overnight. Yield 0.8190g, 95%, m.p 84 – 66 ºC. FT-IR (cm^{-1}): 3082 (C–H), 1614 (C=N), 1591, 1467 (C=C). ^{1}H-NMR (400 MHz, $CDCl_3$-*d1*, δ ppm): 8.65 (1H, d, *J* = 4.76 Hz Ha-C_5H_4N), 8.55 (1H, s, HC=N), 8.28 (1H, d, *J* = 7.88 Hz, Hc-C_5H_4N), 7.89 (1H, t, *J* = 7.60 Hd-C_5H_4N), 7.47 (1H, t, *J* = 4.76 Hz, He-C_5H_4N), 7.15 (2H, s, Hf-C_6H_2). ^{13}C-NMR (400 MHz, DMSO-d6, δ ppm): 152.11 (C=N), 150.01 (Cb-C_5H_4N), 148.45 (Cc-C_5H_4N), 144.56 (Cd-C_5H_2), 138.01 (Cg-C_5H_4N), 134.89 (Ch-C_5H_4N) 126.70 (Ci-C_5H_4N), 131.61 (Ce-C_6H_2), 130.24, 126.81 (Cf-C_5H_2) 124.45 (Cj-C_5H_2). UV-vis (CH_3CN): λ_{max} 208, 245, 310 nm.

3.3.9 (*E*)-2,6-dimethyl-*N*-(quinoline-2-ylmethylene)aniline, ligand (L9)

L9 was prepared using 2,6-dimethylaniline (0.43 mL, 3.627 mmol) and quinoline-2-carboxyaldehyde (0.5491 g, 3.494 mmol). A brown oil was formed after three minutes of grinding. The product was left to dry in open air. Yield 0.8367 g, 92%. m.p 151 – 156 ºC. FT-IR (cm^{-1}): 3053 (C–H), 1627 (C=N), 1485 (C=C), (C=N quinoline) 1595, (C=C quinoline) 1562. ^{1}H-NMR (400 MHz, DMSO-d6, δ ppm): 8.68 (1H, d, *J* = 4.76 Hz, Ha-C_9H_6N), 8.43 (1H, s, HC=N), 8.11 (1H, d, *J* = 7.88 Hz, Hc-C_9H_6N), 7.93 (1H, d, *J* = 7.68 Hd-C_9H_6N), 7.90 (1H, d, *J* = 7.12 Hz, He-C_9H_6N), 7.81 (1H, t, *J* = 7.80 Hz, Hf-C_9H_6N), 7.69 (1H, t, *J* = 7.60 Hz, Hg-C_9H_6N), 7.48 (1H, t, *J* = 7.32 Hz, Hh-C_6H_3), 7.11 (2H, d, *J* = 7.32 Hz, Hi-C_6H_3), 2.32 (6H, s, Hj-CH_3). ^{13}C-NMR (400 MHz, DMSO-d6, δ ppm): 151.71 (C=N), 149.10 (Cb-C_9H_6N), 149.17 (Cc-C_6H_3), 148.03 (Cd-C_9H_6N), 137.55 (Ce-C_5H_4N), 131.37 (Cf-C_5H_4N), 130.45 (Cg-C_6H_3), 130.40 (Ch-C_5H_4N), 128.79 (Ci-C_9H_6N), 128.71 (Cj-C_6H_4), 127.61 (Ck-C_5H_4N),

127.60 (Cl-C_6H_4), 120.25 (Cm-C_5H_4N), 18.91 (Cn-CH_3). UV-vis (CH_3CN): λ_{max} 204, 256, 283 nm.

3.3.10 (*E*)-2,4,6-tri-*tert*-butyl-*N*-(pyridin-2-ylmethylene)aniline, ligand (L10)

L10 was prepared using 2,4,6-tri-*tert*-butylaniline (0.8401 g, 3.213 mmol) and pyridine-2-carboxyaldehyde (0.30 mL, 3.154 mmol). The reaction yielded a brown solid after three minutes. Yield 0.9169 g, 82%, m.p 143 – 145 ºC. FT-IR (cm^{-1}): 2955 (C–H), 1619 (C=N), 1475 (C=C). ^{1}H-NMR (400 MHz, DMSO-d6, δ ppm): 8.75 (1H, s, HC=N), 8.63 (1H, d, *J* = 4.76 Hz Hb-C_5H_4N), 7.84 (1H, d, *J* = 7.88 Hz, Hc-C_5H_4N), 7.75 (1H, t, *J* = 7.68 He-C_5H_4N), 7.62 (1H, t, *J* = 7.12 Hz, Hf-C_5H_4N), 7.35 (2H, s, Hg-C_6H_2), 1.32 (9H, d, Hh-CH_3). ^{13}C-NMR (400 MHz, DMSO-d6, δ ppm): 151.45 (C=N), 149.01 (Cb-C_5H_4N), 148.09 (Cc-C_5H_4N), 141.22 (Cd-C_6H_2), 137.67 (Ce-C_6H_2), 136.89 (Cf-C_5H_4N), 136.14 (Cg-C_5H_4N), 133.19 (Ch-C_6H_2), 126.10 (Ci-C_5H_4N), 123.23 (Cj-C_6H_2), 36.26 (Ck-CCH_3), 34.61 (Cl-CCH_3), 31.27 (Cm-CH_3). UV-vis (CH_3CN): λ_{max} 203, 243, 291 nm.

3.3.11 (*E*)-*N*-(1-(pyridin-2-yl)ethylidene)aniline, ligand (L11)

L11 was prepared using aniline (0.50 mL, 5.148 mmol) and acetylpyridine-2-carboxyaldehyde (0.57 mL, 5.082 mmol). The reaction yielded a brown oil after three minutes. The oily product was dissolved in dry chloroform and rota-vaporised for two hours to remove water and solvent at 80 ºC. A brown oily liquid was eventually obtained as the product. Yield 0.94 mL, 95%. FT-IR (cm^{-1}): 3053, 1627, 1591, 1485, 1467, 1346, 1166, 777, 738, 691, 536, 405. ^{1}H-NMR (400 MHz, $CDCl_3$-d1, δ ppm): 9.17 (1H, d, *J* =0.72 Hz, C_5H_4N), 8.78 (1H, d, 3.84 *J* = C_5H_4N), 8.22 (1H, t, *J* = 4.36 Hz, C_5H_4N), 7.41 (1H, dd, *J* = 4.84 C_5H_4N), 7.14 (2H, t, *J* = 7.92 Hz, C_6H_5), 6.75 (1H, t, *J* = 7.36 Hz, C_6H_5), 6.68 (2H, d, *J* = 7.80 Hz, C_6H_5), 2.63 (3H, s, CC=N). ^{13}C-NMR (400 MHz, $CDCl_3$-d1, δ ppm): 160.67 (N=C), 154.04 (C_5H_4N), 150.45 (C_5H_4N), 149.64 (C_5H_4N), 137.03 (C_5H_4N), 129.32 (C_6H_4) 126.67 (C_5H_4N), 125.55 (C_6H_4), 121.28 (C_5H_4N), 121.09 (C_5H_4).

3.3.12 (*E*)-*N*-(pyridin-3-ylmethylene)aniline, ligand (L12)

L12 was prepared using aniline (0.46 mL, 5.047 mmol) and pyridine-3-carboxyaldehyde (0.49 mL, 5.007 mmol). An amber oil was obtained after three minutes dissolved in dry chloroform and rota-vaporised for two hours at 80 ºC. Yield 88%, m.p 96 – 98 ºC. FT-IR (cm^{-1}): 3053, 1627, 1591, 1485, 1467, 1346, 1166, 777, 738, 691, 536, 405. ^{1}H-NMR (400 MHz, $CDCl_3$-d1, δ ppm): 8.90 (1H, s, Ha-C_5H_4N), 8.57 (1H, d, 3.13 *J* = Hb-C_5H_4N), 8.32 (1H, s, HC=N),

8.14 (1H, d, *J* = 8.40 Hd-C_5H_4N), 7.30 (2H, t, *J* = 8.06 Hz, He-C_6H_5), 7.24 (1H, t, *J* = 4.99 Hz, Hf-C_5H_4N), 7.16 (2H, d, *J* = 9.64 Hz, Hg-C_6H_5), 7.13 (1H, t, *J* = 8.96 Hz,, Hh-C_6H_5). ^{13}C-NMR (400 MHz, DMSO-d6, δ ppm): 160.67 (N=C), 154.04 (Cb-C_5H_4N), 150.45 (Cc-C_5H_4N), 149.67 (Cd-C_5H_4N), 137.01 (Ce-C_5H_4N), 129.35 (Cf-C_6H_4) 126.67 (Cg-C_5H_4N), 125.56 (Ch-C_6H_4), 121.12 (Ci-C_5H_4N), 121.09 (Cj-C_5H_4).

3.3.13 (*E*)-*N*-(pyridin-4-ylmethylene)aniline, ligand (L13)

L13 was prepared using aniline (0.43 mL, 4.717 mmol) and pyridine-4-carboxyaldehyde (0.44 mL, 4.671 mmol). A white powder formed after three minutes and recrystallized in ether. Yield 0.7745g, 91%, m.p 70 – 72 ºC. FT-IR (cm^{-1}): 3084, 1630, 1567, 1468, 1281, 503, 488. ^{1}H-NMR (400 MHz, DMSO-*d6*, δ ppm): 8.75 (2H, d, *J* =5.4 Hz Ha-C_5H_4N), 8.68 (1H, s, HC=N), 7.85 (2H, d, *J* = 5.4 Hz, Hc-C_5H_4N), 7.45 (2H, t, *J* = 7.68 Hd-C_6H_4), 7.34 (2H, d, *J* = 7.28 Hz, He-C_6H_4), 7.30 (1H, t, *J* = 7.36 Hz, Hf-C_5H_4). ^{13}C-NMR (400 MHz, DMSO-*d6*, δ ppm): 159.27 (N=C), 150.54 (Cb-C_5H_4N), 150.45 (Cc-C_5H_4N), 142.45 (Cd-C_6H_4), 129.28 (Ce-C_5H_4N), 126.88 (Cf-C_5H_4N), 122.17 (Cg-C_6H_4), 121.16 (Ch-C_5H_4).

3.3.14 (*E*)-3-nitro-*N*-(pyridin-3-ylmethylene)aniline, ligand (L14)

3-nitroaniline (0.6937 g, 5.022 mmol) and pyridine-3-carboxaldehyde (0.46 mL, 4.900 mmol) was ground for three minutes to form yellow solid. The product was crushed to fine powder and then washed with ether to form white powder (**L14**). Yield: 0.9241 g, 83%, m.p 110 – 112 ºC. FT-IR (cm^{-1}): 3098, 1622, 1606, 1511, 1421, 1350, 1205, 671, 465, 390. ^{1}H-NMR (400 MHz, DMSO-d6, δ ppm): 9.09 (1H, s, Ha-C_5H_4N), 8.84 (1H, s, HC=N), 8.75 (1H, d, *J* = 4.52 Hz, Hc-C_5H_4N), 8.35 (1H, d, *J* = 7.95 Hd-C_6H_4), 8.15 (1H, s, He-C_6H_4), 8.12 (1H, d, *J* = 1.52 Hz, Hf-C_5H_4), 7.77 (1H, d, *J* = 7.88 Hz, Hg-C_5H_4N), 7.73 (1H, t, *J* = 7.80 Hi-C_5H_4N), 7.56 (1H, t, *J* = 4.80 Hz, Hh-C_5H_4) ^{13}C-NMR (400 MHz, DMSO-d6, δ ppm): 159.27 (N=C), 150.54 (Cb-C_5H_4N), 150.45 (Cc-C_5H_4N), 142.45 (Cd-C_6H_4), 129.28 (Ce-C_5H_4N), 126.88 (Cf-C_5H_4N), 122.17 (Cg-C_6H_4), 121.16 (Ch-C_5H_4).

3.4 Microwave-assisted synthesis of ligands

The ligands were also synthesised *via* a microwave-assisted method using minimal absolute dry ethanol (EtOH) as the solvent. The method was employed at 60 ºC, 100 Watts power, 90 psi pressure and three minutes as the reaction time. The product was precipitated by

refrigeration at 4 °C overnight, filtered and then dried under reduced pressure. In some instances, the oily products (**L11** and **L12**) were obtained.

The yields of the ligands were: **L3** = 89%; **L11** = 91%; **L12**% = 85%; **L13**= 88% and **L14** = 85%. All characterisation data were similar to those of products obtained using the solvent-free grinding technique.

3.5 Two-stage synthesis of complexes

The synthesis of complexes was done in two stages; the first stage involved the synthesis of ligands as already described and in the second stage, the synthesis of Cu(I) and Cu(II) Schiff base complexes by reaction of the respective metal salts and ligands, in ethanol and under an inert atmosphere of argon gas, using Schlenk technique. The reactants were stirred at ambient temperature for 3 h (for Cu(I)) and 5 h (for (Cu(II)). The resulting precipitate was filtered under vacuum suction using the Buchner apparatus. The collected residue was washed with EtOH (for Cu(I)) or MeCN (for Cu(II)). The dry solid powder form of complexes was stored in argon flushed desiccator, thereafter, analysed and tested for their antibacterial potency. All the Cu(I) complexes (**1** – **7**) were synthesised following a common procedure and Cu(II) complexes (**8** – **15**) were synthesised following a common procedure.

3.5.1 $[Cu(L1)_2]Cl^-$, complex 1

Complex **1** was synthesised by reacting **L1** (0.21 mL, 0.9987 mmol) with CuCl (0.0494 g, 0.4990 mmol) under inert argon atmosphere in MeCN solvent. Reaction afforded a green precipitate within three hours. The product was filtered under reduced pressure using Buchner apparatus to obtain a green powder. Yield 0.09222 g, 88%, m.p: 319 – 321 °C. FT-IR (cm^{-1}): 2964 (C–H), 2913 (C–H), 1640 (C=N), 1562 (C=C), 624 (Cu–N). ^{1}H NMR (400 MHz, DMSO-*d6*, 30 °C): 7.96 (1H, s, HC=N), 7.01 (2H, d, *J* = 4.92 Hz, Hb-C_5H_4N), 6.95 (1H, t, *J* = 4.68 Hc-C_5H_4N), 6.80 (2H, d, *J* = 4.88 Hz, Hd-C_6H_3), 6.36 (1H, t, *J* = 4.80 Hz, He-C_6H_3), 2.09 (1H, s, Hf-CH_3). UV/Vis (CH_3CN): λ_{max} 201, 232 nm. MS (ESI-TOF) *m/z* (%): Calcd. for $[(CuL1)_2]Cl^-$ 483.1502; found: 483.16 (100).

3.5.2 [(Cu(L2)$_2$Cl$^-$], complex 2

Green powder. Yield 0.3733 g, 85%, m.p: 75 – 77 °C. FT-IR (cm^{-1}): 3016 (C–H), 2945 (C–H), 1638 (C=N), 1572 (C=C), 652 (Cu–N). UV/Vis (CH_3CN): λ_{max} 268 nm. MS (ESI-TOF) *m/z* (%): Calcd. for [Cu(L2)$_2$]Cl$^-$ 483.1368; found: 483.16 (100). Anal. Calcd. (%) for [(CuL2)Cl$^-$]: C, 54.25; H, 3.849; N, 10.37; found: C, 54.25; H, 4.56; N, 9.06.

3.5.3 [Cu(L2)$_2$]Cl$^-$, complex 3

Maroon solid. Yield 1.0268 g, 89%, m.p: 222 – 227 °C (TGA/DSC, Appendix G1). FT-IR: 3048 cm^{-1} (C–H), 1625 cm^{-1} (C=N), (C=C), 1490 cm^{-1}, 489 cm^{-1} (Cu–N), 386 cm^{-1} (Cu–Cl). UV/Vis (CH_3CN): λ_{max} 240, 297 nm. MS (ESI-TOF) *m/z* (%): Calcd. for [Cu(L3)$_2$]Cl$^-$ 427.10; found: 427.0292 (100).

3.5.4 [Cu(L4)$_2$]Cl$^-$, complex 4

Green powder. Yield 0.1271 g, 86%, m.p 220 – 222 °C. FT-IR (cm^{-1}): 3078 (C–H), 28.55 (C–H), 1638 (C=N), 1578 (C=C), 674 (Cu–N). MS (ESI-TOF) *m/z* (%): Calcd. for [Cu(L4)$_2$]Cl$^-$ 595.91; found: 595.3805 (100). Anal. Calcd. (%) for (CuClL4): C, 36.62; H, 2.938; N, 6.87; found: C, 41.17; H, 2.30; N, 8.00.

3.5.5 [CuClL5], complex 5

Green powder. Yield 0.2393 g, 87%, m.p: 294 – 296 °C. FT–IR (cm^{-1}): 30.56 (C–H), 2925 (C–H), 1625 (C=N), 1556 (C=C), 671 (Cu–N). ^{1}H NMR (400 MHz, DMSO-*d6*, 30 °C): 7.96 (1H, s, *J* = HC=N), 8.82 (2H, d, *J* = 4.92 Hz, C_5H_4N), 7.62 (2H, d, *J* = 4.68 C_5H_4N), 6.80 (1H, t, *J* = 4.88 Hz, C_6H_3), 6.36 (2H, d, *J* = 4.80 Hz, C_6H_3). MS (ESI-TOF) *m/z* (%): Calcd. for [CuClL5] 347.90; found: 397.90 (100).

3.5.6 [Cu(L6)$_2$]Cl$^-$, complex 6

Brown powder. Yield 0.02948 g, 89%, m.p: 233 – 235 °C. FT-IR (cm^{-1}): 3093 (C–H), 2937 (C–H), 1623 (C=N), 1568 (C=C), 674 (Cu–N). UV/Vis (CH_3CN): λ_{max} 202, 253, 275 nm. MS (ESI-TOF) *m/z* (%): Calcd. for [Cu(L6)$_2$]Cl$^-$ 517.01; found: 557.0778 (100).

3.5.7 [Cu(L7)$_2$]Cl$^-$, complex 7

Green powder. Yield 0.2061 g, 90%, m.p: 220 – 222 °C. FT-IR (cm^{-1}): 3097 (C–H), 3035 (C–H), 1626 (C=N), 1557 (C=C), 674 (Cu–N). UV/Vis (CH_3CN): λ_{max} 215, 257, 320 nm. MS

(ESI-TOF) *m/z* (%): Calcd. for $[Cu(L7)_2]Cl^-$ 552.04; found: 552.3221 (100). Anal. Calcd. (%) for [CuClL7]: C, 47.34; H, 3.271; N, 13.49; found: C, 44.18; H, 2.78; N, 12.88.

3.5.8 $[Cu(L10)_2]2Cl^-$, complex 8

Complex **8** was synthesised by reacting **L10** (0.1058 g, 0.3413 mmol) with $CuCl_2$ (0. 04874 g, 0.3121 mmol). A green precipitate was formed in the reaction for five hours using ethanol (EtOH) as a solvent. An obtained green powder was recovered by filtration using Buchner apparatus under vacuum. Green powder. Yield 0.09299 g, 85%, m.p: 237 – 238 °C. FT-IR (cm^{-1}): 3049 (C–H), 3016 (C–H), 1638 (C=N), 1567 (C=C), 644 (Cu–N). UV/Vis (CH_3CN): λ_{max} 205, 242, 294 nm. MS (ESI-TOF) *m/z* (%): Calcd. for $[Cu(L10)_2]2Cl^-$ 483.16; found: 483.1603 (100).

3.5.9 $[Cu(L1)_2]2Cl^-$, complex 9

Green powder. Yield 0.5140 g, 84%, m.p: 244 – 248 °C. FT-IR (cm^{-1}): 3041 (C–H), 2970 (C–H), 1639 (C=N), 1561 (C=C), 641 (Cu–N). UV/Vis (CH_3CN): λ_{max} 200, 291, 339 nm. MS (ESI-TOF) *m/z* (%): Calcd. for $[Cu(L1)_2]2Cl^-$ 483.16; found: 483.1602 (100). Anal. Calcd. (%) for $[(Cu(L1)_2)Cl_2]$: C, 49.61; H, 4.861; N, 9.71; found: C, 48.78; H, 4.09; N, 8.13.

3.5.10 $[Cu(L2)_2]2Cl^-$, complex 10

Yellow powder. Yield 0.28 g, 91%, m.p: 240 – 247 °C. FT-IR (cm^{-1}): 3023 (C–H), 2912 (C–H), 1634 (C=N), 1570 (C=C), 651 (Cu–N). UV/Vis (CH_3CN): λ_{max} 237, 391 nm. MS (ESI-TOF) *m/z* (%): Calcd. for $[Cu(L2)_2]2Cl^-$ 483.16; found: 483.1606 (100). Anal. Calcd. (%) for $[Cu(L2)_2Cl_2]$: C, 48.85; H, 3.904; N, 7.98; found: C, 48.78; H, 4.09; N, 8.13.

3.5.11 $[Cu(L9)_2]2Cl^-$, complex 11

Orange powder. Yield 0.4787 g, 86%, m.p: 237 – 238 °C. FT-IR (cm^{-1}): 3059 (C–H), 3024 (C–H), 1637 (C=N), 1563 (C=C), 685 (Cu–N). UV/Vis (CH_3CN): λ_{max} 234, 345 nm. MS (ESI-TOF) *m/z* (%): Calcd. for $[Cu(L9)_2]2Cl^-$ 583.19; found: 583.1932 (100). Anal. Calcd. (%) for $[Cu(L9)_2]2Cl^-$: C, 51.75; H, 3.310; N, 5.64; found: C, 54.78; H, 4.09; N, 7.10.

3.5.12 $[Cu(L3)_2]2Cl^-$, complex 12

Green powder. Yield 1.0268 g, 89%, $m.p_{dec}$: 320 – 325 °C (TGA/DSC, Appendix G2). ^1H NMR (400 MHz, DMSO-*d6*, 25 °C): FT-IR (cm^{-1}): 3049 (C–H), 3016 (C–H), 1638 (C=N),

1567 (C=C), 643 (Cu–N). UV/Vis (CH_3CN): λ_{max} 240, 305 nm. MS (ESI-TOF) *m/z* (%): Calcd. for $[Cu(L3)_2]2Cl^-$ 427.10; found: 427.1106 (100). Anal. Calcd. (%) for $[(Cu(Cl)_2L3)]$: C, 44.92; H, 3.268; N, 8.75; found: C, 45.51; H, 3.18; N, 8.85.

3.5.13 $[Cu(L8)_2]2Cl^-$, complex 13

Green powder. Yield 0.4161 g, 91%, m.p: 299 – 301 °C. FT-IR (cm^{-1}): 3053 (C–H), 2918 (C–H), 1626 (C=N), 1556 (C=C), 685 (Cu–N). UV/Vis (CH_3CN): λ_{max} 204, 241, 280 nm. MS (ESI-TOF) *m/z* (%): Calcd. for $[Cu(L8)_2]2Cl^-$ 723.56; found: 722.7935 (100). Anal. Calcd. (%) for $[(Cu(Cl)_2L8)]$: C, 31.03; H, 1.585; N, 6.10; found: C, 31.03; H, 1.52; N, 6.03.

3.5.14 $[Cu(Cl)_2(L6)_2]$, complex 14

Green powder. Yield 0.41 g, %, $m.p_{dec}$: 257 – 258 °C (TGA/DSC, Appendix G3). FT-IR (cm^{-1}): 3076 (C–H), 2967 (C–H), 1623 (C=N), 1525 (C=C), 679 (Cu–N). UV/Vis (CH_3CN): λ_{max} 200, 270 nm. MS (ESI-TOF) *m/z* (%): Calcd. for $[Cu(Cl)_2(L6)_2]$ 583.89; found: 588.1314 (100). Anal. Calcd. (%) for $[(Cu(Cl)_2L6)]$: C, 39.02; H, 2.620; N, 11.25; found: C, 39.85; H, 2.51; N, 11.62.

3.5.15 $[Cu(Cl)_2L7]$, complex 15

Green powder. Yield 0.26 g, 94%, m.p: 255 – 256 °C. FT-IR (cm^{-1}): 3080 (C–H), 2984 (C–H), 1631 (C=N), 1557 (C=C), 654 (Cu–N). UV/Vis (CH_3CN): λ_{max} 228, 273 nm. MS (ESI-TOF) *m/z* (%): Calcd. for $[Cu(Cl)_2L7]$ 290.00; found: 292.9977. Anal. Calcd. (%) for $[(CuL7)Cl_2]$: C, 49.30; H, 3.082; N, 13.81; found: C, 44.18; H, 2.78; N, 12.88.

3.6 One-pot synthesis of complexes

The complexes were also synthesised *via* a one-pot technique using reported methods with slight variations.[5-7] For this technique, the ligand starting material was stirred in the Schlenk tube for 5 mins. This was then followed by argon flashing through the reaction to ensure the inert reaction atmosphere. Subsequently, the $CuCl_2$ in dried absolute ethanol was added dropwise with an aid of a syringe through a rubber septum. The reaction was left to proceed at room temperature and formed a precipitated product. In brief, both the metal salts and ligand starting material were reacted in EtOH solvent (10 ml) under inert argon atmosphere using Schlenk line apparatus to afford Cu(II) Schiff base complexes (**8** – **15**). Generally, the reactions took five hours to complete. The formed precipitate was filtered and dried under reduced

pressure using the Buchner apparatus. Thereafter, the solid product was washed with EtOH and dried.

The yields of Cu(II) Schiff base complexes were: **8** = 79%; **9** = 84%; **10** = 88%; C**11** = 80%, **12** = 77%; **13** = 86%; **14** = 89% and **15** = 86%. Similar characterisation data was obtained as for the two-stage reaction techniques results.

3.7 Crystal structure determination and refinement

Single crystals suitable for by X-ray diffraction analysis were selected and glued onto the tips of glass fibre mounted on brass holders. Crystal evaluation and data collection were done on a Bruker Smart APEXII diffractometer with graphite monochromated Mo Kα radiation (λ = 0.71073 Å) equipped with an Oxford Cryostream low-temperature apparatus operating at 100 K. The initial cell matrix was determined from three series of scans containing twelve frames collected at intervals of 0.5° in a 6° range with the exposure time of ten seconds per frame and the reflections indexed using the *APEXII* program suite.[8] Data collection involved the use of omega scans of 0.5° width with 20 seconds exposure time per frame. The total number of images was based on results from the program *COSMO*, whereby the expected redundancy was to be 4.0 and completeness of 100% out to 0.75 Å. Cell parameters were retrieved using *APEXII* and refined using *SAINT* on all observed reflections. Data reduction was performed using the *SAINT*[8] software and the scaling and absorption corrections were applied using *SADABS*[9] multi-scan technique. The structure was solved and refined by the direct method using the *SHELXS* program.[9] The visual crystal structure analysis was performed using *ORTEP*-3 system software.[10] Non-hydrogen atoms were first refined isotropically and then by anisotropic refinement with a full-matrix least-squares method based on F^2 using *SHELXL*.[9] All hydrogen atoms were positioned geometrically, allowed to ride on their parent atoms and refined isotropically. The crystal data and structural refinements obtained are summarised in Table 3.1 and were evaluated using online checkCIF and CCDC Mercury.

Table 3.1: The SC-XRD data and structural refinement results of **10_{py}** and **12_{py}**

	10_{py}	**12_{py}**
Formula	$C_{19}H_{19}Cl_2CuN_3$	$C_{17}H_{15}Cl_2CuN_3$
Dcalc./g cm^{-3}	1.518	1.597
Abs coefficient/mm^{-1}	1.472	1.652
Formula weight	423.81	395.76
Crystal size/mm^3	0.33×0.24×0.17	0.21×0.14×0.08
T/K	100(2)	100(2)
Crystal system	Orthorhombic	triclinic
Space group	P 2_1 2_1 2_1	P $\bar{1}$
a/Å	9.2584(5)	8.1445(3)
b/Å	13.6509(7)	9.0100(4)
c/Å	14.6752(7)	12.3725(5)
a/°	90	69.531(2)
b/°	90	86.310(3)
g/°	90	75.496(4)
V/Å^3	1854.73(16)	823.22(6)
Z (Z')	4 (1)	2 (1)
Wavelength/Å	0.71073	0.71073
Q_{min} and Q_{max}/°	2.038 and 28.426	1.757 and 28.248
Measured Refl.	19330	17805
Independent Refl.	4645	3886
Parameters	228	208
Restraints	0	0
Largest Peak/e.Å^{-3}	0.302	0.915
Deepest Hole/e.Å^{-3}	-0.297	-0.575
GooF	1.026	1.094
wR2 (all data)	0.0501	0.1076
wR2	0.0495	0.1023
R1 (all data)	0.0210	0.0401
R1	0.0193	0.0331

3.8 Media used for antibacterial testing

Nutrient Broth (NB) (Biolab, South Africa) solution was prepared by dissolving 16 g of NB powder in 1 L of distilled water. This was dispensed in 10 ml aliquots into stoppered test tubes and autoclaved at 121 °C for 15 minutes. Mueller-Hinton Agar (Biolab, South Africa) (MHA) was prepared by mixing 38 g of MHA powder in 1 L of distilled water and autoclaving at 121 °C for 15 minutes. Thereafter, the agar (approximately 20 mL) was poured into sterile disposable 90 mm petri dishes and allowed to set at room temperature.

3.9 Preparation of bacteria

In this study, the *Escherichia coli* ATCC 25922 (*E. coli*), *Staphylococcus aureus* ATCC 25923 (*S. aureus*), Methicillin-resistant *Staphylococcus aureus* ATCC 700699 (MRSA), *Pseudomonas aeruginosa* ATCC 27853 (*P. aeruginosa*), *Klebsiella pneumoniae* ATCC 31488 (*K. pneumonia*) and *Salmonella typhimurium* ATCC 14028 (*S. typhimurium*) bacteria were used. The broth cultures of the bacteria were prepared by inoculating a single colony of the bacterial strain in the prepared NB. This was incubated at 37 °C in a shaking incubator (100 r.p.m) for 18 hours. After incubation, the density of the broth cultures was adjusted with sterile distilled water to achieve a concentration equivalent to 0.5 McFarland's Standard (i.e., 1.5 x 10^8 colony forming units (CFU)/mL) using a densitometer (DEN-1B, Latvia).

3.10 Antimicrobial evaluation

The test compounds were initially screened for their antibacterial activities using a modification of the disc diffusion method. The test compounds (1 mg) were dissolved in 1 ml of dimethyl sulfoxide (DMSO). The MHA plates were lawn inoculated with the prepared bacterial cultures using a sterile throat swab. The plates were spotted with 10 µL of each compound, allowed to stand for 30 minutes at room temperature and then incubated at 37 °C for 18 hours. After incubation, the zones of inhibition were noted. Zones of inhibition (clear areas at the site of spotting) indicated antibacterial activity and compounds showing antibacterial activity were further tested to determine the minimum inhibitory concentrations (MICs).

The MICs were determined using a modification of the broth dilution method. This enabled the determination of the lowest dose that is required to prevent the visible bacterial growth for different compounds. The compounds were serially diluted with DMSO to achieve concentrations ranging from 1000 to 0.20 µg mL^{-1}. MHA plates were lawn inoculated with a sterile throat swab and 10 µL of concentration was spotted on the MHA plates. This was allowed to stand for 30 minutes at room temperature and then incubated at 37 °C for 18 hours. After incubation, the MICs were carried out to determine the lowest concentration that inhibits the growth of the bacteria. The DMSO solvent was used as a negative control, whilst the ciprofloxacin was employed as a positive control. The MIC determinations were carried out in triplicate.

References

1. G. Y. Nagesh and B. H. M. Mruthyunjayaswamy, *Journal of Molecular Structure*, 2015, **1085**, 198.
2. E. M. Njogu, B. Omondi and V. O. Nyamori, *Journal of Coordination Chemistry*, 2017, **70**, 2796.
3. R. V. Singh, P. Chaudhary, S. Chauhan and M. Swami, *Spectrochimica Acta Part A: Molecular and Biomolecular Spectroscopy*, 2009, **72**, 260.
4. P. K. Kadaba, *Journal of Heterocyclic Chemistry*, 1975, **12**, 143.
5. S. Yavuz and H. Yildirim, *Journal of Chemistry*, 2013, **2013**, 7.
6. M. M. Abd-Elzaher, A. A. Labib, H. A. Mousa, S. A. Moustafa, M. M. Ali and A. A. El-Rashedy, *Beni-Suef University Journal of Basic and Applied Sciences*, 2016, **5**, 85.
7. C. Biewer, C. Hamacher, A. Kaiser, N. Vogt, A. Sandleben, M. T. Chin, S. Yu, D. A. Vicic and A. Klein, *Inorganic Chemistry*, 2016, **55**, 12716.
8. Bruker, *Bruker AXS Inc., Madison, Wisconsin, USA*, 2009.
9. G. Sheldrick, *University of Göttingen: Germany*, 2013.
10. L. J. Farrugia, *Applied Crystallography*, 2012, **45**, 849.

Chapter 4

4 Results and discussions

This chapter discusses the results from the synthesis and characterisation of ligands (**L1** – **L14**) and complexes (**1** – **15**), containing the copper(I) and copper(II) metal centres.

4.1 Synthesis of Schiff base ligands

The solvent-free grinding of reactants and microwave-assisted methods were employed in the synthesis of ligands. Nine pyridinyl Schiff base ligands (**L1** – **L8** and **L10**) and one quinoline Schiff base (**L9**) ligand derivatives (Scheme 4.1) were synthesised *via* a solvent-free grinding of reactants. In the former method, the product was obtained through neat grinding of an aniline derivative and an appropriate carboxaldehyde in mortar and pestle. In the case of **L3** and **L11** – **L14** (Scheme 4.2), both methods were employed. In both techniques, the aniline to aldehyde mole ratio was kept at 1:1.1, a slight excess of aniline derivatives provided a manageable purification procedure. In this case, a minimal amount of dry diethyl ether was used to wash off the unreacted aniline impurities from the product (ligand).[1,2] Ligands, **L1** – **L4**, **L6**, **L7**, **L9** and **L10** had similar physical and spectral properties compared to the same ligands that are reported in literature.[3-9]

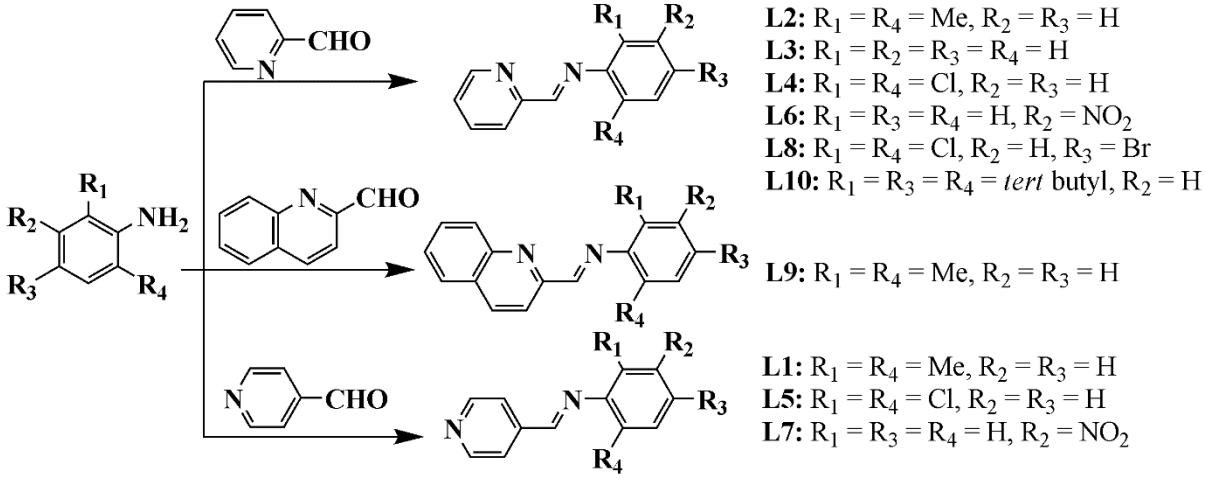

L2: $R_1 = R_4 = Me$, $R_2 = R_3 = H$
L3: $R_1 = R_2 = R_3 = R_4 = H$
L4: $R_1 = R_4 = Cl$, $R_2 = R_3 = H$
L6: $R_1 = R_3 = R_4 = H$, $R_2 = NO_2$
L8: $R_1 = R_4 = Cl$, $R_2 = H$, $R_3 = Br$
L10: $R_1 = R_3 = R_4 = tert$ butyl, $R_2 = H$

L9: $R_1 = R_4 = Me$, $R_2 = R_3 = H$

L1: $R_1 = R_4 = Me$, $R_2 = R_3 = H$
L5: $R_1 = R_4 = Cl$, $R_2 = R_3 = H$
L7: $R_1 = R_3 = R_4 = H$, $R_2 = NO_2$

Scheme 4.1: Solvent-free grinding synthesis of Schiff base ligands, **L1** – **L10**

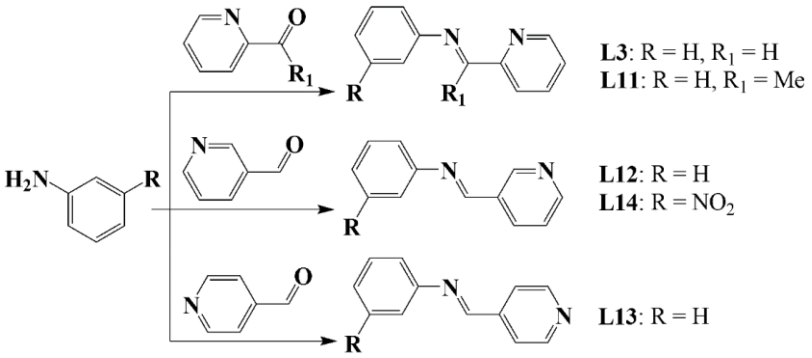

Scheme 4.2: Solvent-free grinding and microwave-assisted synthesis of **L3** and **L11** – **L14**

Both techniques were simple, fast and high yielding (Table 4.1). Ethanol which was used in the microwave-assisted synthesis has the essence of green attributes but is not as green as water. Thus, the solvent-free grinding surpasses the microwave-assisted technique in terms of greenness and the facileness. It is a better method since it is cheaper, simpler and generates less waste.[10-12]

Table 4.1: Ligand yields obtained from the solvent-free grinding and microwave-assisted method

	Solvent-free grinding		Microwave-assisted	
Ligand	Time/mins	Yield%	Time/mins	Yield%
L1	3	94	-	-
L2	3	95	-	-
L3	3	93	3	89
L4	3	94	-	-
L5	3	90	-	-
L6	3	98	-	-
L7	3	96	-	-
L8	3	95	-	-
L9	3	92	-	-
L10	3	82	-	-
L11	3	95	3	91
L12	3	88	3	85
L13	3	91	3	88
L14	3	83	3	85

(-) not synthesised with the microwave-assisted technique

In all cases, the synthesised Schiff base ligands were found to be stable under (dry) normal room conditions. However, they hydrolyse under water or moist conditions.[13] The resonance structures of the aromatic aldehyde moiety enhances the formation of the ligands by offering a resonance, which eventually favours the dehydration process and product formation.[14] As an example, for the formation of **L3**, the first step is the nucleophilic attack by *N*-atom lone pair to the carbonyl carbon (Figure 4.3(a)). This is followed by the proton abstraction by negatively charged oxygen atom (Figure 4.3(b)). The moisture provides water that protonates the alcohol (Figure 4.3(c)), the hydroxyl group deprotonates the amine group to form an imine bond and water is eliminated as a good leaving group (Figure 4.3(d)) to (Figure 4.3(e)).

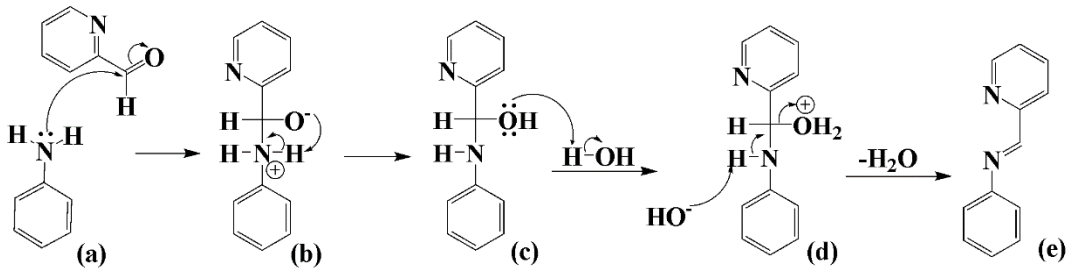

Scheme 4.3: Mechanism for the formation of **L3** under solvent-free conditions

The substituents on the phenyl ring of the anilines did not seem to affect the yield of Schiff bases (SBs) to a certain extent, especially when the solvent-free grinding method was employed.[8,15] However, the higher yields when the electron-withdrawing group (EWG) is on the *meta*-position of the anilines. This is evident from the high yields of **L6** and **L7** (Table 4.1). The reason for this is probably the resonance effect and its correlation to the basicity of the lone-pair electrons of the Schiff base nitrogen as per *meta*-directing property.[16,17] However, much lower yields were recorded (Table 4.1) for **L10**, when bulkier tertiary butyl substitutions were on the aniline precursor (Figure 4.1). This could be as a result of steric hindrance, where the nucleophilic *N*-atom is somehow shielded by the bulky groups. Thus, this to a certain extent, slows down the attack towards the electrophilic carbonyl carbon.

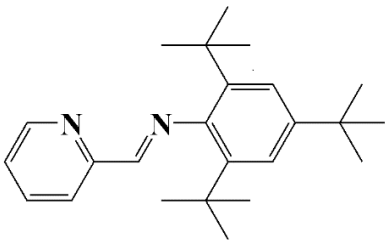

Figure 4.1: Structure of **L10**, showing the tertbutyl groups on the aniline ring

4.1.1 Infrared spectral data of ligands

The frequency of vibrating amine functional group *v*(N–H) of the aniline is observed around 3150 – 3450 cm^{-1}, *e.g.*, (Figure 4.2(a)). However, upon the formation of the imine, this peak disappears, and a peak at 1620 – 1650 cm^{-1} is observed for the formed SBs. Similarly, the vibrational band for the carbonyl of the aldehyde *v*(C=O) occurs around 1700 – 1780 cm^{-1}, e.g., (Figure 4.2(b)), disappears upon ligand formation.[18,19] The disappearance of the two functional groups confirm the formation of a new amine (C=N) band was a confirmation of the ligand formation, *e.g.*, (Figure 4.2(c)).[12,20-28] The stretching absorption bands at around 2900 – 3000 cm^{-1} and 1500 – 1590 cm^{-1} are due the C–H (aromatic) and C=C (conjugated) bond, respectively, for the ligands.[29-31] Schiff base ligands **6** and **7** showed the nitro *v*(N–O) vibrational bands at 1300 – 1400 (symmetric) and 1500 – 1550 (asymmetric) stretches.[13,28] The related IR data for other ligands are provided in Chapter 3 and Appendix A.

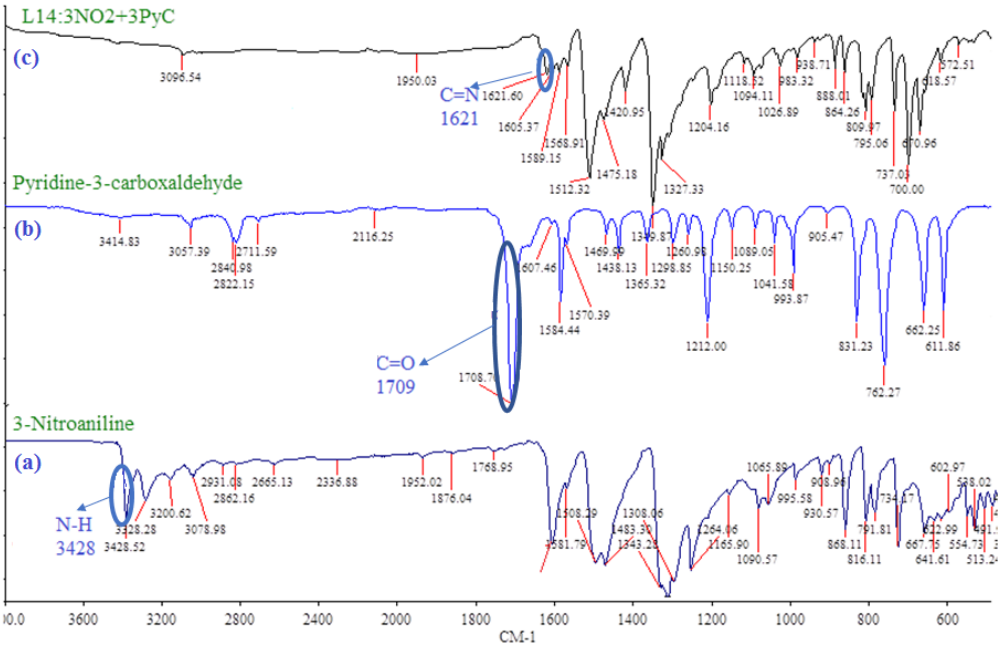

Figure 4.2: Representative IR spectra of (a) 3-nitroaniline, (b) pyridine-3-carboxaldehyde and (c) **L14**

4.1.2 ^{1}H- and ^{13}C-NMR spectral data of ligands

The new imine protons of the synthesised ligands appeared as singlets between 8.3 – 8.8 ppm, while the aldehyde and amine signals disappeared from the starting materials at 9.8 – 10.4 and 1.5 – 2.3 ppm, respectively, in ^{1}H-NMR spectra, *e.g.*, (Figure 4.3). The peak positions were in agreement with those of similar ligands that are reported in the literature. [22,28] Hence, this was a confirmation of the successful synthesis of ligands. The aromatic protons of ligands appeared

in the 6.5 – 8.5 ppm range, whereas the aromatic protons were found to resonate from 6.5 – 8.0 and 7.3 – 8.9 ppm, for aniline and aldehyde derivatives, respectively. This confirmed the successful synthesis of ligands and this also was in agreement with similar ligands in literature.[21,26,32,33] The NMR results showed that the aromatic protons resonated from 6.5 – 8.5 ppm in ^{1}H-NMR, suggesting that the ligands exist in the *enol*-form in solution, since they resonate above 6 ppm, *e.g.*, Figure 4.3(c). There was no peak depicting the *keto*-form (frequencies $\delta < 6$ ppm).[13]

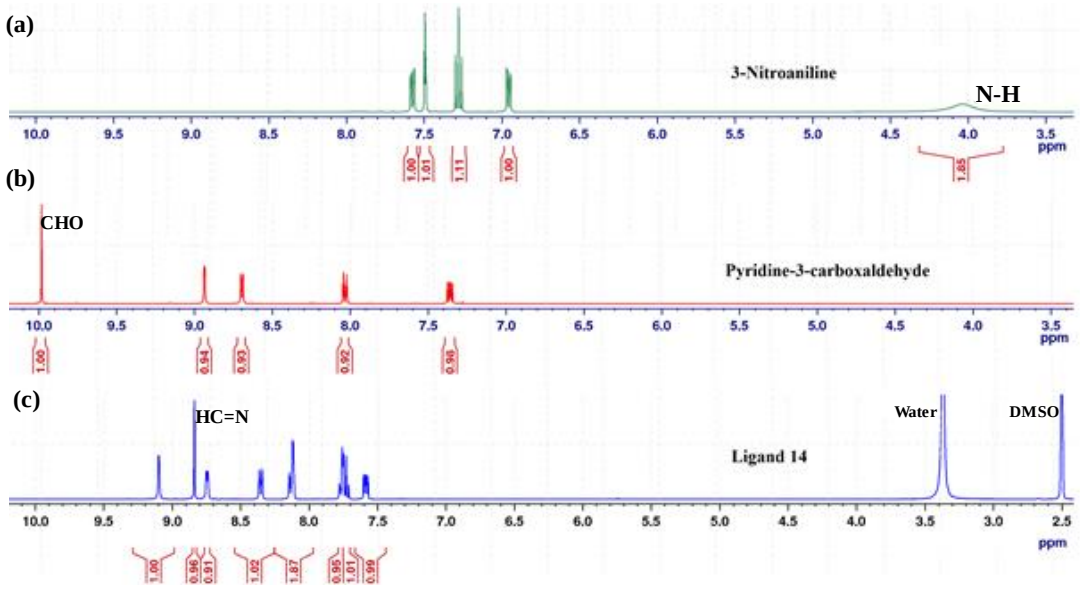

Figure 4.3: ^{1}H-NMR of (a) 3-nitroaniline, (b) 3-pyridinecarboxaldehyde and (c) **L14**

In ^{13}C-NMR, the ligand formation was confirmed by presence of an azomethine carbon formation within 155 – 164 ppm.[22,26,34,35] Also, the ^{13}C-NMR signal disappeared in the region of 185 – 195 ppm which are due to the aldehyde carbons of the precursors in the respective spectre of ligands, postulating the reaction of CHO group. The aromatic carbons resonated around 90 – 155 ppm in the ligands, whereas the aromatic carbons appeared from 115 – 148 and 112 – 155 ppm in the starting materials of the aniline and aldehydes, respectively. The related NMR data for other ligands are provided in Chapter 3 and Appendix B.

4.1.3 UV-vis spectral data of ligands

The ligands have two absorptions maxima below 250 nm due to intra-ligand transitions as explained in literature.[36-39] However, this was not the case for **L8** and **L10**, which have substituents on three positions of the benzene ring, while **L9** have quinoline in place of

pyridine. These minor structural differences led to the differences in the wavelength of absorption of these ligands. The two maxima absorbing wavelengths are due to different electron transitions, *i.e.*, л→л* (sharp peaks, from the aromatic ring) and n→л* (broad peak, from an imine moiety) transitions (Figure 4.4).[31,39] In all cases, n→л* was observed as the longer wavelength absorption band, since it required less energy for an electron transition.[40]

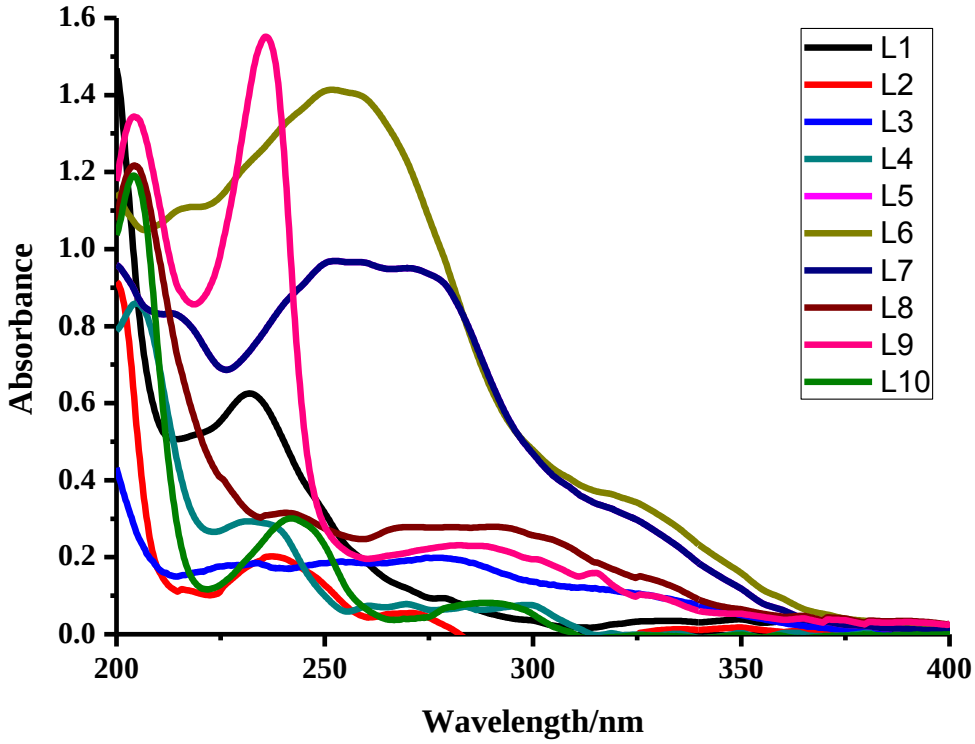

Figure 4.4: UV-vis overlay spectrum of **L1** – **L10**

4.2 Synthesis of complexes

The Cu(I) and Cu(II) complexes were synthesised using two methods; *i.e.*, two-stage and one-pot synthesis approach. The two-stage approach entails the synthesis of ligands and complexes in separate reactions, *i.e.*, a two distinct batch synthesis approach. A one-pot approach involves the synthesis of complexes in one reaction, *i.e.*, the metal salt and the precursors to the ligand were mixed together in one pot. Seven Cu(I) complexes (**1** – **7**) were synthesised using only a two-stage approach since one-pot reaction resulted in aqueous medium where Cu(I) can easily get oxidised. In the synthesis of Cu(I) complexes (Scheme 4.4), dried MeCN was used to avoid the oxidation and disproportionation of Cu(I) to Cu(II) complexes. This is because Cu(I) complexes are unstable and rather oxidise to Cu(II) complexes which forms relatively stable coordination complexes with *N*-donor SBs as predicted by the Pearson's (HSAB) theory.[41-44] Also, MeCN ensures the solubility of reactants, which enhances the reaction rate.[45]

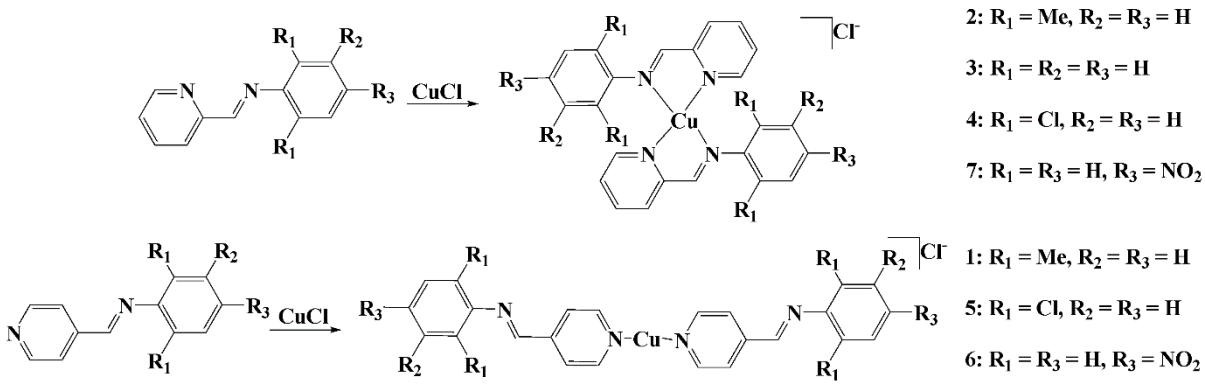

Scheme 4.4: Synthesis of Cu(I) Schiff base complexes (**1** – **7**) using a two-stage approach

The advantage of a two-stage reaction approach is the provision of easier monitoring of the reaction progress, *i.e.*, from ligands to the final complexes. Better yields were obtained at lower reaction times. However, in the two-stage approach, the purification of ligands and complexes was noted as a disadvantage. This was time consuming to isolate and purify the product before proceeding to the next step of the reaction. Eight copper(II) complexes **8** – **15** (Scheme 4.5) were synthesised using both a two-stage and one-pot reaction methods. This approach was used to compare yields and greenness (minimal clean-up) of the reaction.

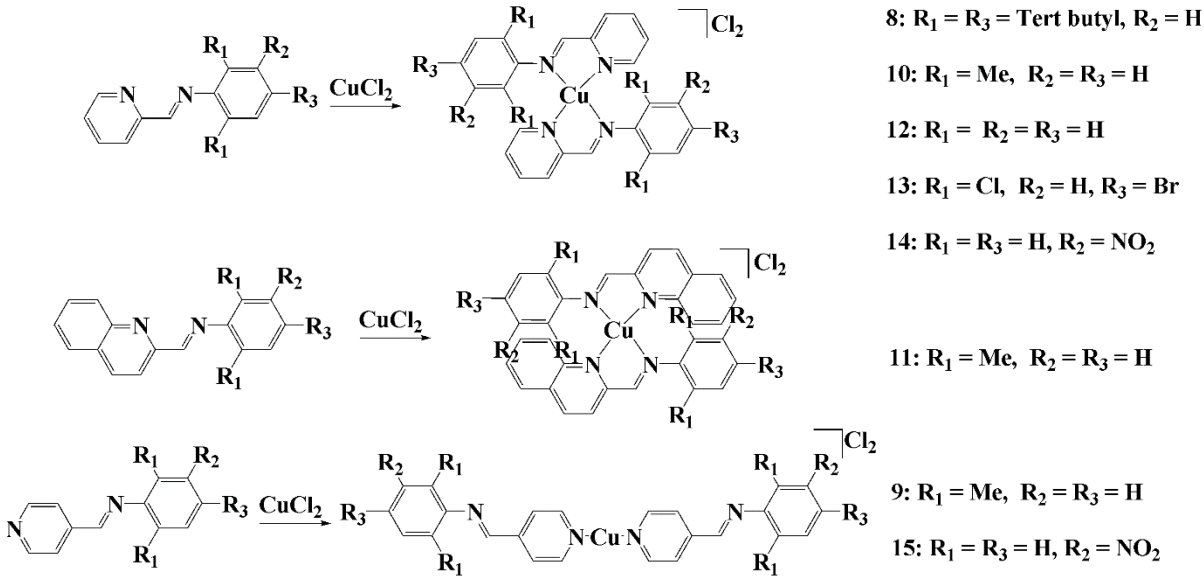

Scheme 4.5: Synthesis of Cu(II) Schiff base complexes (**8** – **15**) *via* a two-stage and one-pot approach

The one-pot synthesis is facile and devoid of stage related purifications from ligands to the synthesis of complexes. In this case, the isolation and purification of the product were conveniently done in one step. This is because the solubility properties of complexes greatly differ from that of the starting reagents, which enabled selective separation through washing.

However, the one-pot reaction time is relatively longer than the two-stage approach (excluding separation and purification times). The reaction is faster in the two-stage synthesis because Cu(II) metal ion served as an organizational centre for the formation of the imine bond from a pre-assembled (*via* coordination) precursors forming the Schiff base. Also, the one-pot approach was found to be unsuitable for the synthesis of copper(I) complexes since there is a formation of water molecules in the reaction. This is because the Cu(I) complexes can disproportionate or oxidise in an aqueous medium. Thus, the Cu(I) complexes were not obtained using this technique.

Nonetheless, the two methods were successfully applied and compared in the synthesis of Cu(II) Schiff base complexes (**8** – **15**) and both had relatively high yields between 77 – 89 % (Table 4.2). One-pot approach was simpler but exhibited relatively lower yields, while the two-stage approach afforded higher yields. Hence, a two-stage approach was found to be suitable for the synthesis of both Cu(I) and Cu(II) Schiff base complexes.

Table 4.2: Results obtained from two-stage and one-pot synthetic techniques

Entry	Two-stage		One-pot	
(C)	Time/hrs	Yield%	Time/hrs	Yield%
1	3	88	-	-
2	3	85	-	-
3	3	89	-	-
4	3	86	-	-
5	3	87	-	-
6	3	89	-	-
7	3	90	-	-
8	5	85	5	79
9	5	89	5	84
10	5	91	5	88
11	5	86	5	80
12	5	89	5	77
13	5	91	5	86
14	5	94	5	89
15	5	89	5	86

(-) Cu(I) complexes were not obtained with this technique

The copper(II) Schiff base complexes were found to be relatively stable under normal room conditions. This was not the case with copper(I) Schiff base complexes, which changed colour immediately when left in open air environment. Thus, Copper(I) complexes required special storage, under inert argon atmosphere and in a vacuum-sealed desiccator, to avoid unwanted post-reactions and to keep the complexes stable.

4.2.1 Infrared spectral data of complexes

Coordination of ligands to the Cu(I) and Cu(II) metal salts was confirmed by IR spectroscopy. The medium intense band due to *ν*C=N stretching frequency in the ligand was bathochromically shifted to 1614 – 1670 cm^{-1}. The bathochromic shift (~8 cm^{-1}), relative to the imine for the ligand (Table 4.3, entry 2 – 4, 6, 8, 10 – 14)[21,22,40,46-48], thereby confirming the formation of the complexes.[29,49,50] This shift is due to donation of electron density by nitrogen to copper which made the Cu–N stronger as the imine band *ν*(C=N) became weaker. This was the case for all the bidentate ligands where an imine *N*-atom coordinates to the metal ion and this is similar to those reported for similar complexes in the literature.[31,47,49] Figure 4.5 presents the IR spectrum of **L2** and its corresponding complex (**10**) illustrating the changes accompanying the coordination of ligands, where an imine band shift from 1637 to 1634 cm^{-1} from **L2** to complex (**10**), respectively.

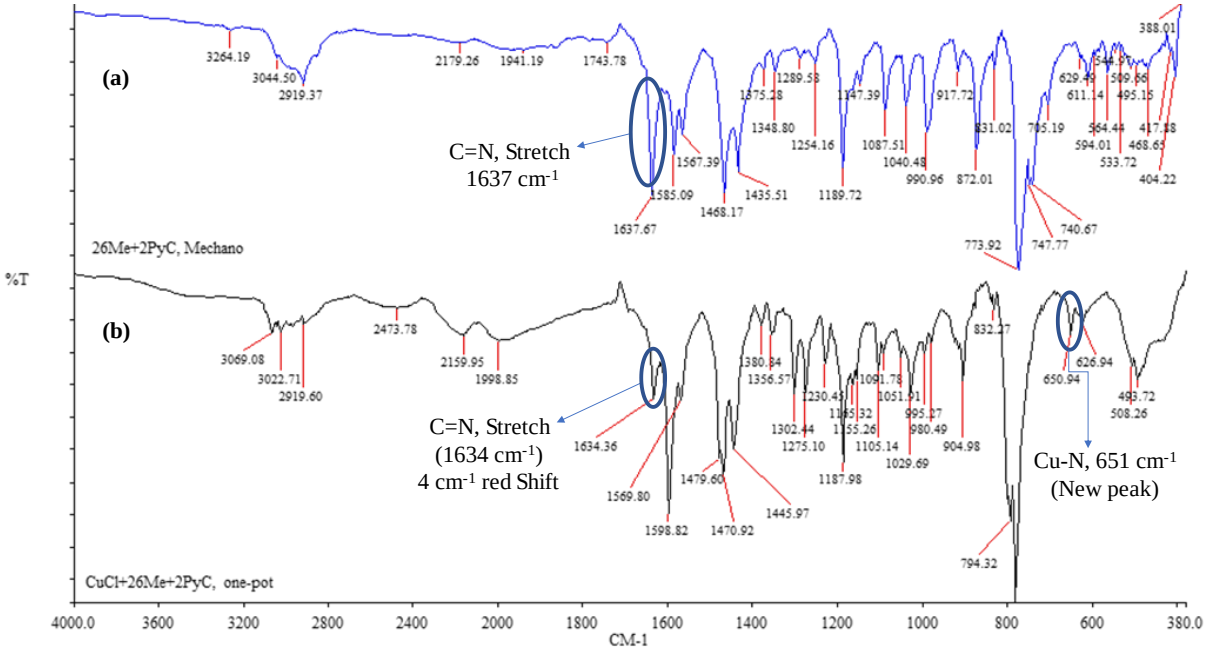

Figure 4.5: IR overlay spectrum of (a) **L2** and (b) its corresponding complex (**10**)

Table 4.3: IR imine peaks of ligands and their corresponding complexes

Entry	Ligand (**Complex**)	IR Wavelength/cm^{-1}	Peak/ppm H^1 NMR	Peak/ppm C^{13} NMR
1	L1 **(1)**	1640 **(1640)**	8.14 **(7.96)**	162.1 **(161.8)**
2	L2 **(2)**	1638 **(1635)**	8.31 **(-)**	152.2 **(-)**
3	L3 **(3)**	1627 **(1625)**	8.59 **(-)**	160.7 **(-)**
4	L4 **(4)**	1643 **(1637)**	8.78 **(-)**	152.1 **(-)**
5	L5 **(5)**	1670 **(1670)**	8.41 **(7.96)**	160.0 **(159.2)**
6	L6 **(6)**	1632 **(1616)**	8.67 **(-)**	151.8 **(-)**
7	L7 **(7)**	1632 **(1615)**	8.45 **(-)**	160.3 **(-)**
8	L10 **(8)**	1619 **(1616)**	8.75 **(-)**	151.5 **(-)**
9	L1 **(9)**	1639 **(1639)**	8.80 **(-)**	161.1 **(-)**
10	L2 **(10)**	1637 **(1634)**	8.50 **(-)**	152.2 **(-)**
11	L9 **(11)**	1627 **(1636)**	8.43 **(-)**	151.7 **(-)**
12	L3 **(12)**	1627 **(1624)**	8.59 **(-)**	160.7 **(-)**
13	L8 **(13)**	1639 **(1635)**	8.55 **(-)**	150.1 **(-)**
14	L6 **(14)**	1620 **(1622)**	8.67 **(-)**	151.8 **(-)**
15	L7 **(15)**	1632 **(1631)**	8.79 **(-)**	160.3 **(-)**

(-) not analysed/obtained with this technique

Some Schiff base ligands such as **L1**, **L5** and **L7** coordinate to copper in a monodentate fashion. This is supported in the IR spectra by the appearance of a new weak peak *v*(Cu–N) with stretching vibration bands at 400 – 700 cm^{-1} (Figure 4.6(c)) to confirm this monodentate coordination of these ligands.[29,50] The peak is relatively weak since the metal coordination does not occur at the imine *N*-atom, rather it involves the pyridinyl *N*-atom. Hence, the red shift was not observed in the monodentate ligands (Table 4.3, entry 1, 5, 7, 9 and 15) as reported in the literature.[51] As an example, **L1** and **1** both have an imine band appeared at 1640 cm^{-1} (Figure 4.6(b)), where a monodentate **L1** was used to form **1**, and did not show imine shift. The related IR data for other complexes are provided in Chapter 3 and Appendix A.

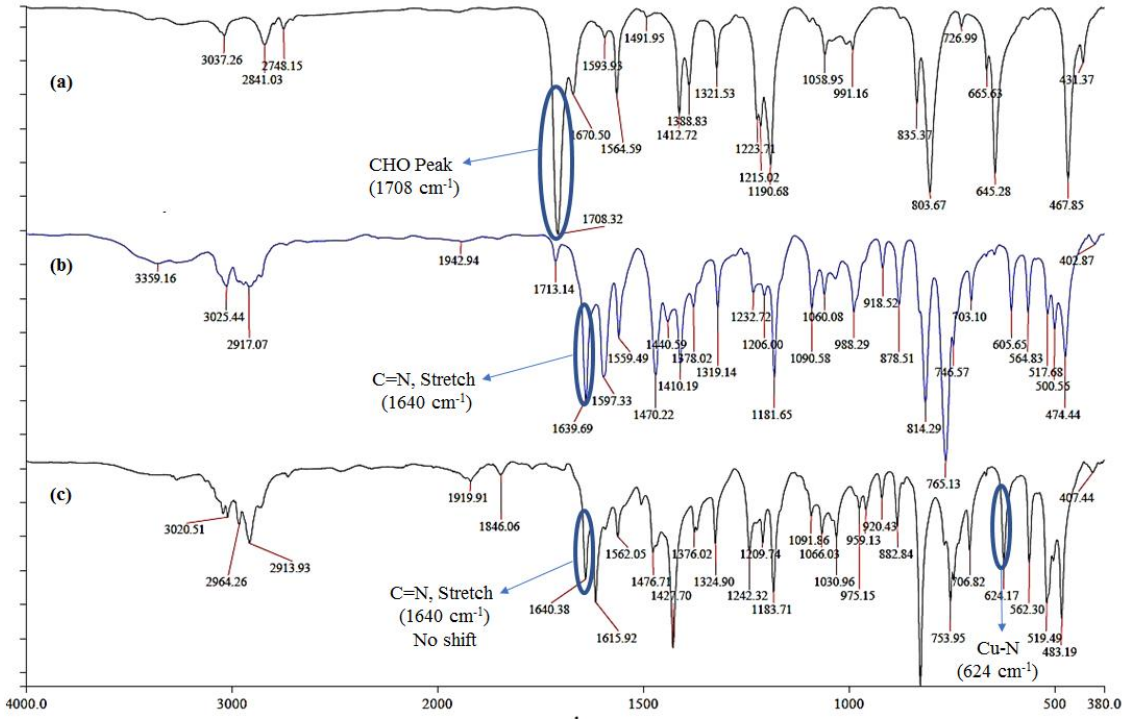

Figure 4.6: IR overlay spectrum of (a) pyridine-2-carboxaldehyde, (b) **L1** and (c) complex (**1**)

4.2.2 Mass spectral data of complexes

The molecular ion peaks in the high resolution-mass spectroscopy (HR-MS) were used to confirm the structural molecular mass of complexes. For example, the HR-MS molecular ion peak of 297.9836 amu (Figure 4.7) corresponded to the M+ ion of **3**. In this case, the Cu(I) metal centre is coordinated to a single bidentate ligand and one chlorine atom as a ligand to afford a coordination number of three around the Cu(I) complex centre. This may be just the most stable fragmentation ion after loss of one of the bidentate ligand (**L3**) in the basal plane from the parental $[Cu(L3)_2]Cl^-$. The related MS data for other complexes are provided in Chapter 3 and Appendix D.

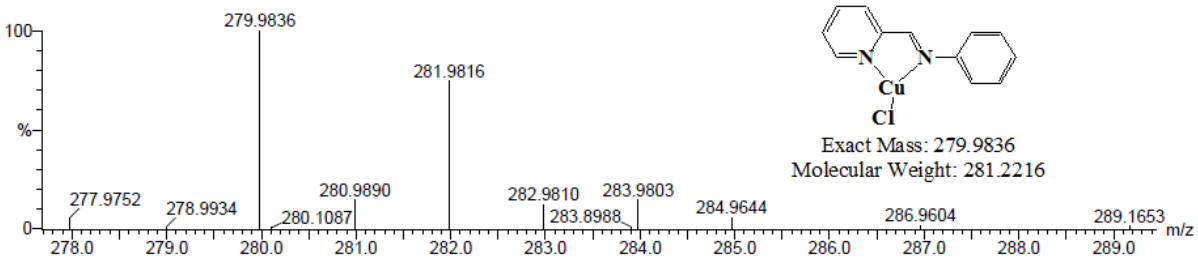

Figure 4.7: Representative HR-MS spectrum of **3**

The low resolution-mass spectroscopy (LR-MS) was also used to investigate all the fragmented peaks within a sample. The LR-MS showed the most abundant structure, for example, **3** (Figure 4.8(b)) is 279.94 amu (base peak), which corresponded with the molecular ion peak in HR-MS (Figure 4.7). The 461.9930 amu indicates that **3** can be constituted of two bidentate ligands and a coordinated chlorine ligand (Figure 4.8d) in solution. Thus, **3** possibly exists as a penta-coordinated complex in solution, which is an unstable coordination number for a Cu(I) complex. The complex might undergo fragmentation to exist in numerous structures (Figure 4.8a – d). **3** may fragment to different mass fragments, which are in Figures 4.8(a), (b) and (c). This was observed in **1**, **3** – **7** and **12** – **14**. The related MS data for other complexes are provided in Chapter 3 and Appendix D.

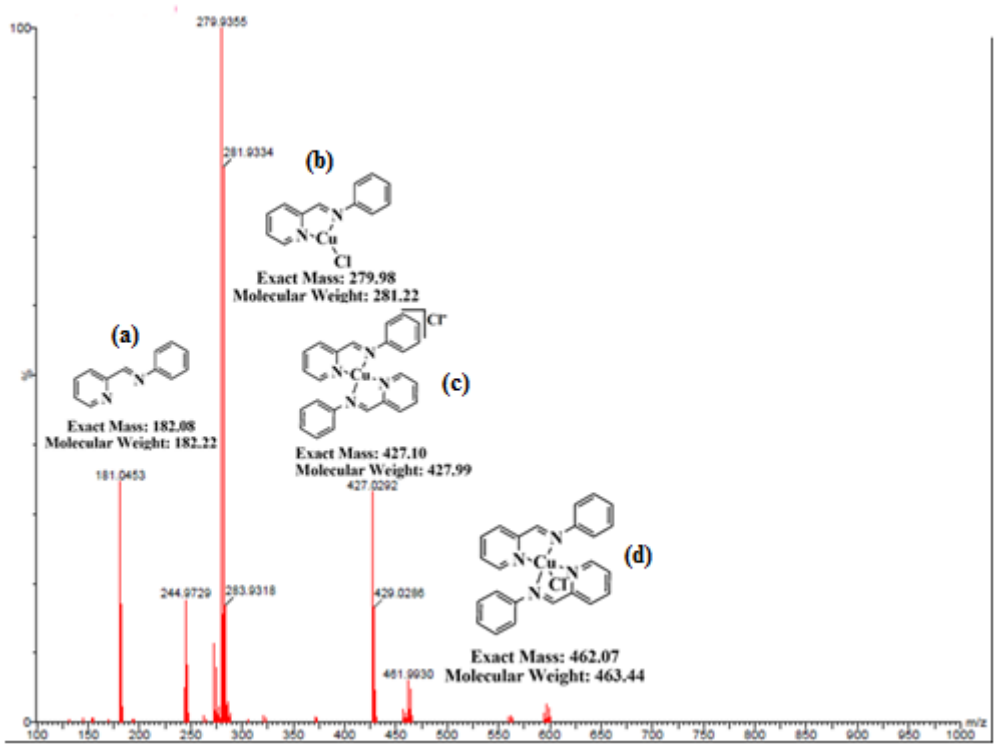

Figure 4.8: Representative LR-MS spectrum of **3**

4.2.3 UV-vis spectral data of complexes

The complexes (**2**, **3**, **4**, **6**, **8**, **10**, **11**, **12**, **13** and **14**) showed red shifts (attributed to n–π*) in relation to their Schiff base precursor ligands. This redshift suggested imine coordination to a metal centre, which is also reported in the literature.[31,36,37] However, the complexes (Table 4.4, entry 1,5,7,9 and 15) did not show any shift upon complexation and this also has been reported for similar complexes (with monodentates) in literature.[46] **13** (Table 4.4, entry 13) is the only complex with a hypsochromic shift, this is not common but has been reported.[39]

Table 4.4: The UV-vis studies of ligands and their corresponding complexes

Entry	L **(C)**	UV-vis Wavelength/nm	UV-vis Assignment
1	L1 **(1)**	200, 231 **(201, 232)**	π–π*, n–π* **(π–π*, n–π*)**
2	L2 **(2)**	238, 271 **(238, 268)**	π–π*, n–π* **(π–π*, n–π*)**
3	L3 **(3)**	230, 283 **(240, 297)**	π–π*, n–π* **(π–π*, n–π*)**
4	L4 **(4)**	205, 233 **(261)**	π–π*, n–π* **(n–π*)**
5	L5 **(5)**	207, 290 **(221, 290)**	π–π*, n–π* **(π–π*, n–π*)**
6	L6 **(6)**	253 **(202, 275)**	n–π* **(π–π*, n–π*)**
7	L7 **(7)**	213,252 **(215, 257, 320)**	π–π*, n–π* **(π–π*, π–π*, n–π*)**
8	L10 **(8)**	203, 243, 291 (**205, 243, 294**)	π–π*, π–π*, n–π* **(π–π*, π–π*, n–π*)**
9	L1 **(9)**	200, 231 **(339, 291)**	π–π*, n–π* **(π–π*, n–π*)**
10	L2 **(10)**	238, 271 **(238, 391)**	π–π*, n–π* **(π–π*, n–π*)**
11	L9 **(11)**	204, 232, 283 **(255, 335)**	π–π*, π–π*, n–π* **(π–π*, n–π*)**
12	L3 **(12)**	230, 283 **(240, 305)**	π–π*, n–π* **(π–π*, n–π*)**
13	L8 **(13)**	208, 245, 310 **(204, 241, 280)**	π–π*, π–π*, n–π* **(π–π*, π–π*, n–π*)**
14	L6 **(14)**	215, 253 **(240, 270)**	π–π*, n–π* **(π–π*, n–π*)**
15	L7 **(15)**	213, 252 **(228, 273)**	π–π*, n–π* **(π–π*, n–π*)**

The ligands showed only the n–π* transition, whereas **6** and **7** (Table 4.4, entry 6 and 7) had an extra band attributed to π–π*. For example, **L6** (Figure 4.9) contains only one absorption peak (n–π*) labelled "**a**", while its corresponding complex (**6)** displayed two signal bands, labelled "**a** and **b**" for n–π* and π–π*, respectively. The new peaks in the complexes could be attributed to the redshift as transitions require less energy upon coordination.[52] Hence, the formation of a new π–π* azomethine metal to ligand charge transfer (MLTC) was observed and the complexes might have exhibited an extra band, as a result of the copper d-d transitions upon coordination.[53] The related UV data for other complexes are provided in Chapter 3 and Appendix c.

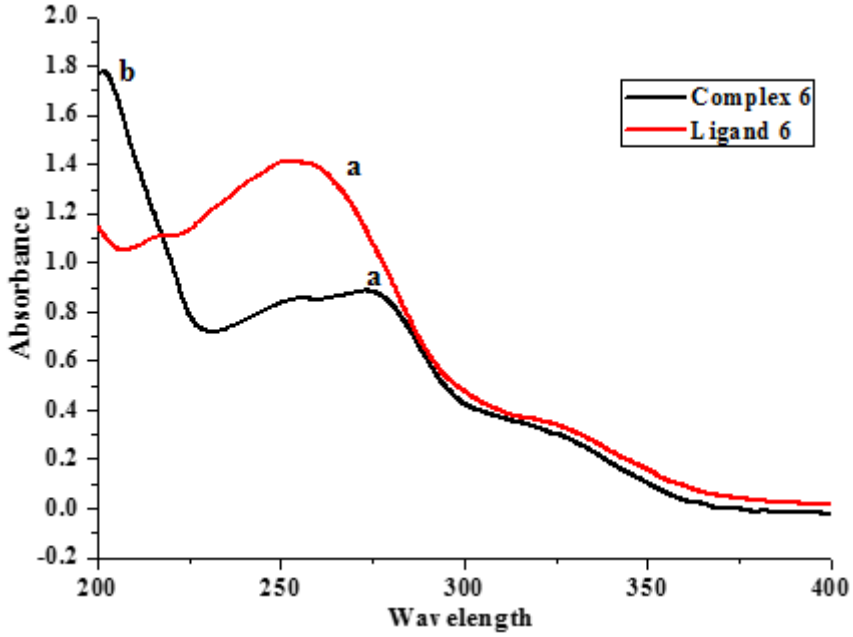

Figure 4.9: UV-vis overlay of **L6** and its corresponding complex (**6**)

4.2.4 Elemental analysis

The elemental analysis results of Schiff base complexes are given in Table E1. Some experimental mass percentage of individual elements were found to be consistent with the expected distribution of respective element mass percentage, which was calculated from expected empirical formula and those reported in the literature.[54] The correlation between the expected and literature mass percentage confirmed the purity of samples and this was observed in some Schiff base complexes. However, this was not the case for **4**, **7** and **11**, which deviated significantly (greater than 0.5%) and this was as a result of sulphur impurities.

4.2.5 Crystal structure description of $\mathbf{10_{py}}$ and $\mathbf{12_{py}}$

$\mathbf{10_{py}}$ crystallised in the orthorhombic $P2_12_12_1$ space group, while $\mathbf{12_{py}}$ crystallised in the triclinic P $\bar{1}$ space group. In both cases, the asymmetric unit consists of a complete molecule, which comprises of a Cu(II) metal centre, pyridine moiety and (*E*)-2.6-dimethyl-*N*-(pyridin-2-ylmethylene)aniline (**L2**) or (*E*)-*N*-(pyridin-2-ylmethylene)aniline (**L3**). The latter coordinates through azomethine (N3)/(N1) and pyridinyl (N2)/(N3) *N*-atoms to form $\mathbf{10_{py}}$ and $\mathbf{12_{py}}$ (Figure 4.10), respectively. The ligand, L2 or L3 and Cu(II) centre form a five-membered metallocycle encompassing Cu1 — N2 — C10 — C11 — N3 and Cu1 — N3 — C8 — C7 — N1, which is almost coplanar with dihedral angles of 3.060(3)° and 6.660(3)° to the ligand pyridinyl moiety, for $\mathbf{10_{py}}$ and $\mathbf{12_{py}}$, respectively. The deviation from planarity is more pronounced in $\mathbf{12_{py}}$

because it contains methyl group, which inductively induces electrons to the ring structure, causing increased electron repulsion.

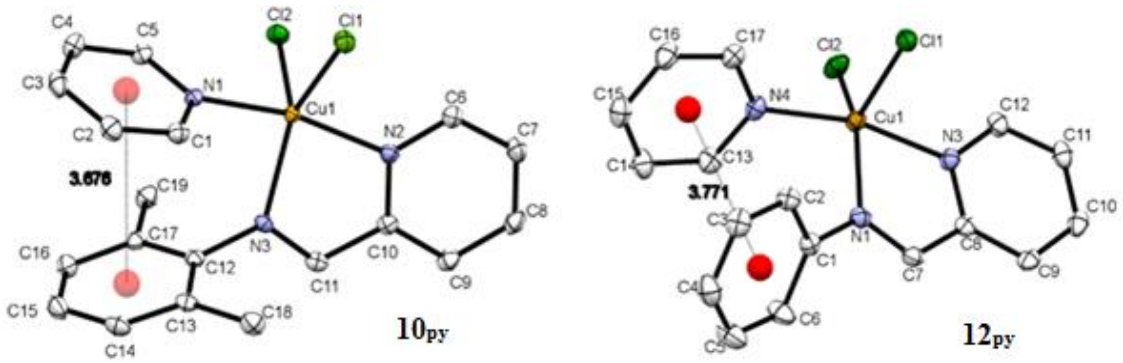

Figure 4.10: ORTEP diagram of **10**$_{py}$ and **12**$_{py}$ drawn at 50% thermal ellipsoid probability level. All hydrogen atoms have been omitted for clarity.

A pyridine solvent coordinates in the complexes, probably through ligand substitution which may indicate the instability of these complexes in solution. Two chlorine ligands occupy the other two sites to form neutral Cu(II) complexes. Thus, a five-coordination number around Cu(II) centre was achieved. The coordinated pyridine and the aniline ring are facing the same direction with $\pi_{\text{pyridine}}\ldots\pi_{\text{aniline}}$ distances of 3.676 Å and 3.771 Å in **10**$_{py}$ and **12**$_{py}$, respectively.[55] Structures of **10**$_{py}$ and **12**$_{py}$ show induced π–π parallel offset stacking, since their centroid are all less than 4 Å. The offset stacking might be stabilising the distorted conformation of complexes, which was observed in both structures.

12$_{py}$ with unsubstituted methylene(aniline) moiety show a relatively higher centroid distance which could be due to the lack of extra electron donating groups towards the phenyl ring.[56] On the contrary, the presence of electron-donating methyl group in **10**$_{py}$ was found to increase the electron density towards the methylene(aniline) ring. Thus, rendering it slightly negative (electron-rich), while the *N*-atom in the pyridinyl ring pulls more electrons towards itself, leaving the entire pyridinyl ring slightly positive (electron-deficient). This enhances the electrostatic aromatic interaction between two π–bonded rings.[57]

Structures of **10**$_{py}$ and **12**$_{py}$ adopt the distorted trigonal bipyramidal geometry around Cu(II) centre with bond angles around the metal centre lying between 79.36(7) ° to 167.35(7)° and 79.12(7)° to 165.57(8)°, in **10**$_{py}$ and **12**$_{py}$, respectively. Figure 4.11 provides the crystal structure of **10**$_{py}$ as an example. The average Cu—N distances were 2.037(18) – 2.0864(16) Å and Cu—CI was 2.292(5) – 2.342(5) Å, is in the range of reported similar Cu(II) complexes.[55,58,59] The ligand (**L2** or **L3**), pyridinyl and one chlorine atom are in the basal

position, while the other chlorine ligand is in the apical position. The axial chlorine ligand bond lengths are profoundly longer, with bond distances of 2.4326(6) and 2.4521(5) (Table 4.5), in **10$_{py}$** and **12$_{py}$**, respectively. The axial elongated bond length feature indicates weak bonding of chlorine atom resulting in Jahn-Teller effect tetragonal distortion.[58]

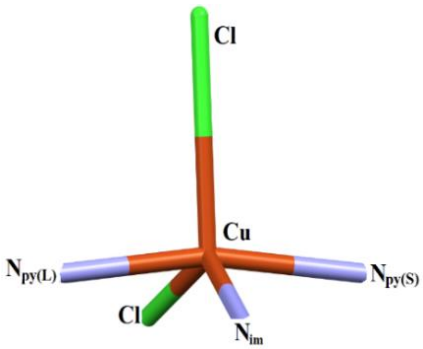

Figure 4.11: Crystal structure of **10$_{py}$** showing geometry around the Cu(II) centre

Table 4.5: Metal coordination bond lengths and angles of **10$_{py}$** and **12$_{py}$**

Parameters	Bond distances/Å		Bond angles/°	
	10$_{py}$	**12$_{py}$**	**10$_{py}$**	**12$_{py}$**
$N_{py(L)}$—Cu	2.020(2)	2.008(2)	-	-
N_{im}—Cu	2.086(2)	2.111(2)	-	-
$N_{py(S)}$—Cu	2.004(2)	1.991(2)	-	-
Cl**1**—Cu	2.4326(6)	2.4521(5)	-	-
Cl**2**—Cu	2.2941(5)	2.2905(5)	-	-
$N_{py(S)}$—Cu—$N_{py(L)}$	-	-	167.35(7)	165.57(8)
Cl**1**—Cu—Cl**2**	-	-	106.90(2)	113.58(2)
Cl**1**—Cu—N_{im}	-	-	108.83(5)	98.20(4)
Cl**2**—Cu—N_{im}	-	-	143.73(5)	147.70(5)
Cl**1**—Cu—$N_{py(L)}$	-	-	92.58(5)	93.84(5)
Cl**1**—Cu—$N_{py(S)}$	-	-	98.10(5)	97.33(5)
Cl**2**—Cu—$N_{py(S)}$	-	-	90.30(5)	91.20(5)
Cl**2**—Cu—$N_{py(L)}$	-	-	93.05(5)	92.67(5)
N_{im}—Cu—$N_{py(S)}$	-	-	90.75(7)	90.24(7)
N_{im}—Cu—$N_{py(L)}$	-	-	79.36(7)	79.12(7)

$N_{py(L)}$ = Ligand pyridinyl *N*-atom,
$N_{py(S)}$ = Pyridine *N*-atom
N_{im} = Azomethine *N*-atom.

The two obtained structures were overlaid with a root mean squared deviation (RMSD) value of 0.418 Å. This shows that **10_{py}** and **12_{py}** are closely similar in structure. A noticeable difference in conformation was brought by the ligand (aniline) phenyl ring (Figure 4.12). The N—C_{Ph} bond distance measured in **10_{py}** (1.440(3) Å) is longer than that of the free ligand (1.419(3) – 1.423(3) Å) and this could be attributed to the back-bonding feature. Furthermore, it appears that the N—C_{Ph} bond length measured in **12_{py}** (1.428(3) Å) is shorter than that of the free ligand (1.442(3) – 1.447(3) Å). An imine bond is also elongated in complexes as shown in Table 4.6, upon its ligand coordination to form a complex.[49] This trait supports what is observed as red shifts on the spectroscopic UV-vis and IR spectra.

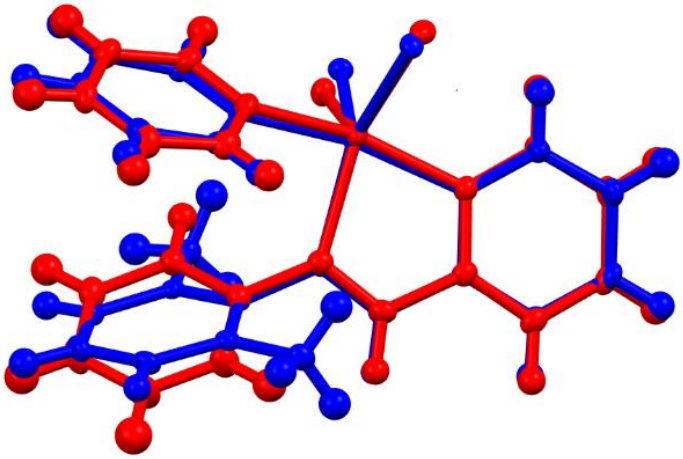

Figure 4.12: Structural overlay diagram of **10_{py}** (blue) and **12_{py}** (red)

Table 4.6: Bond lengths of free ligands (**L2** and **L3**) and **10_{py}** and **12_{py}**

Compounds	Bond distances/Å	
	N=CH	**N—Ph**
L2	1.250(3)	1.419(3)
	1.260(3)	1.423(3)
10_{py}	1.277(3)	1.440(3)
L3	1.229(5)	1.442(8)
	1.231(6)	1.447(5)
12_{py}	1.277(3)	1.428(2)

Numbers in parentheses are estimated standard deviations in the last significant figures

The dihedral angles between the phenyl ring and pyridyl moiety of the free ligands was determined to be 79.82 – 84.75° and 0.00° in **L2** and **L3**, respectively. It can be postulated that the ligand phenyl ring methyl substituents contribute to the deviation of the final ligand from structural planarity. The planarity of **L3** changed by a noticeable conformation upon coordination to 51.49° in $\mathbf{12_{py}}$. The dihedral angle between the pyridinyl and phenyl moiety was measured to be 80.65° in $\mathbf{10_{py}}$. This showed that the free ligand conformation was not greatly affected during the complexation and this is evident since the torsion angle of 80.65° in $\mathbf{10_{py}}$ was still in range (79.82 – 84.75°) for a free ligand (**L2**).

The crystal packing analysis revealed that $\mathbf{10_{py}}$ contains four mononuclear molecules (Z = 4) within its unit cells, whilst the unit cell of $\mathbf{12_{py}}$ consisted of just two mononuclear molecules (Z =2). The mononuclear $\mathbf{10_{py}}$ and $\mathbf{12_{py}}$ form three dimensional (3-D) supramolecular network structures with non-classical intermolecular C-H…Cl hydrogen bonding patterns as shown in blue for clarity in Figure 4.13. These interactions ultimately determine the packing order of a molecule.[60] The supramolecular network determines the physical and chemical properties of a complex. These properties include the melting point or decomposition temperature and biological applications of a compound.

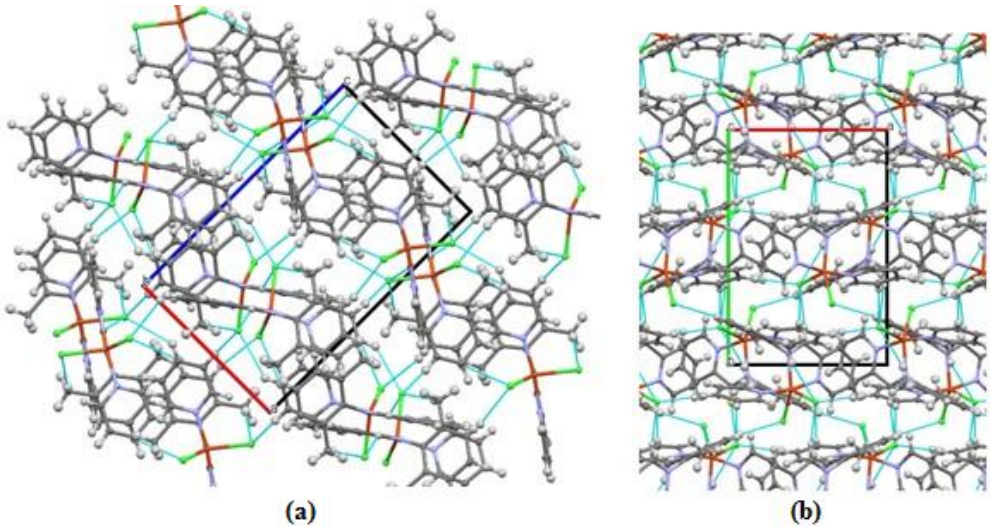

Figure 4.13: Intermolecular C—H…Cl hydrogen bonding patterns observed in the crystal packing of $\mathbf{10_{py}}$, viewed down the crystallographic (a) b- and (b) c-axis

Table 4.7 shows the H-bonding pattern across atoms within the 3-D supramolecular network structures of $\mathbf{10_{py}}$ and $\mathbf{12_{py}}$. The 3-D network was also observed as protonated Schiff base ligands and complexes are suitable for hydrogen-bonding.[59] Most importantly, the H-bonding

affecting the network structures are the electrostatic forces between the hydrogen and most electronegative chlorine atoms.

Table 4.7: Hydrogen bond information for $\mathbf{10_{py}}$ and $\mathbf{12_{py}}$

D	H	A	(D-H)/Å	(H-A)/Å	(D…A)/Å	D-H…A/°
Complex 10_{py}						
C4	H4	$Cl2^{1}$	0.95	2.82	3.643(2)	145.7
C11	H11	$Cl2^{2}$	0.95	2.78	3.650(2)	153.3
Complex 12_{py}						
C7	H7	$Cl2^{1}$	0.95	2.60	3.531(2)	165.2
C13	H13	$Cl2^{4}$	0.95	2.78	3.711(2)	168.4
C16	H16	$Cl1^{5}$	0.95	2.82	3.555(2)	135.4

^{1}-1/2+x,1/2-y,-z; ^{2}1-x,-1/2+y,1/2-z (**10_{py}**)

^{1}-1+x,+y,+z; ^{2}1-x,2-y,1-z; ^{3}-x,2-y,1-z; ^{4}1-x,1-y,1-z; ^{5}1-x,1-y,2-z (**12_{py}**)

4.3 Summary of results

Schiff base ligands **L1** – **L14** were synthesised by condensation between the phenyl amines and the corresponding phenyl carboxaldehydes. The identities of ligands (**L1** – **L14**) were established by ^{1}H- and ^{13}C-NMR and IR spectroscopic techniques. The ^{1}H-NMR of **L1** – **L14** at room temperature displayed a typical azomethine peak in the region of 8.41 – 8.89 ppm and the aromatic protons in the 6.42 – 8.81 ppm region. In the ^{13}C-NMR, imine peak ranged from 149.2 – 160.1 ppm while in the IR spectra, the peak was observed at 1614 – 1640 cm^{-1} range.

Their corresponding copper Schiff base complexes were obtained as fine powders in various colours (mostly green in colour), with high melting points and decomposition temperatures from 150 – 325 °C. The crystallographic trigonal bipyramidal structures of complex derivatives of **10** and **12** where pyridine (py) is coordinated (**10_{py}** and **12_{py}**) were obtained. All complexes were not soluble in common organic solvents, except in pyridine, DMSO and very few were completely soluble in acetonitrile (MeCN). Based on various analysis techniques, the structure of complexes was suggested to have a 1:2 metal to ligand ratio. The copper(II) Schiff base complexes were found to be relatively stable at normal room conditions. This was not the case with copper(I) Schiff base complexes, which required special storage, under inert argon atmosphere and in a vacuum-sealed desiccator, to keep the complexes stable.

References

1. M. Zbačnik, K. Pičuljan, J. Parlov-Vuković, P. Novak and A. Roodt, *Crystals*, 2017, **7**, 25.
2. N. S. Radulović, A. B. Miltojević and R. D. Vukićević, *Comptes Rendus Chimie*, 2013, **16**, 257.
3. E. M. Njogu, B. Omondi and V. O. Nyamori, *Journal of Coordination Chemistry*, 2017, **70**, 2796.
4. G. Song, L. Guo, Q. Du, W. Kong, W. Li and Z. Liu, *Journal of Organometallic Chemistry*, 2018, **858**, 1.
5. A. Mechria, S. Dridi and M. Msaddek, *Inorganica Chimica Acta*, 2015, **427**, 173.
6. V. Rosar, D. Dedeic, T. Nobile, F. Fini, G. Balducci, E. Alessio, C. Carfagna and B. Milani, *Dalton Transactions*, 2016, **45**, 14609.
7. G. Pampaloni, M. Guelfi, A. Sommazzi, G. Leone, F. Masi, S. Zacchini and G. Ricci, *Inorganica Chimica Acta*, 2019, **487**, 331.
8. B. Ž. Jovanović, M. Mišić-Vuković, A. Marinković and V. Vajs, *Journal of Molecular Structure*, 1999, **482**, 375.
9. V. V. Kouznetsov, L. Y. V. Méndez, M. Sortino, Y. Vásquez, M. P. Gupta, M. Freile, R. D. Enriz and S. A. Zacchino, *Bioorganic & Medicinal Chemistry*, 2008, **16**, 794.
10. M. Espino, M. de los Ángeles Fernández, F. J. Gomez and M. F. Silva, *Trends in Analytical Chemistry*, 2016, **76**, 126.
11. T. Baran, I. Sargin, M. Kaya and A. Menteş, *Carbohydrate Polymers*, 2016, **152**, 181.
12. M. Nikoorazm, A. Ghorbani-Choghamarani and M. Khanmoradi, *RCS Advances*, 2016, **6**, 56549.
13. G. T. Tigineh, Y. S. Wen and L. K. Liu, *Tetrahedron*, 2015, **71**, 170.
14. P. K. Kadaba, *Journal of Heterocyclic Chemistry*, 1975, **12**, 143.
15. G. T. Tigineh, Y. S. Wen and L.-K. Liu, *Tetrahedron*, 2015, **71**, 170.
16. K. Bhat, K. J. Chang, M. D. Aggarwal, W. S. Wang, B. G. Penn and D. O. Frazier, *Materials Chemistry and Physics*, 1996, **44**, 261.
17. B. Hemmateenejad, L. Emami and H. Sharghi, *Spectrochimica Acta Part A: Molecular and Biomolecular Spectroscopy*, 2010, **75**, 340.
18. T. Baran, I. Sargin, M. Kaya and A. Menteş, *Carbohydrate Polymers*, 2016, **152**, 181.
19. H. Wei, S. Chai, N. Hu, Z. Yang, L. Wei and L. Wang, *Chemical Communications*, 2015, **51**, 12178.

20. C. Chen, J. Zhang, Y. Zhang, Z. Yang, H. Wu, G. Pan and Y. Bai, *Journal of Coordination Chemistry*, 2015, **68**, 1054.
21. R. V. Singh, P. Chaudhary, S. Chauhan and M. Swami, *Spectrochimica Acta Part A: Molecular and Biomolecular Spectroscopy*, 2009, **72**, 260.
22. M. M. Abd-Elzaher, A. A. Labib, H. A. Mousa, S. A. Moustafa, M. M. Ali and A. A. El-Rashedy, *Beni-Suef University Journal of Basic and Applied Sciences*, 2016, **5**, 85.
23. M. Salehi, F. Rahimifar, M. Kubicki and A. Asadi, *Inorganica Chimica Acta*, 2016, **443**, 28.
24. I. P. Ejidike and P. A. Ajibade, *Molecules*, 2015, **20**, 9788.
25. M. Cindrić, G. Pavlović, R. Katava and D. Agustin, *New Journal of Chemistry*, 2017, **41**, 594.
26. M. Ikram, S. Rehman, F. Subhan, M. N. Akhtar and M. O. Sinnokrot, *Open Chemistry*, 2017, **15**, 308.
27. T. Baran, *Journal of Molecular Structure*, 2017, **1141**, 535.
28. T. Baran, A. Menteş and H. Arslan, *International Journal of Biological Macromolecules*, 2015, **72**, 94.
29. S. Kumari, A. Shekhar and D. D. Pathak, *RSC Advances*, 2016, **6**, 15340.
30. M. Enamullah, M. A. Quddus, M. A. Halim, M. K. Islam, V. Vasylyeva and C. Janiak, *Inorganica Chimica Acta*, 2015, **427**, 103.
31. M. Khorshidifard, H. A. Rudbari, B. Askari, M. Sahihi, M. R. Farsani, F. Jalilian and G. Bruno, *Polyhedron*, 2015, **95**, 1.
32. M. Sutradhar, L. M. D. R. S. Martins, M. F. C. Guedes da Silva and A. J. L. Pombeiro, *Applied Catalysis A: General*, 2015, **493**, 50.
33. G. Y. Nagesh and B. H. M. Mruthyunjayaswamy, *Journal of Molecular Structure*, 2015, **1085**, 198.
34. T. Baran, *Journal of Molecular Structure*, 2017, **1141**, 535.
35. S. Sujarani and A. Ramu, *Journal of Molecular Structure*, 2015, **1079**, 353.
36. T. Thirunavukkarasu, H. A. Sparkes, K. Natarajan and V. G. Gnanasoundari, *Inorganica Chimica Acta*, 2018, **473**, 255.
37. A. Gencer Imer, R. H. B. Syan, M. Gülcan, Y. S. Ocak and A. Tombak, *Journal of Materials Science: Materials in Electronics*, 2018, **29**, 898.
38. N. Raman, A. Kulandaisamy, C. Thangaraja, P. Manisankar, S. Viswanathan and C. Vedhi, *Transition Metal Chemistry*, 2004, **29**, 129.

39. T. Kiran, V. G. Prasanth, M. M. Balamurali, C. S. Vasavi, P. Munusami, K. I. Sathiyanarayanan and M. Pathak, *Inorganica Chimica Acta*, 2015, **433**, 26.
40. M. Salehi, F. Rahimifar, M. Kubicki and A. Asadi, *Inorganica Chimica Acta*, 2016, **443**, 28.
41. P. Chakraborty, S. Purkait, S. Mondal, A. Bauzá, A. Frontera, C. Massera and D. Das, *Crystals Engineering Communications*, 2015, **17**, 4680.
42. P. Chattaraj, *The Journal of Physical Chemistry A*, 2001, **105**, 511.
43. R. M. LoPachin, T. Gavin, A. DeCaprio and D. S. Barber, *Chemical Research in Toxicology*, 2012, **25**, 239.
44. R. Herrera, A. Nagarajan, M. A. Morales, F. Méndez, H. A. Jiménez-Vázquez, L. G. Zepeda and J. Tamariz, *The Journal of Organic Chemistry*, 2001, **66**, 1252.
45. Y. Zhang, J. Fan, B. Yang and L. Ma, *Chemical Engineering Journal*, 2017, **326**, 612.
46. C. Chen, J. Zhang, Y. Zhang, Z. Yang, H. Wu, G. Pan and Y. Bai, *Journal of Coordination Chemistry*, 2015, **68**, 1054.
47. I. P. Ejidike and P. A. Ajibade, *Molecules*, 2015, **20**, 9788.
48. T. Baran, A. Menteş and H. Arslan, *International Journal of Biological Macromolecules*, 2015, **72**, 94.
49. M. Ghosh, M. Layek, M. Fleck, R. Saha and D. Bandyopadhyay, *Polyhedron*, 2015, **85**, 312.
50. L. H. Abdel-Rahman, N. M. Ismail, M. Ismael, A. M. Abu-Dief and E. A. H. Ahmed, *Journal of Molecular Structure*, 2017, **1134**, 851.
51. L. M. Martins, S. Hazra, M. F. C. G. da Silva and A. J. Pombeiro, *RSC Advances*, 2016, **6**, 78225.
52. Y. X. Chi, H. P. Dai, S. M. Li, J. Jin, S. Y. Niu and G. N. Zhang, *Spectrochimica Acta Part A: Molecular and Biomolecular Spectroscopy*, 2013, **106**, 203.
53. S. Kathiresan, S. Mugesh, J. Annaraj and M. Murugan, *New Journal of Chemistry*, 2017, **41**, 1267.
54. N. S. Abdel-Kader, A. L. El-Ansary, T. A. El-Tayeb and M. M. F. Elnagdi, *Journal of Photochemistry and Photobiology A: Chemistry*, 2016, **321**, 223.
55. L. Barhács, M. Czaun, E. Speier, G. Speier, B. Noll and C. Pierpont, *Zeitschrift für Kristallographie-New Crystal Structures*, 2000, **215**, 193.
56. C. Biewer, C. Hamacher, A. Kaiser, N. Vogt, A. Sandleben, M. T. Chin, S. Yu, D. A. Vicic and A. Klein, *Inorganic Chemistry*, 2016, **55**, 12716.

57. S. Alapour, S. Zamisa, J. Silva, C. Alves, B. Omondi, D. Ramjugernath and N. Koorbanally, *Crystals Engineering Communications*, 2018, **20**, 2316.
58. E. Q. Gao, Y. F. Yue, S. Q. Bai, Z. He and C. H. Yan, *Crystal Growth & Design*, 2005, **5**, 1119.
59. J. J. Braymer, N. M. Merrill and M. H. Lim, *Inorganica Chimica Acta*, 2012, **380**, 261.
60. R. Fekri, M. Salehi, A. Asadi and M. Kubicki, *Polyhedron*, 2017, **128**, 175.

Chapter 5

5 Biological studies

This chapter describe methods employed in the biological studies of Cu(I) and Cu(II) pyridinyl Schiff base complexes. This includes testing of the antibacterial activities of the subjected compounds. Finally, the antibacterial activity of the organometallic complexes is discussed in relation to their structural variations.

5.1 Antimicrobial of Cu(I) and Cu(II) complexes

L3, metal salts (CuCl and $CuCl_2$), and 15 copper complexes (**1** – **15**) were tested for their antibacterial potency, *i.e.*, against four gram-negative bacteria (namely: *E. coli* (Ec), *P. aeruginosa* (Pa), *K. pneumonia* (Kp), and *S. typhimurium* (St)) and two gram-positive bacteria (namely: *S. aureus* (Sa) and MRSA). The results are presented in **Error! Reference source not found.**. The CuCl metal salt only demonstrated antibacterial activity against the *S. typhimurium* bacterium, whilst **L3** was active against the *E. coli* and MRSA bacteria. Most of the Cu(I) complexes showed very weak or no activities. For this reason, the MIC values of Cu(I) Schiff base complexes (**1** – **7**) were not further determined.

The Cu(I) Schiff base complexes are very unstable. It is likely that their ligands decoordinate in solution medium, preventing their permeation into the cells which leads to poor activity. Moreover, the bacterial defence mechanism against Cu(I) is pronounced, since it can readily bind with thiolates.[1] This could be a reason why all tested Cu(I) Schiff base complexes (**1** – **7**) exhibited very little or no antibacterial activities (Table 5.1). However, this is not the case with Cu(II) complexes.

Table 5.1: Antibacterial activity of CuCl, **L3**, and Cu(I) complexes at 1 mg mL^{-1}

Compound	Gram -ve				Gram +ve	
	Ec	**Pa**	**St**	**Kp**	**MRSA**	**Sa**
CuCl	**-**	**-**	**A**	**-**	**-**	**-**
L3	**A**	**-**	**-**	**-**	**A**	**-**
1	**A**	**-**	**-**	**-**	**-**	**-**
2	**-**	**-**	**-**	**-**	**-**	**-**
3	**-**	**-**	**-**	**-**	**-**	**-**
4	**-**	**-**	**-**	**-**	**-**	**-**
5	**-**	**-**	**-**	**-**	**-**	**-**
6	**-**	**-**	**-**	**-**	**-**	**-**
7	**-**	**-**	**A**	**-**	**-**	**-**

(A): activity; (-): no activity

E. coli (Ec), *P. aeruginosa* (Pa), *K. pneumonia* (Kp), and *S. typhimurium* (St)), and *S. aureus* (Sa)

The synthesised Cu(II) Schiff base complexes showed greater antibacterial activity against subjected bacteria (Table 5.2). The results revealed that the $CuCl_2$ is effective against three gram-negative bacteria, except the *K. pneumonia* bacteria. However, it did not show any potency against gram-positive bacteria. The Cu(II) Schiff base complexes are quite stable even in solution medium. These Cu(II) complexes have better antibacterial potency against the studied bacteria than $CuCl_2$. This could be due to the low degree at which the metal centre and ligands dissociate in DMSO solution to afford free copper ion, thus disrupting the biochemical pathways in a microorganism.[2] Based on their initial antibacterial screening results presented in Table 5.2, **L3**, $CuCl_2$, and Cu(II) Schiff base complexes (**8** – **15**) were further tested to determine their minimum inhibitory concentration (MIC) values.

Table 5.2: Antibacterial activity of $CuCl_2$, **L3** and Cu(II) complexes at 1 mg mL^{-1}

Compound	Gram -ve				Gram +ve	
	Ec	**Pa**	**St**	**Kp**	**MRSA**	**Sa**
$CuCl_2$	**A**	**A**	**A**	**-**	**-**	**-**
L3	**A**	**-**	**-**	**-**	**A**	**-**
8	**A**	**A**	**A**	**-**	**-**	**-**
9	**A**	**A**	**A**	**-**	**-**	**A**
10	**A**	**A**	**A**	**A**	**A**	**-**
11	**A**	**A**	**A**	**A**	**A**	**-**
12*	**A**	**A**	**A**	**A**	**A**	**-**
13	**-**	**-**	**A**	**-**	**-**	**-**
14	**A**	**-**	**-**	**-**	**-**	**-**
15	**A**	**A**	**A**	**-**	**-**	**-**

(A): activity; (-): no activity

E. coli (Ec), *P. aeruginosa* (Pa), *K. pneumonia* (Kp), and *S. typhimurium* (St)), and *S. aureus* (Sa)

12*: parent complex

The MICs of **L3**, metal salt ($CuCl_2$) and Cu(II) Schiff base complexes (**8** – **15**) were determined using Broth dilution method as explained in Chapter 3, and results are presented in Table 5.3. Unlike the standard drug, which was active against all six strains, the Cu(II) complexes were inactive against one or more of the bacteria. **10**, **11** and **12** are active against the *K. pneumoniae* bacteria. **9** was the only compound which was active against the *S. aureus* bacteria. The results revealed that the antibacterial potency of **12** is enhanced over its precursor, pyridinyl Schiff base ligand (**L3**). **11** is active against the *P. aeruginosa*, *S. typhimurium*, MRSA and *K. pneumoniae*, and *P. aeruginosa*, with MIC values in the 0.20 – 25.0 µg mL^{-1} range. **12** and the ciprofloxacin standard reference revealed similar MIC values against the *S. typhimurium*.

Gram-positive bacteria (*S. aureus* and MRSA), and gram-negative bacteria (*K. pneumoniae*) are resistant towards **8**, **13**, **14**, and **15**. *E. coli* bacterium was less susceptible towards the studied complexes, except for **9** (Table 5.3) which demonstrated the same activity (MIC value of 0.20 µg mL^{-1}) with the ciprofloxacin standard drug. **13** and **14** are the least active complexes against studied bacteria. In comparison to the ciprofloxacin, **13** and **14** recorded higher MIC values against the *S. typhimurium* and *E. coli* bacteria, respectively.

Table 5.3: MIC (μg mL^{-1}) values of $CuCl_2$, **L3** and copper(II) complexes

Compound	Gram -ve				Gram +ve	
	Ec	**Pa**	**St**	**Kp**	**MRSA**	**Sa**
$CuCl_2$	**12.5**	**100**	**50.0**	**-**	**-**	**-**
L3	**100**	**-**	**-**	**-**	**50.0**	**-**
8	**50.0**	**50.0**	**25.0**	**-**	**-**	**-**
9	**0.20**	**50.0**	**12.5**	**-**	**-**	**1.60**
10	**12.5**	**25.0**	**0.80**	**0.80**	**1.60**	**-**
11	**25.0**	**0.40**	**0.20**	**0.40**	**0.40**	**-**
12*	**12.5**	**0.40**	**0.40**	**0.20**	**0.20**	**-**
13	**-**	**-**	**12.5**	**-**	**-**	**-**
14	**6.30**	**-**	**-**	**-**	**-**	**-**
15	**3.10**	**12.5**	**12.5**	**-**	**-**	**-**
Ciprofloxacin	**0.20**	**0.80**	**0.40**	**1.60**	**25.0**	**25.0**

(-): No activity, 12*: parent complex

E. coli (Ec), *P. aeruginosa* (Pa), *K. pneumonia* (Kp), and *S. typhimurium* (St)), and *S. aureus* (Sa)

L3 was only active against the *E. coli* and MRSA compared to **12** (parent complex) which showed antibacterial activities towards all tested bacteria, except *S. aureus* (Sa) (**Error! Reference source not found.**). **L3** displayed lower potency than **12**, which had higher MIC values. The enhanced antibacterial activities of **12** as compared to **L3** can be explained in two ways, namely; Overtone's concept and the Tweedy's chelation theory.[3-10] According to Overtone's theory of cell permeability, the liposolubility of complexes enhances their interactions with the lipid membrane of a bacteria, whilst the polarity of a metal centre is greatly reduced on chelation since the charge is neutralised by the donor atoms of coordinated ligands.[11]

Out of all the examined complexes, **10**, **11** and **12** produced appreciable activities towards five bacteria, except the *S. aureus* bacteria. **10** and **11** have methyl groups on the phenyl ring of the ligands, whilst the only difference is the pyridine and quinoline moieties, for **10** and **11**, respectively. The parent complex (**12**) has the pyridine moiety and does not have any substituents on the aryl aniline. Hence, their activities could be due to their ability to easily diffuse through the membrane of bacteria, aided by the size, hydrogen bonding, solubility and electronic effects of **10**, **11** and **12**.[12,13] Thus, the antibacterial potency of these complexes is

largely determined by the structural attributes of a coordinated ligands.[8] However, the quinoline moiety in **11** and the aniline methyl groups in **10**, does not seem to affect the antibacterial activities when compared to the parent complex (**12**).

The hydrophobic and hydrophilic properties and the outermost membrane characteristic of a bacteria play a role in antibacterial activities of complexes. In this case, the alkyl (EDG) substituted ligands *e.g.* tertiary butyl substituted (**L10**), formed complexes that are more hydrophobic, enabling greater affinity towards the microbial bilayer membrane. This leads to bactericidal activities of complexes by multiple mechanisms, mostly by binding to the bacterial cell membrane and transporting the compound to the inner organelles.[14-16] In this case, the complexes **13**, **14** and **15** with EWG (Cl, Br or NO_2) substituents yielded better antibacterial activities towards the gram-positive bacteria. This could be attributed to the lipophilic properties of the complexes which enabled them to bind and disrupt the lipophilic cell wall and proteins of the bacteria.[17] This tendency was not observed in the parent (neutral) complex (**12**), which is active against all, except the gram-positive (*S. aureus*) bacteria. Therefore, the chemical constituents of a bacterial outer membrane play a role in antibacterial activities of the subjected complex.

None of the tested copper Schiff bases complexes were active in all tested strains. The Cu(II) Schiff base complexes demonstrated low MIC values. However, the parent complex (**12**) recorded lower MIC values (Table 5.3). This was expected since **12** is neutral (coordinated ligand is unsubstituted) and does not show any specific preference to the binding of either the gram-negative or gram-positive bacteria based on their outer most membrane.

The tested Cu(II) Schiff base complexes, including the parent complex (**12**) showed more potency towards the gram-negative bacteria than the gram-positive ones. This may be due to the differences in bacterial cell walls. The cell wall of gram-negative bacteria has an extra lipid bilayer. This, in turn, favours the permeation of lipophilic compounds.[2,18] The gram-negative bacteria are usually responsible for several health-related issues, *e.g.*, some *E coli* bacterial strains have been reported to cause food and blood poisoning, pneumonia, urinary tract infections, and diarrhoea, amongst other diseases.[19] These results are somehow be indicative of structures that are potent towards bacteria, especially the gram-negative strains. Thus, going forward, these results could pave a way for the better design of compounds with biological potential and also, providing a good direction for better organometallic structural design as structural templates for design of antimicrobial agents.

5.2 Summary of the biological application results

The synthesised and characterised compounds (ligand and complexes) were tested for their antibacterial potency against six bacteria. Out of six bacteria, four gram-negative bacteria were *E. coli*, *P. aeruginosa*, *S. typhimurium*, and *K. pneumonia*, while two gram-positive bacteria were *S. aureus* and MRSA. Upon comparison of **L3** and **12**, it was found that **12** showed greater antibacterial activities than the precursor organic ligand (**L3**). Furthermore, the studied bacteria were established to be more susceptible to Cu(II) Schiff base complexes.

The test compounds were not active in all strains of bacteria. **10**, **11** and **12** showed bactericidal activities against all, except the *S. aureus* bacterium. Results showed that unsubstituted ligands form complexes with higher biological activities. The introduction of the quinoline moiety for the pyridine ring has no effect on the antimicrobial activity. Further, gram-negative bacteria were the most susceptible to the test compounds. Lastly, some of the Cu(II) Schiff base complexes that were subjected to the MIC studies had lower MIC values in comparison with the ciprofloxacin which used as a standard reference.

References

1. X. Hao, F. Lüthje, R. Rønn, N. A. German, X. Li, F. Huang, J. Kisaka, D. Huffman, H. A. Alwathnani, Y. G. Zhu and C. Rensing, *Molecular Microbiology*, 2016, **102**, 628.
2. E. M. Njogu, B. S. Martincigh, B. Omondi and V. O. Nyamori, *Applied Organometallic Chemistry*, 2018, **32**, e4554.
3. K. Singh, Y. Kumar, P. Puri, M. Kumar and C. Sharma, *European Journal of Medicinal Chemistry*, 2012, **52**, 313.
4. O. A. El-Gammal, M. M. Bekheit and M. Tahoon, *Spectrochimica Acta Part A: Molecular and Biomolecular Spectroscopy*, 2015, **135**, 597.
5. R. Murcia, S. Leal, M. Roa, E. Nagles, A. Muñoz-Castro and J. Hurtado, *Molecules*, 2018, **23**, 2013.
6. M. T. Kaczmarek, M. Zabiszak, M. Nowak and R. Jastrzab, *Coordination Chemistry Reviews*, 2018, **370**, 42.
7. C. Giri, P. K. Sahoo, R. Puttreddy, K. Rissanen and P. Mal, *Chemistry–A European Journal*, 2015, **21**, 6390.
8. R. Fekri, M. Salehi, A. Asadi and M. Kubicki, *Polyhedron*, 2017, **128**, 175.
9. D. Sriram, P. Yogeeswari, N. S. Myneedu and V. Saraswat, *Bioorganic & Medicinal Chemistry Letters*, 2006, **16**, 2127.
10. M. Cindrić, G. Pavlović, R. Katava and D. Agustin, *New Journal of Chemistry*, 2017, **41**, 594.
11. K. Singh, R. Thakur and V. Kumar, *Beni-Suef University Journal of Basic and Applied Sciences*, 2016, **5**, 21.
12. G. M. Decad and H. Nikaido, *Journal of Bacteriology*, 1976, **128**, 325.
13. T. D. Davis, C. J. Gerry and D. S. Tan, *American Chemical Society: Chemical Biology*, 2014, **9**, 2535.
14. M. Zbačnik, K. Pičuljan, J. Parlov-Vuković, P. Novak and A. Roodt, *Crystals*, 2017, **7**, 25.
15. T. Baran, *Journal of Molecular Structure*, 2017, **1141**, 535.
16. A. M. Abu-Dief and L. A. E. Nassr, *Journal of the Iranian Chemical Society*, 2015, **12**, 943.
17. C. O. Kappe and D. Dallinger, *Nature Reviews Drug Discovery*, 2006, **5**, 51.
18. M. Nikoorazm, A. Ghorbani-Choghamarani and M. Khanmoradi, *RCS Advances*, 2016, **6**, 56549.

19. Y. Zhang, X. Liu, Y. Wang, P. Jiang and S. Quek, *Food Control*, 2016, **59**, 282.

Chapter 6

6 Conclusion and future work

Cu(I) and Cu(II) Schiff base complexes were successfully prepared by using two copper metal salts and evaluated in detail. The characterisation techniques employed included techniques, such as ^{1}H-NMR, ^{13}C-NMR, IR, UV-Vis, ESI-MS, EA, TGA/DSC and SC-XRD. Furthermore, the synthesised **L3** and 15 complexes (**1** – **15**) were evaluated for their antibacterial potency against four gram-negative and two gram-positive bacteria.

6.1 Synthesis summary

One quinoline Schiff base and 13 derivatives of pyridinyl Schiff base ligands were designed and synthesised. The ligands (**L1** – **L14**) were synthesised *via* a solvent-free grinding technique where aniline or its substituted derivatives and an appropriate carboxaldehyde was neatly ground together using a mortar and pestle. The synthesis of **L3** and **L11** – **L14** was carried out by means of both the solvent-free grinding and microwave-assisted (MW-assisted) approaches for comparison of the two techniques. Both techniques were found to be easy, timeous, high yielding, clean and economically viable. However, the solvent-free grinding technique was found to be a better technique because it is relatively greener, unlike the MW-assisted technique which uses a solvent and energy, and thus is relatively expensive.

Out of 14 synthesised ligands, **L1** – **L10** were used to synthesise of 15 Schiff base copper(I) and copper(II) complexes that were evaluated for their antibacterial activity. The copper(I) and copper(II) complexes were synthesised *via* a conventional technique, with either a two-stage or one-pot approach, where an appropriate ligand and metal salt was reacted under inert argon atmosphere in a Schlenk line apparatus. The complexation techniques both gave high yields and are considered green. The two-stage method is a better approach since it gave relatively higher yields and can be used in the synthesis of both Cu(I) and Cu(II) Schiff base complexes.

6.2 Antibacterial evaluation summary

1 – **7** were tested for their antibacterial activities and found to exhibit little to no activity. Hence, no further tests were conducted at lower concentrations. However, the Cu(II) complexes revealed appreciable antibacterial activities. For this reason, the MIC of **8** – **15**, **L3** and $CuCl_2$ were tested by means of the dilution method. Most of tested complexes had higher MIC values than the parent complex (**12**). All tested compounds did not demonstrate wide-spectrum antibacterial activities. **10**, **11** and **12** showed appreciable activities towards five bacteria, except the *Staphylococcus aureus* bacterium. The results implied that neutral (unsubstituted) ligands form complexes with higher activities and that the introduction of a quinoline moiety in place of pyridinyl ring did not significantly affect their antibacterial activities. It is noteworthy that the gram-negative bacteria were more susceptible to the tested complexes. Gram-negative bacteria lack a cell wall but consist of a lipid bilayer outer membrane. This could be the reason why they were more susceptible, as these complexes can easily diffuse into the microbes as a result of their high affinity towards the lipid outer membrane. The substituents on the Schiff base ligands, as well as increasing either the EDG or EWG density on the ligands of the complexes, decreased their biological activities.

6.3 Recommendations and future work

Since copper(I) complexes may easily oxidise, disproportionate or even substitute for ligands in DMSO solvent, stabilising ligands may be employed first before their biological studies are carried out to ensure a true reflection of results. Similarly, ligands with soft sulphur- or phosphorous-donor atoms can be coordinated to copper(I) to improve the stability of the Cu(I) Schiff base complexes. The mechanisms of action of the tested complexes will need to be studied for a better understanding and in order to design future compounds.

With the knowledge that **9** – **12** showed higher antibacterial activities, copper centres with different (apart from the chloride anions) counter ions of Cu(I) and Cu(II) Schiff base complexes can be synthesised to investigate their effect in structural and biological activities. Also, the Schiff base ligands can then be appended with biologically active molecules (BAMs) with known antibacterial activities and mechanisms of action. The appended BAMs will enable the complexes to specifically target desired enzymes within a bacterium. This might result in improved activity of complexes with less or no downsides. Furthermore, other metal centres, like ruthenium and rhenium, may be used during complexation.

The very same compounds can be tested for other biological activities, i.e., anticancer, antifungal, antioxidant and antibiofilm. Not only do they have huge potency in pharmacological evaluations, but in catalysis too, thus, they can be employed as catalysts in homogeneous reactions, for example, in octane oxidation reactions. Lastly, they can also be evaluated as catalysts in the polymerisation of environmentally friendly polymers with slight structural modifications or along with benzyl alcohol (BnOH) as an initiator. Thus, there is much scope for testing these or similar complexes for a number of different applications.

Appendix A

IR spectra

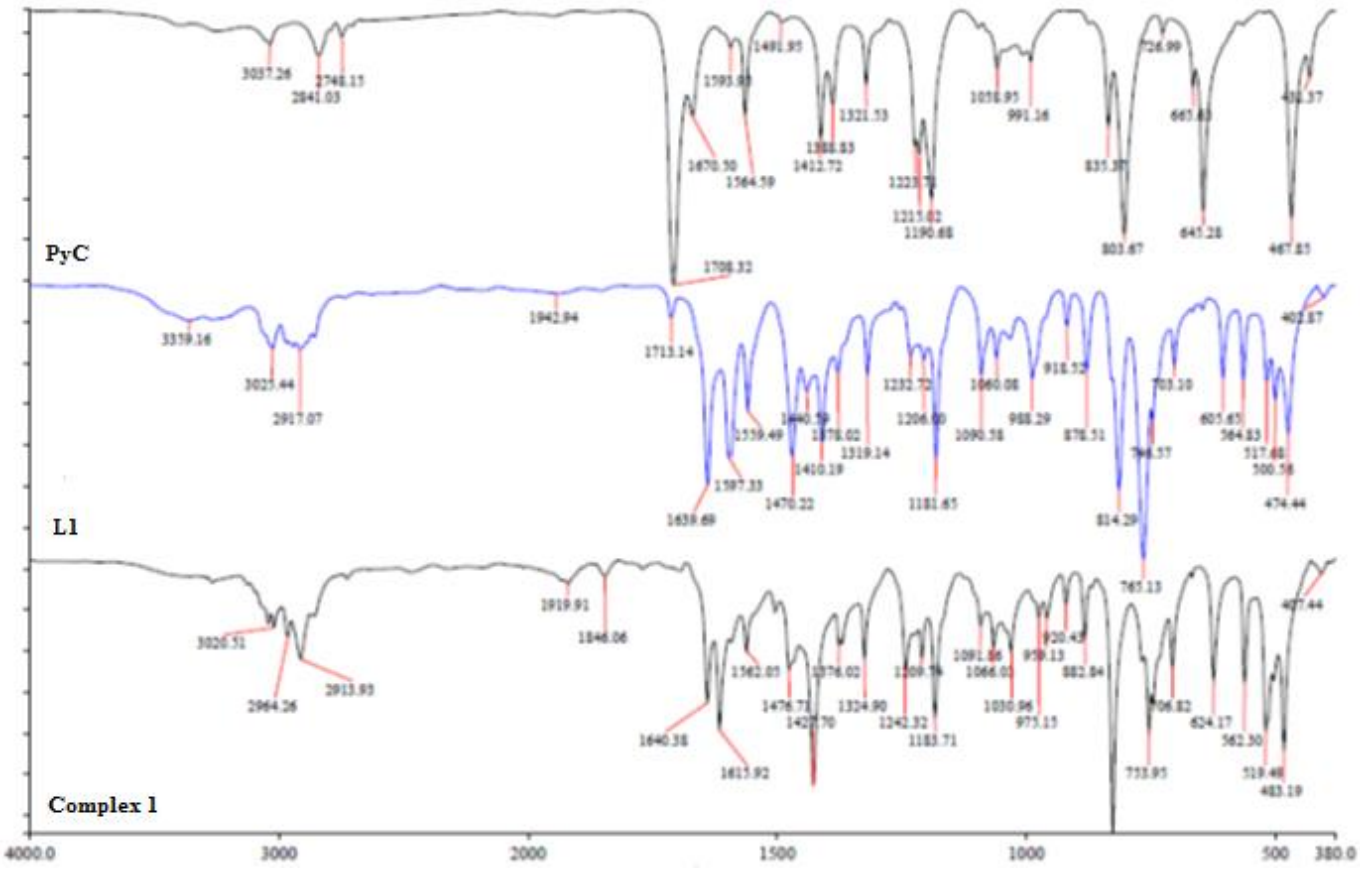

A1: Stacked IR of ligand (**L1**) and complex **1**

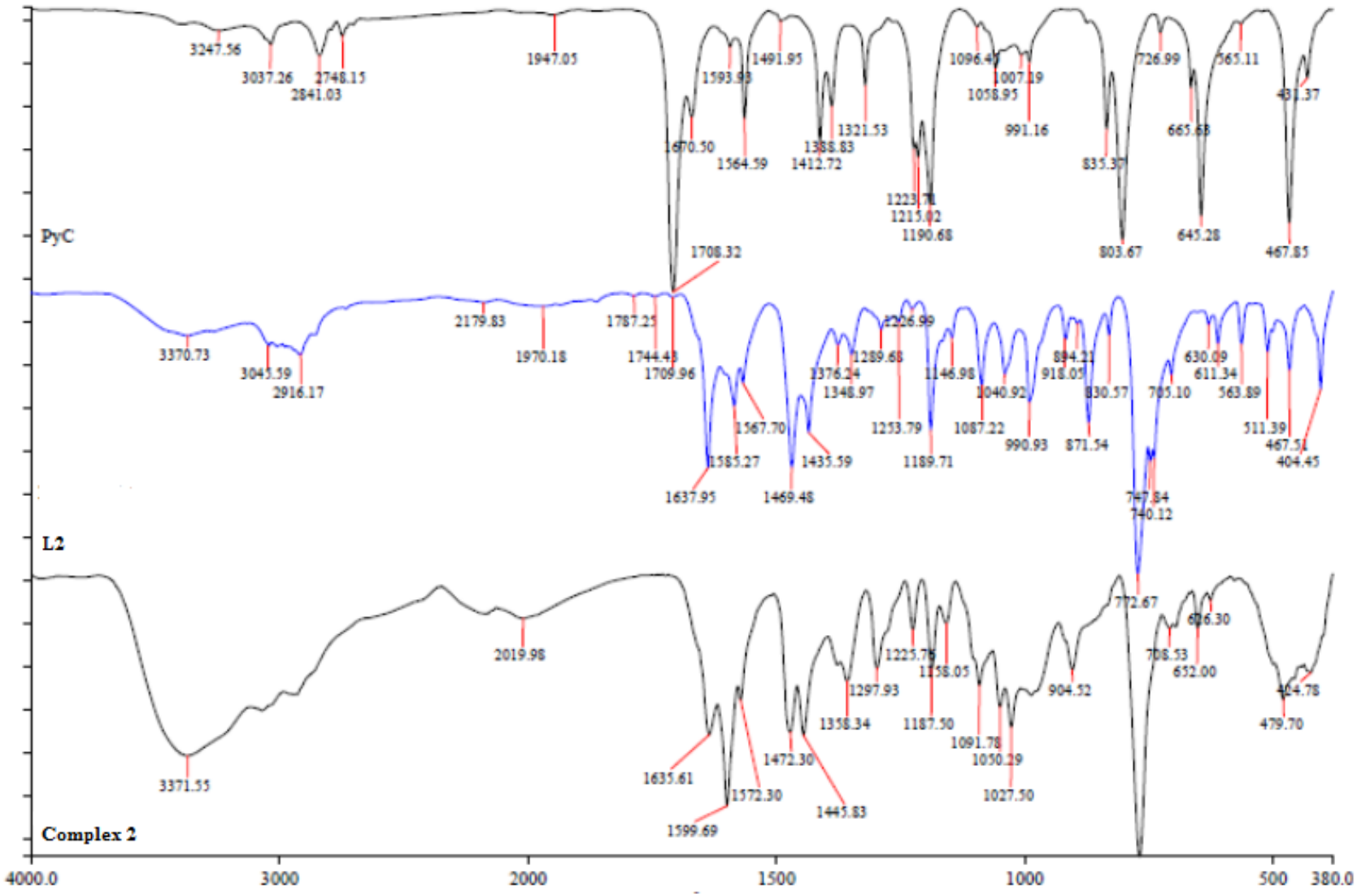

A2: Stacked IR of ligand (**L2**) and complex **2**

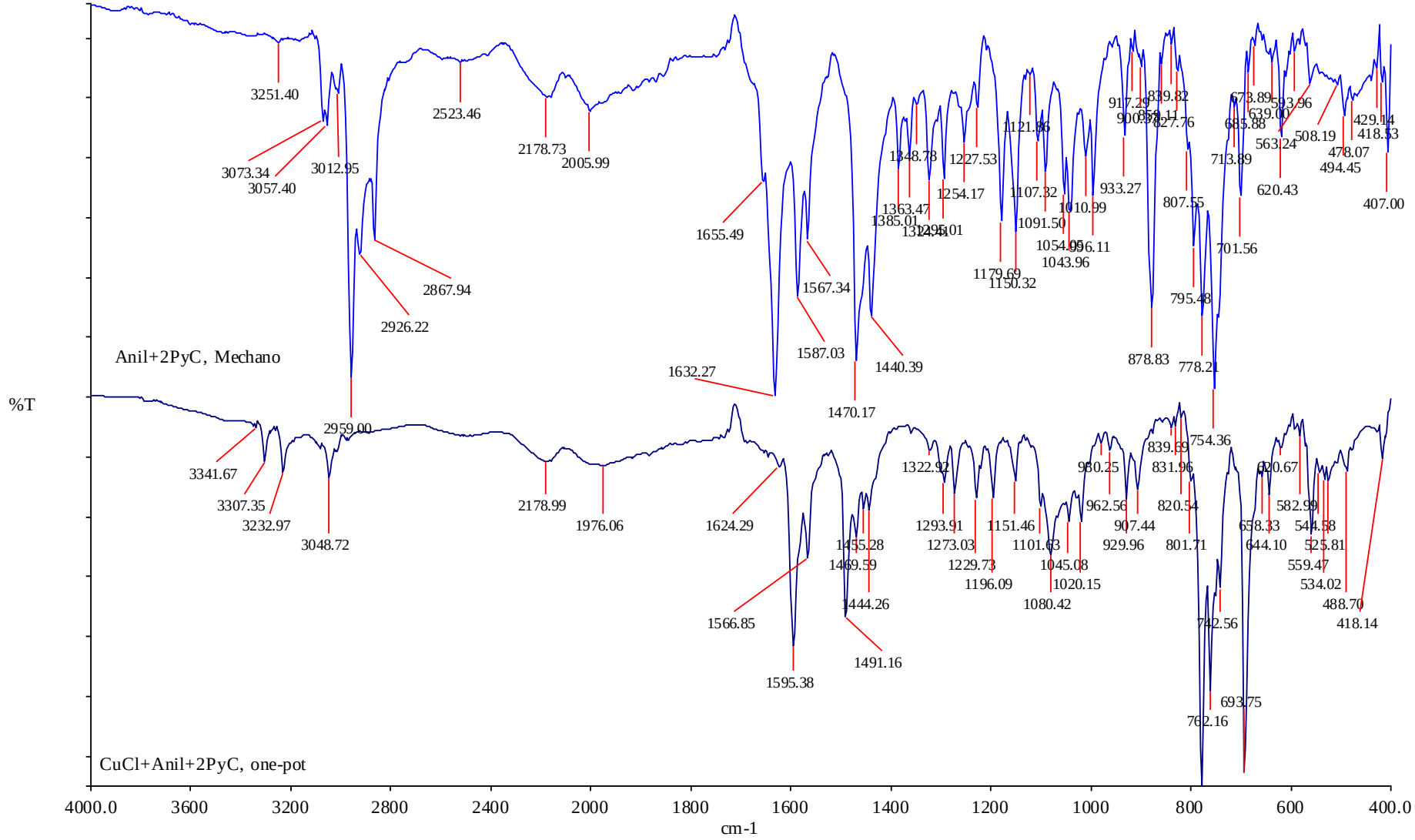

A3: Stacked ligand **(L3)** and complex **3**

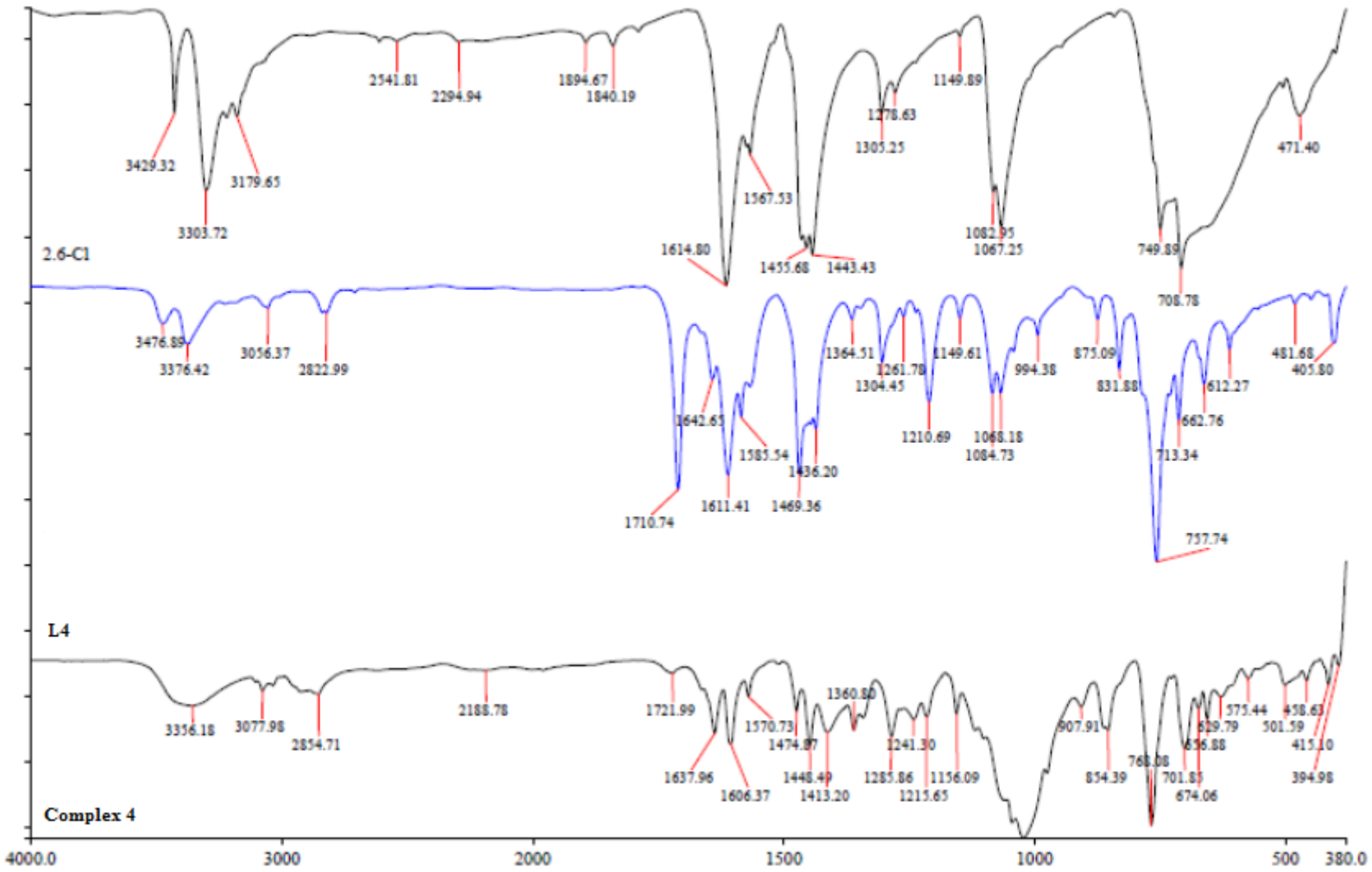

A4: Stacked IR spectre of ligand (**L4**) and complex **4**

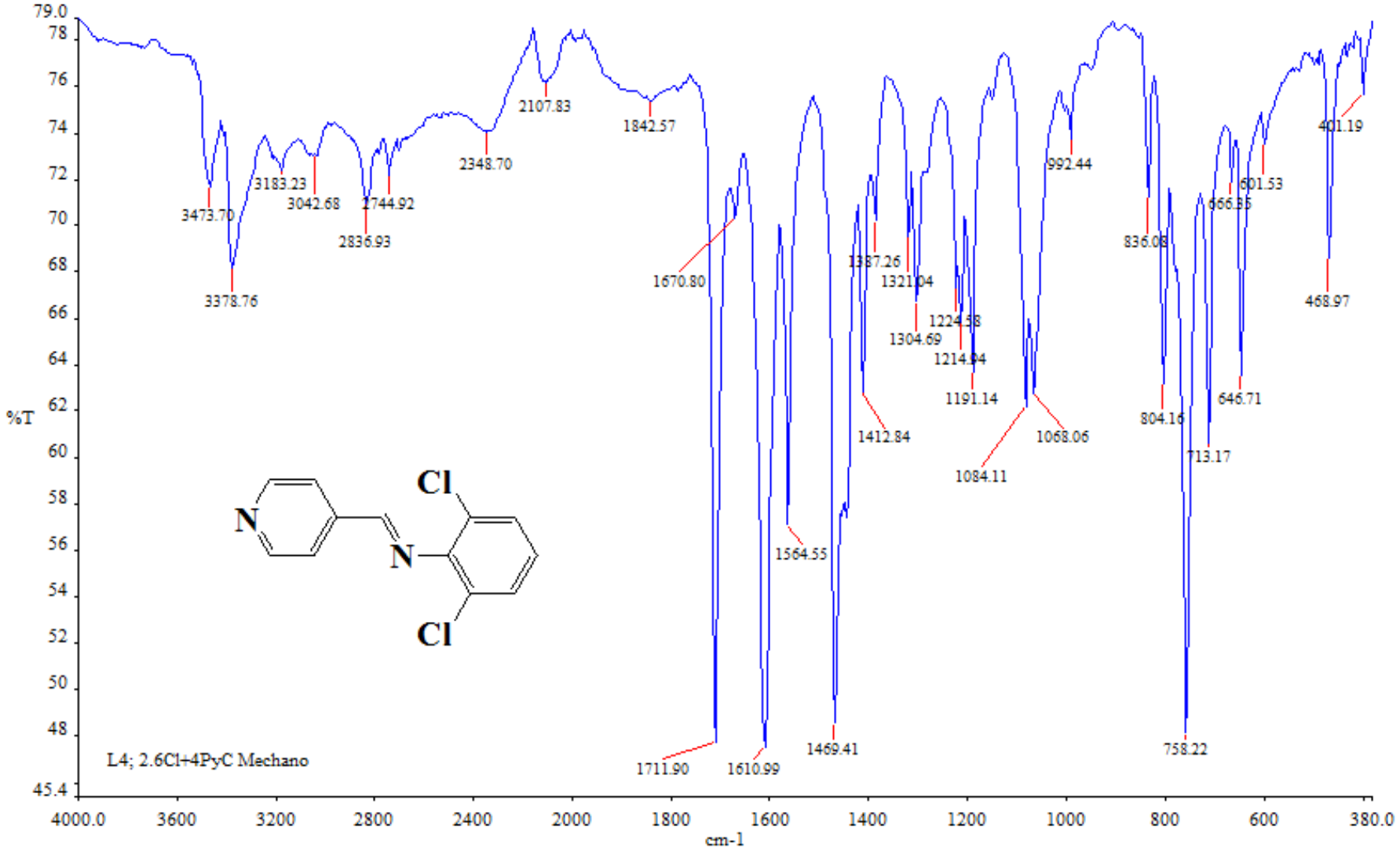

A5: IR spectrum of ligand (**L5**)

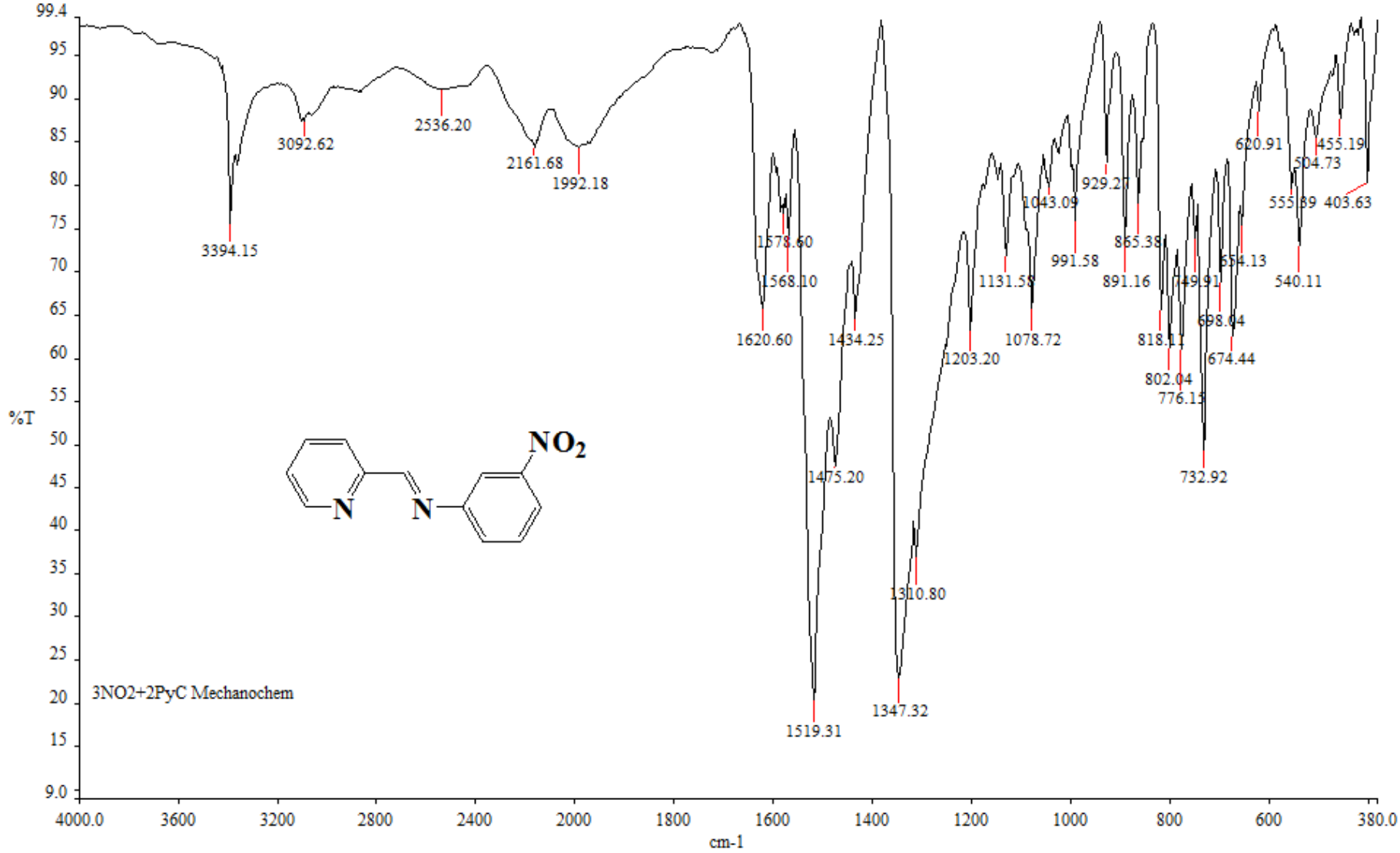

A6: IR spectrum of ligand (**L6**)

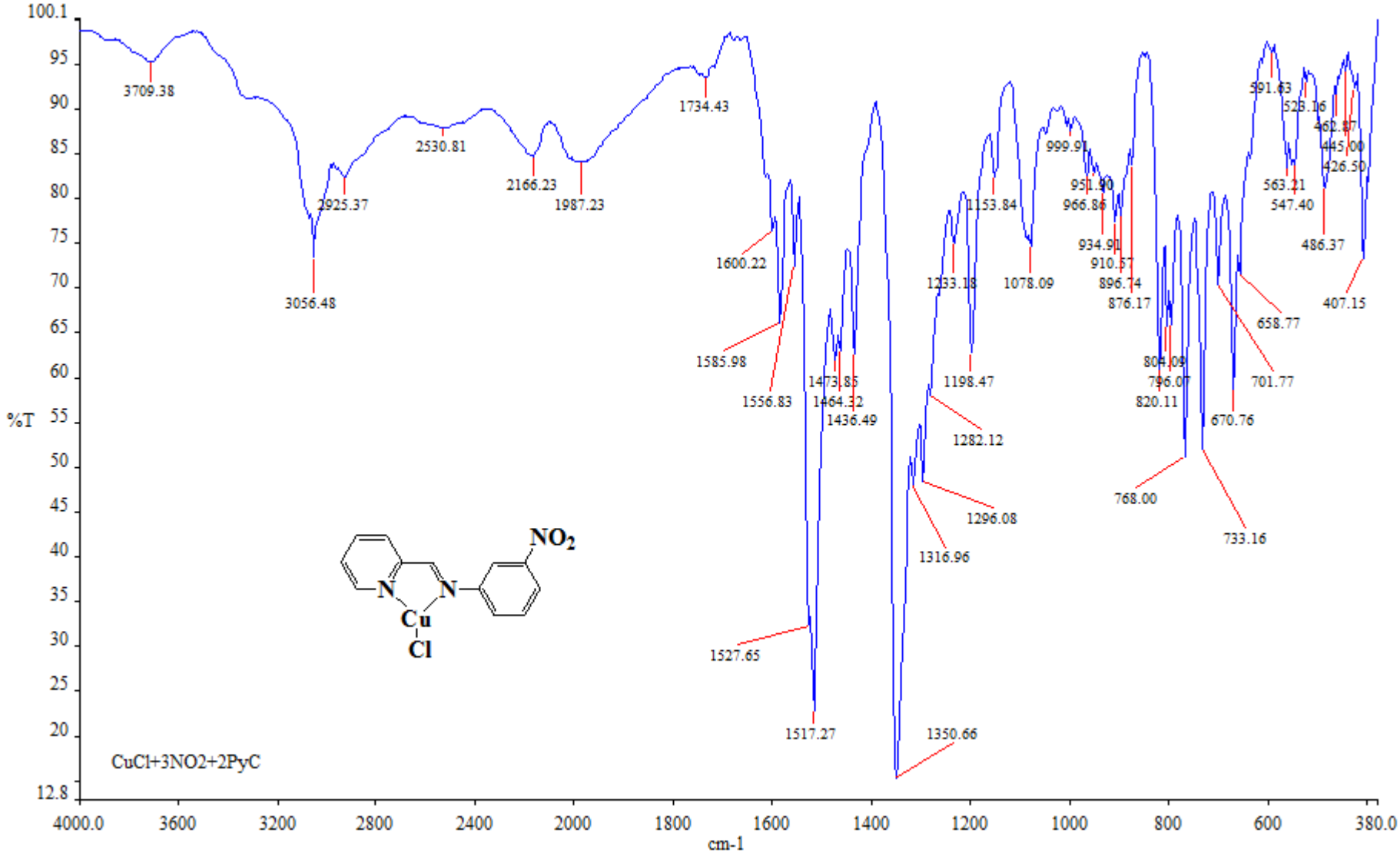

A7: IR spectrum of complex **6**

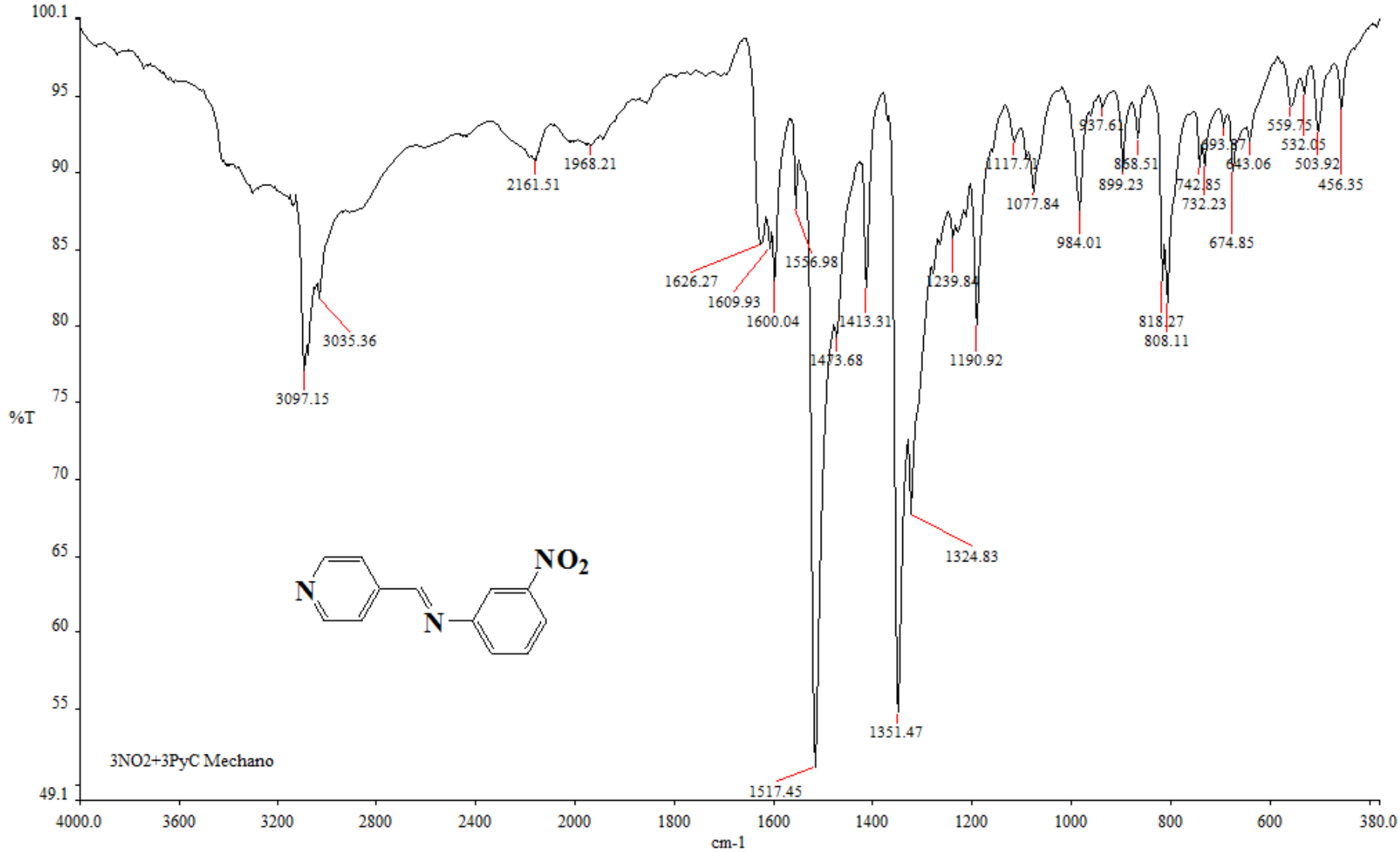

A8: IR spectrum of ligand (**L7**)

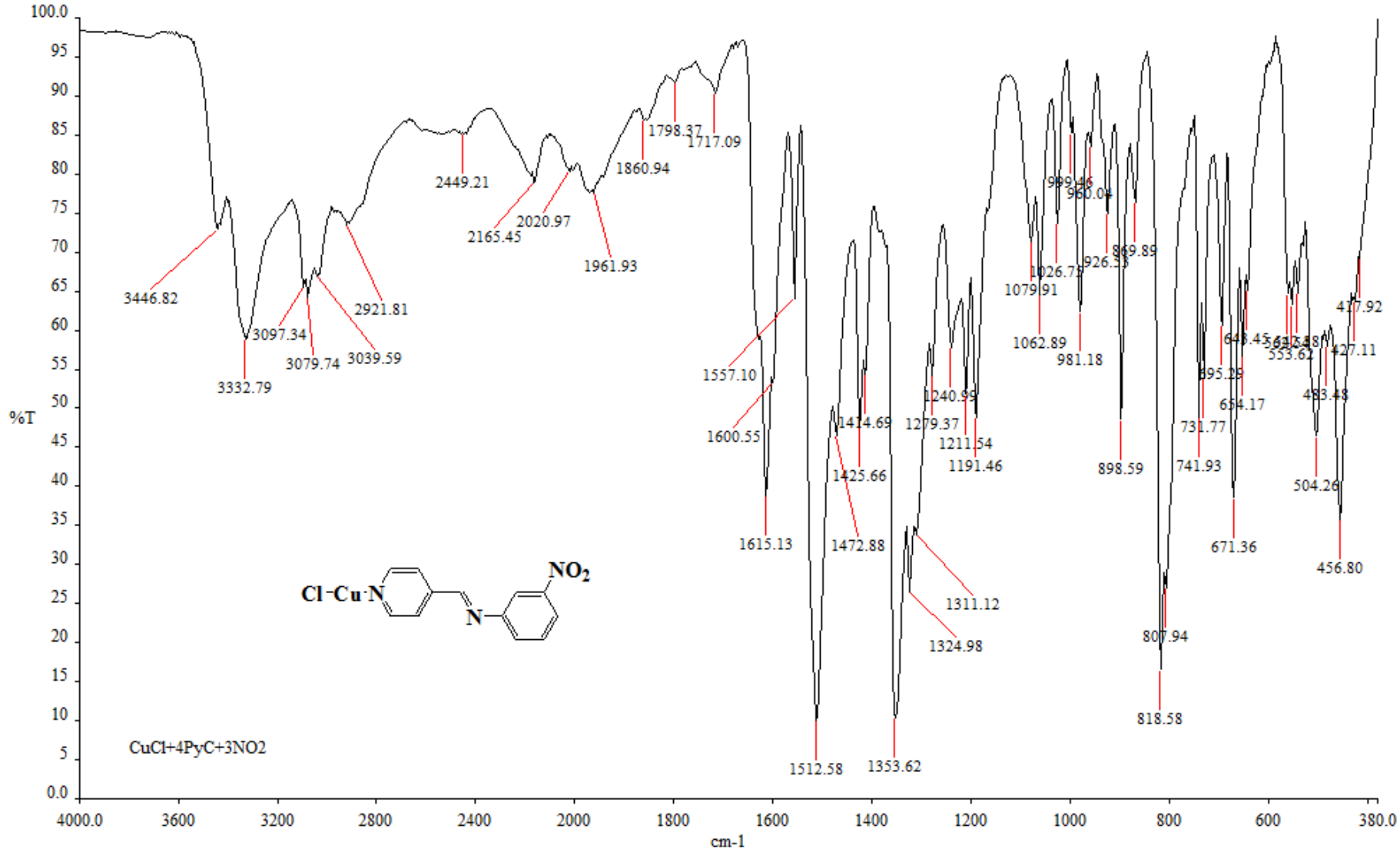

A9: IR spectrum of complex **7**

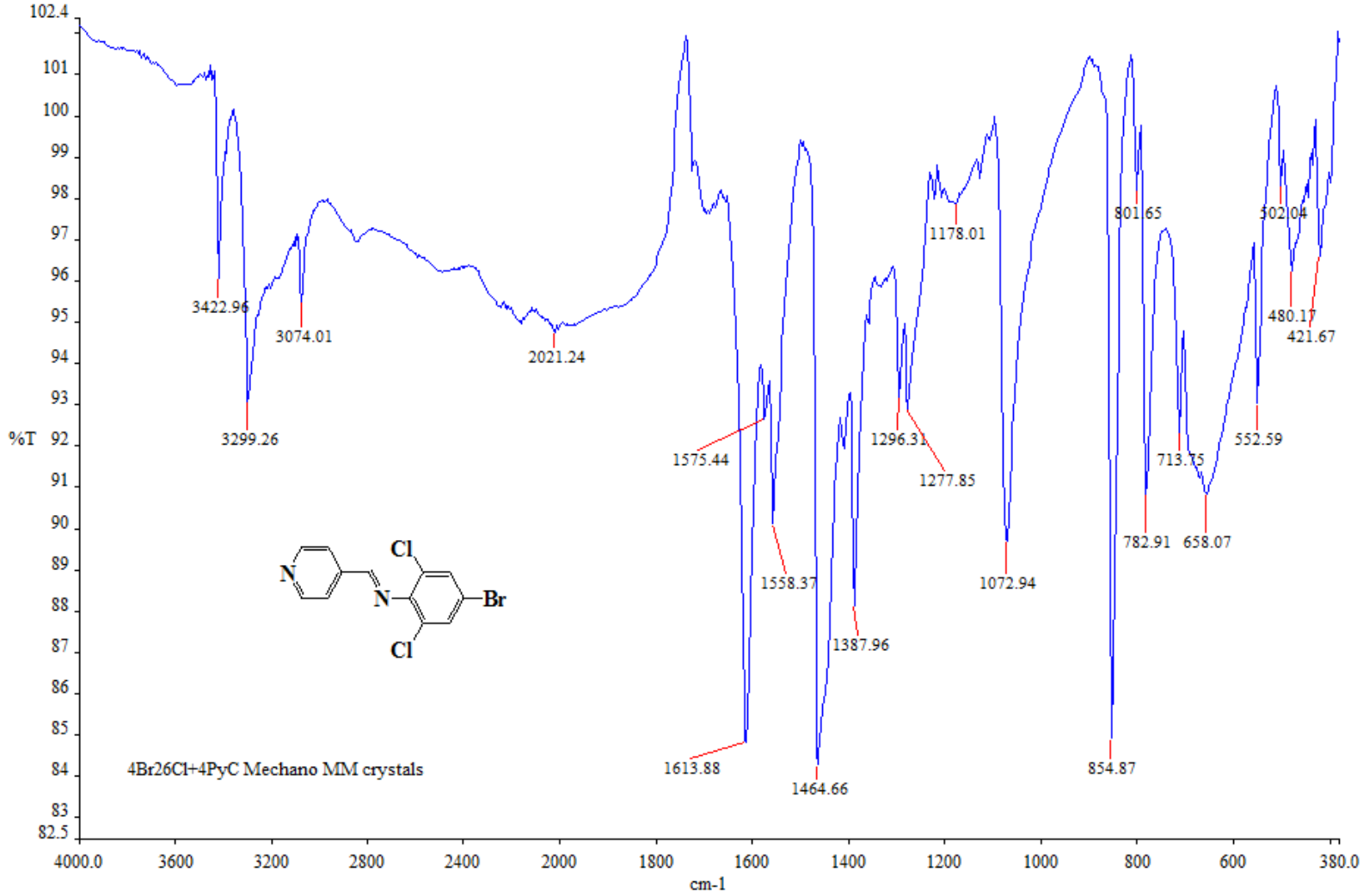

A10: IR spectrum of ligand (**L8**)

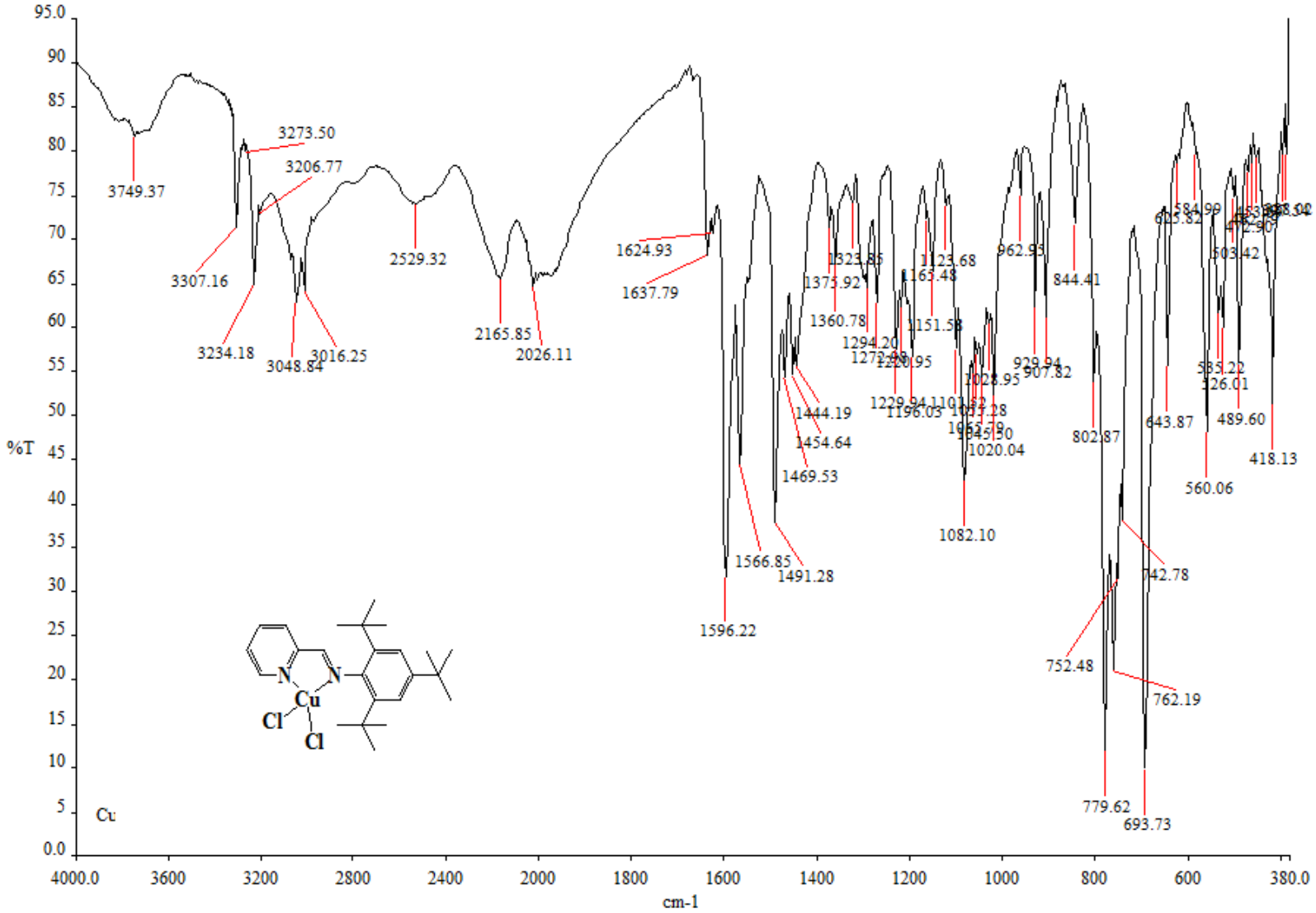

A11: IR spectrum of complex **8**

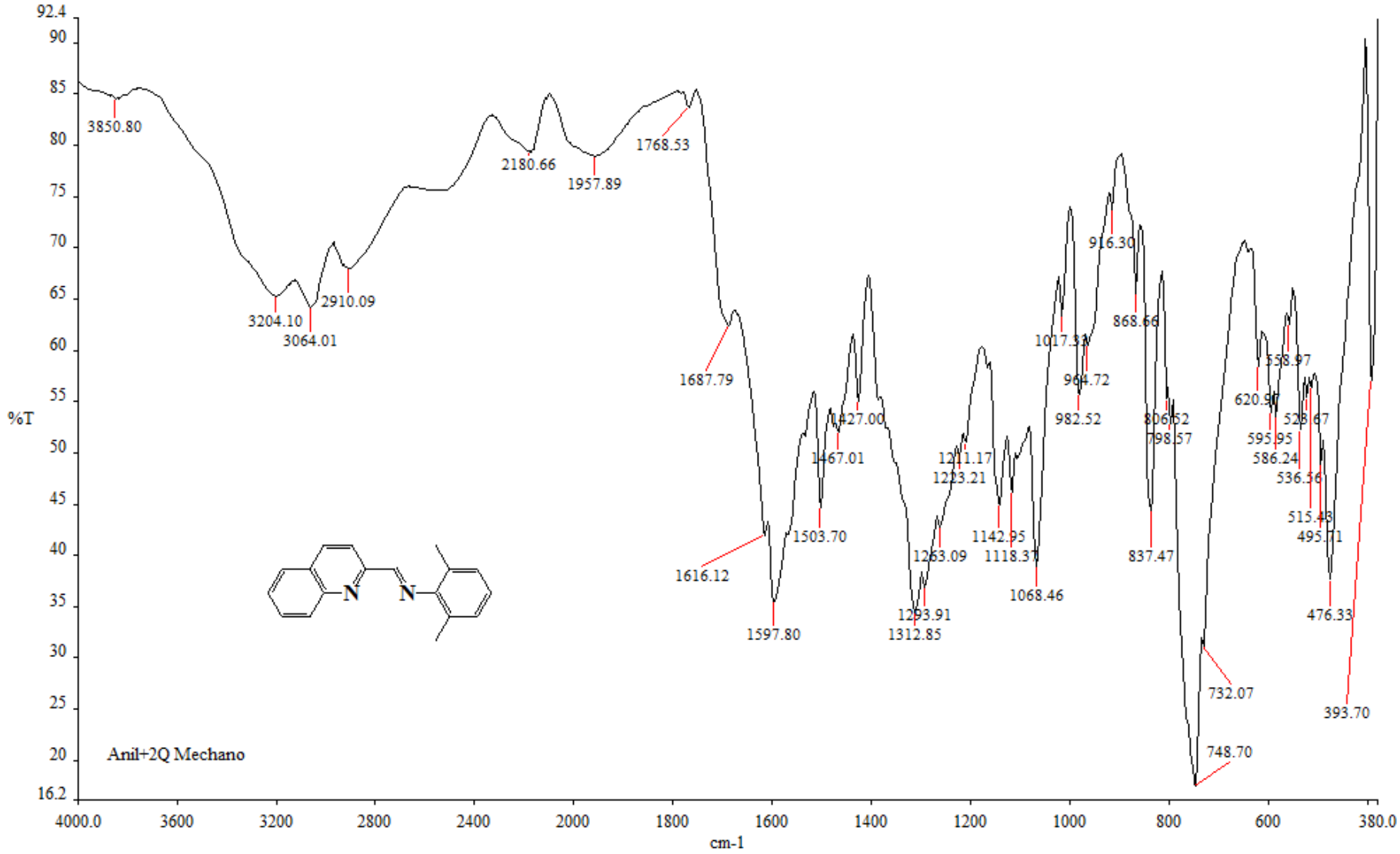

A12: IR spectrum of ligand (**L9**)

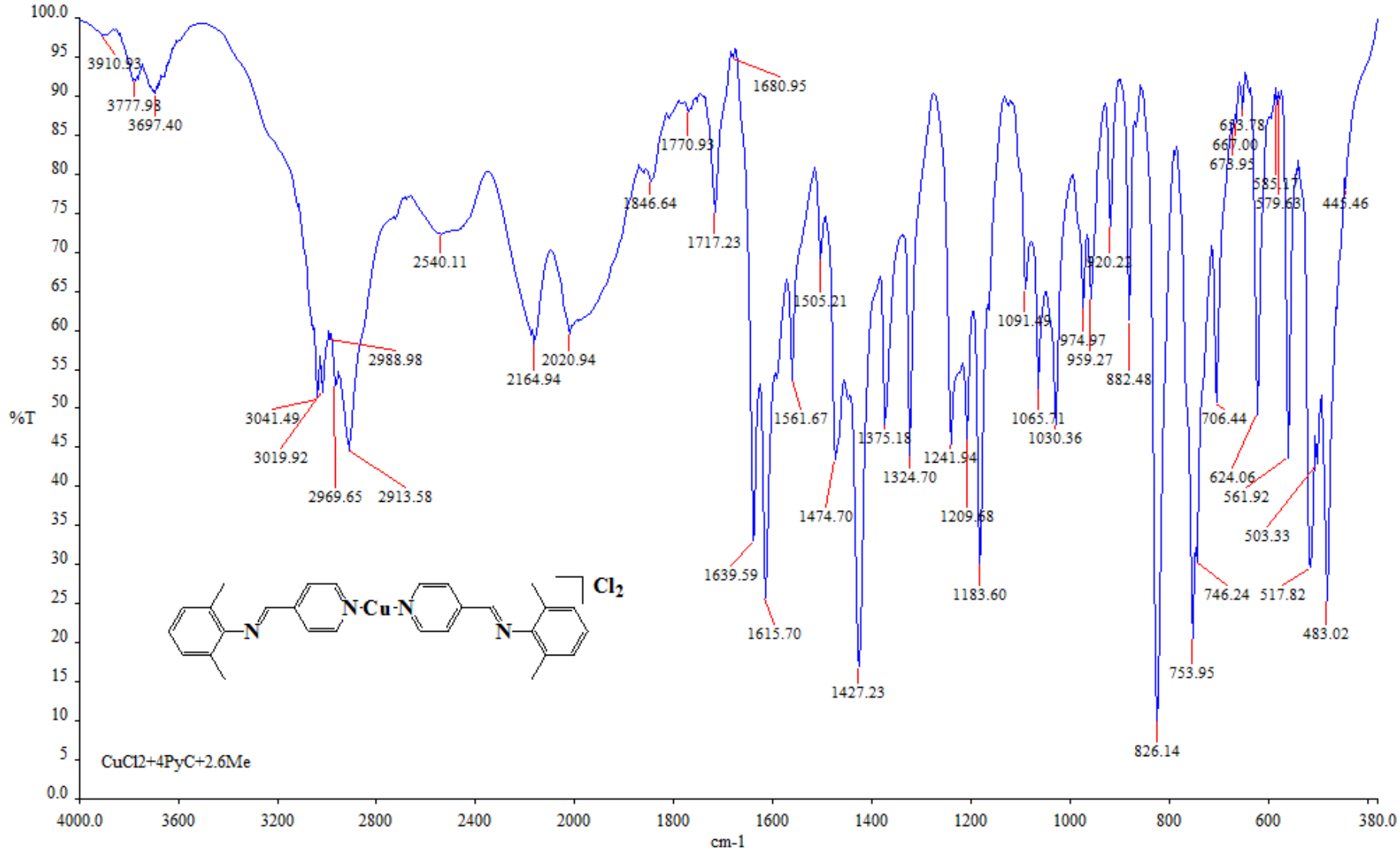

A13: IR spectrum of complex **9**

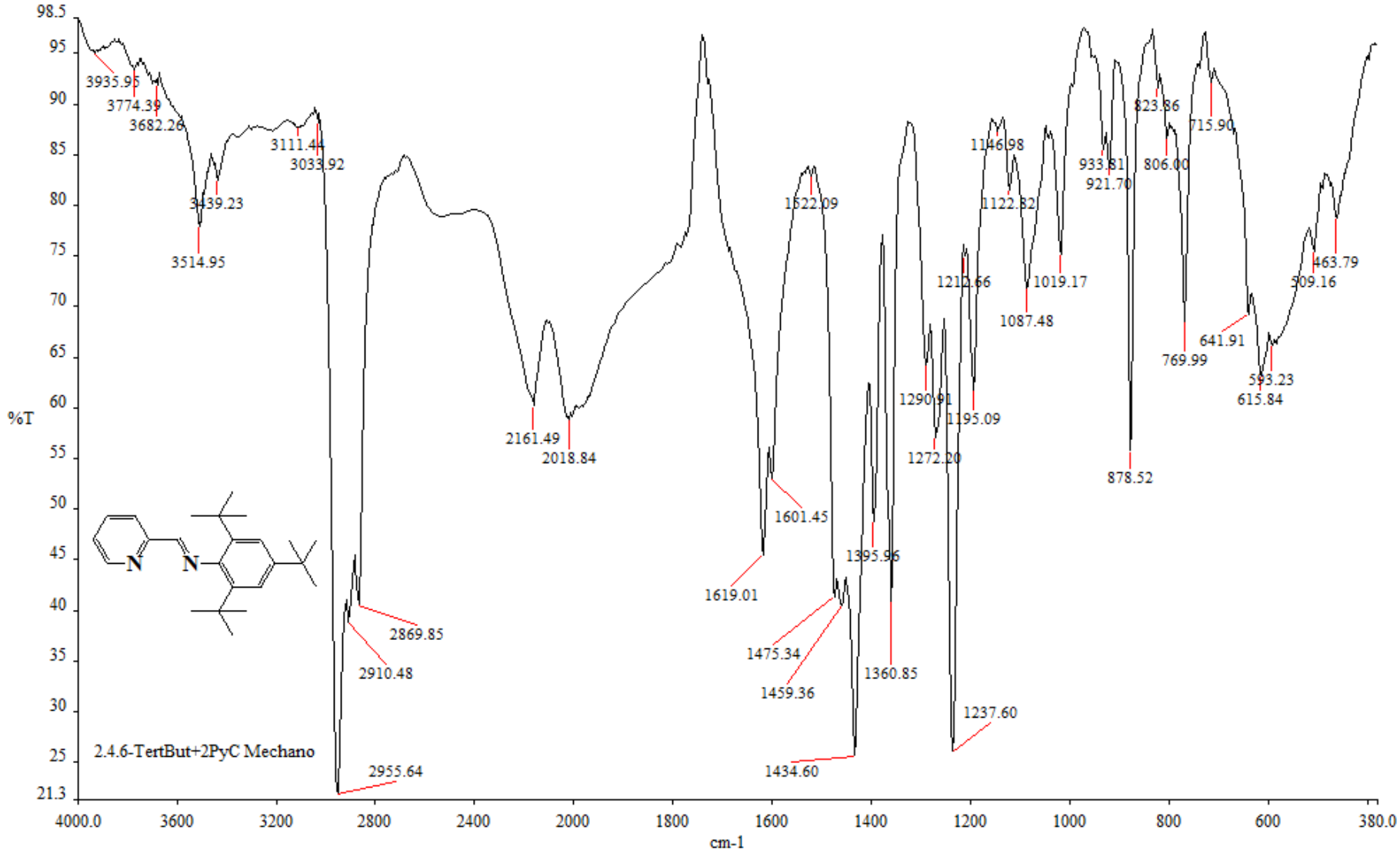

A14: IR spectrum of ligand (**L10**)

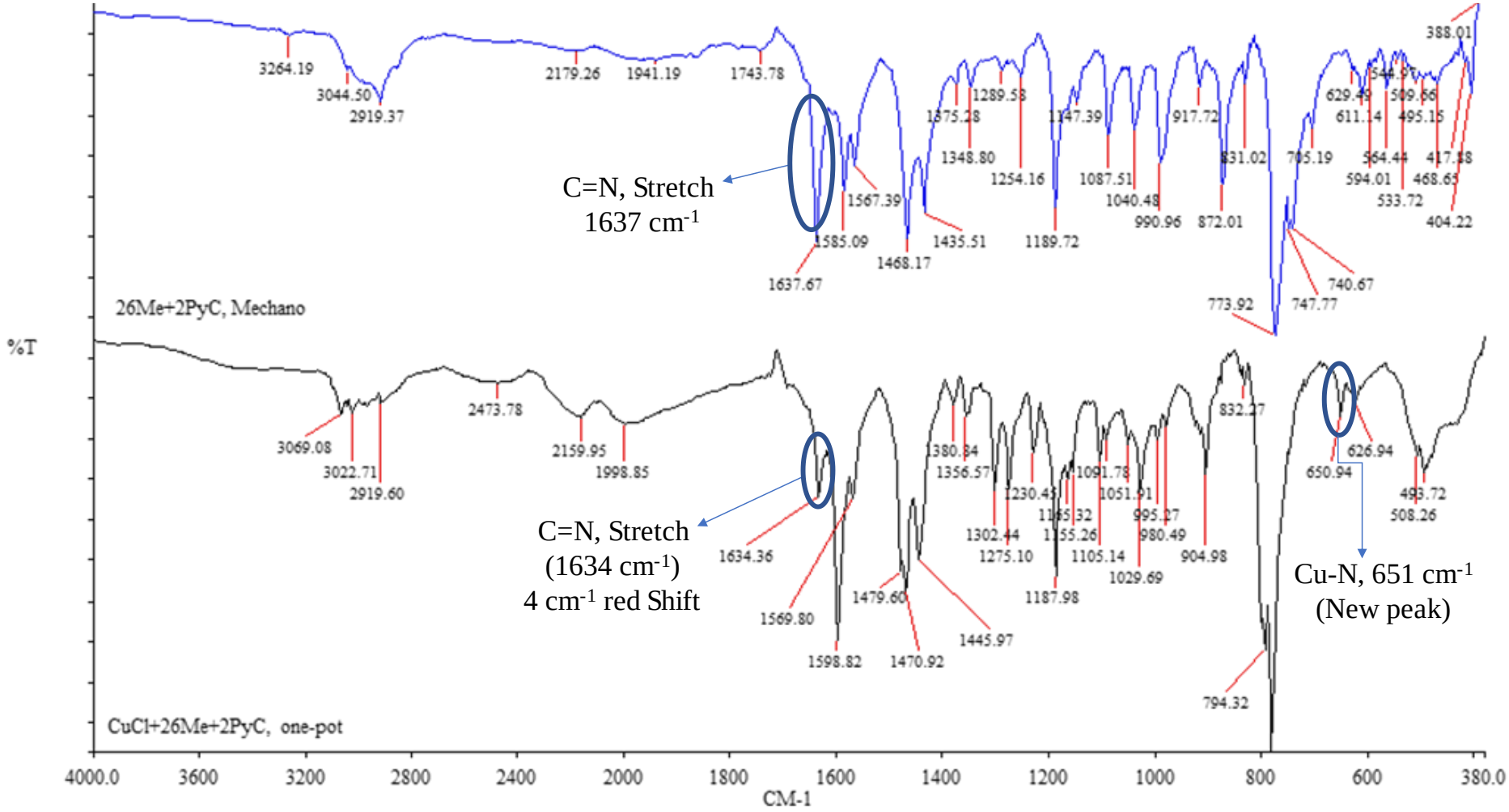

A15: Overlaid IR spectre of **L2** and **10**

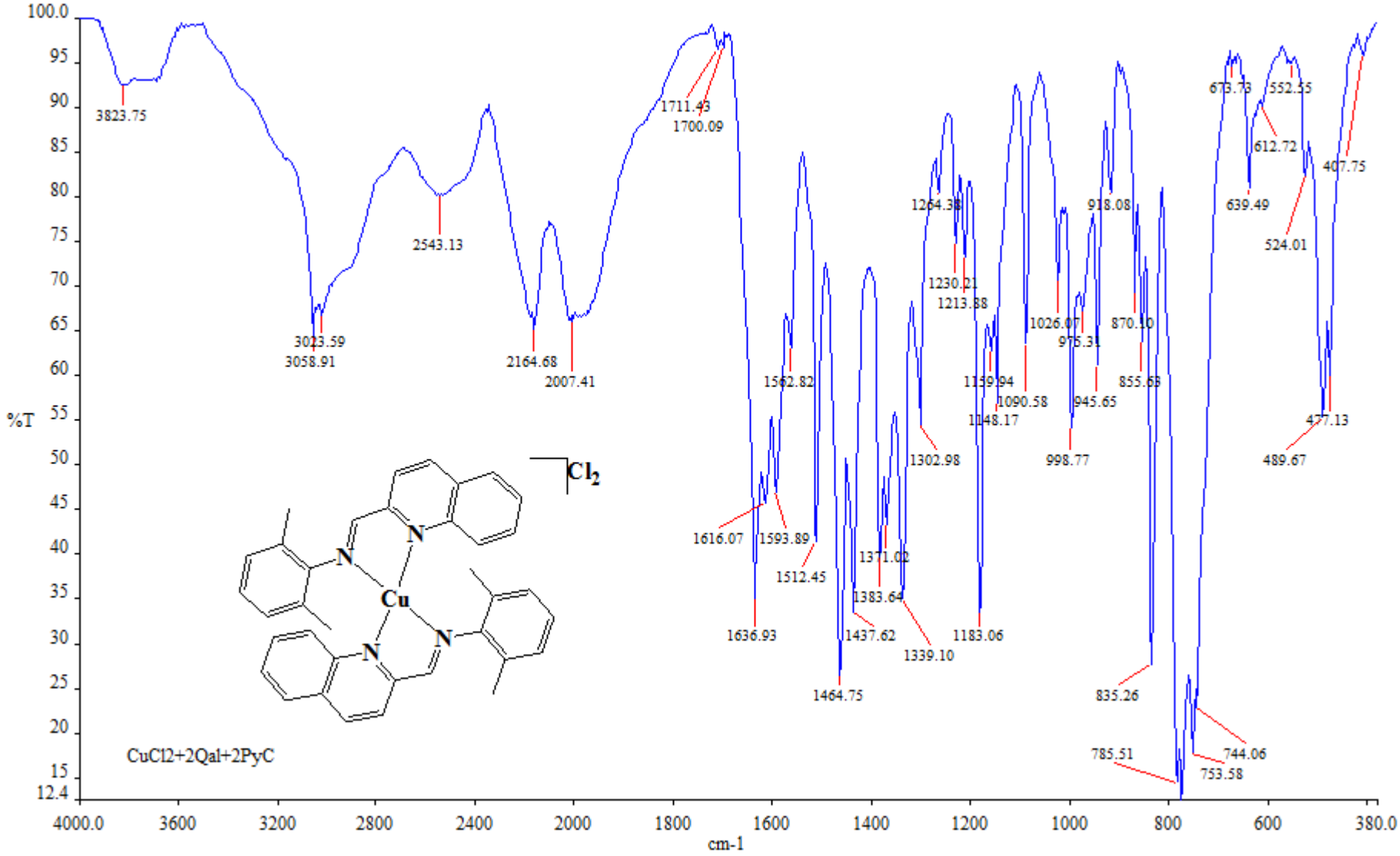

A16: IR spectrum of complex **11**

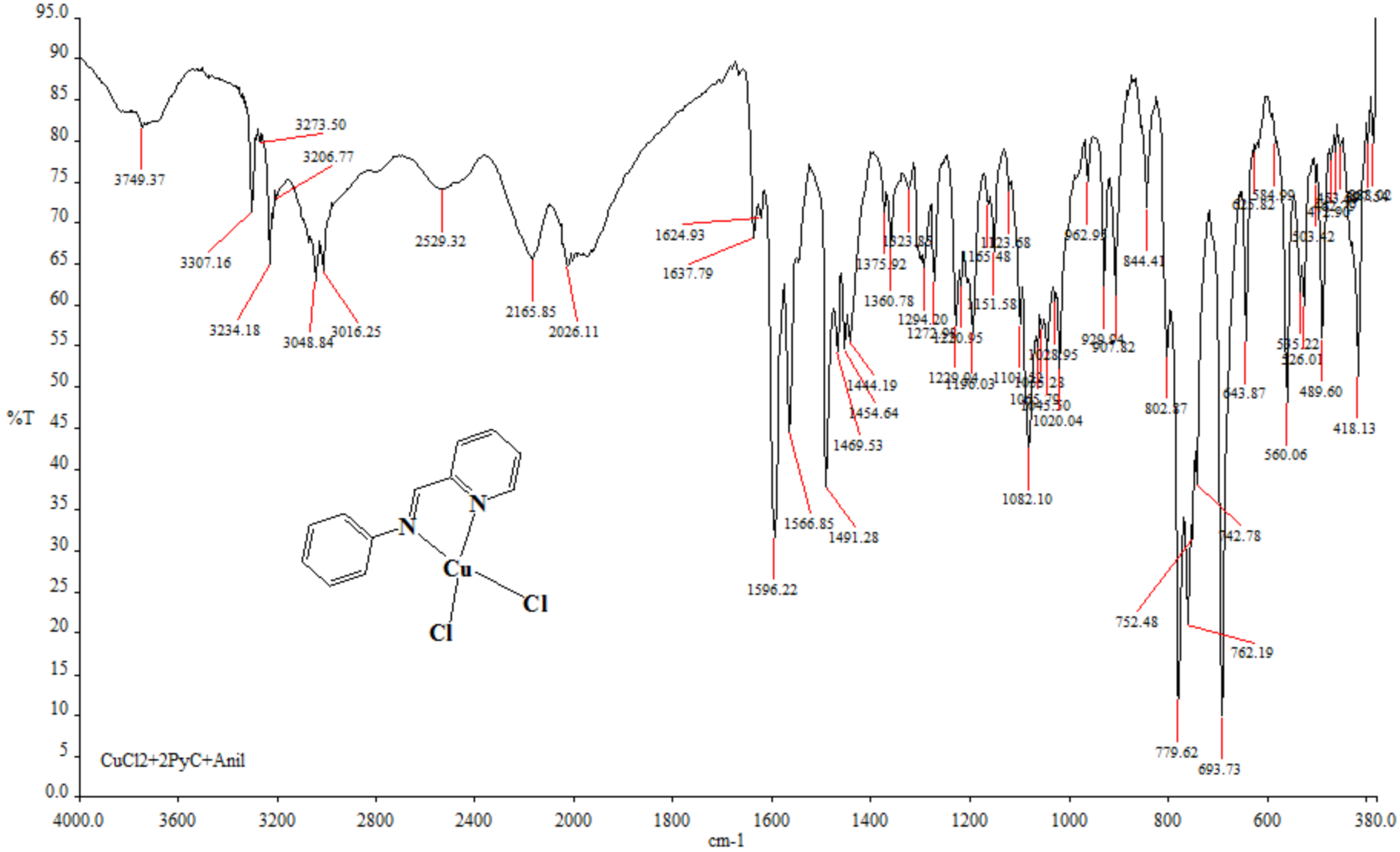

A17: IR spectrum of complex **12**

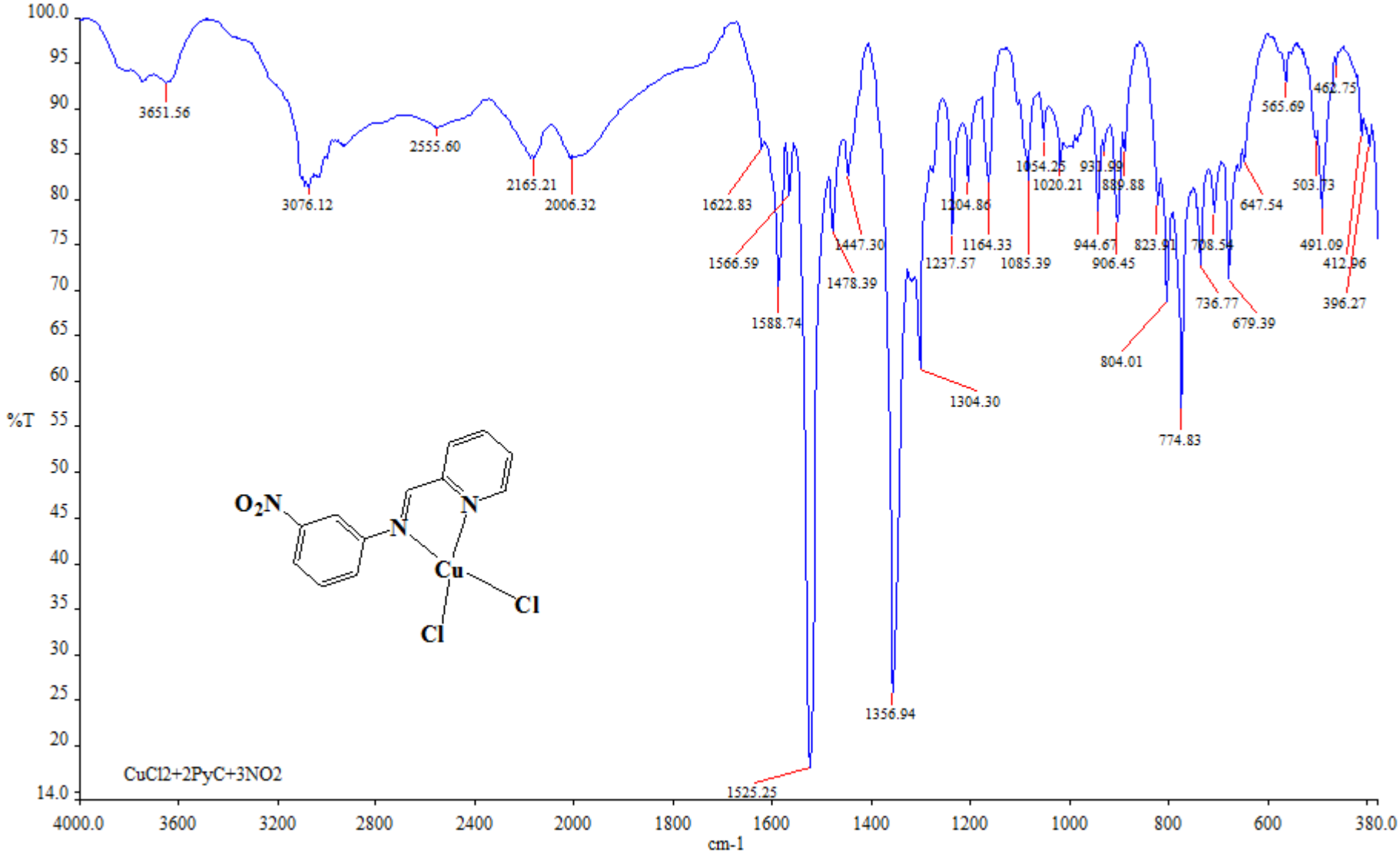

A18: IR spectrum of complex **14**

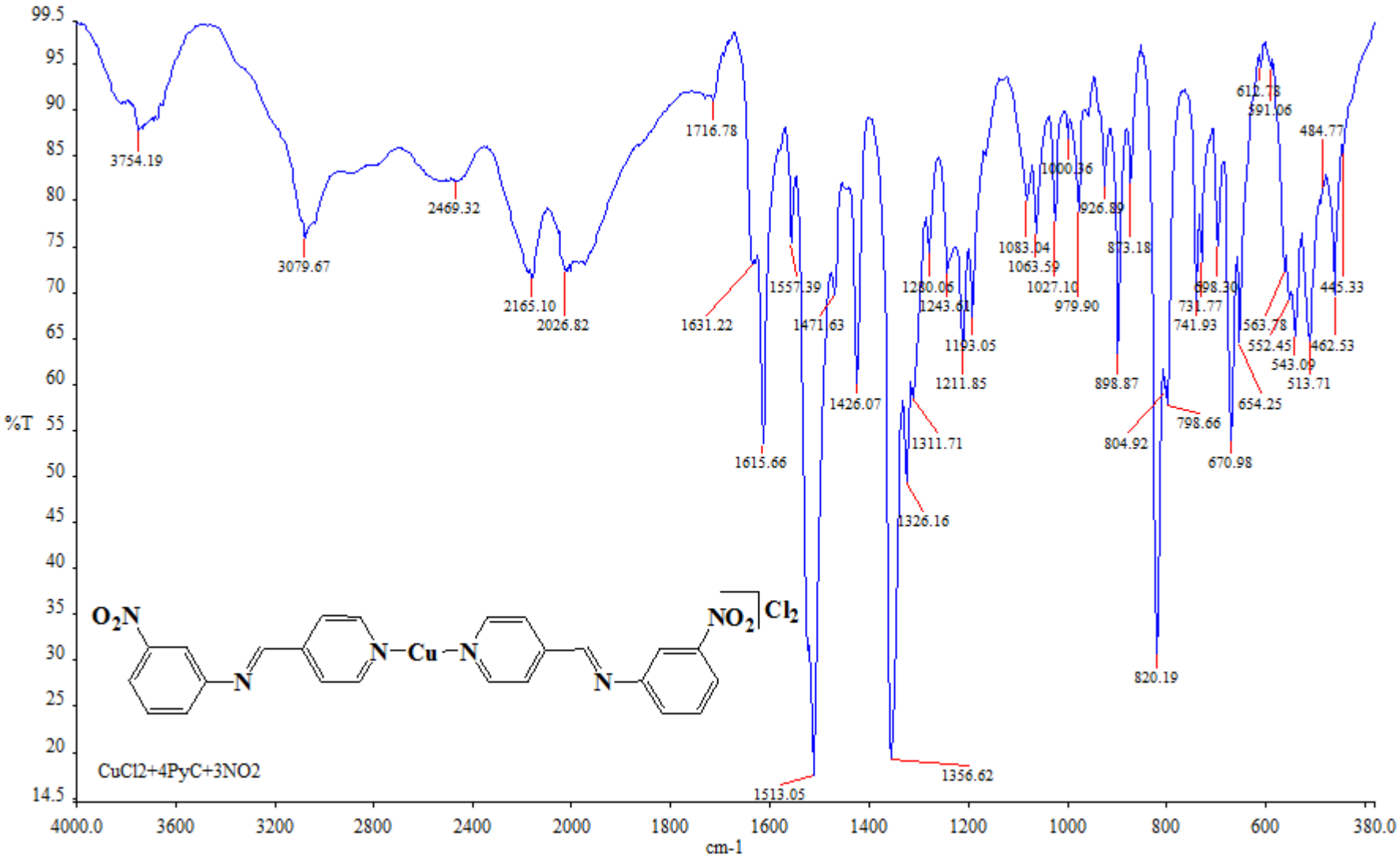

A19: IR spectrum of complex **15**

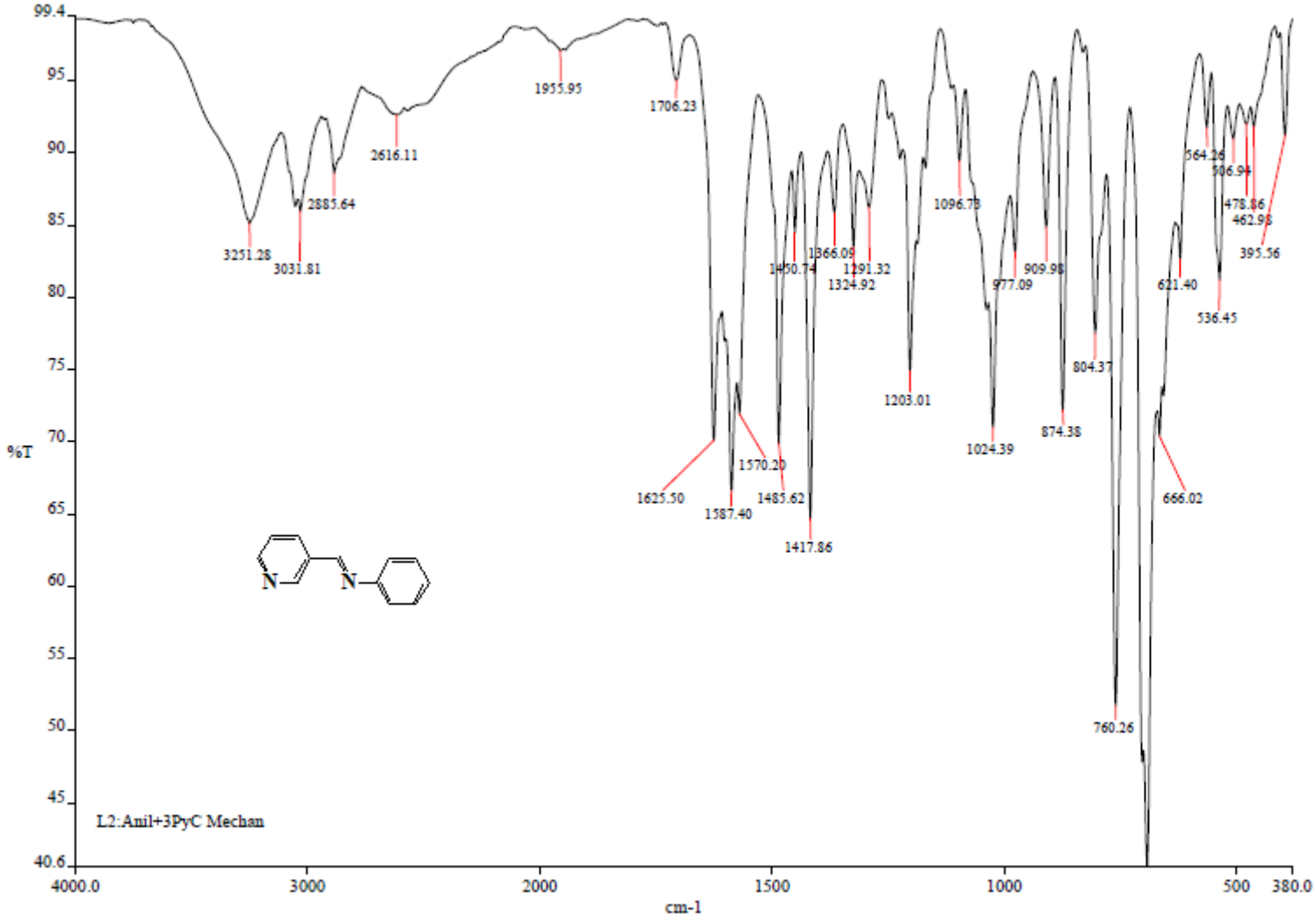

A20: IR spectrum of ligand (**L12**)

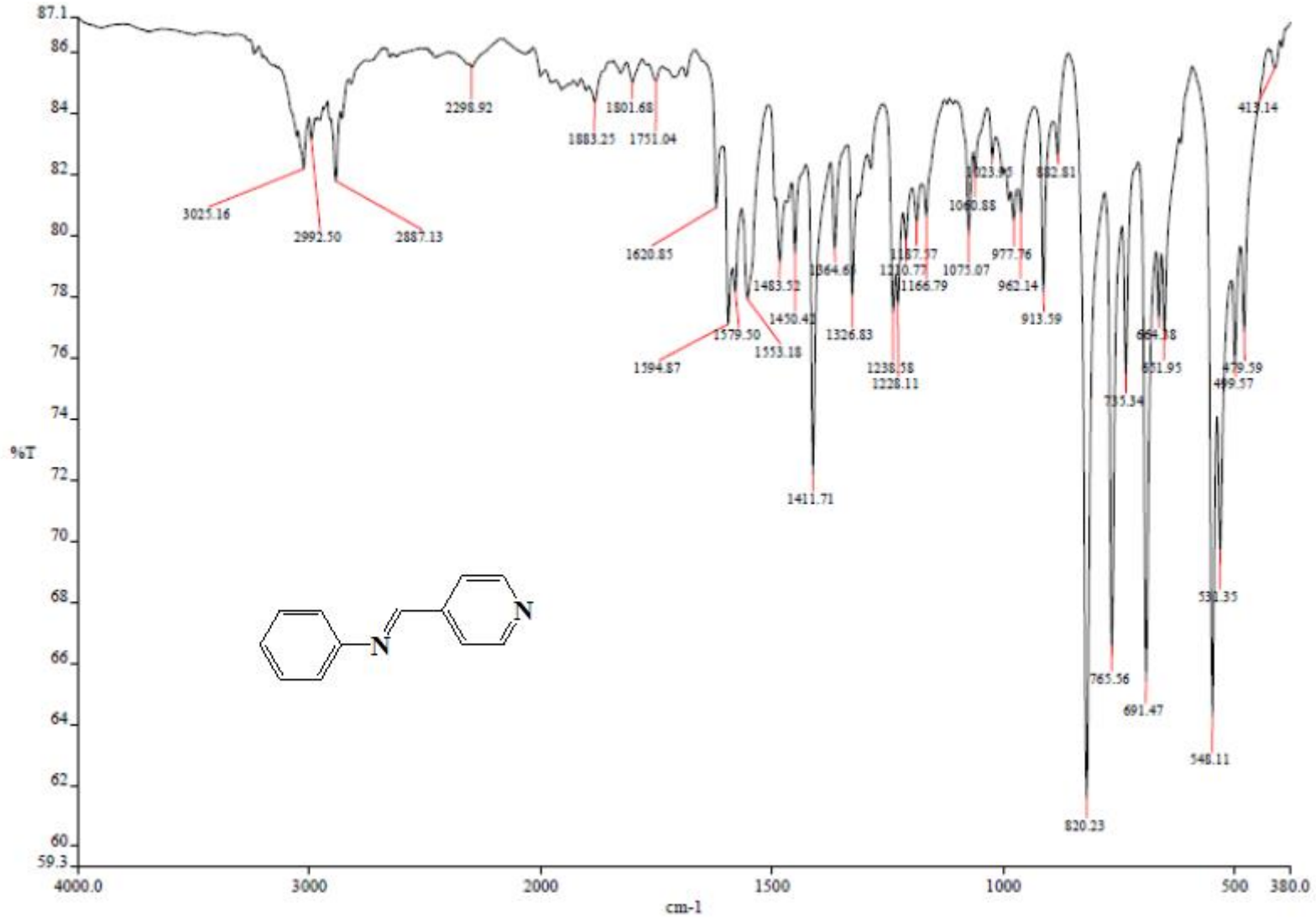

A21: IR spectrum of ligand (**L13**)

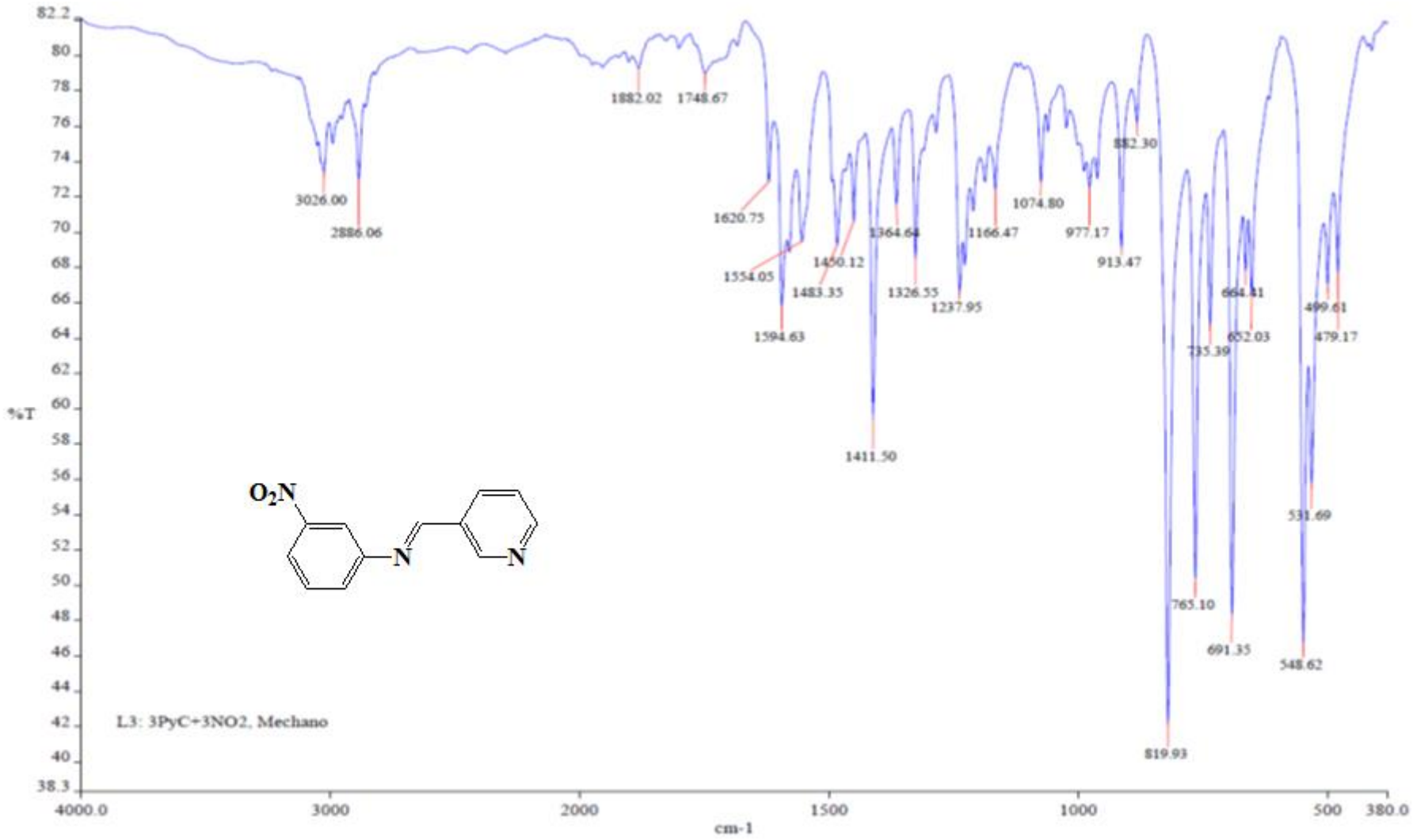

A22: IR spectrum of ligand (**L14**)

Appendix B

^{1}H-NMR and ^{13}C-NMR spectra

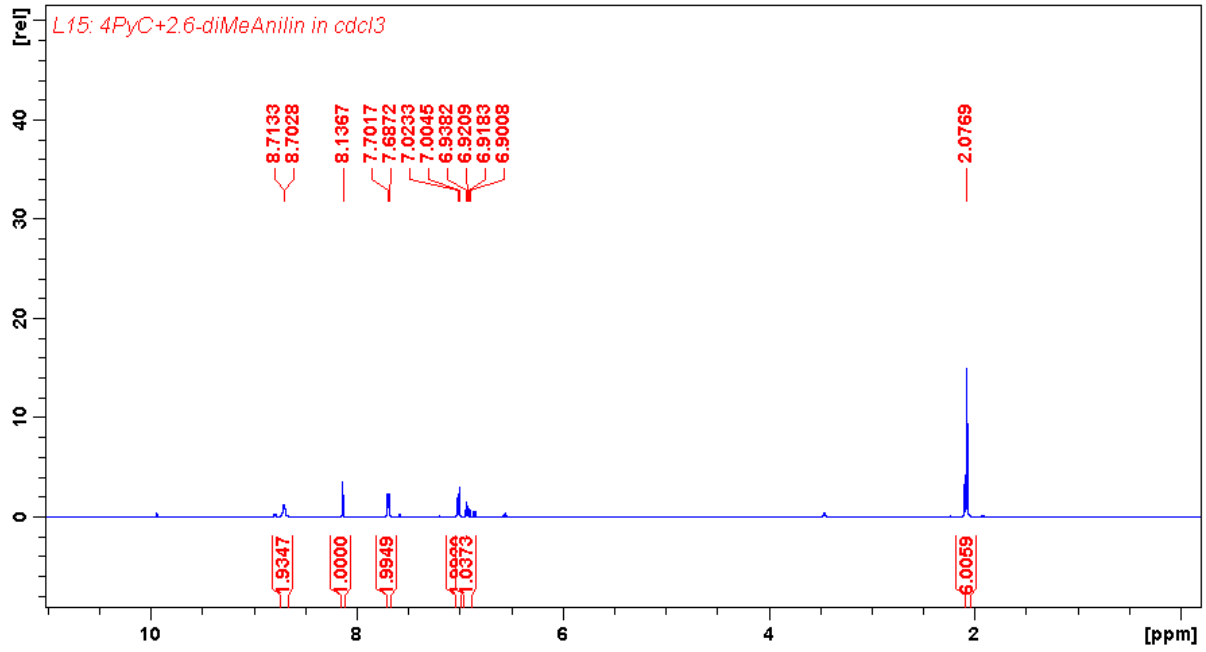

B1: ^{1}H-NMR of ligand (**L1**)

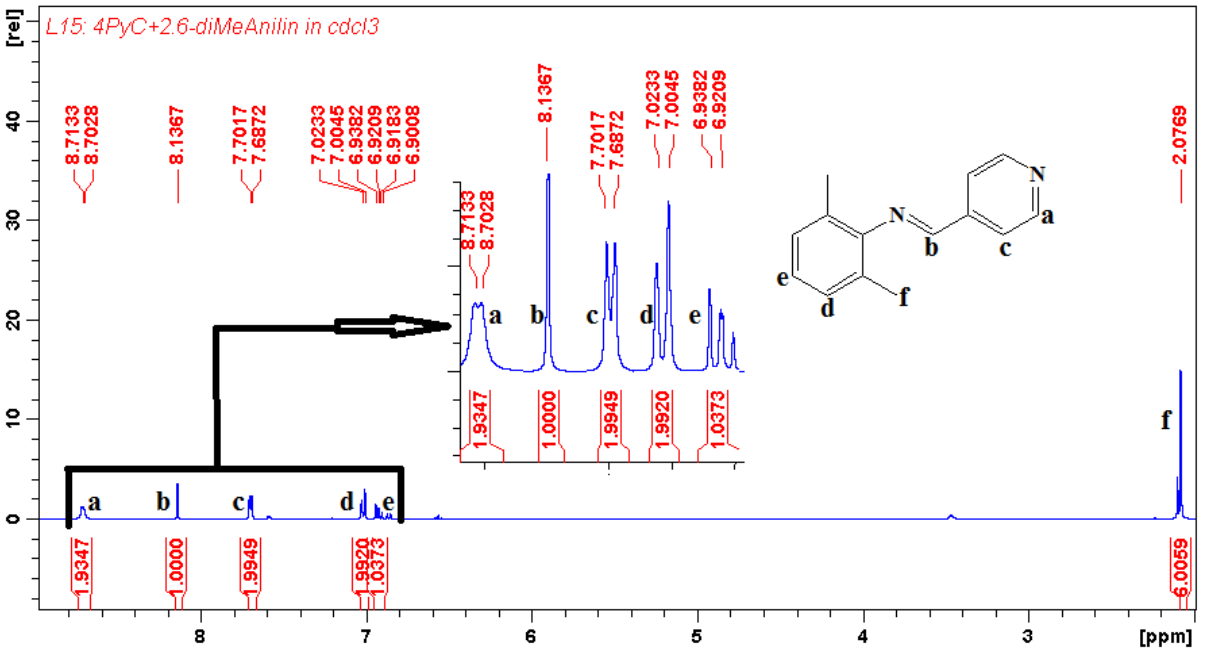

B2: Expanded ^{1}H-NMR of ligand (**L1**)

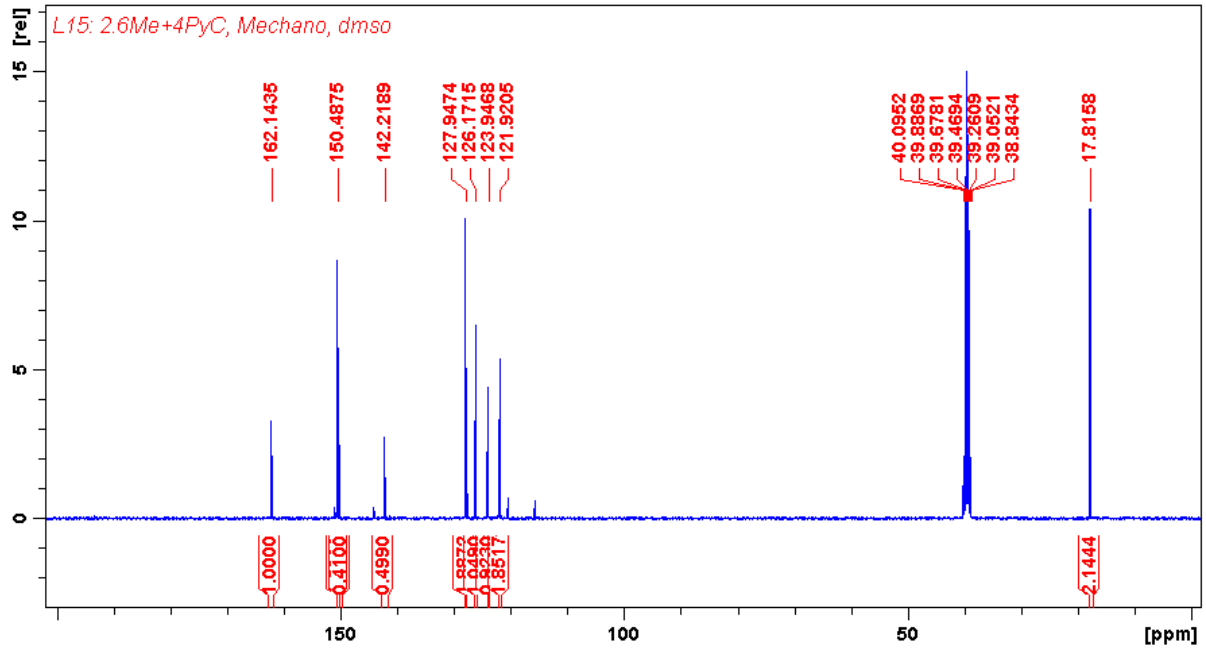

B3: ^{13}C-NMR of ligand (**L1**)

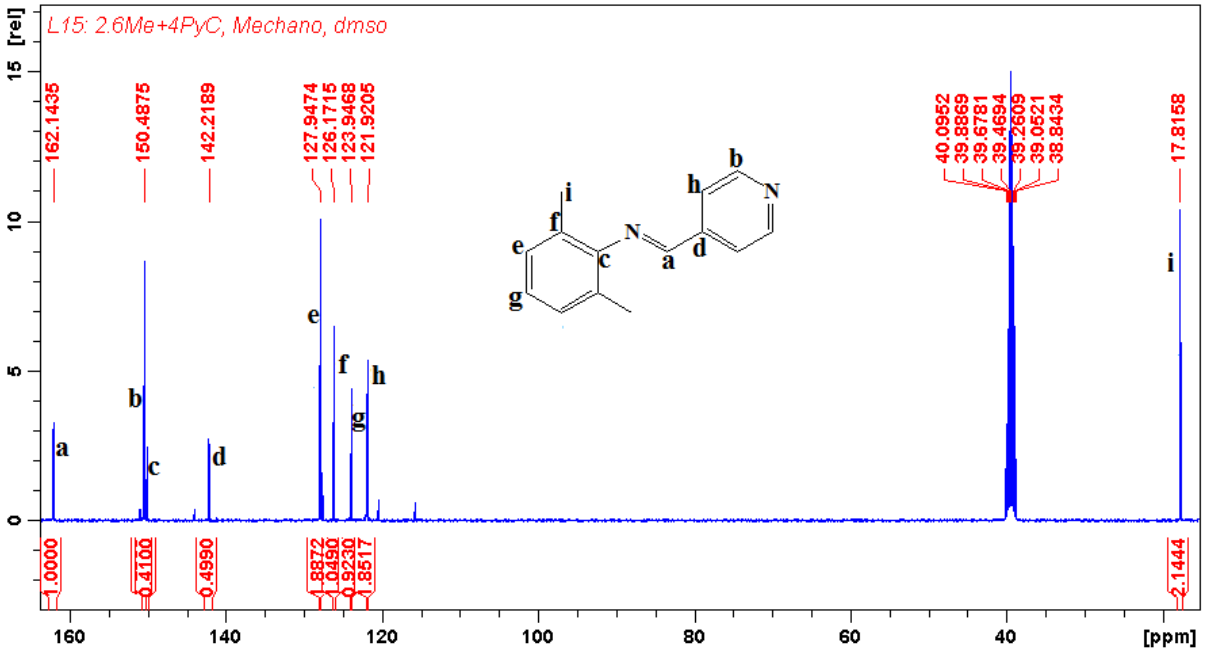

B4: Expanded ^{13}C-NMR of ligand (**L1**)

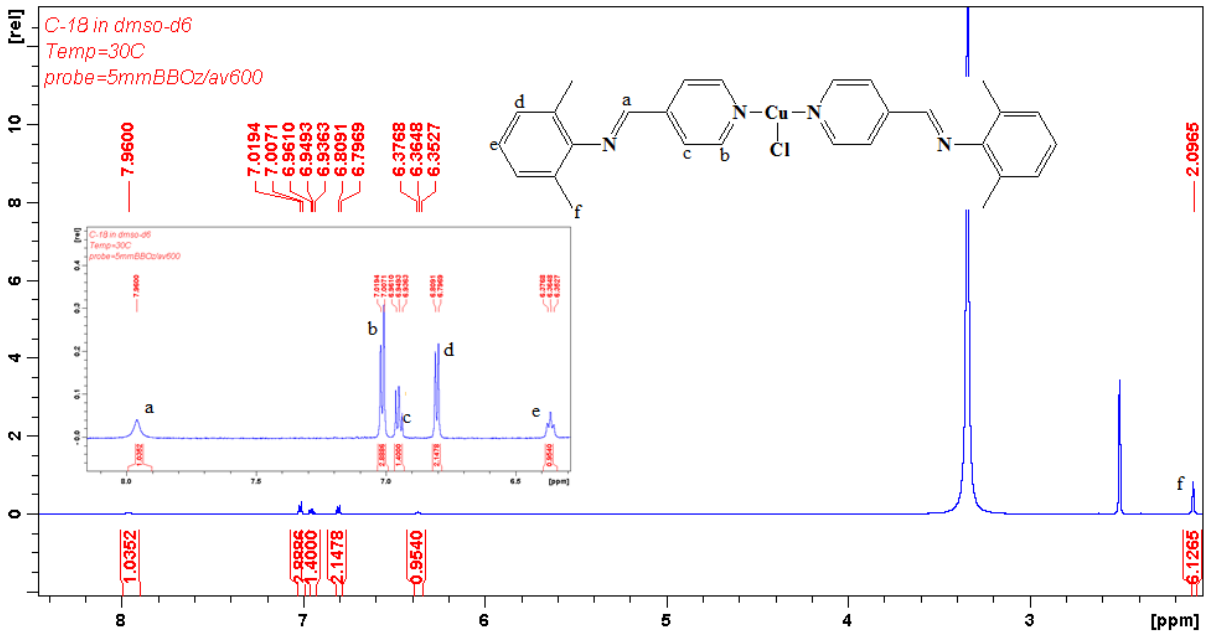

B5: Expanded ^{1}H-NMR of complex **1**

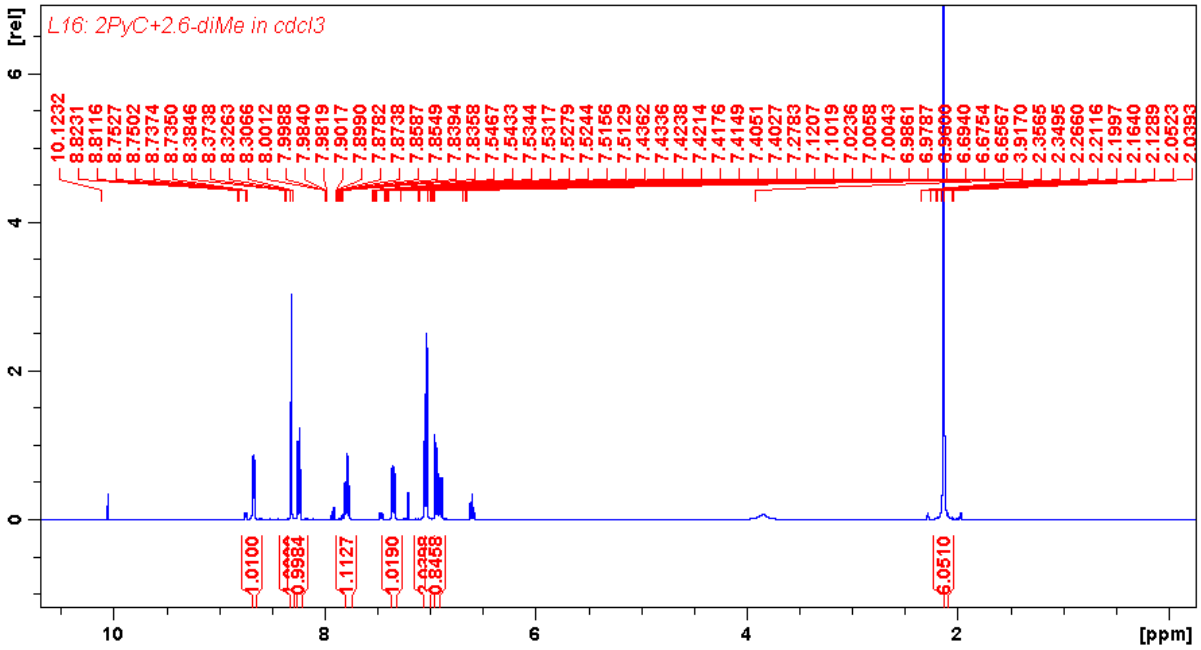

B6: ^{1}H-NMR of ligand (**L2**)

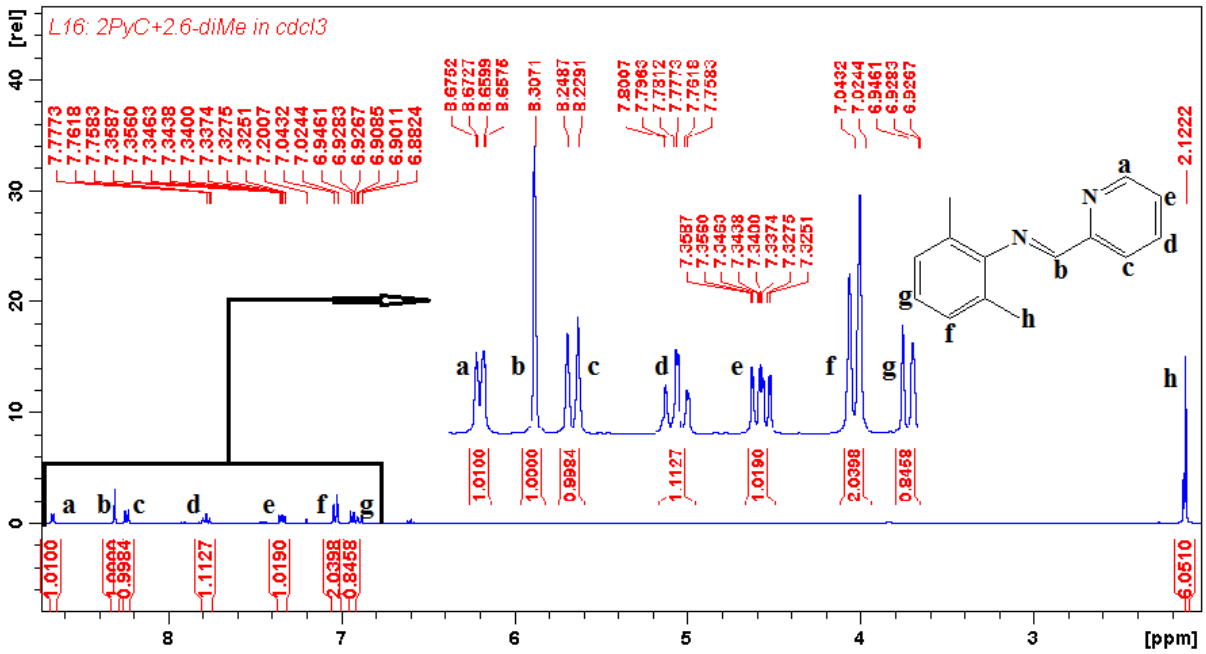

B7: Expanded ^{1}H-NMR of ligand (**L2**)

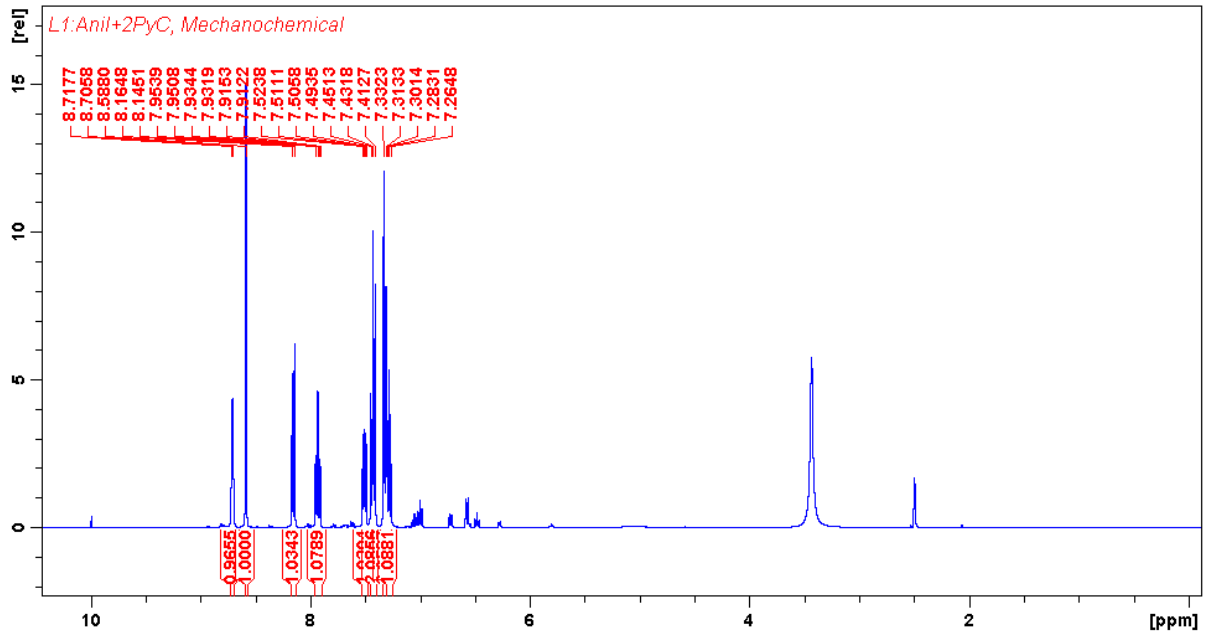

B8: ^{1}H-NMR of ligand (**L3**)

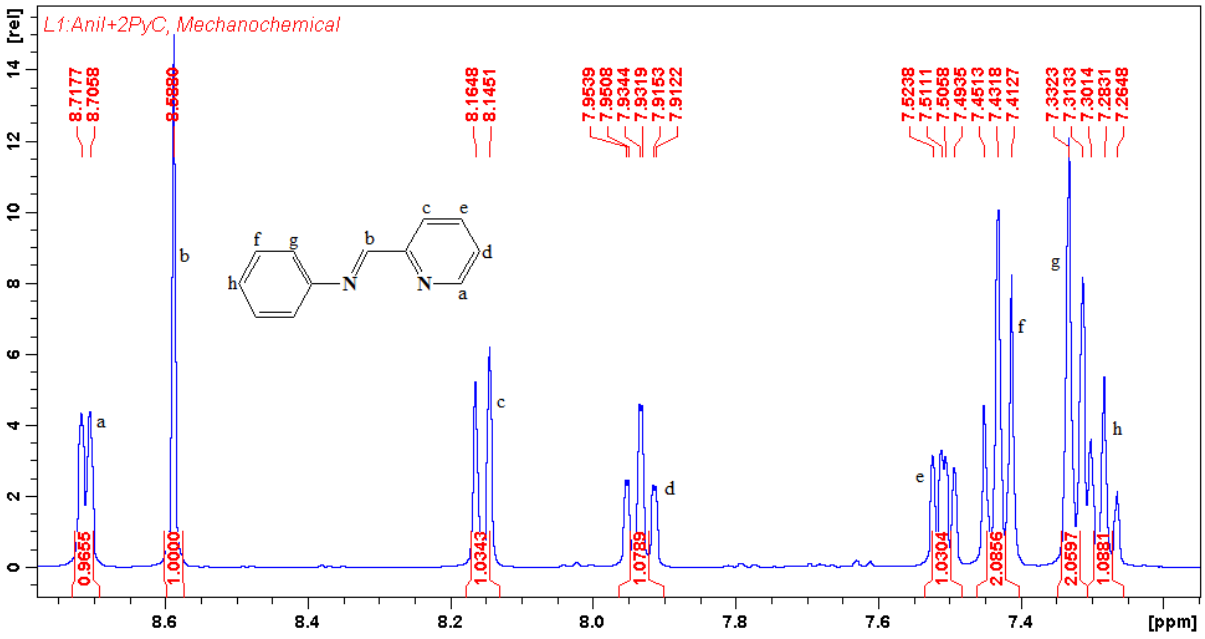

B9: Expanded ^{1}H-NMR of ligand (**L3**)

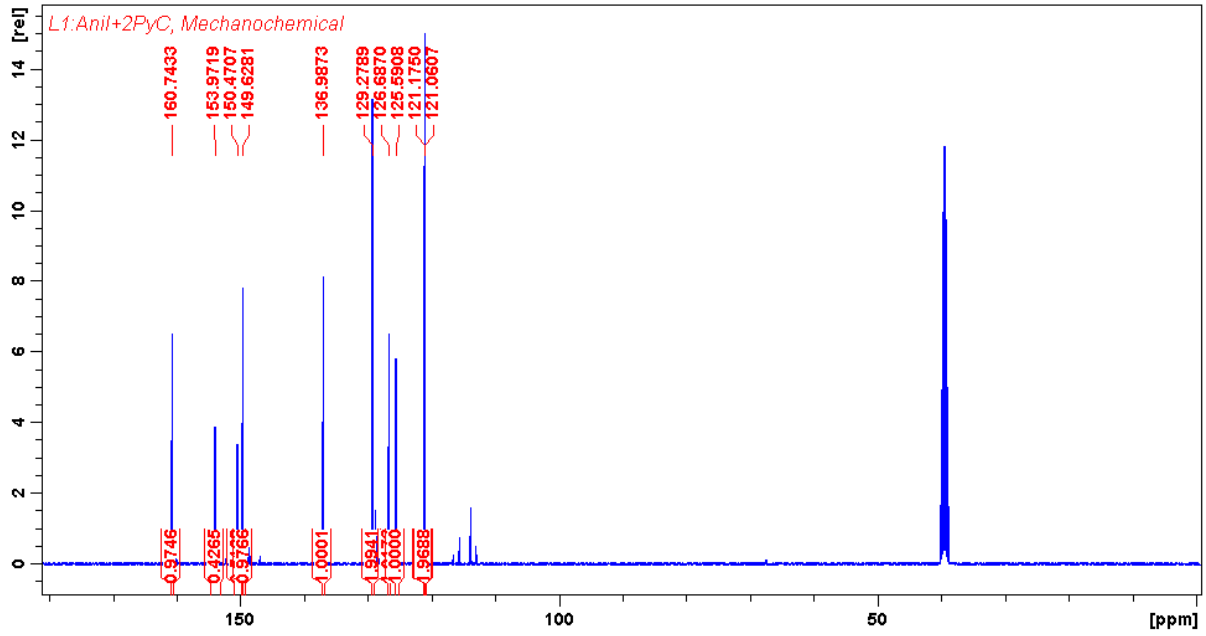

B10: ^{13}C-NMR of ligand (**L3**)

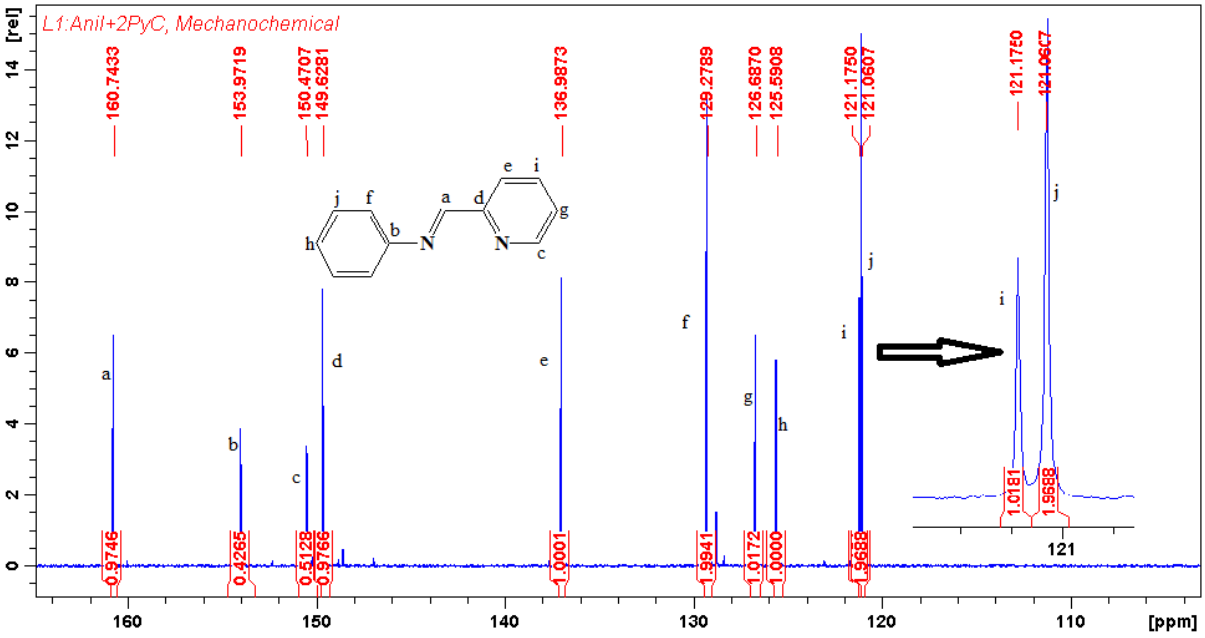

B11: Expanded ^{13}C-NMR of ligand (**L3**)

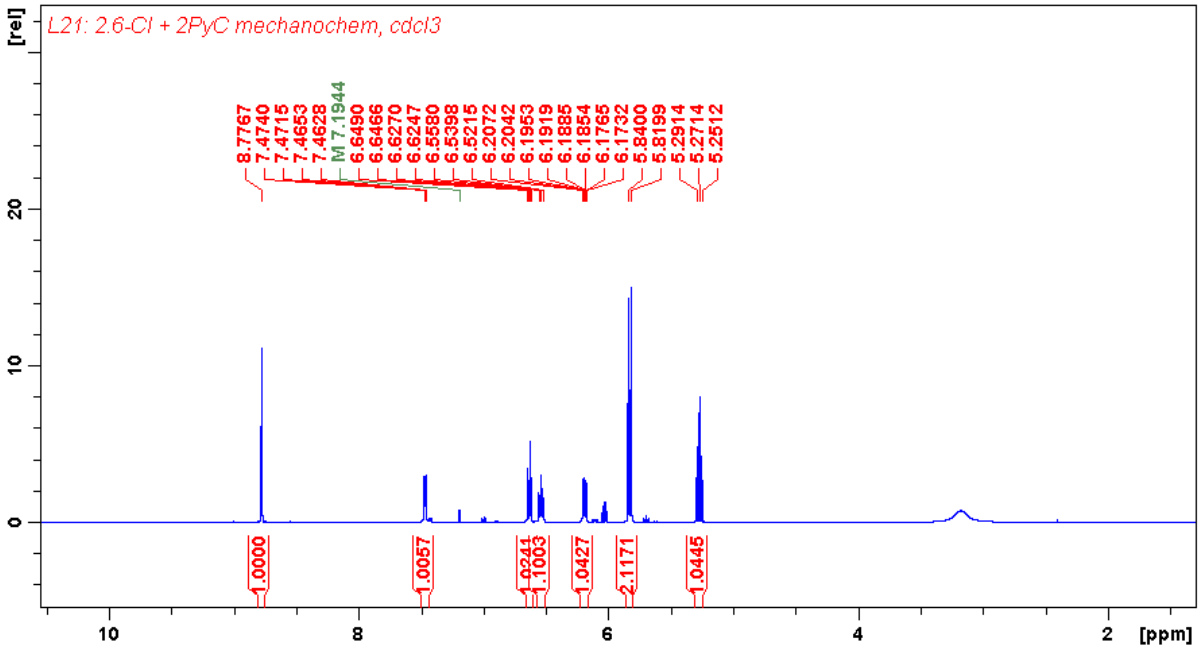

B12: ^{1}H-NMR of ligand (**L4**)

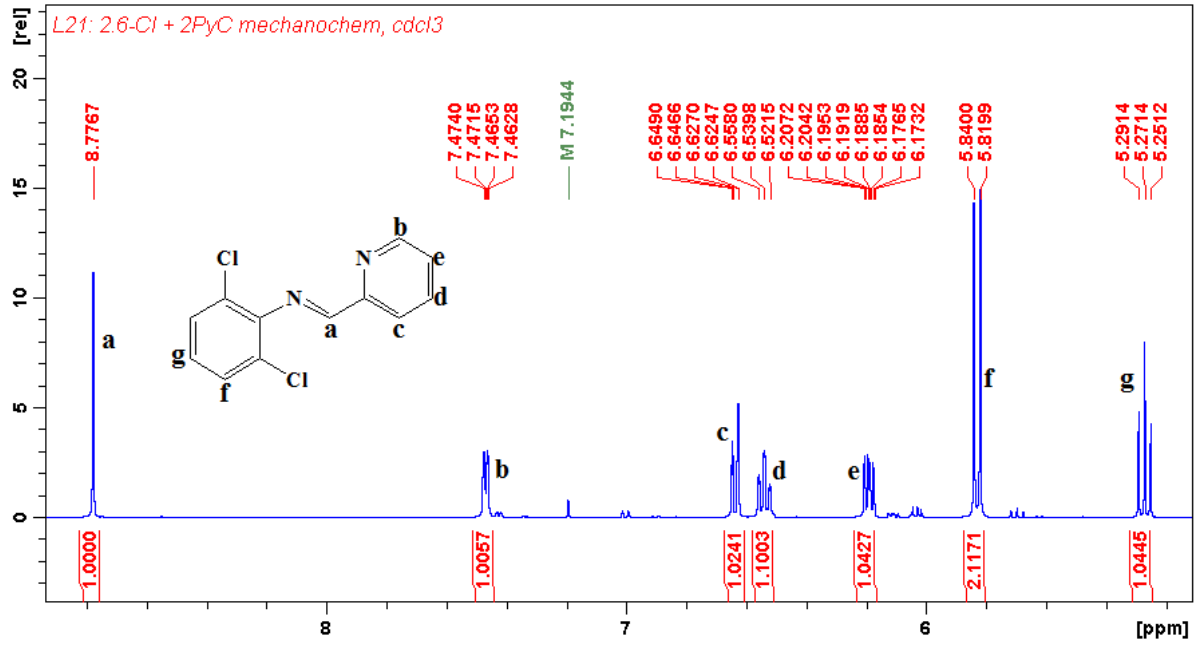

B13: Expanded ^{1}H-NMR of ligand (**L4**)

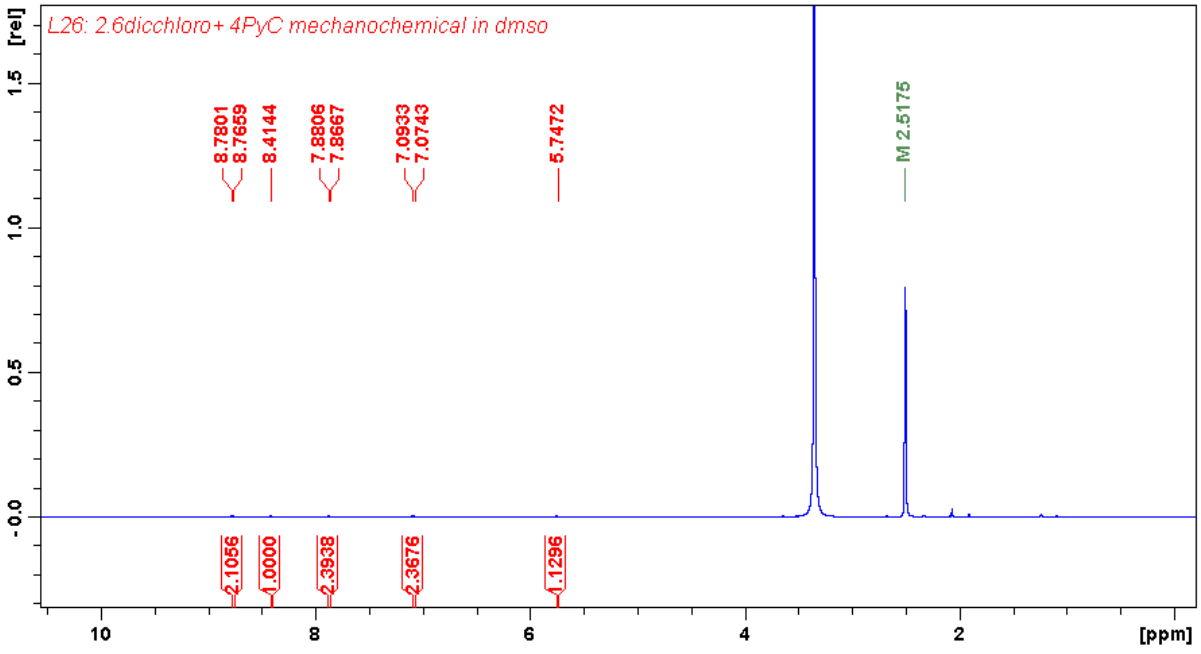

B14: ^{1}H-NMR of ligand (**L5**)

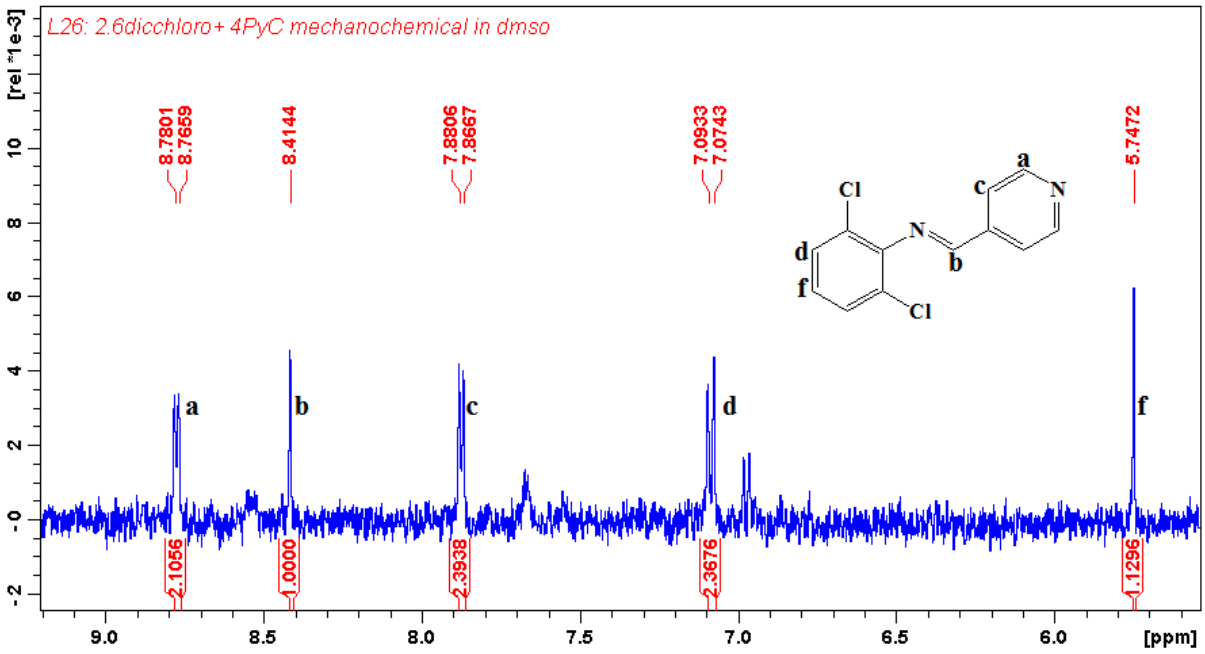

B15: Expanded ^{1}H-NMR of ligand (**L5**)

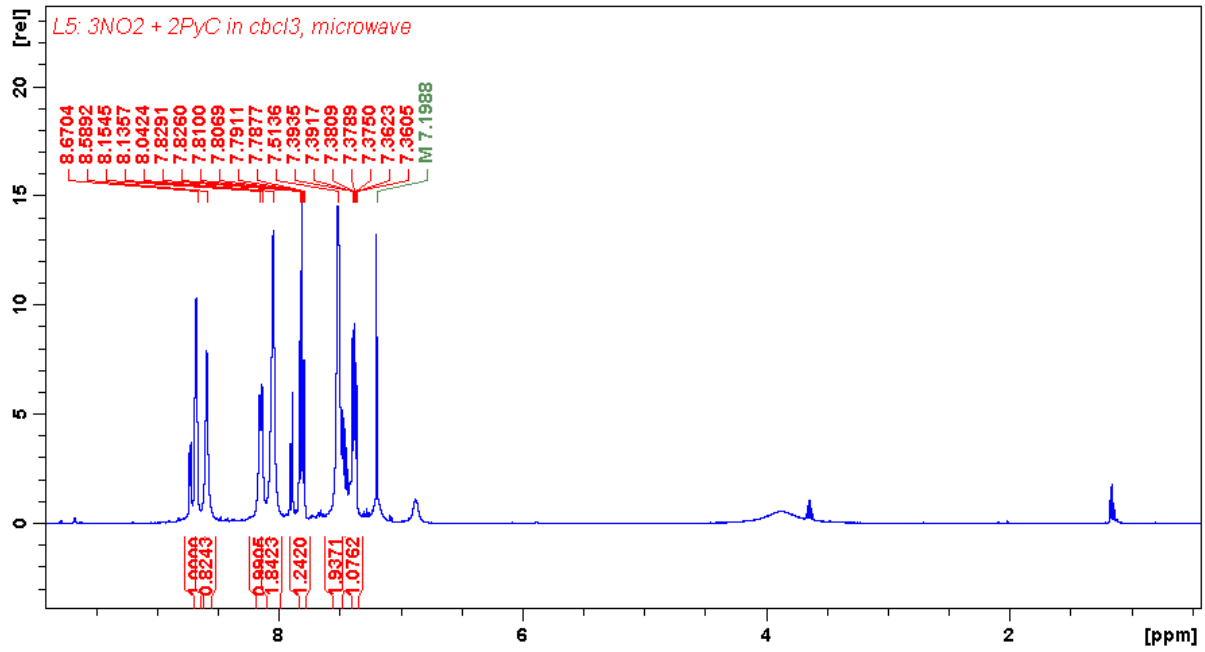

B16: ^{1}H-NMR of ligand (**L6**)

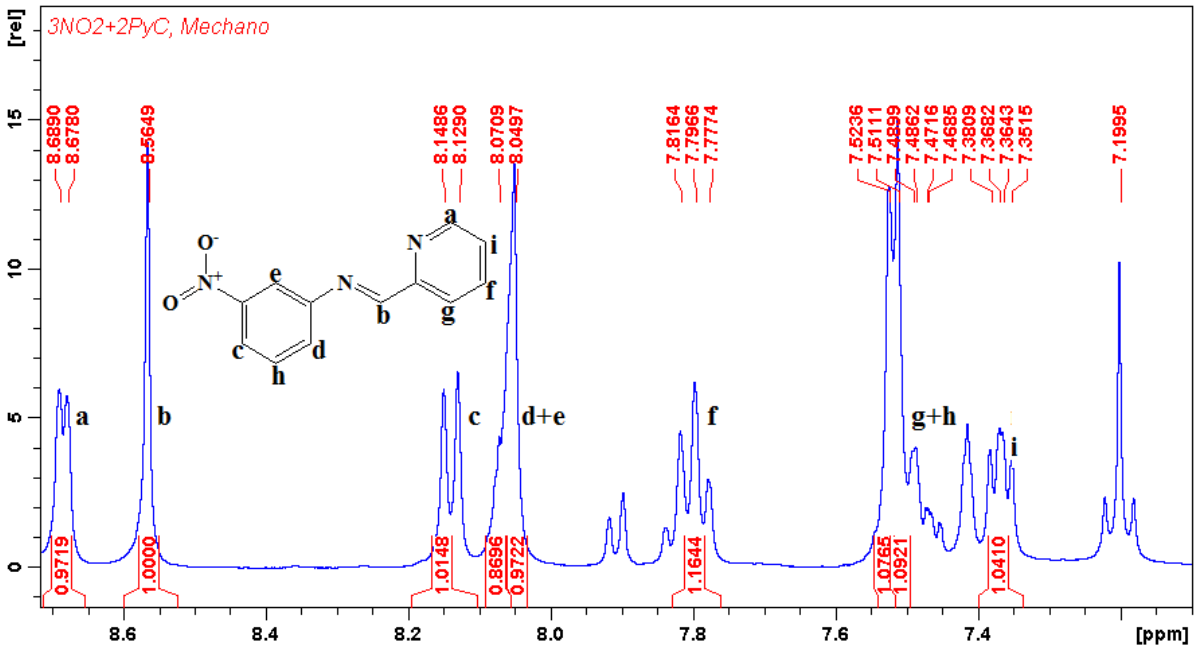

B17: Expanded ^{1}H-NMR of ligand (**L6**)

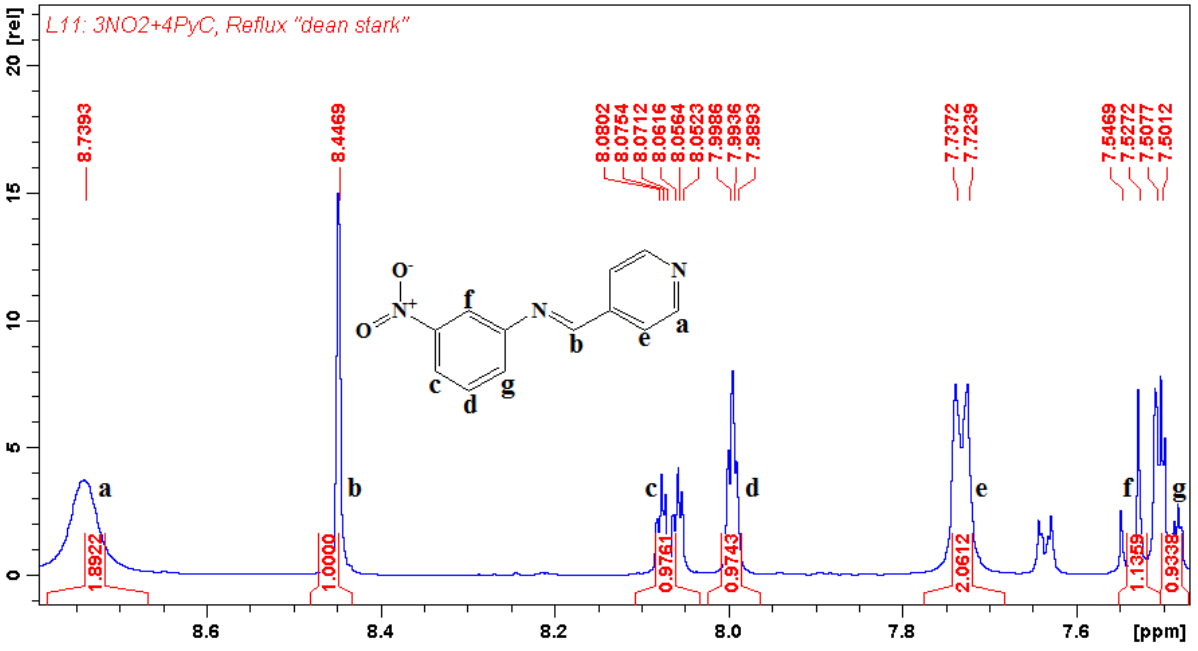

B18: Expanded ^{1}H-NMR of ligand (**L7**)

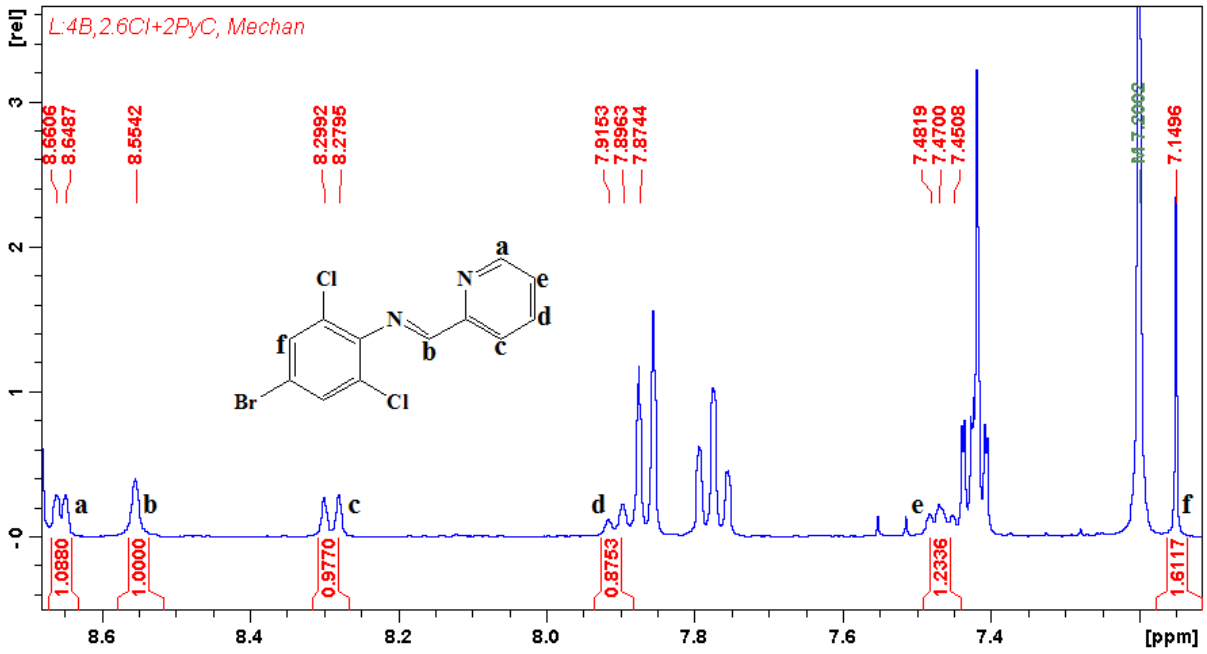

B19: Expanded ^{1}H-NMR of ligand (**L8**)

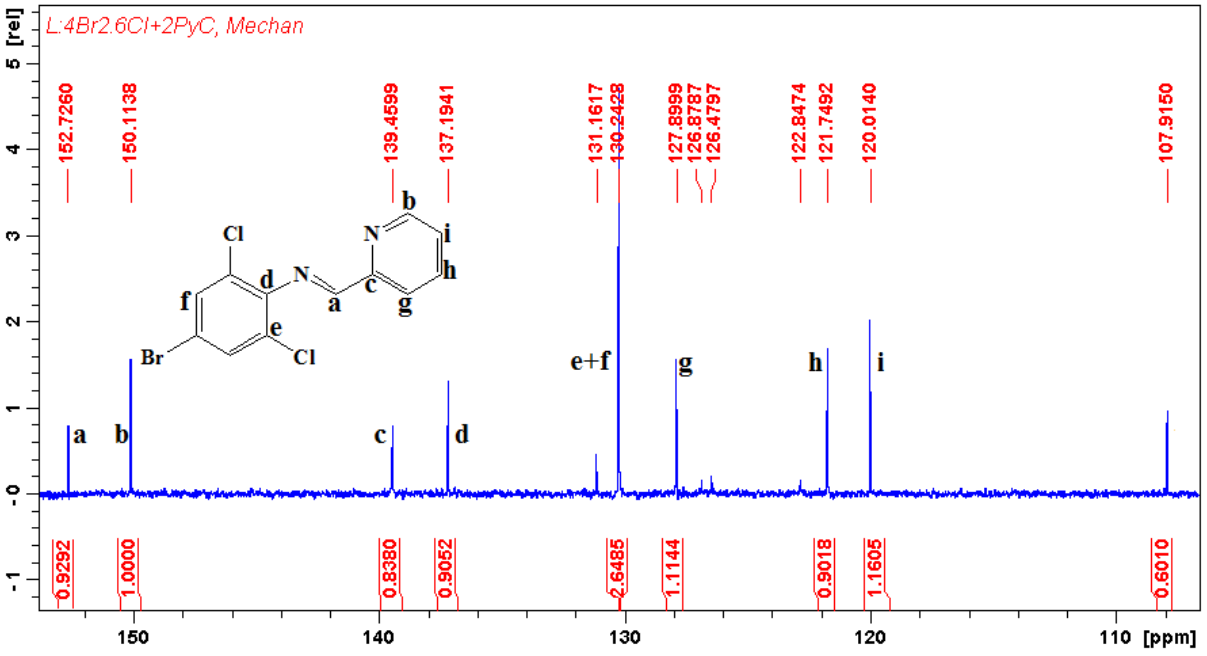

B20: Expanded ^{13}C-NMR of ligand (**L8**)

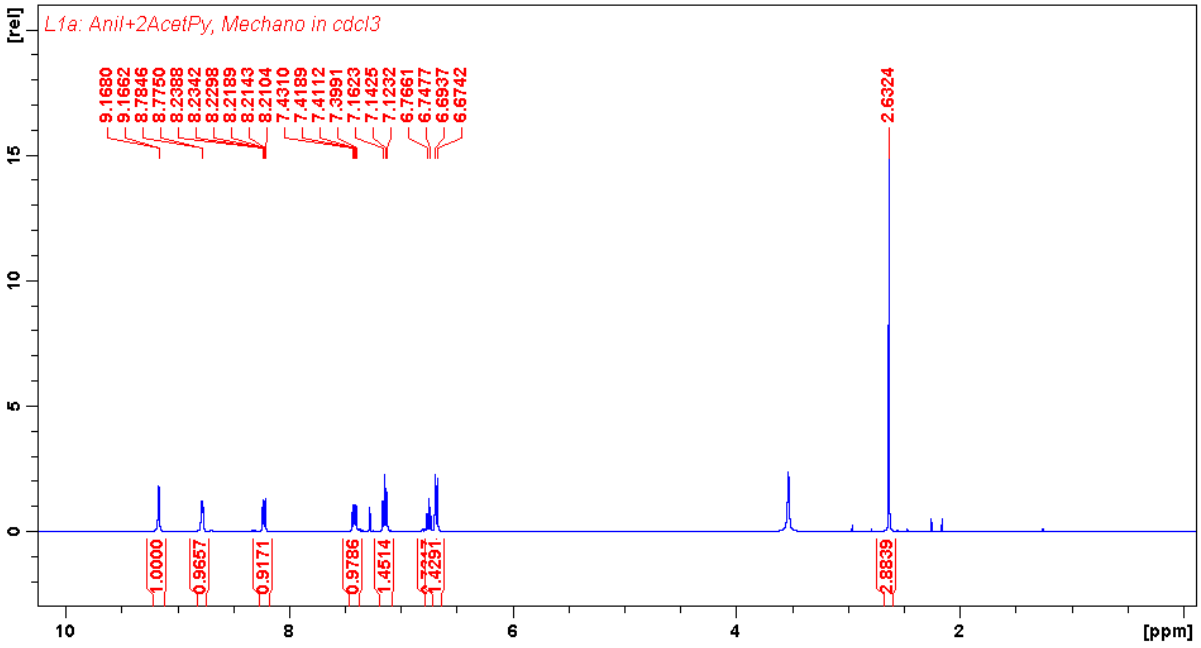

B21: ^{1}H-NMR of ligand (**L11**)

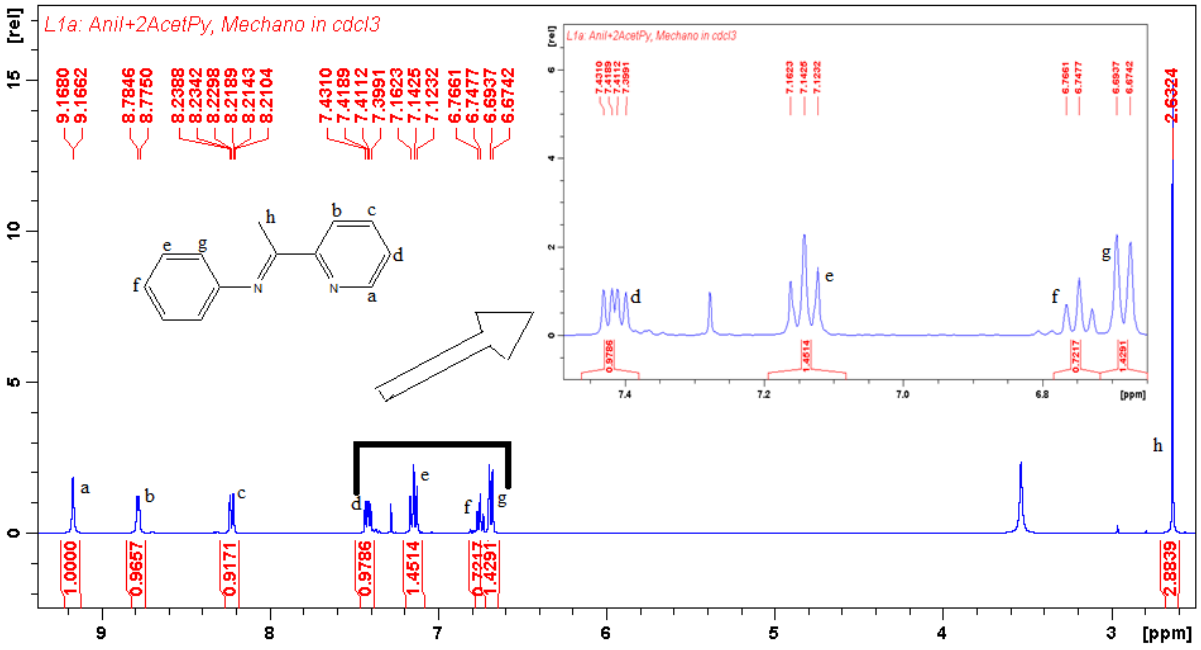

B22: Expanded ^{1}H-NMR of ligand (**L11**)

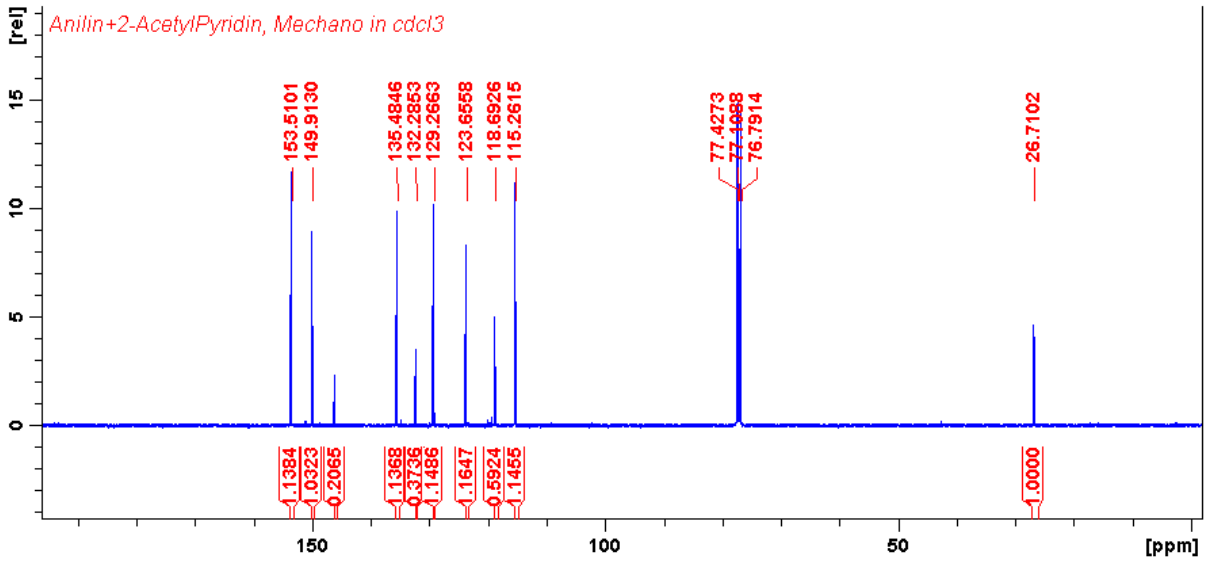

B23: ^{13}C-NMR of ligand (**L11**)

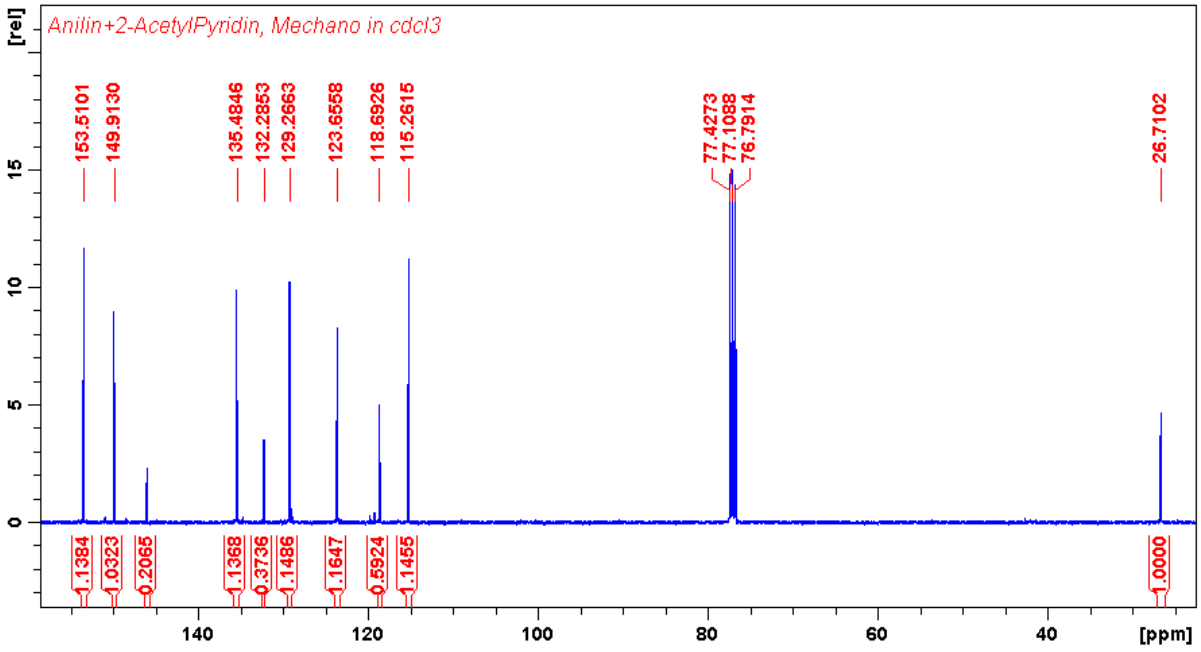

B24: Expanded ^{13}C-NMR of ligand (**L11**)

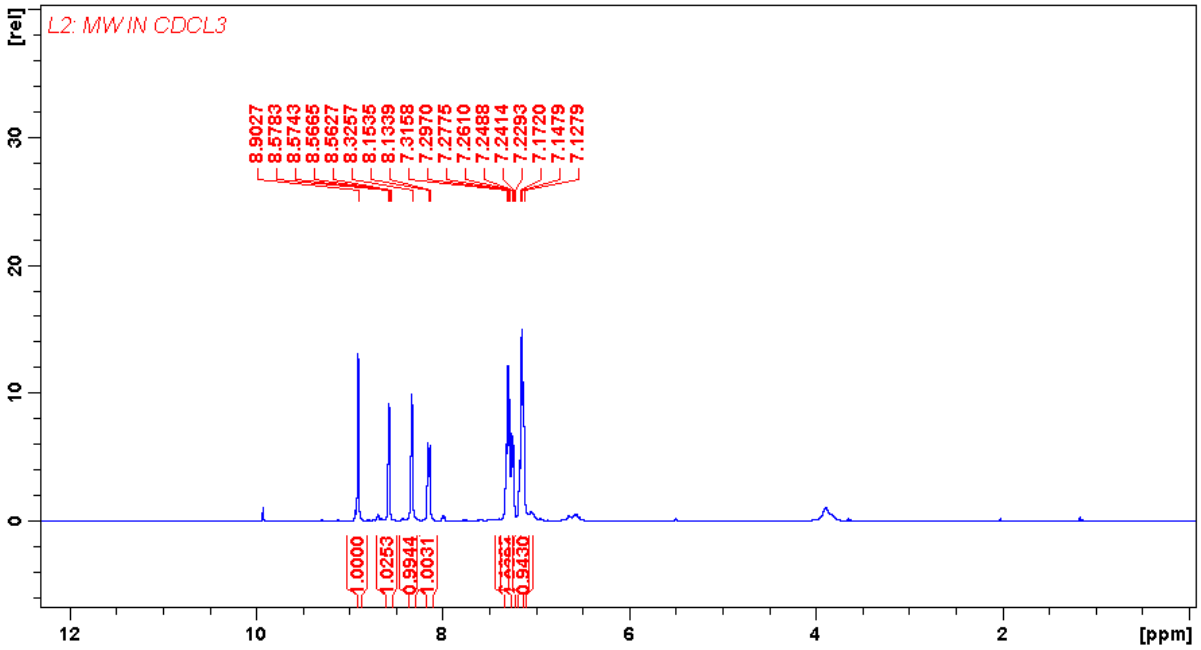

B25: ^{1}H-NMR of ligand (**L12**)

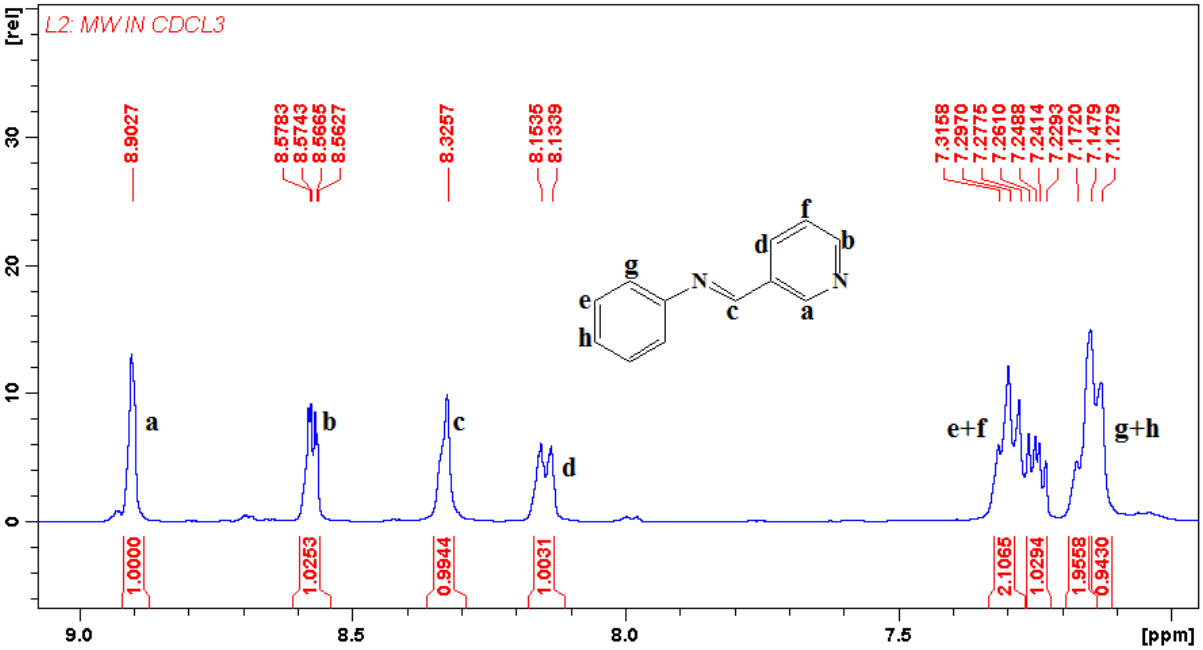

B26: Expanded ^{1}H-NMR of ligand (**L12**)

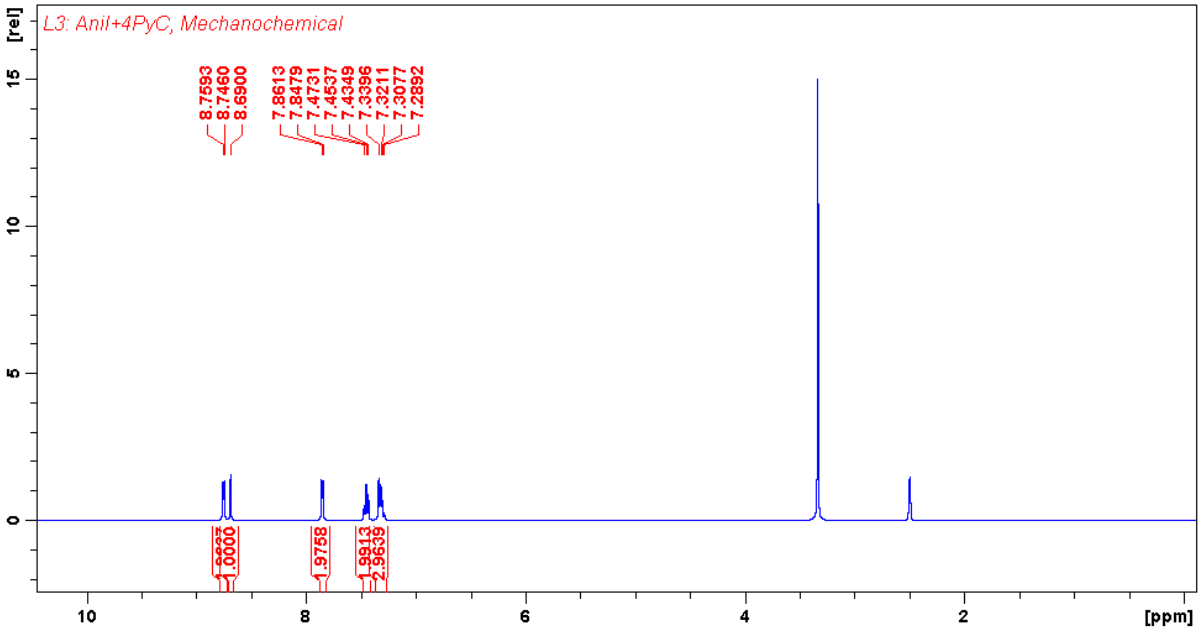

B27: ^{1}H-NMR of ligand (**L13**)

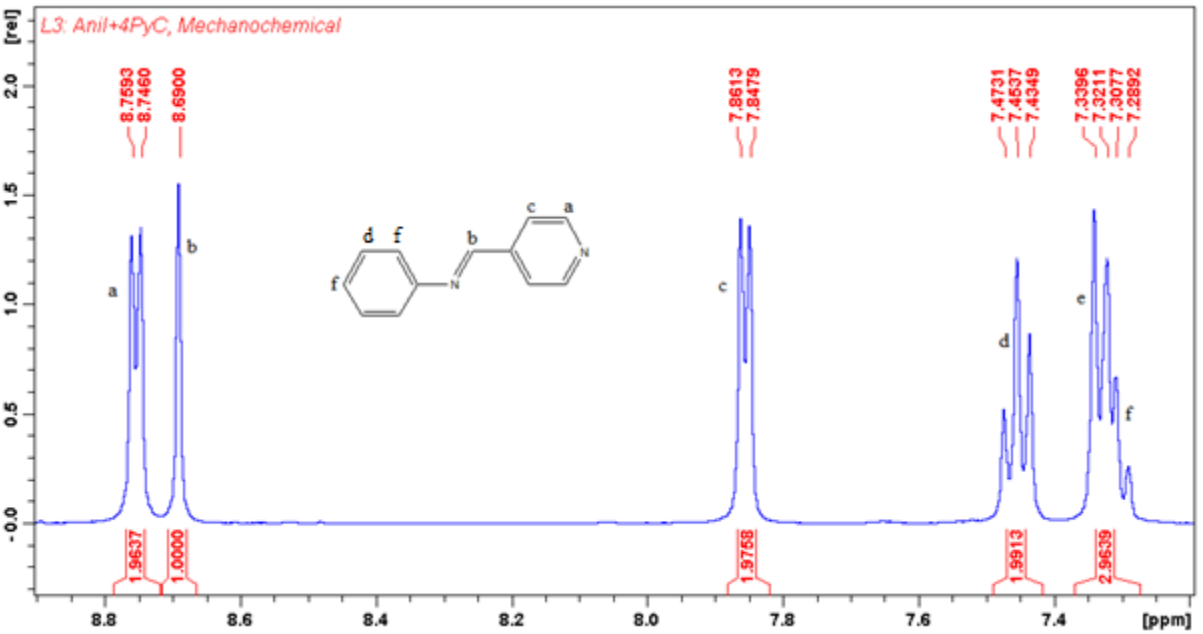

B28: Expanded ^{1}H-NMR of ligand (**L13**)

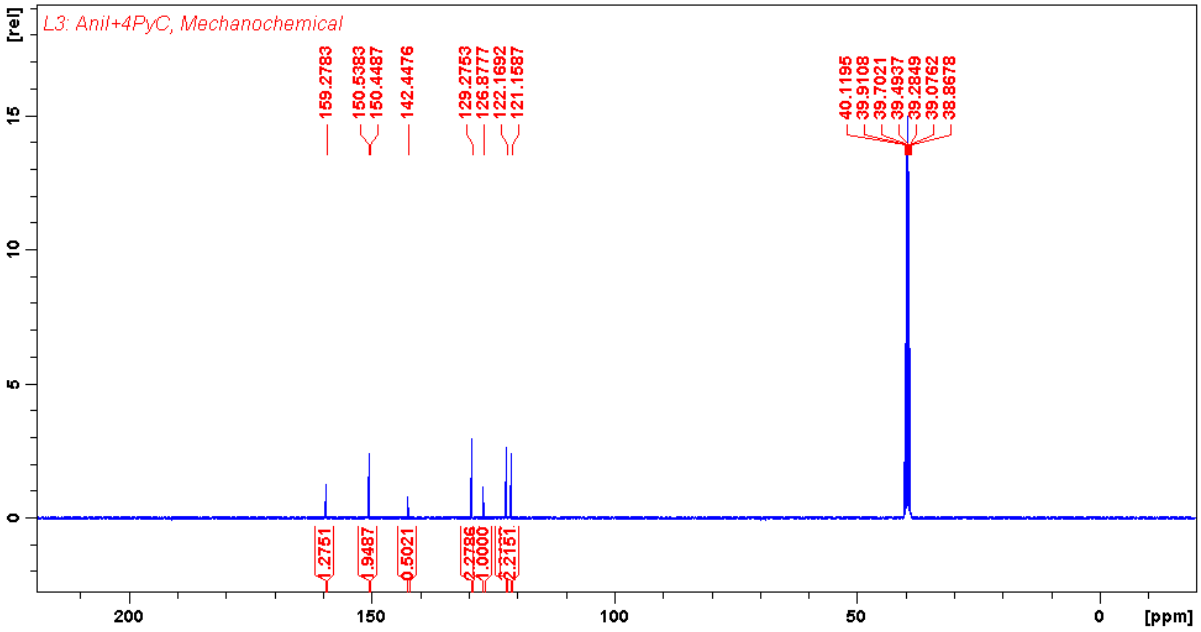

B29: ^{13}C-NMR of ligand (**L13**)

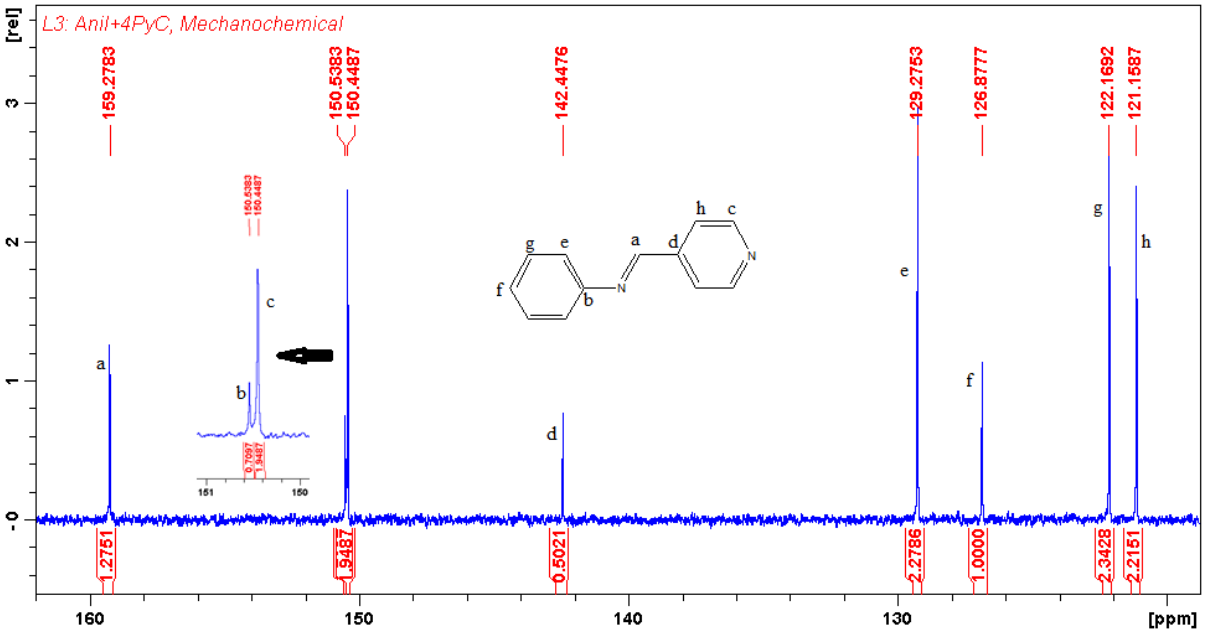

B30: Expanded ^{13}C-NMR of ligand (**L13**)

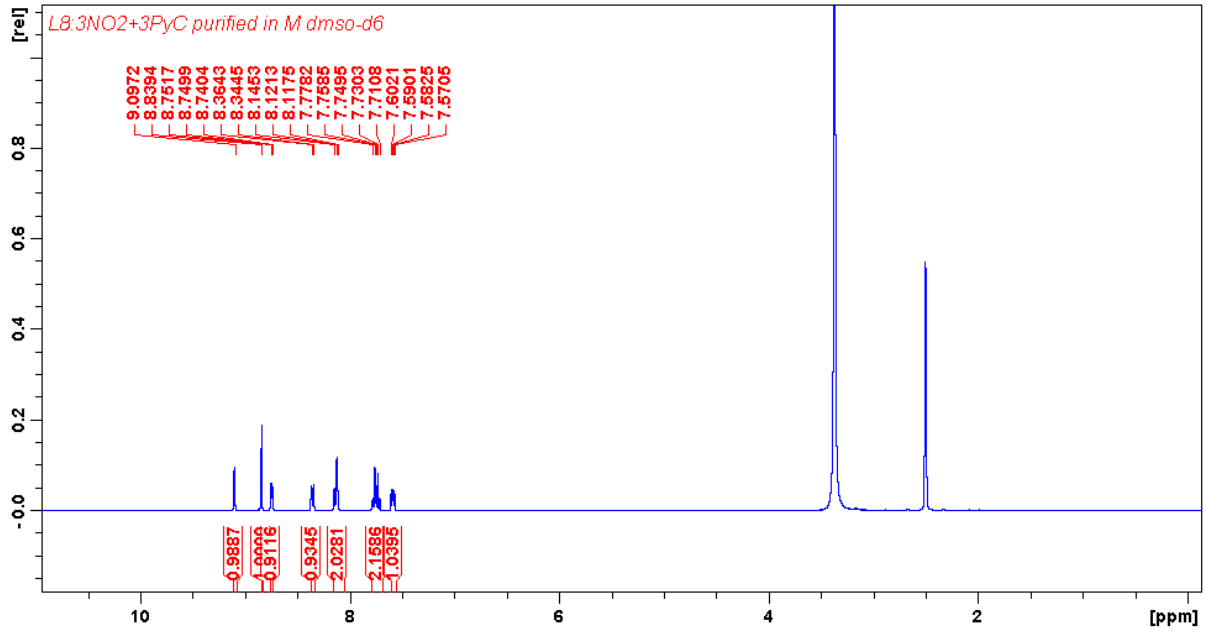

B31: ^{1}H-NMR of ligand (**14**)

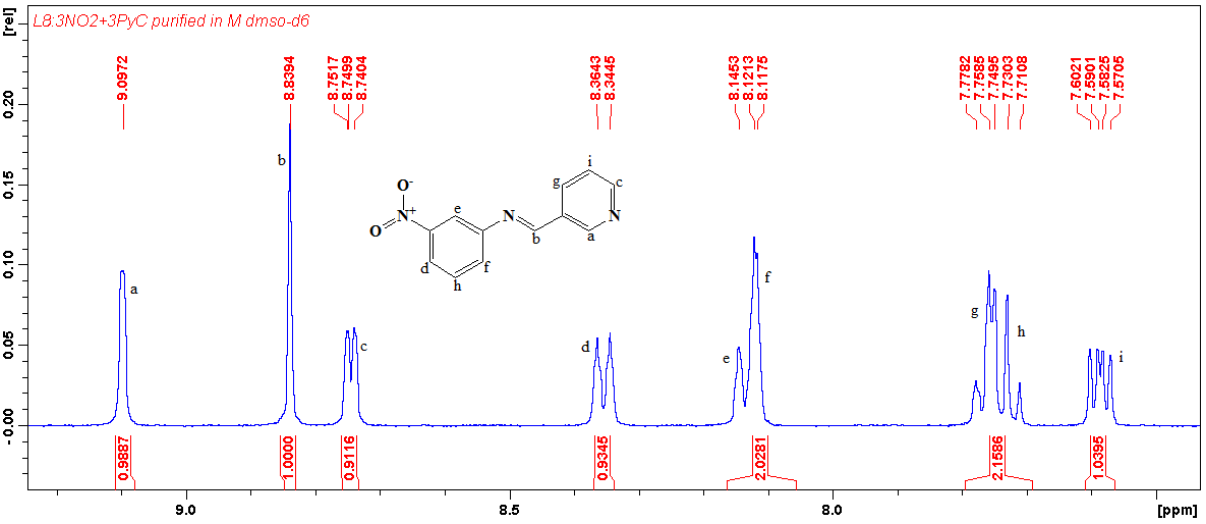

B32: Expanded ^{1}H-NMR of ligand (**L14**)

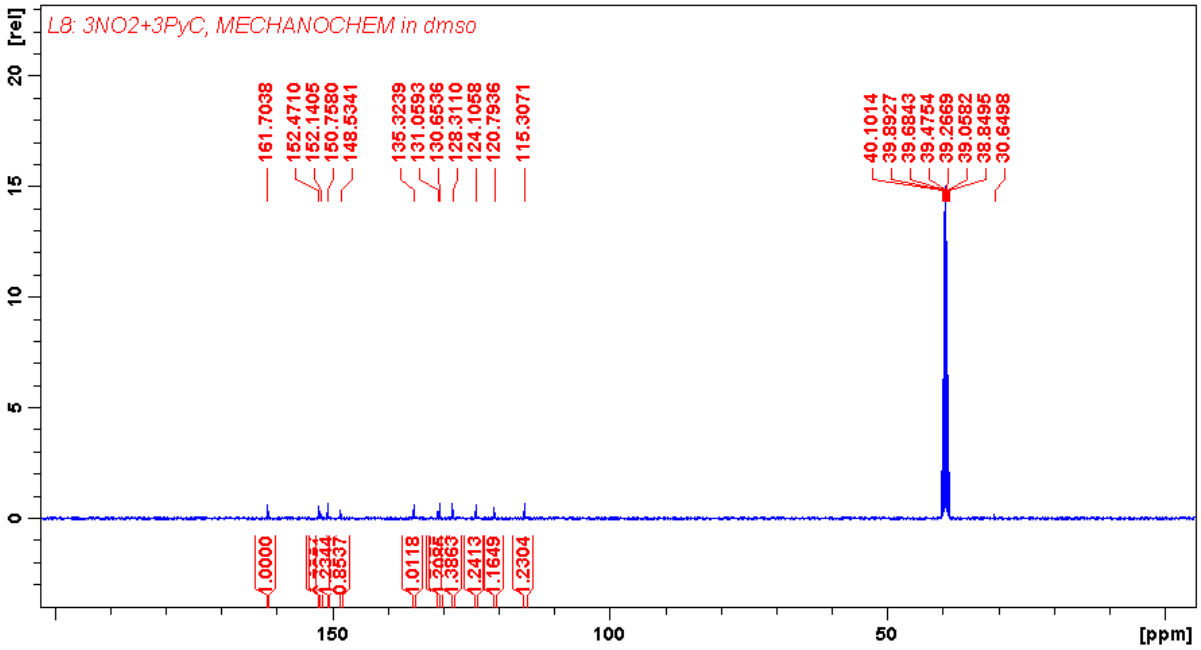

B33: ^{13}C-NMR of ligand (**L14**)

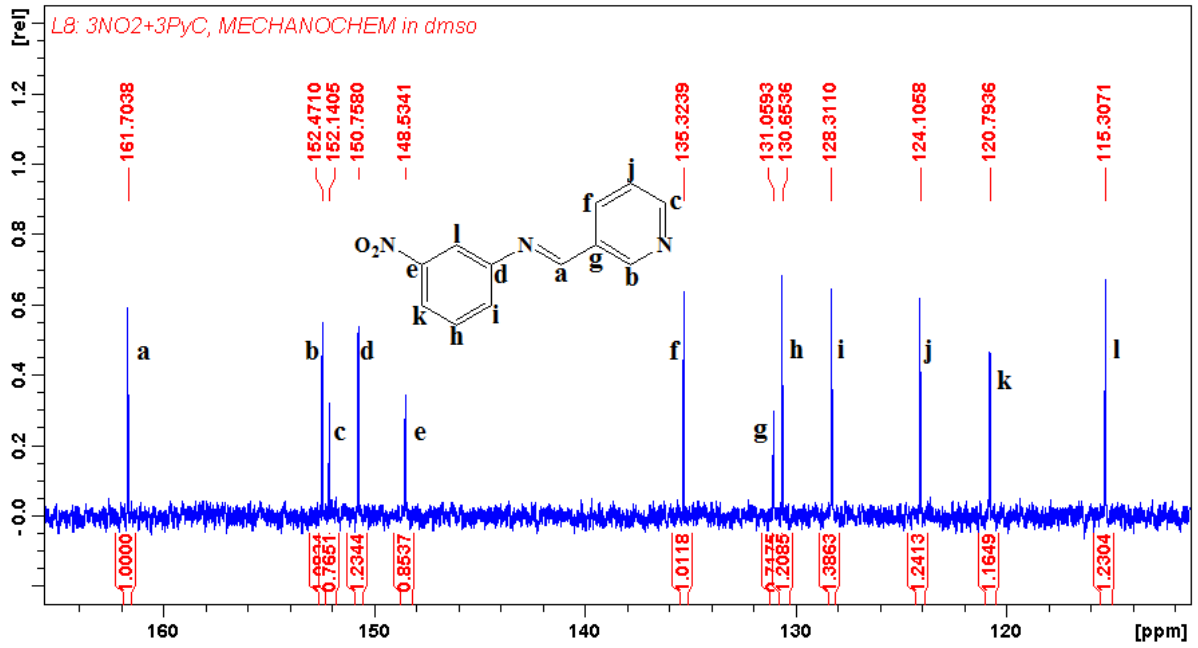

B34: Expanded ^{13}C-NMR of ligand (**L14**)

Appendix C

UV-vis spectra

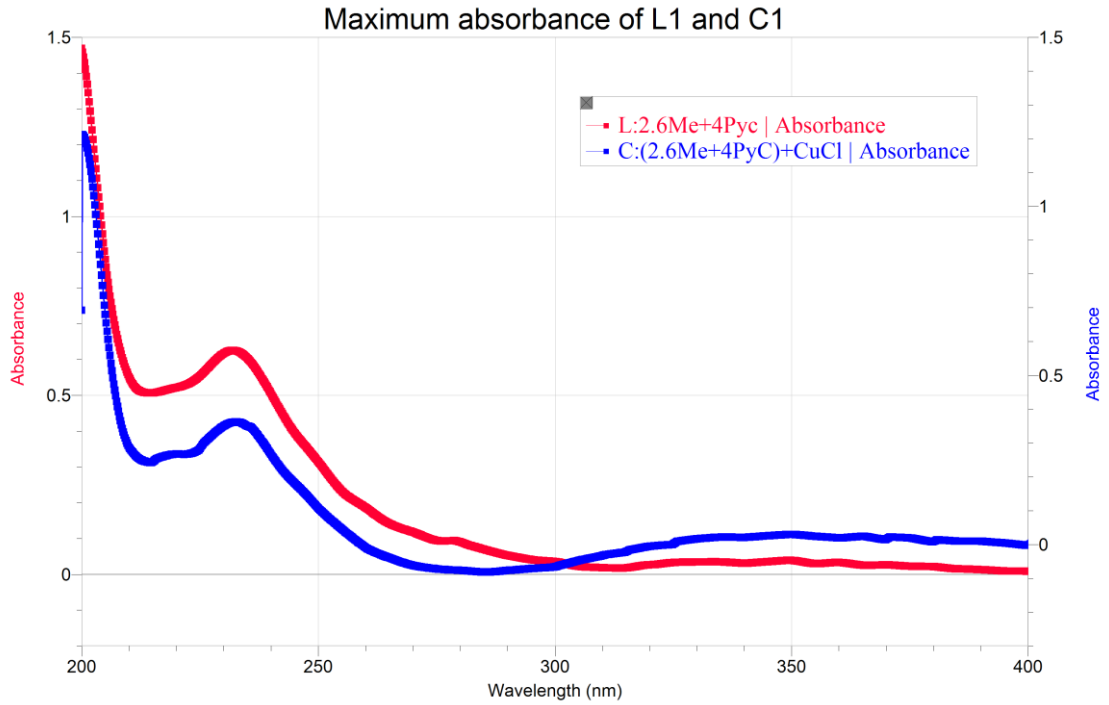

C1: UV-vis spectra of ligand (**L1**) and complex **1**

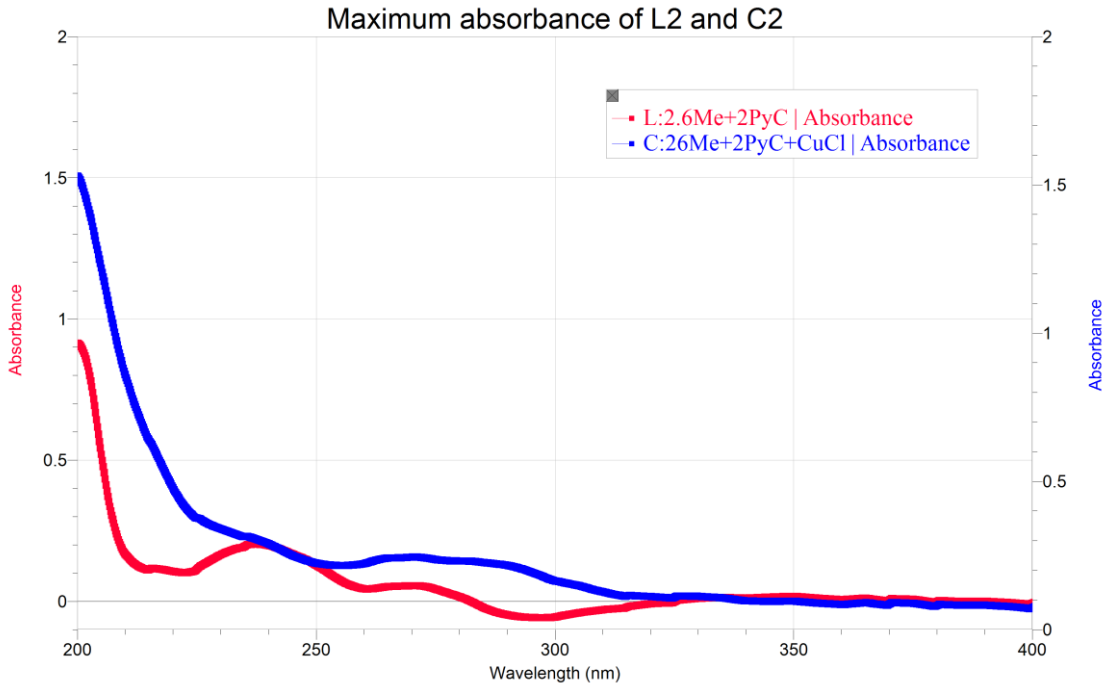

C2: UV-vis spectra of ligand (**L2**) and complex **2**

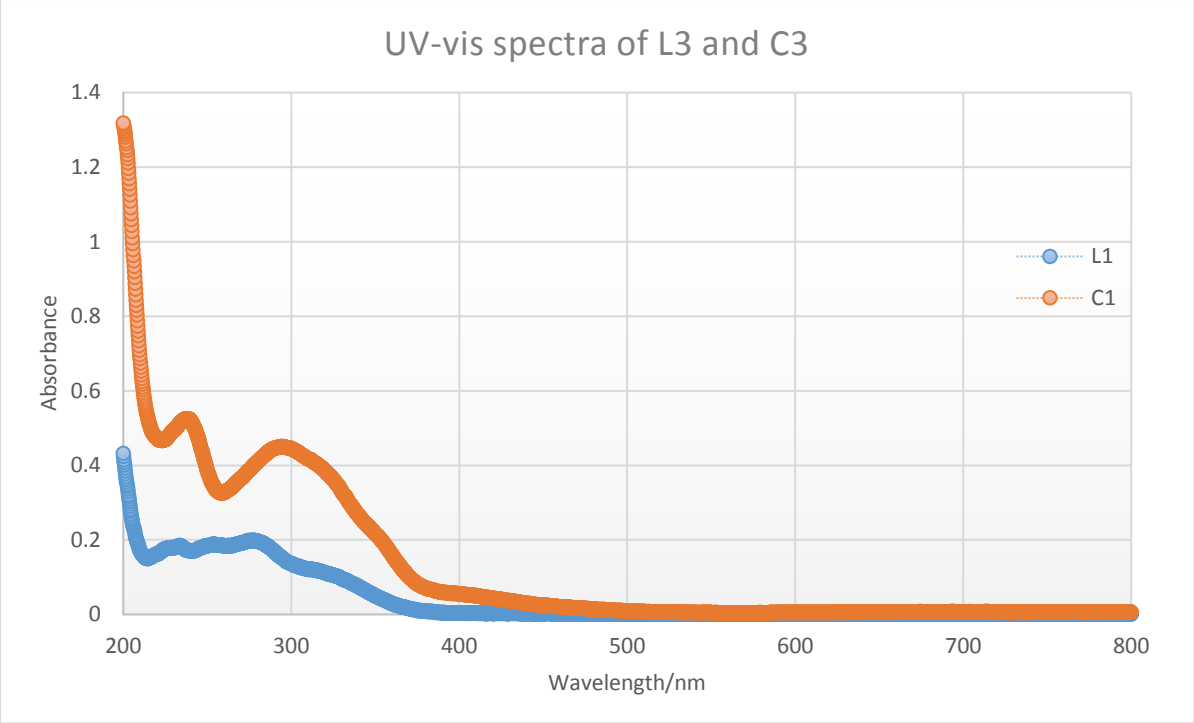

C3: UV-vis spectra of ligand (**L3**) and complex **3**

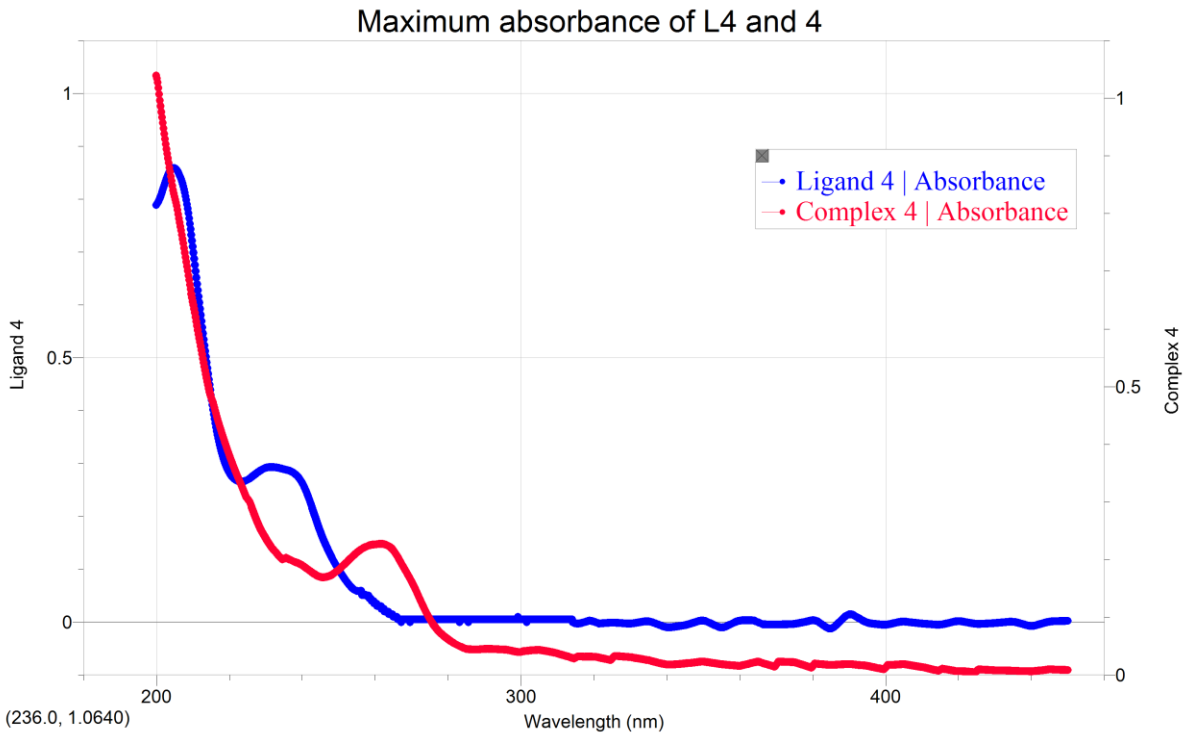

C4: UV-vis spectra of ligand (**L4**) and complex **4**

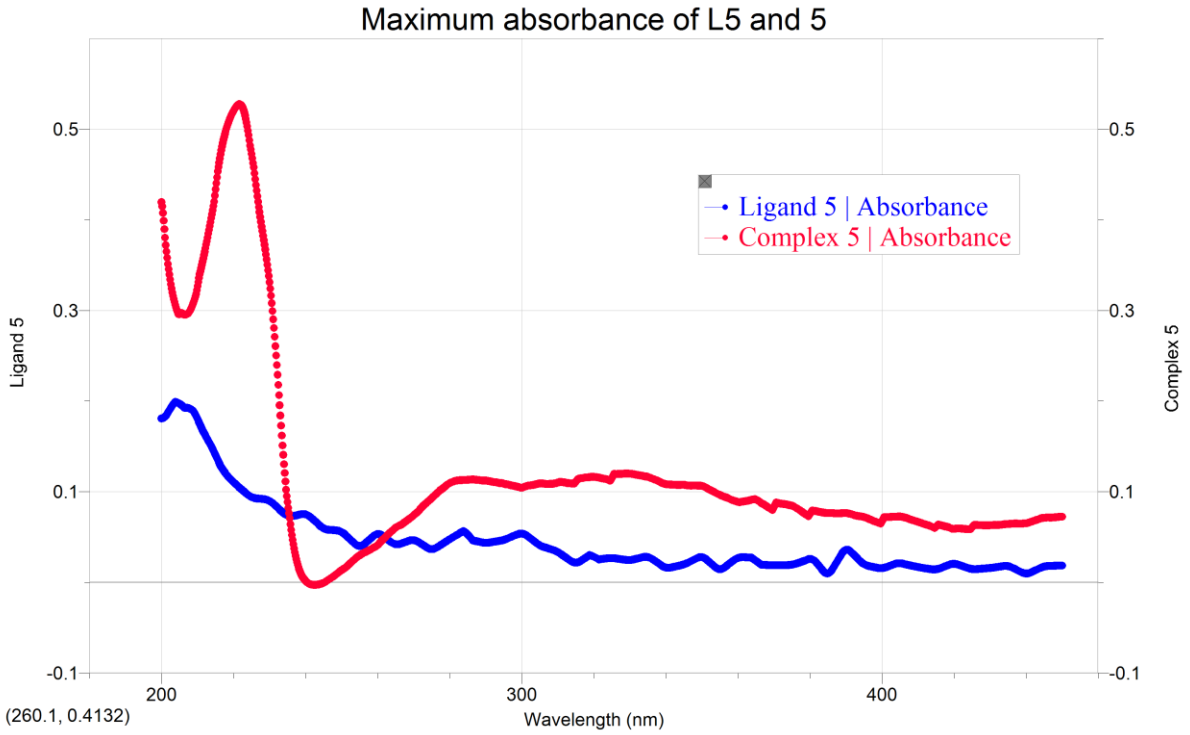

C5: UV-vis spectra of ligand (**L5**) and complex **5**

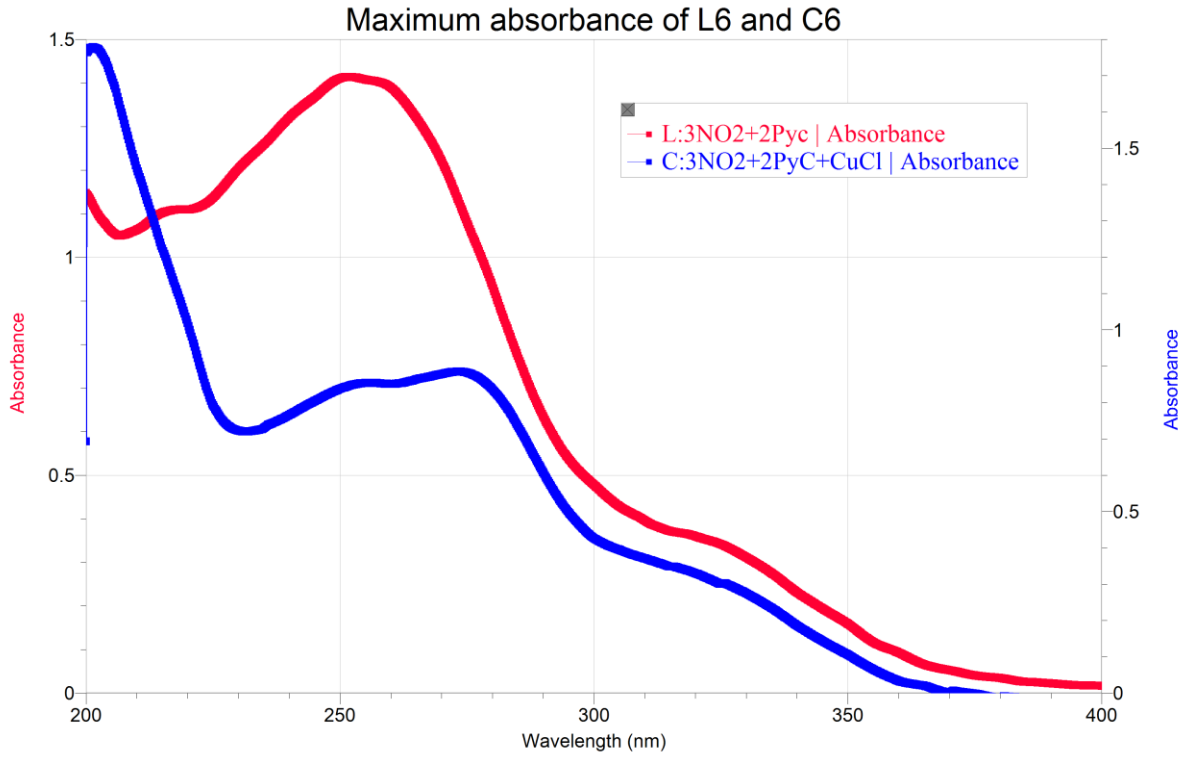

C6: UV-vis spectra of ligand (**L6**) and complex **6**

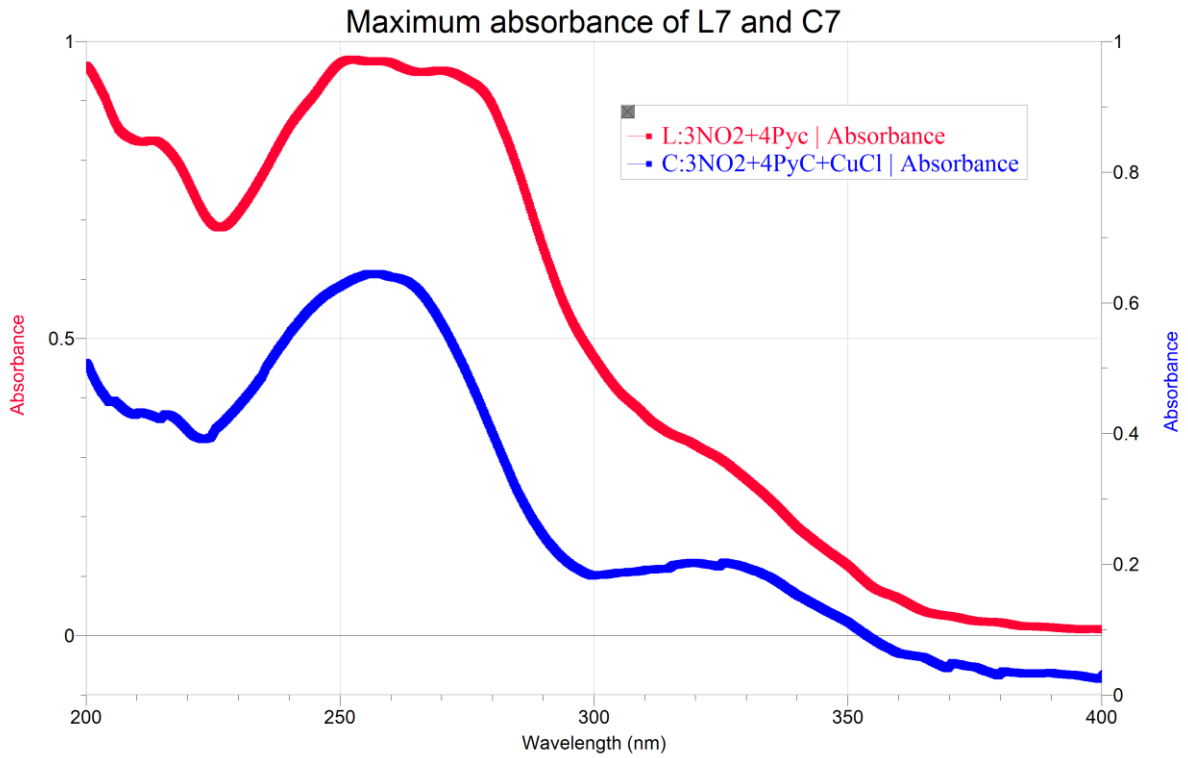

C7: UV-vis spectra of ligand (**L7**) and complex **7**

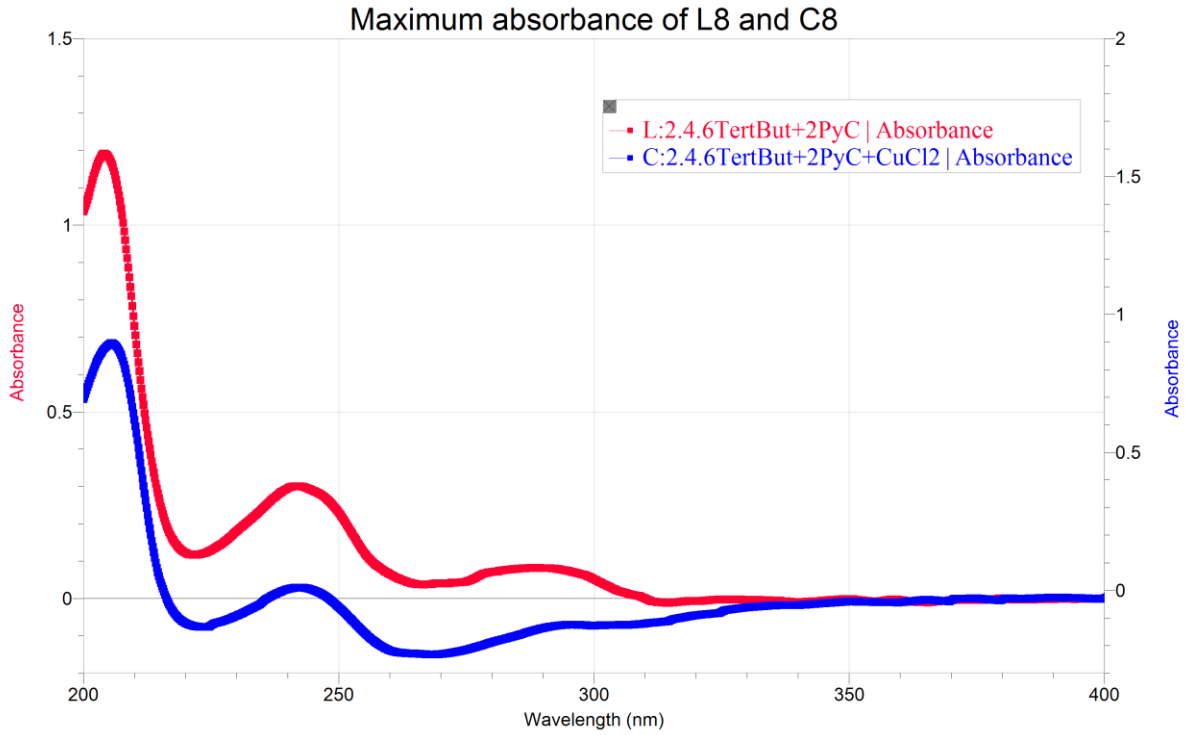

C8: UV-vis spectra of ligand (**L10**) and complex **8**

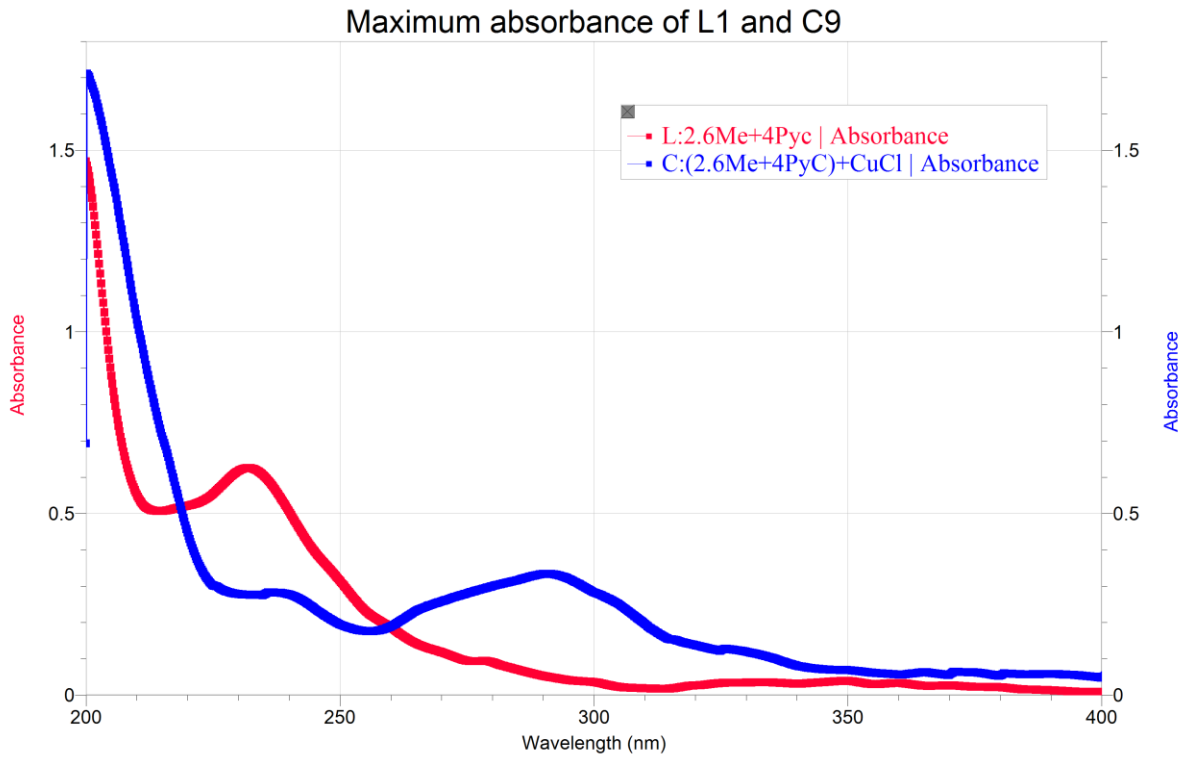

C9: UV-vis spectra of ligand (**L1**) and complex **9**

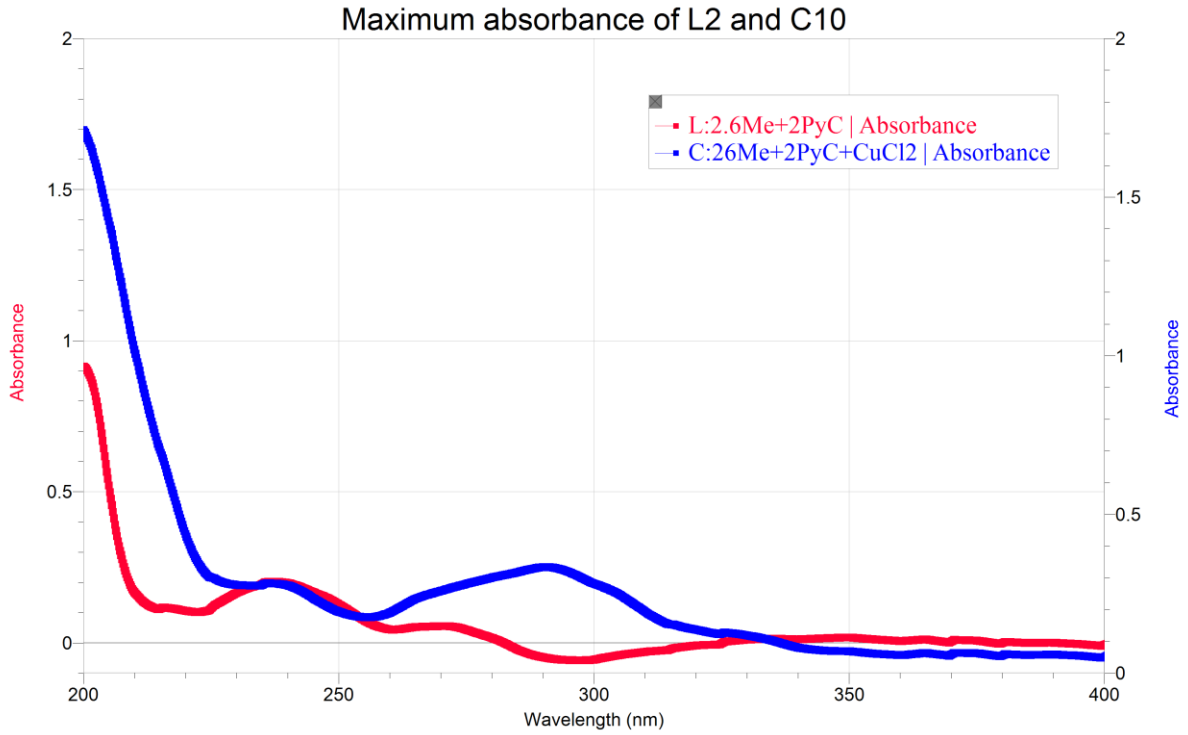

C10: UV-vis spectra of ligand (**L2**) and complex **10**

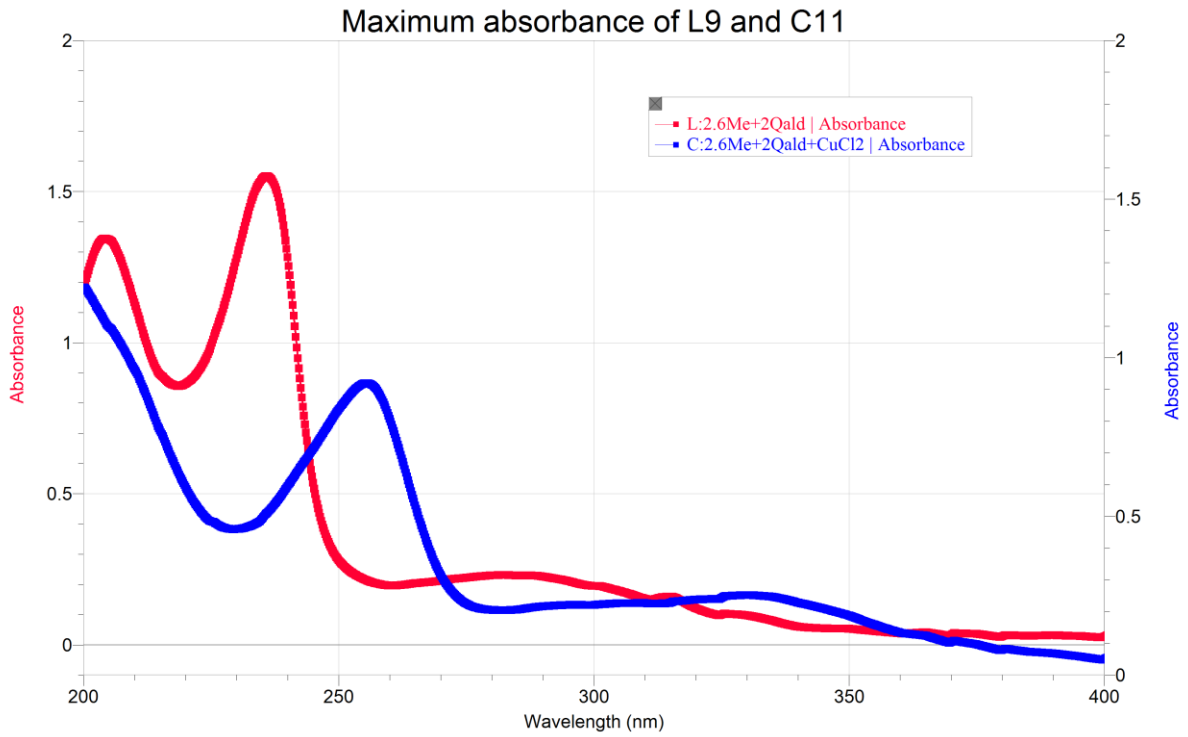

C11: UV-vis spectra of ligand (**L9**) and complex **11**

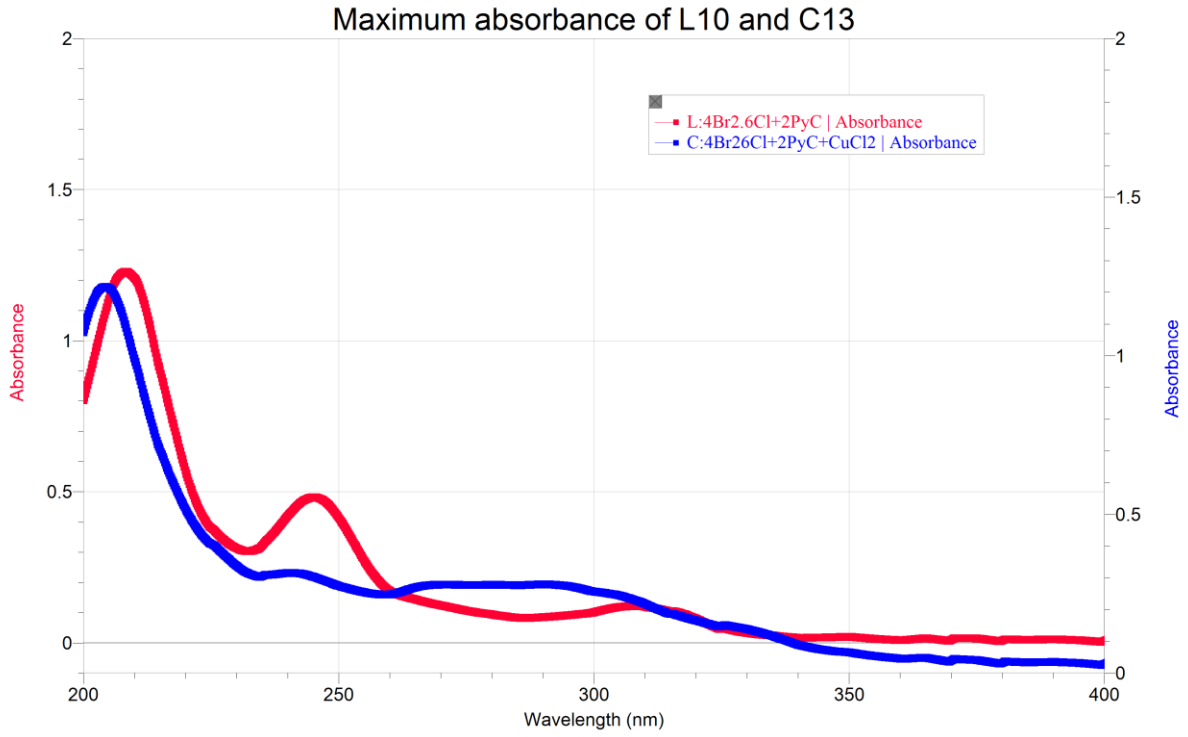

C12: UV-vis spectra of ligand (**L8**) and complex **13**

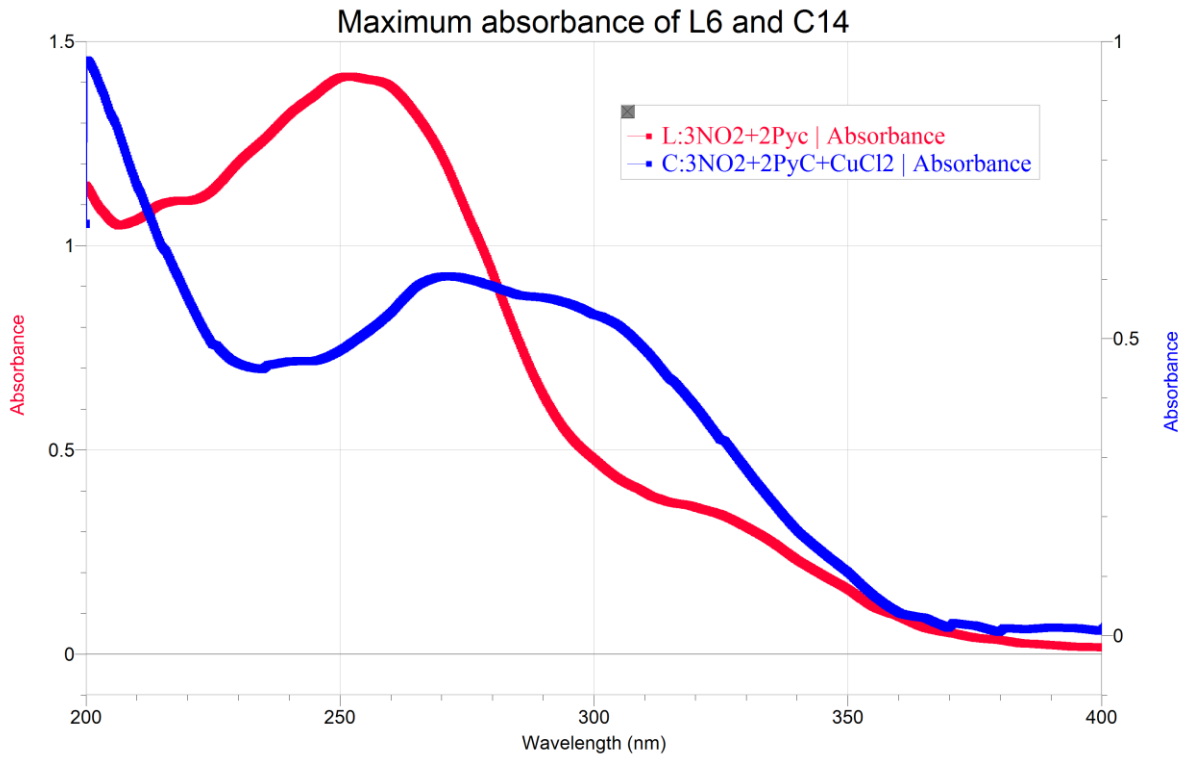

C13: UV-vis spectra of ligand (**L6**) and complex **14**

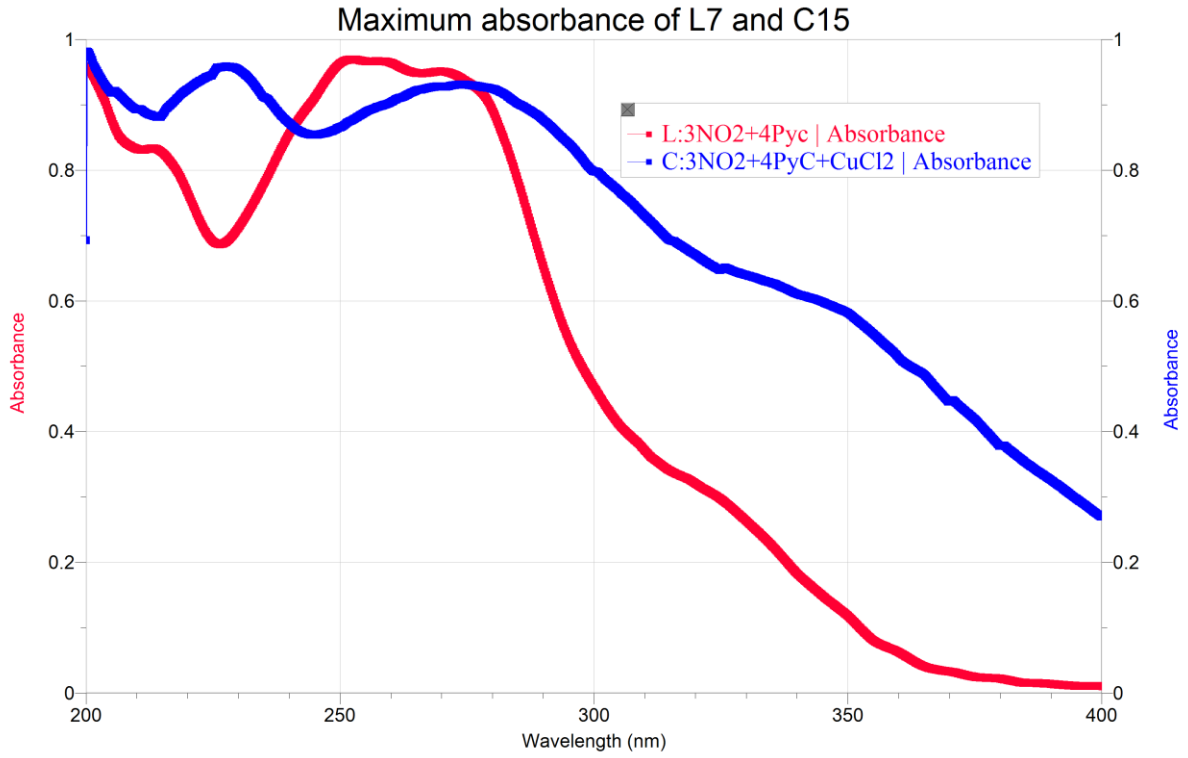

C14: UV-vis spectra of ligand (**L7**) and complex **15**

Appendix D

LR-MS and HR-MS spectra

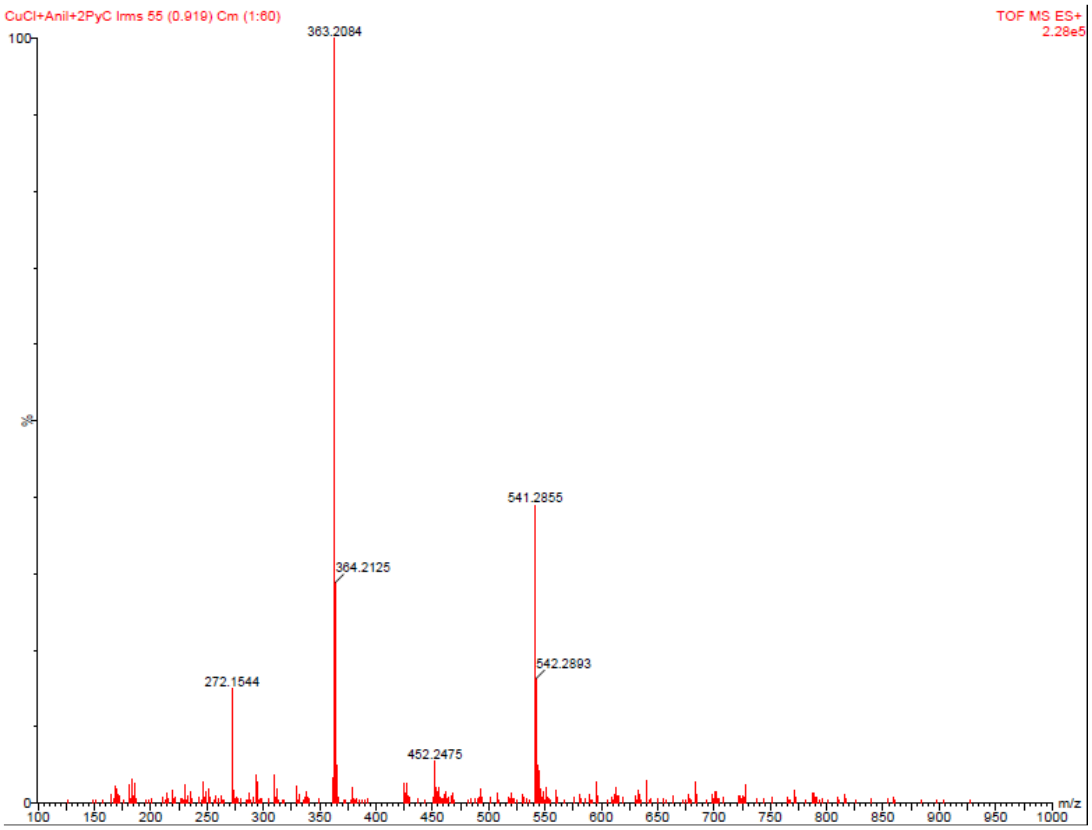

D1: LR-MS of complex **1**

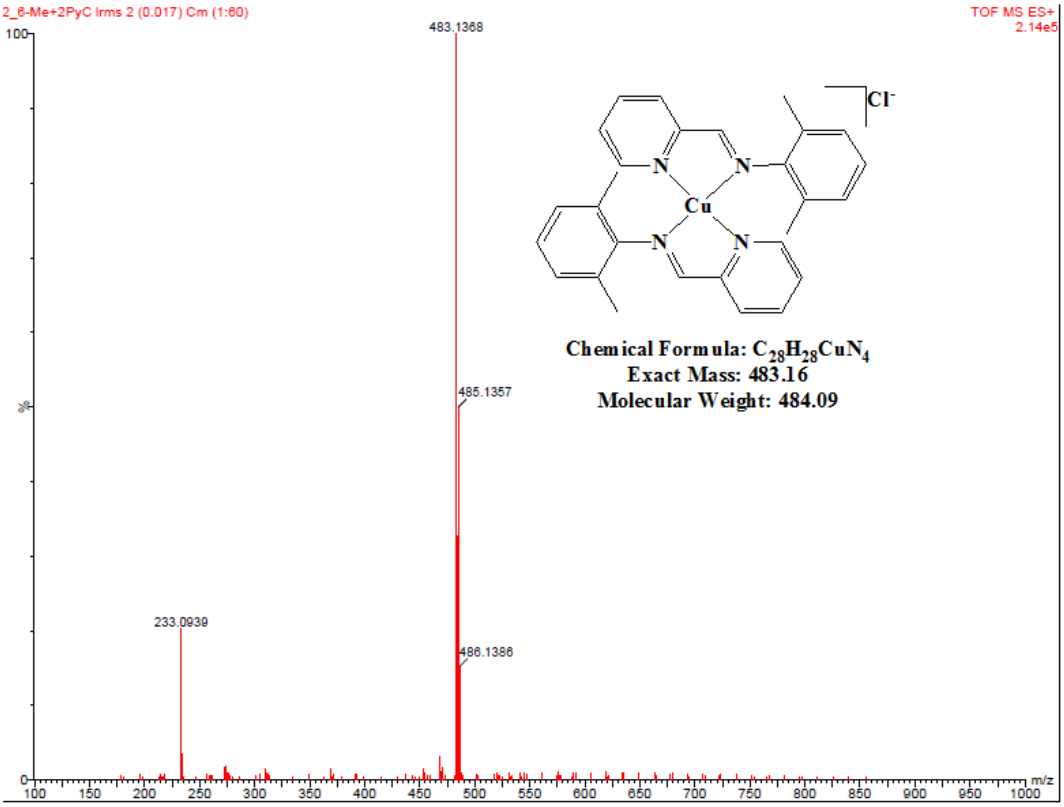

D2: LR-MS of complex **2**

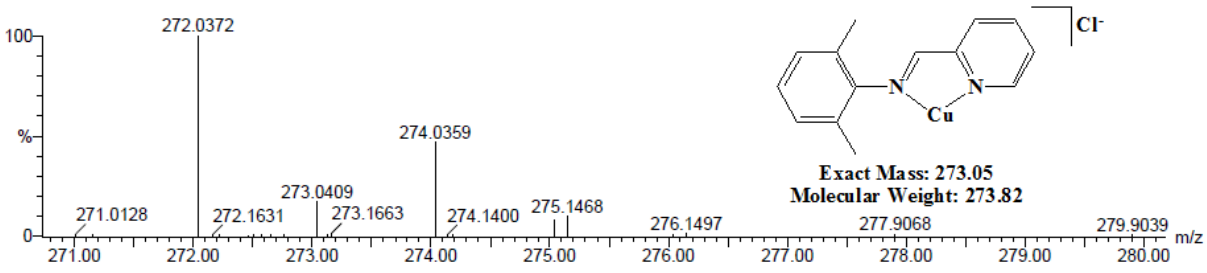

D3: HR-MS of complex **2**

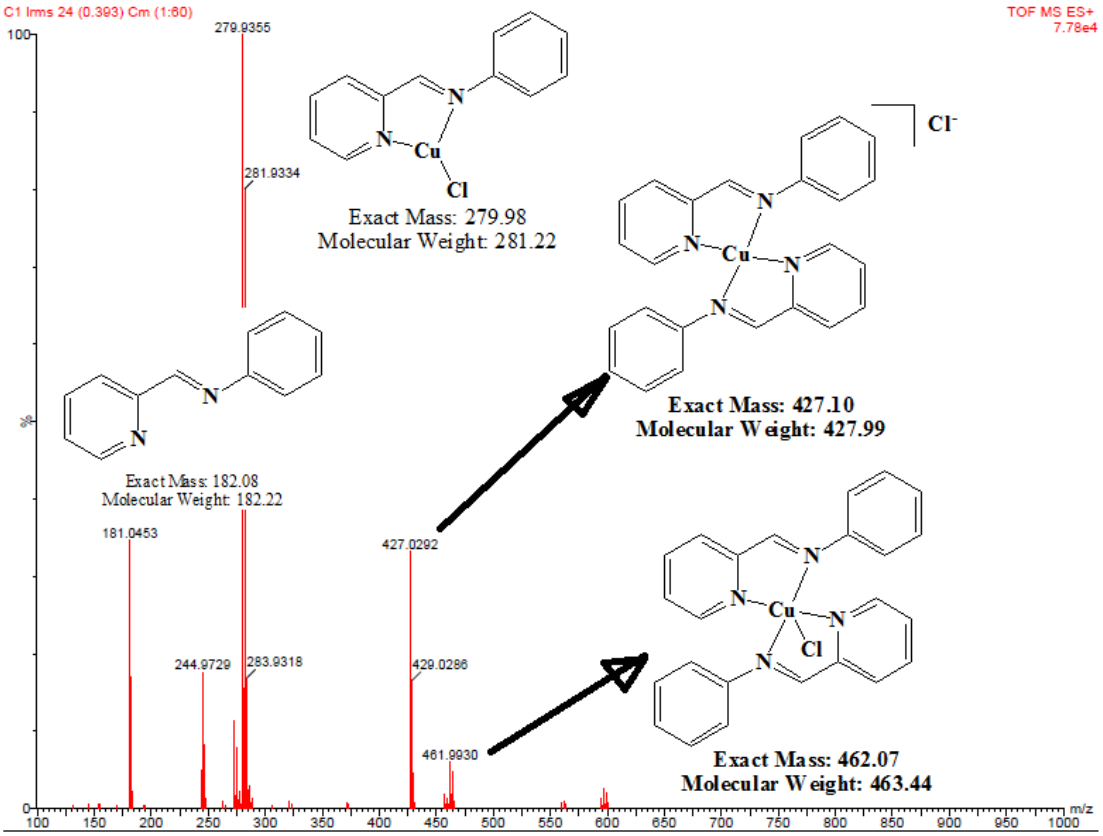

D4: LR-MS of complex **3**

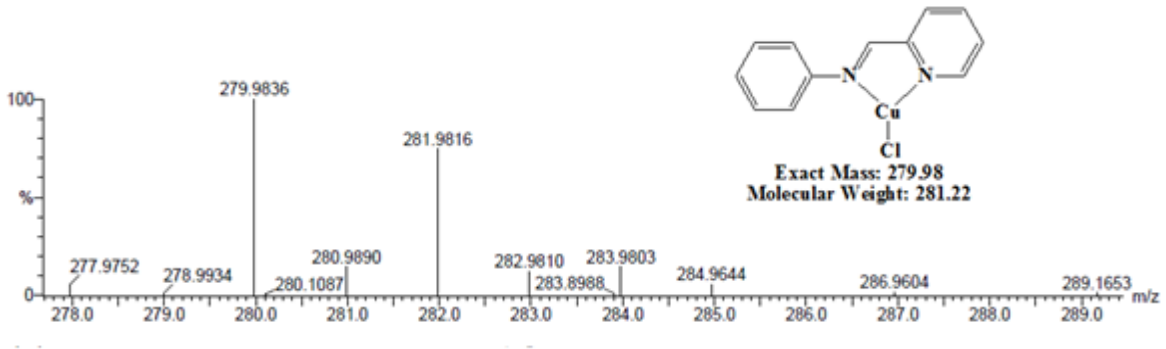

D5: HR-MS of complex **3**

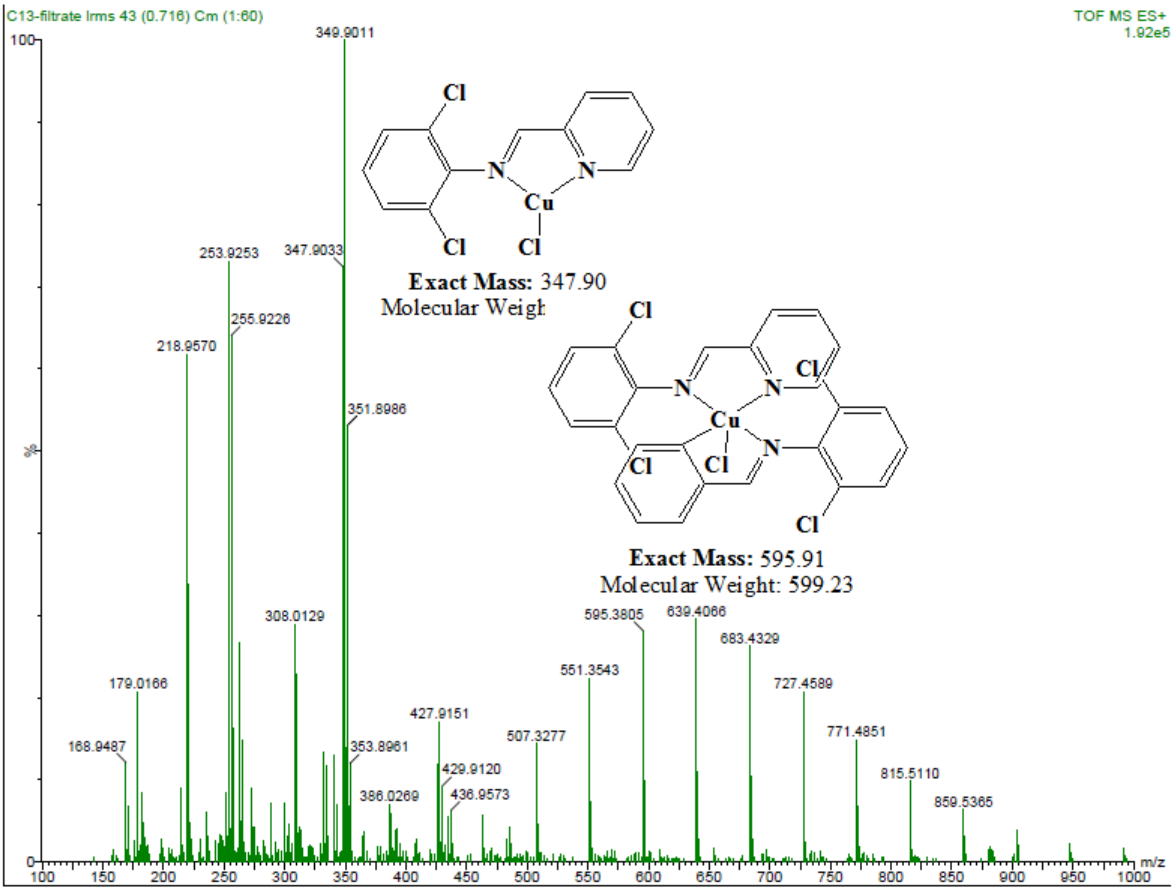

D6: LR-MS of complex **4**

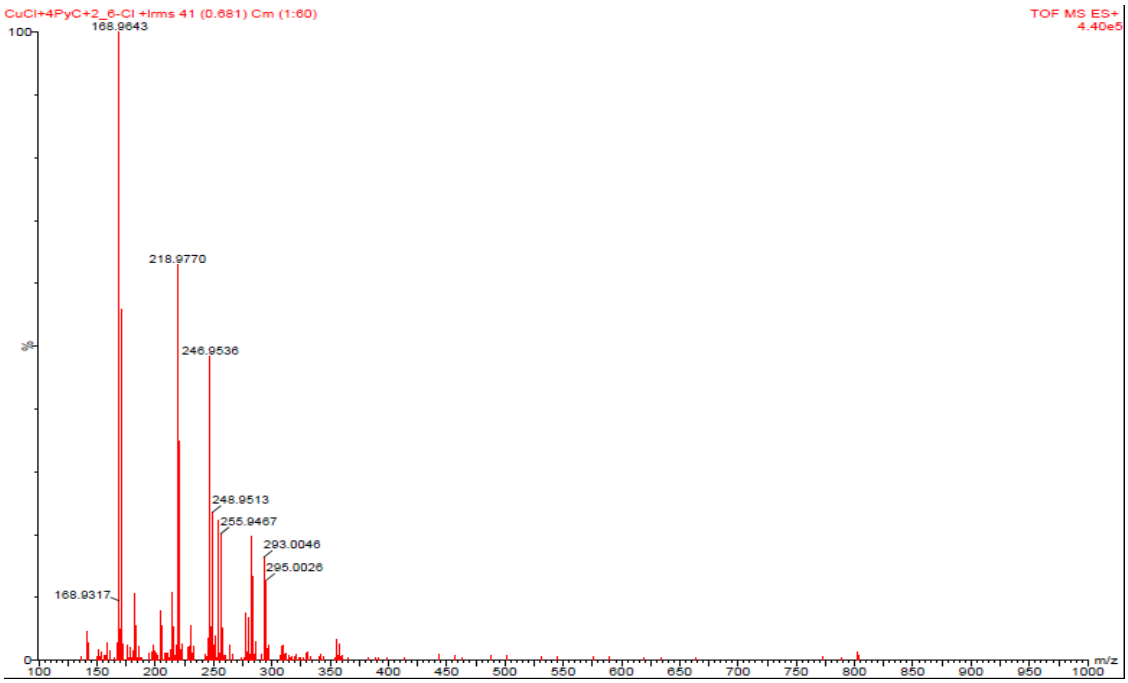

D7: LR-MS of complex **5**

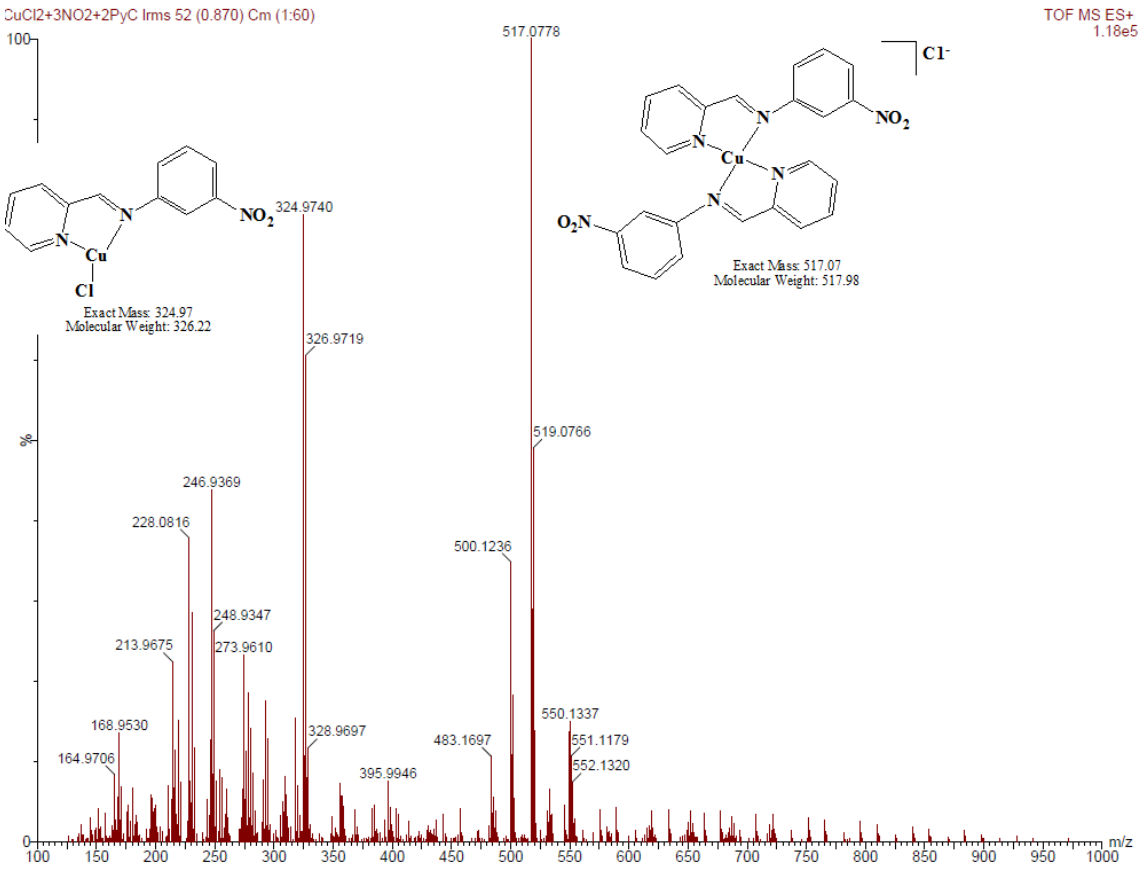

D8: LR-MS of complex **6**

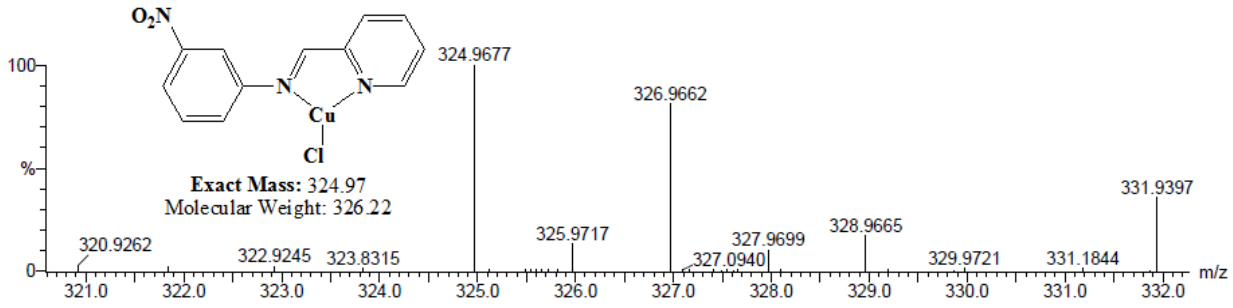

D9: HR-MS of complex **6**

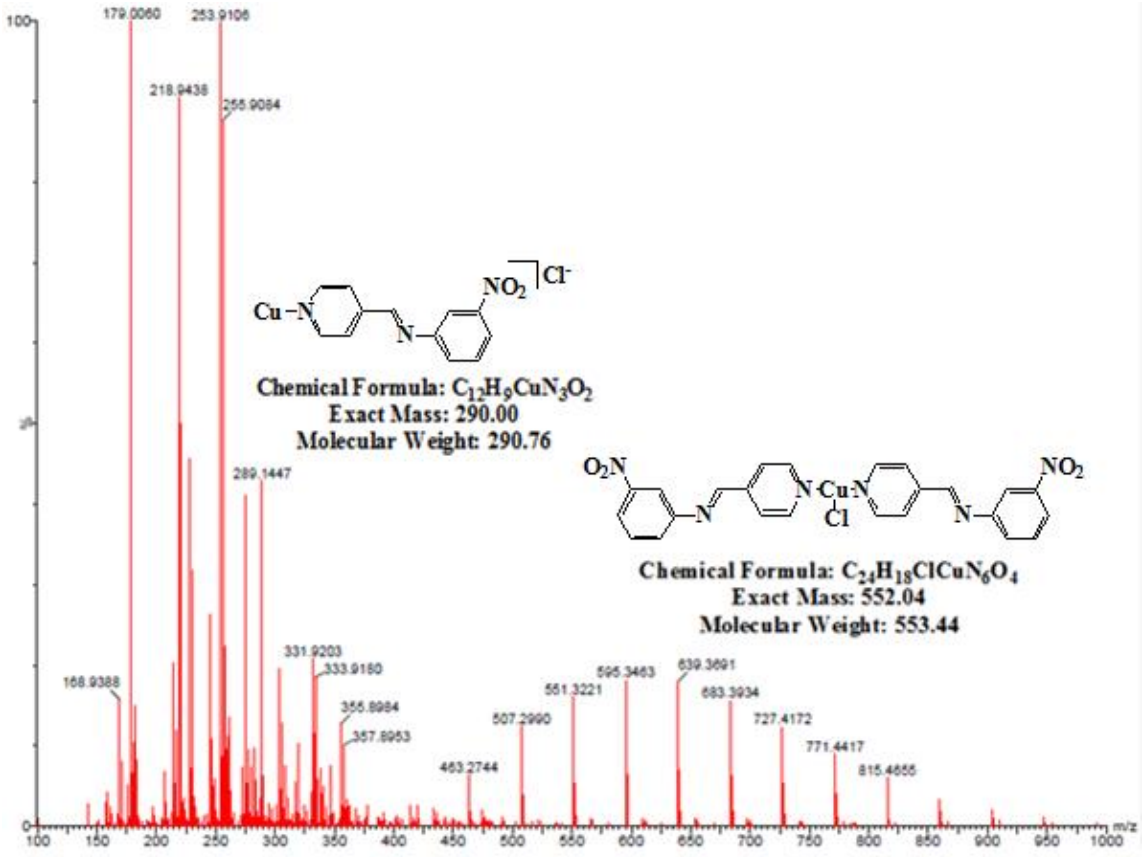

D10: LR-MS of complex **7**

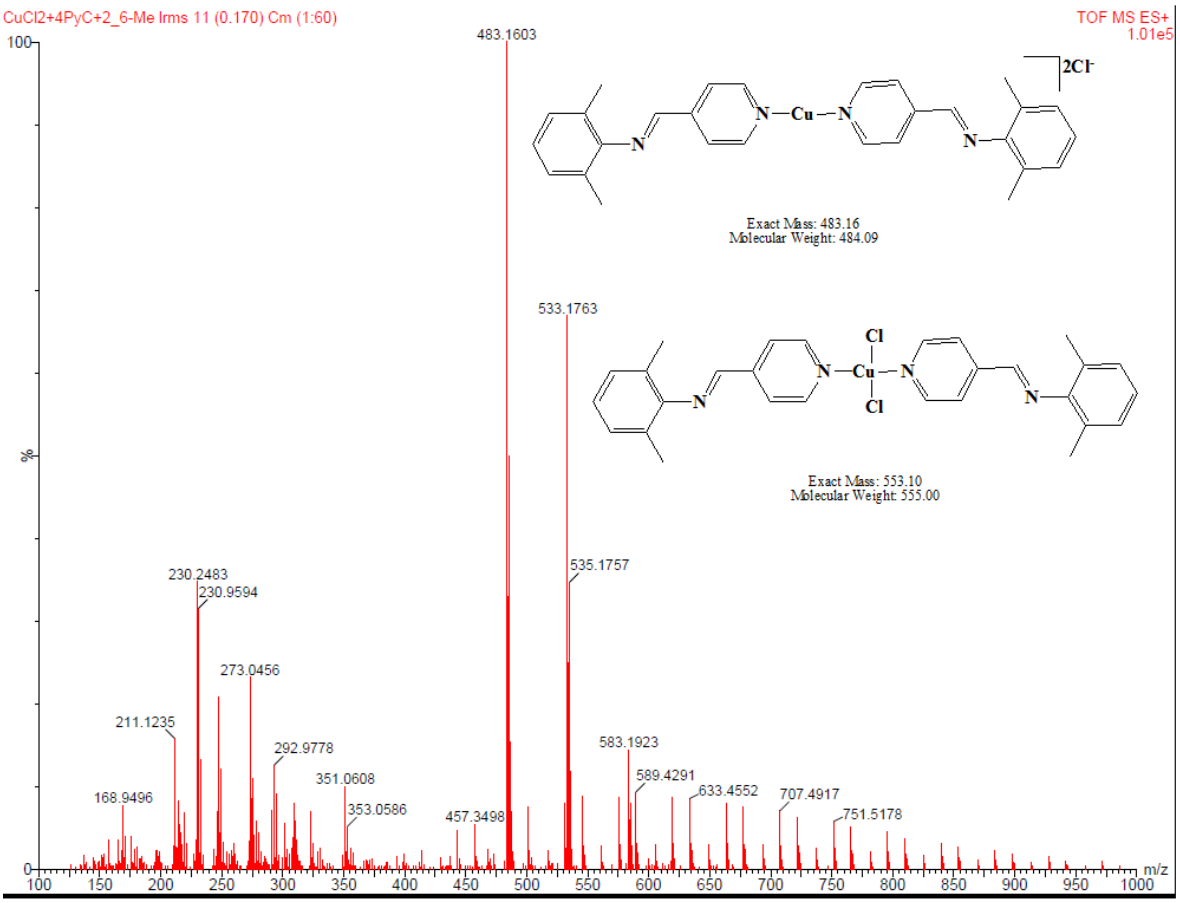

D11: LR-MS of complex **9**

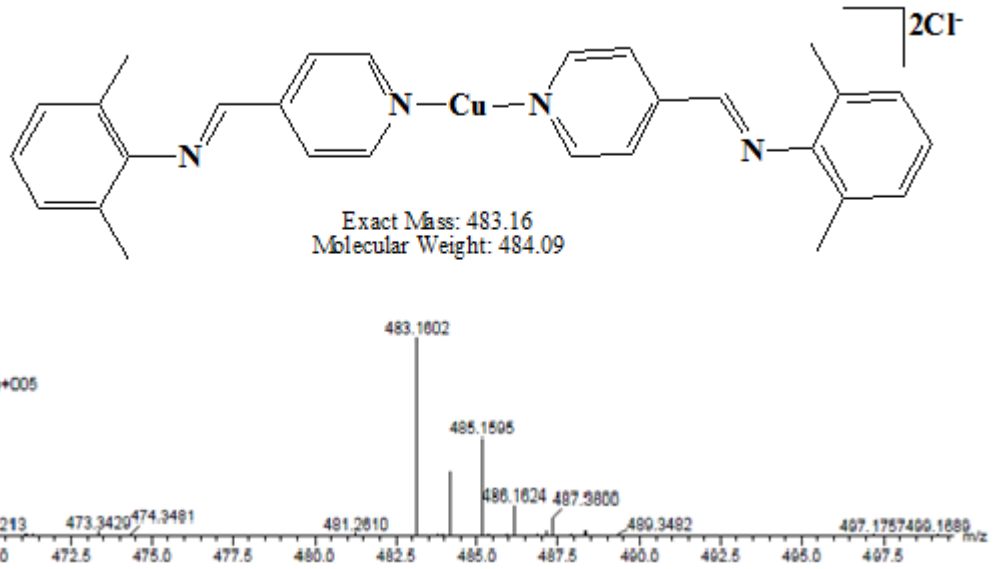

D12: HR-MS of complex **9**

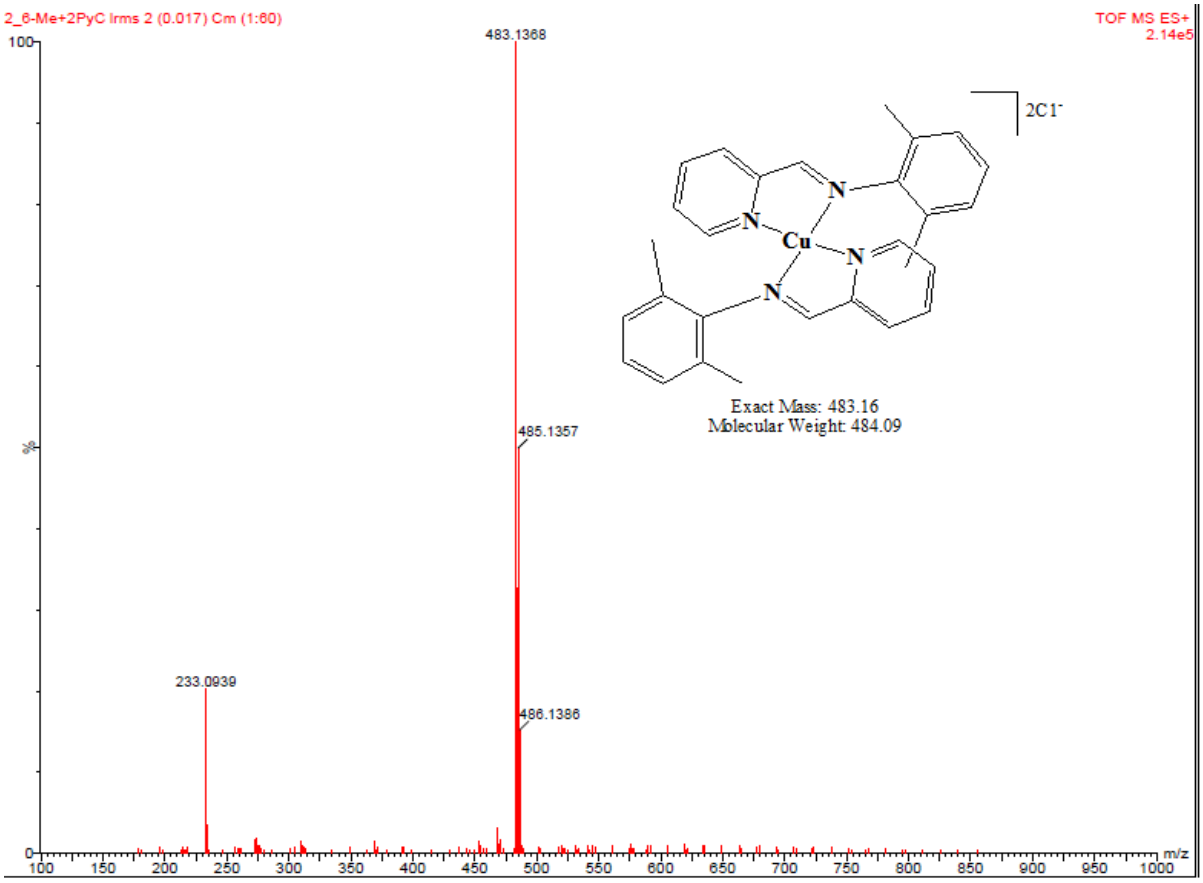

D13: LR-MS of complex **10**

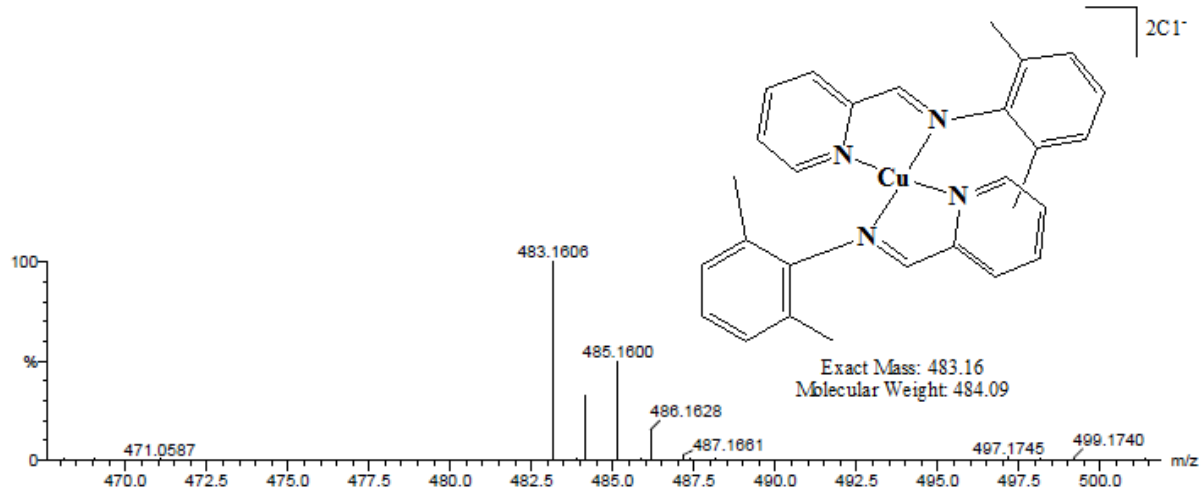

D14: HR-MS of complex **10**

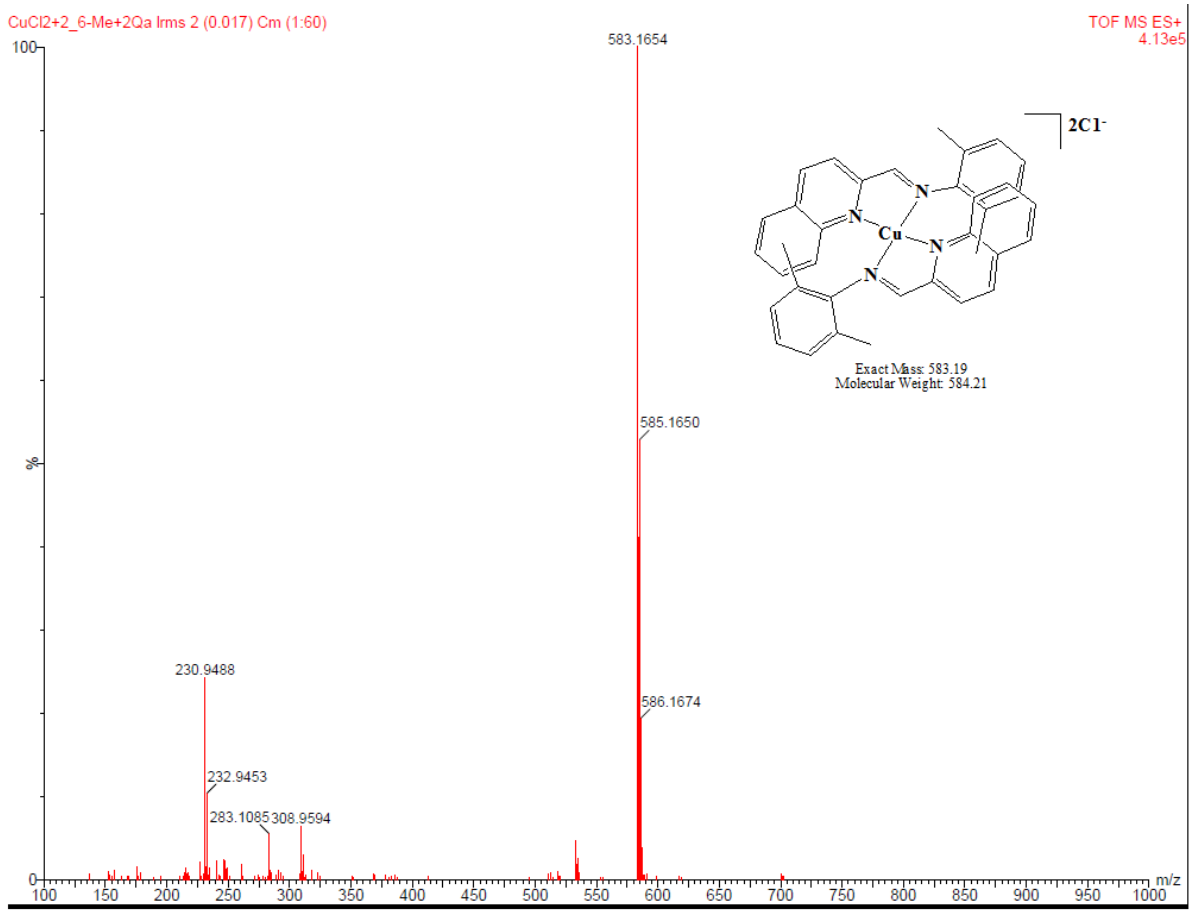

D15: LR-MS of complex **11**

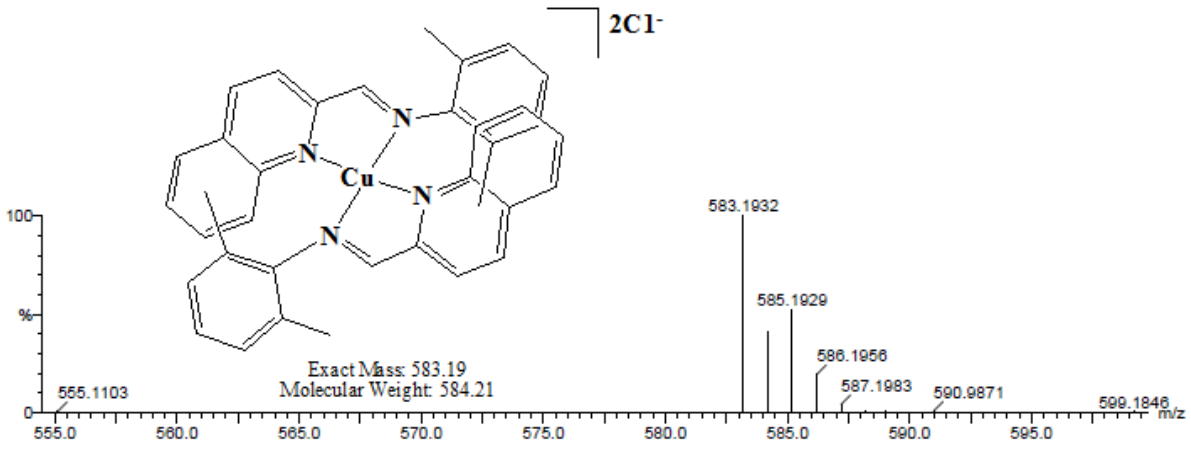

D16: HR-MS of complex **11**

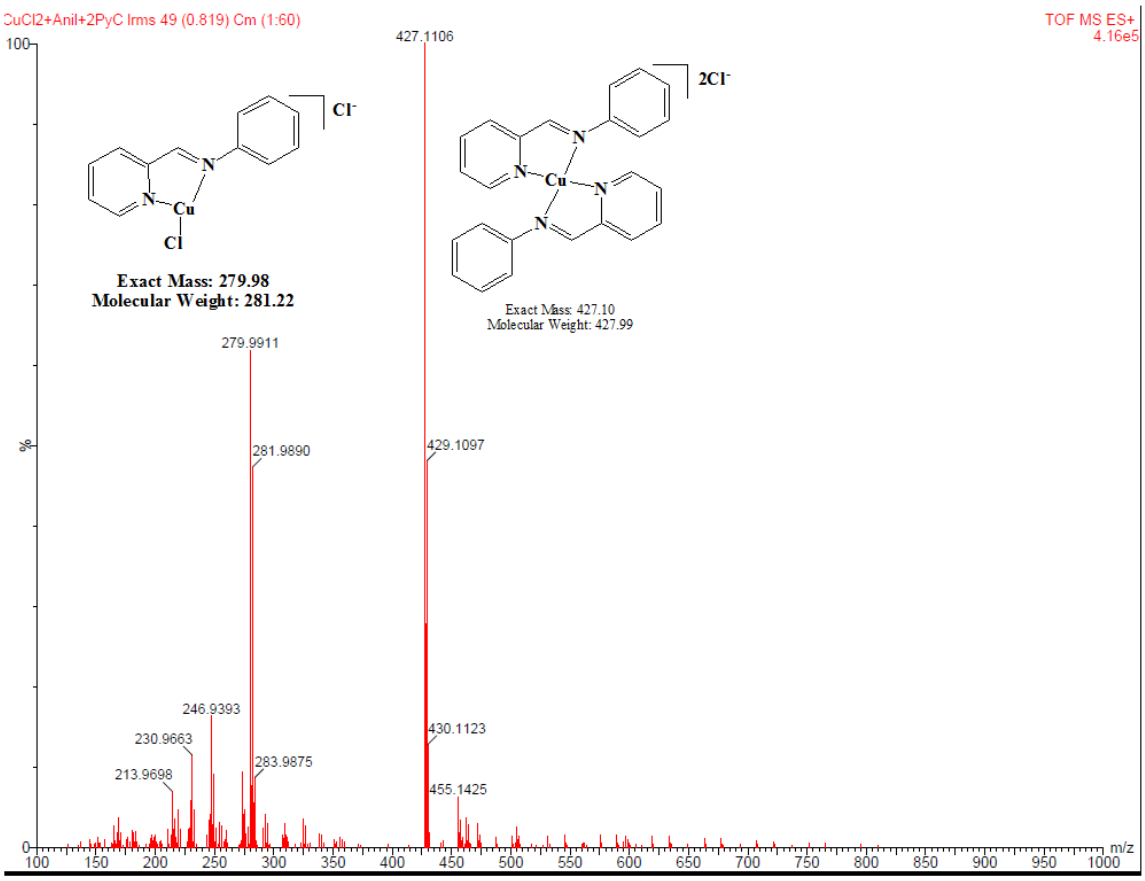

D17: LR-MS of complex **12**

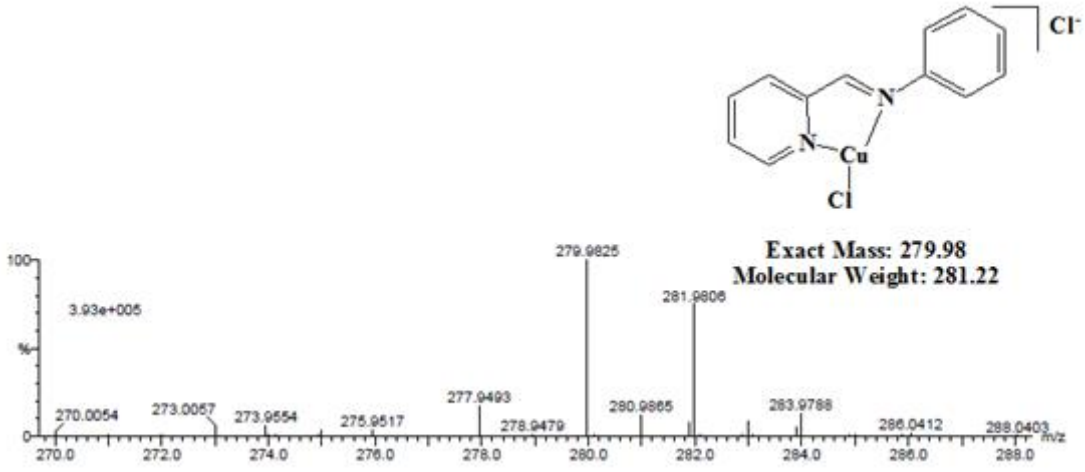

D18: HR-MS of complex **12**

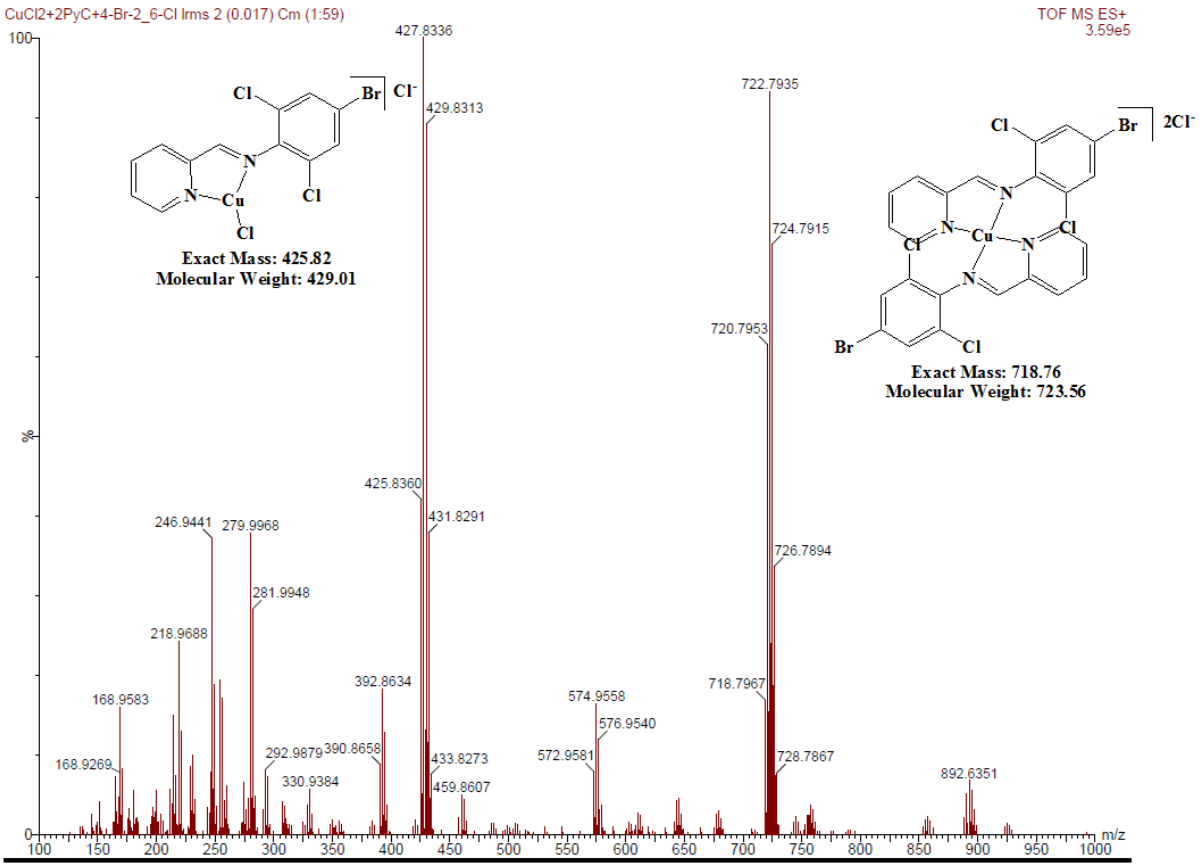

D19: LR-MS of complex **13**

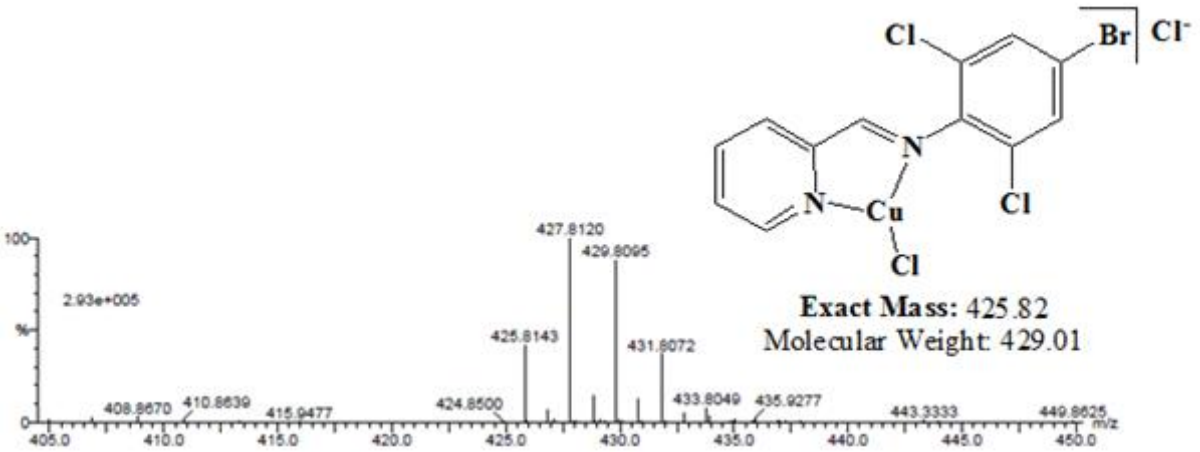

D20: HR-MS of complex **13**

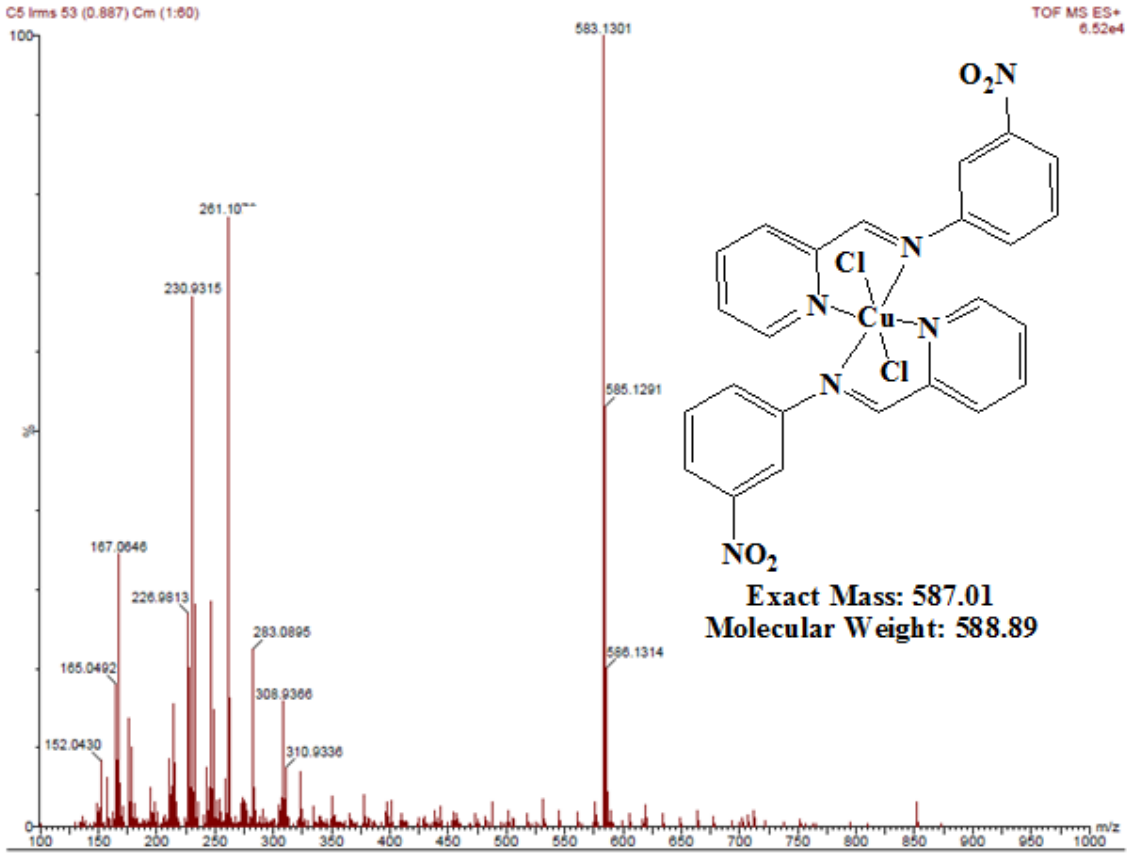

D21: LR-MS of complex **14**

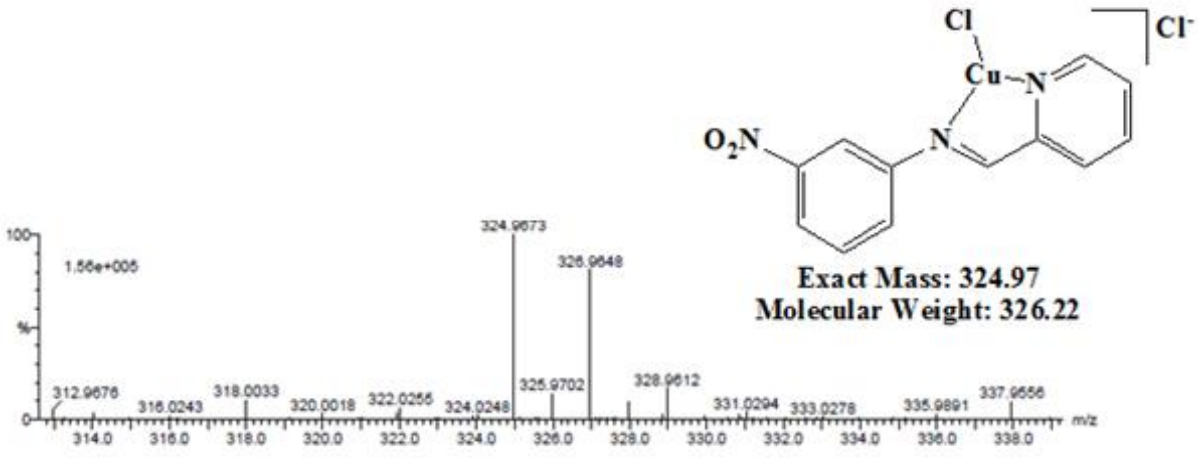

D22: HR-MS of complex **14**

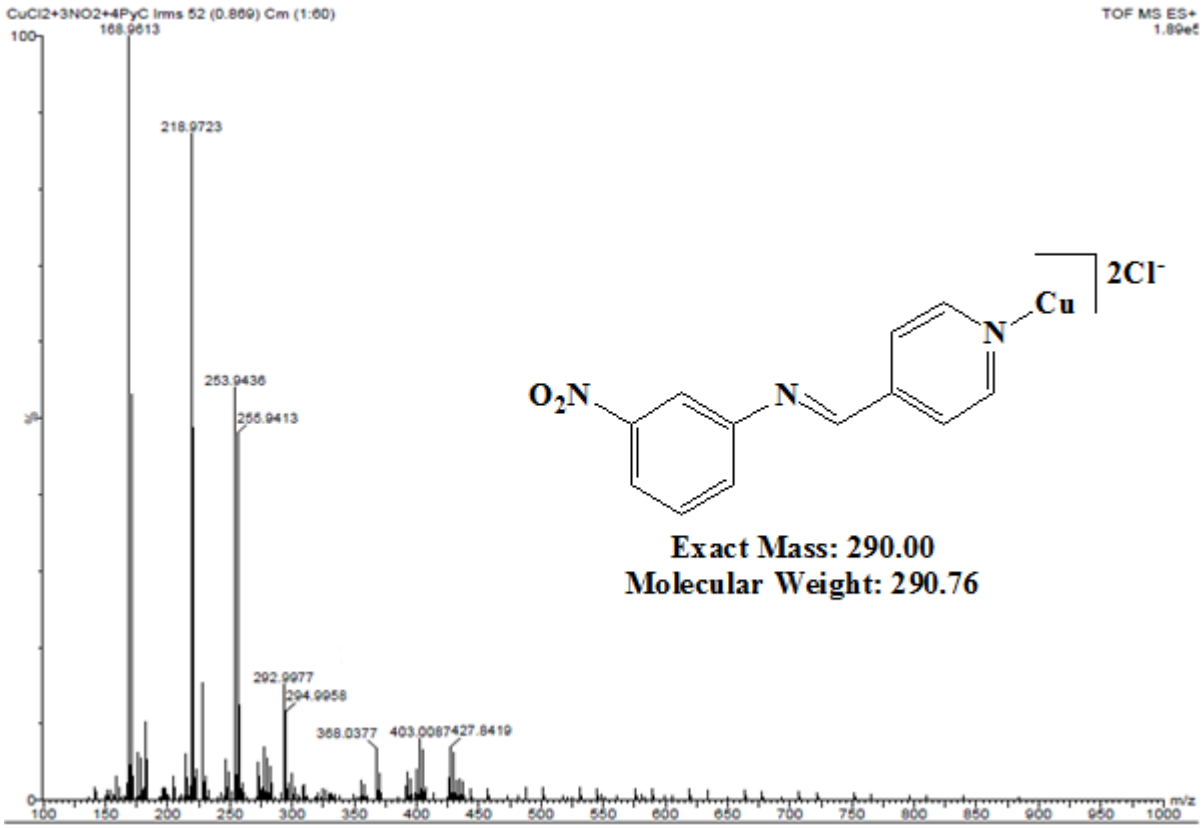

D23: LR-MS of complex **15**

Appendix E

Elemental analysis results

Table E1: The elemental analysis results of complexes

C	C% **Actual** (Theoretical)	H% **Actual** (Theoretical)	N% **Actual** (Theoretical)
2	**54.25** (54.25)	**3.849** (4.56)	**10.37** (9.06)
4	**36.62** (41.17)	**2.938** (2.30)	**6.87** (8.00)
7	**47.34** (44.18)	**3.271** (2.78)	**13.49** (12.88)
9	**59.61** (60.59)	**4.861** (5.09)	**9.71** (10.09)
10	**48.85** (48.78)	**3.904** (4.09)	**7.98** (8.13)
11	**51.75** (54.78)	**3.310** (4.09)	**5.64** (7.10)
12	**44.92** (45.51)	**3.268** (3.18)	**8.75** (8.85)
13	**31.67** (31.03)	**1.585** (1.52)	**6.10** (6.03)
14	**39.02** (39.85)	**2.620** (2.51)	**11.25** (11.62)
15	**47.81** (49.45)	**3.082** (3.09)	**13.81** (14.45)

Appendix F

TGA/DSC derivative graphs

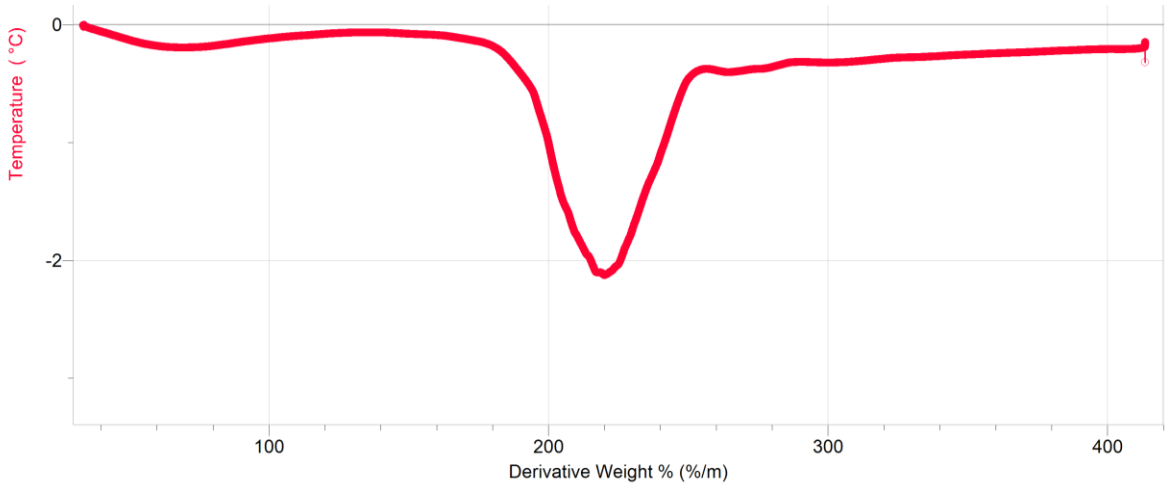

F1: TGA/DSC first derivative graph of complex **3**

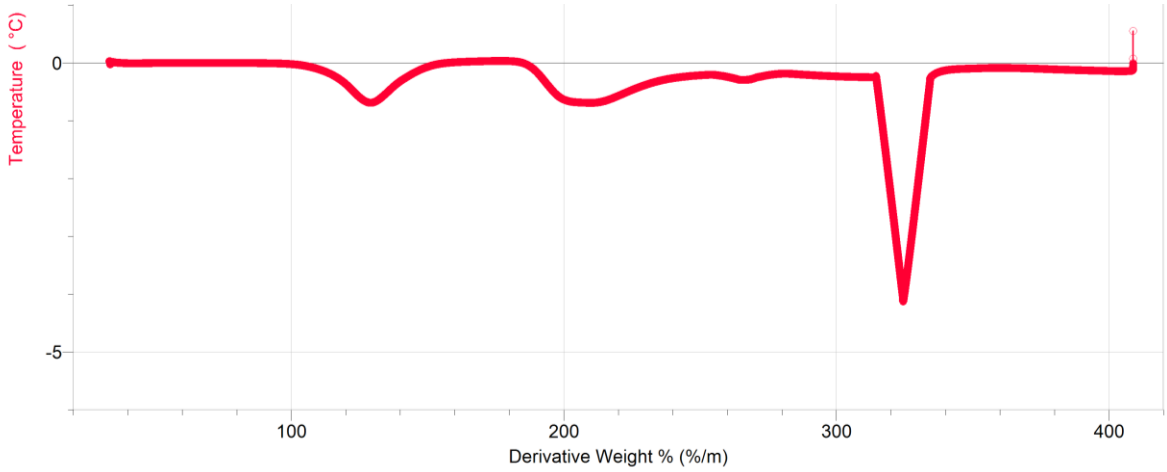

F2: TGA/DSC first derivative graph of complex **12**

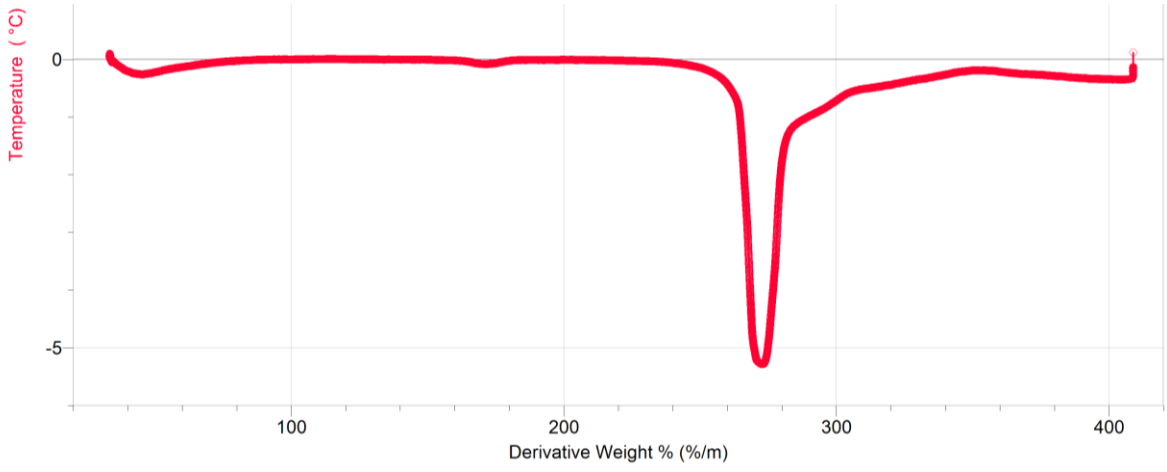

F3: TGA/DSC first derivative graph of complex **14**